UNIVERSITÉ DU QUÉBEC À MONTRÉAL

TRACEURS MICROPALÉONTOLOGIQUES (DINOKYSTES ET COCCOLITHES) DE L'HYDROGRAPHIE ACTUELLE ET HOLOCÈNE AUX MOYENNES ET HAUTES LATITUDES DE L'ATLANTIQUE NORD

THÈSE
PRÉSENTÉE
COMME EXIGENCE PARTIELLE
DU DOCTORAT EN SCIENCES DE L'ENVIRONNEMENT

PAR
SANDRINE SOLIGNAC

FÉVRIER 2008

AVANT-PROPOS

Cette thèse a été rédigée sous forme de trois articles en anglais formant chacun un chapitre. Le premier a été publié en 2006 dans une revue à comité de lecture. Le deuxième a été soumis pour publication. Le troisième article a quant à lui été accepté et est en voie d'être publié, également dans une revue à comité de lecture. La mise en page de ces trois chapitres suit donc les directives propres à chaque revue. Pour cette raison, les titres et figures de chaque chapitre ne sont pas numérotés selon le Guide de présentation des mémoires et thèse; à la place, les numéros tels qu'apparaissant dans les articles ont été conservés. De plus, les formats des références sont légèrement différents d'un chapitre à l'autre, afin de rester conformes aux revues dans lesquelles ils ont été ou seront publiés.

Mon travail a consisté à analyser les assemblages de dinokystes dans chacune des quatre carottes présentées dans les chapitres I et III. J'ai aussi, pour le chapitre II, mis sur pieds une base de données moderne d'assemblages de coccolithes dans l'Atlantique Nord à partir de données de comptage précédemment publiées ainsi que de nouveaux échantillons que j'ai analysés moi-même. J'ai donc harmonisé les données provenant des diverses sources, afin entre autres de standardiser les espèces identifiées. J'étais également responsable des analyses statistiques faites sur l'ensemble des données des trois chapitres, de l'interprétation des résultats et de la rédaction des manuscrits à des fins de soumission, le tout sous la supervision de ma directrice, Madame Anne de Vernal. Les co-auteurs des différents articles ont participé à mes recherches en fournissant échantillons et données, ainsi que par des échanges stimulants sur l'interprétation des résultats.

Le premier chapitre est un article publié en 2006 dans la revue *Paleoceanography* (vol. 21, PA2004, doi:10.1029/2005PA001175) et ayant pour titre « Holocene sea surface conditions in the western North Atlantic: Spatial and temporal heterogeneities », avec pour co-auteurs Jacques Giraudeau et Anne de Vernal. Il porte sur les variations au cours de l'Holocène de l'hydrographie de surface dans le détroit du Danemark, situé entre l'Islande et le Groenland, dans une région-clé de la circulation océanique de l'Atlantique Nord.

Le deuxième chapitre, « Reorganisation of the upper ocean circulation in the mid-Holocene in the northeastern Atlantic », est un article soumis à la *Revue canadienne des sciences de la Terre* et co-écrit avec Michael Grelaud, Anne de Vernal, Jacques Giraudeau,

Matthias Moros, Ian Nicholas McCave et Babette Hoogakker. Il expose les variations de l'hydrographie de surface au cours de l'Holocène sur la ride de Reykjanes et dans le Chenal des Féroé-Shetland, dans le nord-est de l'Atlantique Nord. Ces deux régions sont influencées par des courants océaniques transportant des eaux atlantiques vers le nord et sont donc particulièrement appropriés pour l'étude des fluctuations des transferts de chaleur vers le Pôle Nord.

Le troisième chapitre est un article accepté dans la revue *Marine Micropaleontology*, intitulé « Comparison of coccolith and dinocyst assemblages in the northern North Atlantic: how well do they relate with surface hydrography? ». Écrit en collaboration avec Anne de Vernal et Jacques Giraudeau, il présente une comparaison de la distribution dans le sédiment des assemblages de dinokystes et de coccolithes dans les domaines tempérés à subpolaires de l'Atlantique Nord. La relation entre la distribution des deux groupes d'assemblages et les paramètres hydrographiques de surface de l'océan est également étudiée.

REMERCIEMENTS

Je tiens tout d'abord à remercier ma directrice de thèse, Madame Anne de Vernal, de m'avoir orientée et encouragée tout au long de mes études supérieures, de m'avoir fait confiance et de m'avoir une fois de plus permis de participer à de nombreuses missions, stages et congrès scientifiques. Un immense merci également à mon co-directeur non officiel, Monsieur Jacques Giraudeau, pour son accueil pendant mon séjour à Bordeaux, son aide précieuse, sa patience et son soutien moral.

Je remercie également Monsieur Claude Hillaire-Marcel, grâce à qui j'ai pu participer à une mission extraordinaire en Arctique, Maryse Henry, sans qui bien des analyses n'auraient pas pu être faites et dont le bureau a servi à de nombreuses scéances de consultation psychologique, et Taoufik Radi et Bianca Fréchette qui m'ont aidée dans l'identification des dinokystes et la compréhension des analyses multivariées. Un grand merci également à tous les étudiants qui ont participé aux traitements des échantillons en laboratoire, et surtout aux étudiants et employés que j'ai côtoyés pendant toutes ces années et

qui ont fait de ce doctorat une expérience inoubliable : Benoît, Christelle, Matthieu, Chantal, Christian et tous les autres.

Pendant les moments difficiles, j'ai eu la chance d'être entourée de précieux amis et de ma famille, qui m'ont encouragée et/ou poussée à aller décompresser autour d'une (ou plusieurs) bière(s) : mes parents, Pascal et Catherine, Laurent, l'autre Laurent, Isabelle et bien sûr le groupe des géographes, David (fournisseur officiel d'articles scientifiques introuvables à l'UQAM), Geneviève, Sylvie et Sonya. Je remercie égalemment le Conseil de recherches en sciences naturelles et en génie du Canada (CRSNG), le Fonds québécois de la recherche sur la nature et les technologies (FQRNT) et encore une fois Madame Anne de Vernal pour leur soutien financier.

TABLE DES MATIÈRES

LISTE DES FIGURES

CHAPITRE 1

CHAPITRE 2

CHAPITRE 3

CONCLUSION

LISTE DES TABLEAUX

CHAPITRE 3

LISTE DES ANNEXES

CHAPITRE 3

RÉSUMÉ

Devant le problème du réchauffement planétaire, il est indispensable d'approfondir notre compréhension des mécanismes et des rétroactions qui régulent le climat pour pouvoir prédire les conséquences de tels changements. L'étude des climats passés permet de mettre en évidence la façon dont les événements climatiques s'enchaînent. En particulier, étudier des périodes plus chaudes que l'actuelle permet de mieux comprendre ce vers quoi nous semblons nous diriger. C'est dans cette optique que de nombreuses recherches sont menées sur l'évolution du climat au cours de la présente période interglaciaire, l'Holocène. Notamment, bon nombre de ces études portent sur le milieu océanique, celui-ci étant responsable d'une grande partie des transferts de chaleur à la surface terrestre. De plus, parmi les régions de l'océan susceptibles de réagir fortement à des changements climatiques, l'Atlantique Nord occupe une place de choix. En effet, cette région est actuellement caractérisée par un équilibre entre les apports d'eaux chaudes vers le Pôle Nord via les courants dérivés du Gulf Stream, et les flux d'eaux polaires transportées vers le sud par le courant du Labrador et le courant de l'Est du Groenland. Une modification de l'une des composantes de la circulation actuelle aura donc des conséquences sur l'équilibre de l'ensemble de la région, qui est ainsi particulièrement sensible aux changements hydrographiques et/ou climatiques. En outre, l'Atlantique Nord joue un rôle essentiel dans la circulation thermohaline et la formation d'eau profonde. Des modifications des flux d'eaux atlantiques vers le nord pourraient également avoir des conséquences significatives sur la circulation océanique de surface et profonde à l'échelle du globe.

Cette thèse a pour objectif général de mieux comprendre l'évolution de l'hydrographie de surface de l'Atlantique Nord au cours de l'Holocène, en particulier devant les incertitudes concernant la durée, la chronologie, la distribution spatiale et la cause des perturbations climatiques mises en lumière par les études précédentes. Devant ces incertitudes, deux approches, l'une thématique et l'autre méthodologique, ont été ciblées afin d'améliorer notre compréhension de l'Atlantique Nord à l'Holocène. Le premier volet de cette thèse porte sur la reconstitution quantitative des conditions de surface de l'Atlantique Nord au cours de l'Holocène à partir des assemblages de dinokystes. Cette méthode est privilégiée puisqu'elle permet la reconstitution non seulement de la température de surface de l'océan, mais également de la salinité et de la durée du couvert de glace, qui sont des paramètres jouant un rôle majeur dans le système océanique. De plus, des endroits clés de la circulation océanique de l'Atlantique Nord ont été choisis: le détroit du Danemark, dans l'ouest de l'Atlantique, lieu d'échange d'eaux arctiques et atlantiques, la ride de Reykjanes, plus au centre, sous influence d'eaux atlantiques, et le chenal des Féroé-Shetland, dans l'est de la région, par où s'écoule en surface une grande part des eaux atlantiques vers l'Arctique.

Le deuxième volet concerne un aspect plus fondamental de la paléocéanographie, à savoir la comparaison entre différents traceurs. Il ressort de plusieurs études que des divergences sont apparentes lorsque les signaux fournis par plusieurs traceurs paléocéanographiques sont comparés. Il est essentiel de comprendre la cause de ces divergences pour affiner nos reconstitutions. Dans ce but, une comparaison des assemblages de dinokystes avec ceux d'un autre traceur micropaléontologique, les coccolithes, a été

entreprise, et ce, aussi bien dans des enregistrements holocènes que dans des sédiments actuels. L'objectif ultime est de mettre en évidence d'éventuelles différences au niveau des affinités écologiques de chaque groupe afin de mieux comprendre les informations paléocéanographiques que l'on peut en tirer.

Le premier chapitre présente les résultats de reconstitutions des conditions de surface à partir d'assemblages de dinokystes dans l'ouest de l'Atlantique Nord, dans le détroit du Danemark. Une tendance générale vers des températures d'hiver plus chaudes, des eaux de surface plus salées et un couvert de glace réduit est apparente. Les enregistrements suggèrent que les apports en eaux polaires ont diminué au cours de l'Holocène, au profit des eaux atlantiques transportées par le courant d'Irminger du Nord de l'Islande. La comparaison avec un enregistrement provenant du sud du Groenland, où un refroidissement est observé dans la deuxième moitié de l'Holocène, souligne la forte hétérogénéité des conditions hydrographiques de surface dans l'ouest de l'Atlantique Nord. Cela pourrait s'expliquer par un découplage des deux branches du courant d'Irminger: lorsque celle du Nord de l'Islande est renforcée comme cela semble être le cas dans la deuxième moitié de l'Holocène, la branche principale se dirigeant vers le sud du Groenland est affaiblie. De plus, des similarités entre l'enregistrement marin du sud du Groenland avec un enregistrement continental à proximité suggèrent un étroit couplage avec des processus atmosphériques.

Le deuxième chapitre expose les résultats de reconstitutions des conditions de surface dans l'est de l'Atlantique Nord, à partir d'un site provenant de la ride de Reykjanes et d'un autre du chenal des Féroé-Shetland. Les assemblages de dinokystes aussi bien que de coccolithes mettent enévidence des changements significatifs des conditions de surface de l'océan et suggèrent une réorganisation majeure de la configuration des courants de surface entre 7 et 5.4 ka BP. Des tendances évolutives inverses de température de surface sont observées aux deux sites, avec un refroidissement à partir de 6 ka BP, et un réchauffement dans le chenal des Féroé-Shetland après 5.4 ka BP. Cela suggère que la diminution de l'insolation estivale n'était pas l'unique « forçage » direct à l'origine de ces changements. Il est proposé que ceux-ci résultent d'un découplage entre les deux courants transportant des eaux atlantiques vers le Nord et influençant le chenal des Féroé-Shetland, soit le Courant Nord Atlantique (CNA) et le courant de Pente. Un CNA plus fort dans la première moitié de l'Holocène se serait traduit par des températures plus élevées sur la ride de Reykjanes. Après 5-6 ka BP, un affaiblissement du CNA aurait entraîné un refroidissement sur la ride de Reykjanes, et une plus forte contribution relative du courant de Pente, plus chaud et plus salé, résultant en une hausse des températures et salinités dans cette région. En outre, la comparaison des enregistrements de dinokystes et de coccolithes met en évidence des fluctuations synchrones des assemblages des deux groupes. Cependant, quelques contradictions sont également observées, soulignant la nécessité de mieux comprendre le potentiel paléocéanographique de ces deux traceurs.

Le troisième chapitre porte sur la comparaison de la distribution moderne des assemblages de dinokystes et de coccolithes dans les sédiments de l'Atlantique Nord à partir d'une base de données de 87 échantillons. La comparaison met en évidence une excellente correspondance entre les assemblages de dinokystes, les assemblages de coccolithes et les masses d'eau sus-jacentes, notamment dans les domaines subtropical et tempéré. Dans le

domaine subpolaire, les assemblages de coccolithes sont nettement moins diversifiés en termes d'espèces que ceux de dinokystes, qui reflètent ainsi beaucoup plus clairement l'hydrographie de surface. Des analyses de correspondance canonique menées sur les assemblages de coccolithes et de dinokystes montrent que la température de surface de l'océan est le paramètre environnemental ayant la plus grande influence sur la distribution des deux groupes. Les assemblages de dinokystes semblent également être influencés par la distance à la côte, contrairement aux coccolithes. Les autres facteurs environnementaux significatifs incluent la salinité de surface et la productivité, mais leur importance relative change selon que des échantillons provenant de conditions environnementales « extrêmes » sont inclus ou non dans la base de données. Les résultats suggèrent qu'il est difficile de faire ressortir tous les différents environnements par des analyses multivariées en raison de la complexité des interrelations entre les divers paramètres environnementaux. De plus, la forte cohérence entre les assemblages de dinokystes et de coccolithes ne nous permet pas pour le moment de comprendre la cause de divergences telles que celles observées dans le chapitre deux. Des études supplémentaires sont donc nécessaires non seulement pour mieux détailler l'écologie des deux groupes, mais aussi pour avoir un plus grand éventail d'associations d'assemblages de dinokystes et de coccolithes avec lesquelles comparer nos enregistrements Holocène.

Mots-clés : Atlantique Nord, Holocène, circulation océanique, masse d'eau, dinokyste, coccolithe, distribution, fonction de transfert

INTRODUCTION

Devant le problème du réchauffement planétaire, il est indispensable d'approfondir notre compréhension des mécanismes et des rétroactions qui régulent le climat avant de pouvoir prédire les conséquences de tels changements. Notamment, une meilleure connaissance du milieu océanique est nécessaire, puisqu'une grande partie des transferts de chaleur à la surface terrestre s'opère via l'océan. L'étude des climats passés, à travers la modélisation paléoclimatique ou l'utilisation de traceurs paléo-climatiques, s'avère un moyen efficace de comprendre la façon dont les événements climatiques s'enchaînent, et ce à différentes échelles temporelles. En particulier, étudier le comportement du système climatique au cours de périodes où les températures étaient plus chaudes que de nos jours permettrait de mieux comprendre ce vers quoi le climat actuel semble se diriger.

Dans cette optique, de nombreuses recherches ont été entreprises sur la présente période interglaciaire, l'Holocène, qui a débuté il y ~11.5 milliers d'années. Diverses études suggèrent en effet que les températures au cours d'une partie de cette période ont été supérieures à celles de nos jours (e.g. Mangerud et al., 1974), en raison entre autres d'une insolation estivale plus élevée au début de l'Holocène qu'aujourd'hui (Berger et Loutre, 1991). Cette thèse s'inscrit donc dans le cadre des reconstitutions du climat de l'ensemble de l'Holocène. Plus particulièrement, elle a pour objectif de caractériser les fluctuations climatiques au cours de l'Holocène dans l'Atlantique Nord (59°N à 68°N) à l'aide d'un traceur micropaléontologique, les kystes de dinoflagellés (ou dinokystes), qui donnent accès à différents paramètres hydrographiques (température, salinité, glace de mer). De plus, devant les nombreux résultats contradictoires obtenus à partir de différents traceurs paléocéanographiques, un deuxième volet porte sur la comparaison des variations des assemblages de dinokystes avec celles des assemblages d'un autre traceur micropaléontologique, les coccolithes, et ce, aussi bien dans les sédiments actuels que dans les enregistrements Holocène.

1. L'Atlantique Nord dans le système climatique

Parmi les régions du globe susceptibles de réagir fortement à des changements climatiques, l'Atlantique Nord occupe une place de choix. Actuellement, la distribution des masses d'eau de surface dans l'Atlantique Nord subpolaire (45° à 65°N) est déterminée par l'écoulement vers le sud des eaux froides provenant de l'Arctique le long des côtes ouest (par le biais des courants de l'Est du Groenland et du Labrador), et par l'advection vers le nord d'eaux chaudes de l'Atlantique dans l'est de la région (par le biais de la Dérive Nord Atlantique et du courant d'Irminger, tous deux dérivés du Gulf Stream, et du Courant de Pente longeant les côtes européennes). L'influence relative des eaux polaires et atlantiques détermine les paramètres hydrographiques des masses d'eau (température, salinité, durée du couvert de glace, nutriments, etc.) et se traduit par trois domaines océanographiques majeurs : le domaine polaire, le long de la côte est groenlandaise, essentiellement influencé par les eaux froides et dessalées de l'Arctique, le domaine atlantique, au sud de l'Islande et dans l'est de la mer de Norvège, relativement chaud et salé, et le domaine arctique, au centre des mers nordiques (mers du Groenland, d'Islande et de Norvège), qui naît du mélange d'eaux polaires et atlantiques (Swift, 1986). La configuration actuelle des courants a pour effet d'adoucir le climat européen jusqu'aux hautes latitudes, comme en témoigne par exemple le couvert de glace réduit jusqu'à 80°N dans la mer de Barents, au nord de la Norvège, par comparaison à 50°N dans le secteur ouest de l'Atlantique Nord (National Snow and Ice Data Center, 2003).

En plus de tempérer le climat européen, les apports en eaux chaudes et salées de l'Atlantique vers le pôle Nord jouent également un rôle essentiel dans la circulation thermohaline, étant directement liés à la formation d'eau profonde. Le refroidissement progressif des masses d'eau lorsqu'elles sont transportées vers le nord accroît leur densité jusqu'à une valeur critique dans la mer du Groenland, à partir de laquelle elles s'enfoncent dans l'océan et renouvellent les eaux profondes, qui s'écoulent alors vers le sud de part et d'autre de l'Islande et forment la *North Atlantic Deep Water* (NADW) lorsqu'elles se rejoignent (Rahmstorf, 2006 et références citées). Outre la mer du Groenland, la mer du Labrador est aussi un important site de convection (Marshall et Schott, 1999). La convection, en entraînant les masses d'eau de surface vers les profondeurs, génère à son tour un

phénomène « d'aspiration » et attire les eaux atlantiques, créant ainsi une boucle de rétroaction positive et maintenant le flux d'eaux chaudes vers le nord.

Une modification de l'une des composantes de la circulation actuelle aura donc des conséquences sur l'équilibre de l'ensemble de la région, qui est ainsi particulièrement sensible aux changements hydrographiques et/ou climatiques. La sensibilité même de l'Atlantique Nord en fait une région de choix pour l'étude d'oscillations climatiques d'amplitude relativement faible, telles que celles qui ont ponctué la période interglaciaire dans laquelle nous nous trouvons, l'Holocène. De nombreuses études se sont penchées sur les fluctuations de la vitesse et/ou du volume des courants arctiques et atlantiques, aussi bien au cours des dernières décennies (e.g., Turrel et al., 1999; Blindheim et al., 2000), pour lesquelles on dispose de mesures instrumentales, que sur des périodes beaucoup plus longues (e.g., Jennings et al., 2002; Rasmussen et al., 2002a), et ce, afin d'identifier les conséquences de tels changements sur les moyennes et hautes latitudes de l'Atlantique Nord, ou sur l'intensité de la circulation thermohaline (e.g., Oppo et al., 2003).

2. L'Holocène dans l'Atlantique Nord

L'Holocène a longtemps été considéré comme une période remarquablement stable d'un point de vue climatique (e.g., Dansgaard et al., 1993; Sarthein et al., 1995), particulièrement lorsque comparé à la dernière glaciation, qui a connu de très fortes et parfois rapides oscillations climatiques (e.g., Rasmussen et al., 2002b). Pourtant, une tendance générale de refroidissement à partir de l'Holocène moyen à l'échelle de l'Atlantique Nord et de ses bassins marginaux a été identifiée par de nombreux auteurs (e.g., Eiriksson et al., 2000a, b; Duplessy et al., 2001; Klitgaard-Kristensen et al., 2001; Marchal et al., 2002) et est généralement attribuée à un changement de l'insolation (e.g., Alley et al., 1999; Marchal et al., 2002; Koç et Jansen, 2002). De plus, il semblerait que des oscillations de plus haute fréquence soient superposées à cette tendance. Entre autres, Bond et al. (1997, 2001) ont mis en évidence des pics de froid quasi-cycliques (~1500 ans) associés à de l'advection d'eaux arctiques dans l'Atlantique Nord. Cependant, de fortes divergences sont observées avec d'autres études, que ce soit au niveau de la fréquence des oscillations climatiques (e.g., Chapman et Shackleton, 2000; Schultz et Paul, 2002), de leur distribution spatiale (Solignac

et al., 2004; de Vernal et Hillaire-Marcel, 2006) ou même de leur présence (Risebrobakken et al., 2003; voir aussi Solignac, 2005 pour une synthèse des oscillations rapides au cours de l'Holocène). Les causes de ces fluctuations sont également sujettes à débat. Les forçages mis en avant, qu'ils soient internes (instabilité des calottes glaciaires actuelles, oscillation interne du système océanique et/ou atmosphérique, Maslin et al., 2003; Paul et Schulz, 2002; Schulz et Paul, 2002; Noren et al., 2002) ou externes (variations de l'irradiance solaire – Denton et Karlén, 1973; O'Brien et al., 1995; Sarnthein et al., 2003; etc. – ou de la force des marées – Keeling et Whorf, 2000, volcanisme – Nesje et Johannessen, 1992; Zielinski et al., 1994) souffrent de nombreuses incertitudes et se contredisent d'une étude à l'autre (Solignac, 2005).

Il semblerait donc que nous soyons arrivés à une nouvelle étape dans l'étude de l'Holocène. Maintenant qu'il a été clairement établi que des perturbations climatiques ont ponctué cette période, il importe de déterminer avec précision la durée, la chronologie, la distribution spatiale et les causes de celles-ci. Une meilleure connaissance des événements climatiques au cours de l'Holocène permettrait de mettre en évidence les forçages de la variabilité climatique ainsi que les modes de transmission de ces anomalies. Pour améliorer nos connaissances, il est cependant essentiel de comprendre les causes des divergences entre les études.

Des biais méthodologiques, tels qu'une chronostratigraphie imprécise ou une résolution temporelle des analyses insuffisante, sont parfois invoqués pour expliquer le manque de cohérence entre les enregistrements. Il a également été proposé que les divergences résultent de mécanismes climatiques régionaux entraînant une réponse non linéaire à des phénomènes globaux tels que des changements d'insolations. Cette réponse serait à l'origine des disparités spatiales de l'évolution du climat rappelant certains modes de variabilité climatique actuels tels que l'Oscillation Nord Atlantique (e.g., Schulz et Paul, 2002; Lorenz et al. 2006). Enfin, il est aussi possible que les différents traceurs paléoclimatiques ne permettent pas de reconstituer les mêmes facteurs environnementaux. De telles différences sont particulièrement apparentes lorsque plusieurs traceurs paléocéanographiques sont analysés sur les mêmes échantillons et donnent des enregistrements en apparence contradictoires (e.g., Dolven et al., 2002; Marchal et al., 2002). Plusieurs études de ce genre ont mené les auteurs à penser que les divers traceurs utilisés

reflètent les conditions hydrographiques de différentes profondeurs de la colonne d'eau et/ou de différentes saisons (Chapman et al., 1996; Sikes et Keigwin, 1996; Marchal et al., 2002; Cortese et al., 2005). Si tel est le cas, mieux connaître les spécificités des différents traceurs s'avère un atout puisque cela pourrait permettre de plus détailler les environnements passés, par exemple en reconstituant le cycle saisonnier des températures, ou encore la stratification de la colonne d'eau.

Il est donc primordial non seulement de faire la part entre les différentes sources possibles d'incohérence entre les enregistrements, mais aussi de mieux comprendre les informations paléocéanographiques fournies par les différents traceurs.

3. Dinokystes et coccolithes, deux traceurs micropaléontologiques

En milieu océanique, de nombreux indicateurs sont utilisés dans le but de reconstituer certains paramètres hydrographiques. Ces traceurs peuvent être sédimentologiques (granulométrie, débris transportés par les icebergs, etc.), isotopiques ($\delta^{18}O$, $\delta^{13}C$, etc.), biochimiques (alkénones) ou micropaléontologiques. Notamment, les foraminifères sont les traceurs micropaléontologiques les plus souvent utilisés (e.g. Kucera, 2007). Ils présentent des avantages certains, dont leur abondance dans les sédiments, la simplicité des traitements nécessaires pour les récupérer, ou encore la possibilité de mener des analyses isotopiques de leurs tests. Cependant, plusieurs espèces de foraminifères évoluent à la subsurface de l'océan, jusqu'à plusieurs centaines de mètres de profondeur (e.g., de Vernal et Hillaire-Marcel, 2006 et références citées; Kucera, 2007). Les communautés de foraminifères, ainsi que leurs compositions isotopiques, ne sont pas forcément directement influencées par les processus de surface de l'océan et peuvent refléter les conditions environnementales plus en profondeur dans la colonne d'eau. D'autres traceurs micropaléontologiques sont donc nécessaires pour reconstituer l'hydrographie de surface de l'océan. Parmi ceux-ci, les coccolithes et les dinokystes occupent une place de choix en raison de leur abondance et, en particulier dans le cas des dinokystes, de leur potentiel de préservation dans les sédiments marins.

Les dinoflagellés sont des protistes algaires de la division des *Dinoflagellata* (Fensome et al., 1993) et constituent, aux côtés des coccolithophores et des diatomées, l'un

des principaux groupes de producteurs primaires dans l'océan. Près de la moitié des dinoflagellés sont autotrophes, l'autre moitié se composant d'organismes hétérotrophes, mixotrophes, parasitiques ou symbiotiques (de Vernal et Marret, 2007 et références citées). Au cours de leur cycle de vie, environ 10 à 20% des dinoflagellés forment un kyste protégeant la cellule pendant une période de dormance plus ou moins longue (e.g. Wall et Dale, 1968). Ces kystes – appelés dinokystes – sont composés d'une matière organique extrêmement résistante, la dinosporine (de Vernal et Marret, 2007 et références citées), ce qui leur permet d'être préservés dans les sédiments marins lorsque la cellule meurt. Ce sont ces fossiles qui sont utilisés comme traceurs paléocéanographiques.

Les coccolithophores sont des protistes algaires, pour la plupart autotrophes, regroupés dans les ordres des Isochrysidales et des Coccolithales (classe des Prymnesiophycées, division des Haptophytes). En plus d'être d'importants producteurs primaires dans l'océan, ils représentent la première source de boues calcaires marines (Giraudeau et Beaufort, 2007). Ces organismes ont en effet la particularité de former des plaques calcaires recouvrant la cellule vivante, et dont la morphologie est propre à chaque espèce. Lorsque la cellule meurt, une partie de ces plaques, ou coccolithes, se déposent sur le fond marin, où elles sont peu à peu enfouies et fossilisées. Ce sont ces fossiles qui servent de traceurs paléoenvironnementaux.

Les coccolithes et les dinokystes (du moins les autotrophes) évoluent dans la zone photique des océans afin de pouvoir faire la photosynthèse. Ils sont ainsi exposés à différents paramètres environnementaux, tels que la température, la salinité, la durée du couvert de glace, l'abondance en nutriments ou l'intensité lumineuse, qui déterminent la distribution des différentes espèces (Eide, 1990; Samtleben et Schröder, 1992; Brand, 1994). Cependant, divers processus (prédation, bioturbation, dissolution préférentielle, transport, etc.; e.g. Matthiessen et al. 2001) affectent la sédimentation des dinokystes et coccolithes, causant une altération des assemblages fossiles par rapport aux communautés vivantes (e.g., Samtleben et Schröder, 1992; Andruleit, 1997). Malgré cela, de nombreuses études ont montré une étroite relation entre les caractéristiques des masses d'eau de surface et les assemblages de dinokystes et coccolithes fossiles directement en dessous (Siesser, 1993; Rochon et al., 1999; Baumann et al., 2000; Boessenkool et al., 2001; Marret et al., 2004). Cette relation en fait des traceurs de l'hydrographie de surface plus adéquats que les foraminifères, et des méthodes

quantitatives de reconstitution des paramètres environnementaux de surface ont été développées à partir des dinokystes et des coccolithes. Dans le cas des dinokystes, elles permettent la reconstitution des températures de surface estivale hivernale (et donc de la saisonnalité), des salinités de surface estivale et hivernale, et de la durée du couvert de glace à partir de la méthode des meilleurs analogues et d'une base de données de la distribution des assemblages de dinokystes couvrant la côte est du Pacifique Nord, l'Atlantique Nord et leurs mers marginales (Guiot, 1990; de Vernal et al., 1994, 2005). Les assemblages de dinokystes apportent donc d'importantes informations complémentaires sur les conditions physico-chimiques de la colonne d'eau, ce qui leur confère un intérêt manifeste sur d'autres traceurs paléocéanographiques à partir desquels seule la température de surface est reconstituée (e.g., alkénones, diatomées, etc.). Dans le cas des coccolithes, quelques méthodes quantitatives de reconstitution de la température de surface de l'océan ont été mises sur pied (Geitzenauer et al., 1976; Bollmann et al., 2002), mais dans l'ensemble, les études paléocéanographiques basées sur les coccolithes s'appuient essentiellement sur une interprétation qualitative des assemblages (e.g., Baumann et Matthiessen, 1992; Giraudeau et al., 2000).

Les dinokystes et les coccolithes partagent donc de nombreux points communs. Malgré cela, des caractéristiques propres à chaque groupe sont apparentes. Le maximum de productivité des coccolithophores est observé en milieu océanique ouvert et la plupart des espèces vivent dans des eaux chaudes, stratifiées et oligotrophes (Brand, 1994). La diversité des espèces diminue également des basses aux hautes latitudes. De plus, la dissolution de la calcite modifie fortement les assemblages, d'autant plus qu'elle est sélective et s'attaque de préférence aux espèces les moins résistantes. Dans les bassins subpolaires, quatre espèces constituent plus de 95% des assemblages (Haq, 1998; Rahman et de Vernal, 1994) en raison non seulement d'un faible nombre d'espèces vivantes, mais également d'une forte dissolution (Andruleit, 1997). À l'inverse, les dinokystes sont particulièrement abondants dans les mers marginales et sur les plateaux continentaux, avec une diversité relativement élevée dans les milieux subpolaires (de Vernal et Marret, 2007). Extrêmement résistants, ils ne sont pas affectés par la dissolution, mais certaines espèces montrent une certaine sensibilité à l'oxydation (Zonneveld et al., 2001).

Ainsi, chaque groupe de microfossiles présente des avantages et des inconvénients particuliers en tant que traceur paléocéanographique; les utiliser conjointement devrait

permettre de réduire quelque peu les limites inhérentes à chaque traceur. Des différences écologiques pourraient permettre d'apporter des informations complémentaires sur les fluctuations climatiques passées et donc d'affiner les reconstitutions paléo-environnementales. À l'inverse, des affinités écologiques communes permettraient dans une certaine mesure de faire la part entre des signaux écologiques et des processus taphonomiques, et ainsi d'obtenir des reconstitutions plus solides.

Quelques études comparatives des dinokystes et des coccolithes ont été menées, mais elles reposent essentiellement sur un nombre réduit d'échantillons provenant d'un domaine géographique de l'Atlantique Nord (e.g. Hass et al., 2001) ou d'un milieu totalement différent (par exemple, le système du Benguela au large de la Namibie; Vink et al., 2003). Il importe donc de parfaire nos connaissances sur les affinités écologiques des dinokystes et des coccolithes, afin de pouvoir identifier avec précision les paramètres environnementaux déterminant leur distribution spatiale.

4. Objectifs

Au vu de cet état des connaissances, cette thèse s'articule autour de deux volets, l'un, thématique, concernant les changements de conditions de surface dans l'Atlantique Nord au cours de l'Holocène et l'autre, plus méthodologique, portant sur la comparaison de deux traceurs micropaléontologiques, les dinokystes et les coccolithes. Plus spécifiquement, les objectifs sont de :

1. Mieux comprendre l'évolution de l'hydrographie de surface de l'Atlantique Nord au cours de l'Holocène à l'aide de reconstitutions quantitatives basées sur les assemblages de dinokystes. Une attention toute particulière est portée à l'étendue spatiale des changements hydrographiques afin de mieux comprendre les mécanismes qui les sous-tendent. Dans cette optique, des endroits clés de la circulation océanique de la région sont ciblés: le détroit du Danemark, où des échanges d'eaux arctiques et atlantiques ont lieu, la ride de Reykjanes, sous influence d'eaux atlantiques issues de la Dérive Nord Atlantique et du courant d'Irminger, et le Chenal des Féroé-Shetland, site d'importants apports d'eaux atlantiques vers le nord. L'utilisation des méthodes quantitatives paléocéanographiques basées sur les

assemblages de dinokystes est privilégiée puisqu'elle permet la reconstitution de divers paramètres hydrographiques (température, salinité, saisonnalité, durée du couvert de glace) jouant un rôle majeur dans le système océanique.

2. Comparer les variations des assemblages de dinokystes et de coccolithes dans des enregistrements Holocène de l'Atlantique Nord afin de déterminer si les deux traceurs donnent des résultats concordants, ou au contraire de comprendre les causes d'éventuelles divergences et si possible d'en tirer des informations paléoenvironnementales complémentaires.

3. Comparer la distribution actuelle des assemblages de dinokystes et de coccolithes dans les sédiments de surface de l'Atlantique Nord afin de mettre en évidence d'éventuelles différences au niveau des affinités écologiques de chaque groupe, ou au contraire une forte cohérence. Des analyses statistiques multivariées sont utilisées pour voir la relation entre les deux types d'assemblages et les caractéristiques physico-chimiques des masses d'eau.

CHAPITRE I

HOLOCENE SEA SURFACE CONDITIONS IN THE WESTERN NORTH ATLANTIC: SPATIAL AND TEMPORAL HETEROGENEITIES

Sandrine Solignac[1], Jacques Giraudeau[2] and Anne de Vernal[1]

[1]GEOTOP-UQAM, C.P. 8888, Succursale Centre-ville, Montréal, QC, H3C 3P8

[2]Environnements et Paléoenvironnements Océaniques, UMR CNRS 5805, Université Bordeaux 1, Avenue des Facultés, 33405 Talence cedex, France

Article publié en 2006 dans la revue *Paleoceanography*, Vol. 21, PA2004, doi:10.1029/2005PA001175.

Résumé

Des enregistrements des conditions de surface de l'océan au cours de l'Holocène dans l'ouest des mers Nordiques ont été obtenus à partir d'assemblages de kystes de dinoflagellés. Deux carottes sédimentaires provenant des plates-formes continentales de l'est du Groenland et du nord de l'Islande fournissent des informations détaillées sur la dynamique à long et court termes des écoulements opposés des eaux arctiques et atlantiques. Une tendance générale vers des températures d'hiver plus chaudes, des eaux de surface plus salées et un couvert de glace réduit est apparente dans les enregistrements de certaines espèces de dinokystes ainsi que dans les reconstitutions quantitatives. La diminution du couvert de glace est mise en évidence par une étroite relation entre l'abondance relative d'une espèce atlantiques, *Nematosphaeropsis labyrinthus* et des enregistrements de débris transportés par la glace (DTG). Il est proposé que l'augmentation des DTG à l'Holocène supérieur dans le détroit du Danemark est en grande partie le résultat d'une combinaison d'un couvert de glace réduit en raison d'apports accrus en eaux atlantiques et d'un vêlage d'icebergs plus intense lié à la réavancée de la calotte glaciaire du Groenland. Nos enregistrements suggèrent donc que les apports en eaux polaires ont diminué au cours de l'Holocène, bien que la date des changements de régime diffère entre l'ouest et l'est du détroit du Danemark. Enfin, la comparaison de nos enregistrements avec une carotte au sud du Groenland souligne la forte hétérogénéité des conditions hydrographiques de surface dans l'ouest de l'Atlantique Nord. Cela pourrait s'expliquer par un découplage des deux branches du courant d'Irminger. Des similarités entre l'enregistrement marin du sud du Groenland et un enregistrement continental à proximité suggèrent un étroit couplage avec des processus atmosphériques, rappelant ainsi une configuration spatiale climatique ressemblant à l'Oscillation Nord Atlantique.

Abstract

Holocene records of sea surface conditions in the western Nordic seas were obtained from quantitative reconstructions based on dinoflagellate cyst assemblages. Two sediment cores from the east Greenland and the north Iceland shelves provide a detailed account of the long- and short-term dynamics of the opposing flows of Arctic versus Atlantic waters. Both marker species and quantitative reconstructions depict an overall trend toward warmer winter temperatures, saltier surface waters and decreased sea ice extent. The latter is supported by a close relationship between relative abundances of an Atlantic dinocyst species, *Nematosphaeropsis labyrinthus*, and ice-rafted debris (IRD) records. We propose that the late Holocene increased IRD delivery in the Denmark Strait region was primarily induced by a combination of less extensive sea ice cover under increased Atlantic water inflow and sustained iceberg calving tied to the readvance of the Greenland ice sheet. Our records thus suggest diminishing polar waters supplies throughout the Holocene, although the timing of regime changes differs between the western and eastern sides of the Denmark Strait. Finally, comparison of our records with a core from southern Greenland points to very heterogeneous sea surface conditions in the western North Atlantic, which could be explained by the decoupled dynamics of the two Irminger Current branches. Similarities between the southern Greenland marine record and a continental record nearby suggest a close coupling with atmospheric processes, reminiscent of a North Atlantic Oscillation-like climate pattern.

1. Introduction

Holocene climate variability has been the focus of numerous studies in the recent years. There is a general consensus on a climate transition in the mid-Holocene [e.g. *Steig*, 1999], generally attributed to insolation changes [e.g. *Alley et al.*, 1999; *Marchal et al.*, 2002]. In addition, growing evidence suggest that higher-frequency oscillations are superimposed on this long-term trend, in atmospheric [*O'Brien et al.*, 1995], continental [*Campbell et al.*, 1998], sea surface [*Bond et al.*, 1997], as well as deep-sea [*Bianchi and McCave*, 1999] records. However, many inconsistencies are observed between the records, with respect for instance to the timing of these oscillations, their periodicities, their cause and their spatial extent [e.g. *Solignac et al.*, 2004].

The spatial extent of climate fluctuations, either on a long or short term, is an important factor to assess as it can shed light on climate mechanisms (e.g. seesaw patterns as in the North Atlantic Oscillation versus global temperature trends). Here we aim at understanding sea surface changes throughout the Holocene in different domains of the Nordic seas, which are characterized by pronounced temperature and salinity gradients due to the presence of very contrasting water masses, as well as by a strong sensitivity to climate changes related to their high-latitude setting. In particular, the Denmark Strait is a central region when addressing the sea surface variability of the Nordic seas as it extends over very different interacting environments, characterized by Arctic water outflow to the west and by the influence of warm and saline North Atlantic waters to the east. Recent paleoenvironmental studies have highlighted the sensitivity of this oceanic realm to subtle changes in climate variations and ocean processes throughout the last 10,000 years [*Andrews et al.*, 2002; *Jennings et al.*, 2002; *Knudsen et al.*, 2004; *Andresen et al.*, 2005]. Two study sites were thus chosen on each side of the Denmark Strait in order to document the recent history of Atlantic and Arctic sea surface and its influence on the heat and salt budget of the western North Atlantic.

Sea surface parameters (temperature, salinity and sea ice extent) were reconstructed for the past 10,000 calibrated years based on organic-walled dinoflagellate cyst (dinocyst) assemblages. Dinocysts are a sensitive proxy for sea surface conditions and allow the

reconstruction of hydrographical parameters including temperature and salinity of the coldest and warmest months and sea ice cover extent [e.g. *de Vernal et al.*, 1994, 2005].

2. Oceanographic setting

The cold and relatively fresh East Greenland Current (EGC) flows south from the Arctic Ocean in a narrow band along the Greenland coast. Part of it splits and feeds the Jan Mayen Current (JMC) in the Greenland Sea, as well as the East Iceland Current (EIC) in the Iceland Sea. The ice-free EIC usually carries arctic water to the northern Iceland shelf; however, the EIC can acquire a true polar character, in connection with a strengthened EGC and northerly wind conditions [Malmberg, 1985; Olafsson, 1999].

The Irminger Current (IC) branches from the warm and saline North Atlantic Drift. Part of it flows westward into the Irminger basin, whereas the other branch circulates anticyclonically around Iceland (Figure 1) [*Johannessen*, 1986]. Hence west and north of Iceland, close to the coast, warmer water is brought by the slightly modified northern branch of the IC, the North Iceland Irminger Current (NIIC). The environment of the northern Icelandic shelf is thus highly variable and primarily controlled by the balance between the relative strength of the Atlantic NIIC and the Arctic EIC [*Malmberg and Jónsson*, 1997].

The presence of hydrographically contrasting water masses in the Nordic seas gives rise to the formation of two major oceanic fronts (Figure 1). The Polar Front corresponds with the maximum extent of summer sea ice and marks the boundary between the purely polar waters carried by the EGC and the Arctic waters of the Greenland and Iceland seas, which are saltier and warmer due to the influence of Atlantic waters brought by the Irminger and Norwegian Atlantic currents [*Johannessen*, 1986] (Figure 1). The Polar Front thus closely follows the eastern Greenland coast. The Arctic Front coincides with the maximum winter sea ice extent and separates the Arctic waters from the Atlantic waters flowing north along the Norwegian coast as the Norwegian Atlantic Current (NAC, Figure 1).

The surface currents described above have obvious consequences on the sea ice formation and distribution. On the northeastern margin of Greenland, sea ice cover in the fjords and on the shelf lasts several months a year, in the form of either landfast ice or drifting polar pack ice [*Andrews et al.*, 2002; *Jennings et al.*, 2002]. In summer and fall,

higher solar radiation allows runoff from the continent and melts the sea ice and icebergs, hence reducing the sea surface salinity [*Andrews et al.*, 2002].

Generally, no sea ice is observed on the Iceland shelf, except in a few bays. Sea ice formation can nevertheless occur on the northern shelf in winter when surface salinity decreases. Severe ice conditions can also develop there in times of high export of sea ice from the Arctic Ocean and east Greenland shelf, when influence of the Actic EIC dominates over that of the IC waters [*Hopkins*, 1991; *Andrews et al.*, 2001b, 2002]. The Great Salinity Anomaly (GSA) in the 1960s is a good example of such a phenomenon. Enhanced northerly winds induced by a strengthened Greenland High increased the strength of the EGC, as well as the export of sea ice from the Arctic Ocean through the Fram Strait, resulting in a higher contribution of the polar water to the EIC. The EIC salinity then decreased to 34.7, allowing stratification and sea ice formation on the north Icelandic shelf [*Belkin*, 1998; *Visbeck et al.*, 2003].

3. Materials and methods

Core JM96-1207/1-GC (68°06'N, 29°21'W; water depth 404 m) was collected in the Nansen trough on the inner east Greenland shelf in 1996 aboard the Norwegian R/V *Jan Mayen* [*Jennings et al.*, 2002]. The site lies in an area influenced by the EGC and is therefore characterized by low temperatures and salinity of $\leq$ 0°C, and $\leq$ 34.5 respectively. Sea ice cover lasts over 6 months a year and icebergs from the Greenland ice sheet and glaciers can be carried to the south by the ECG [*Andrews et al.*, 1997, *Jennings et al.*, 2002].

Core B997-327 (66°38'N, 20°52'W; water depth 373 m) was retrieved on the northern Iceland continental shelf during the summer 1997 cruise of R/V *Bjarni Saemundsson* [*Helgadóttir*, 1997]. MD99-2269 (66°37'N, 20°51'W, water depth 365 m) was raised at the same site during the IMAGES V cruise of R/V *Marion Dufresne* in 1999. The northern Iceland shelf is under the influence of the warm and ice free NIIC (7-12°C, 35). However, the NIIC influence can diminish in favour of polar waters ($\leq$ 0°C) brought by the EIC, in which case severe ice conditions establish [*Andrews et al.*, 2002].

Cores will be referred to in the text as 1207, 327 and 2269.

3.1. Chronologies

The stratigraphic framework for core 1207 has been described by *Jennings et al.* [2002]. It is based on 7 AMS ^{14}C dates, three of which having been measured on a nearby core (JM96-1206, 68°06'N, 29°26' W; water depth 402 m) correlated to the 1207 with the use of their respective volume magnetic susceptibility profiles. A marine reservoir correction of 550 years was applied to all dates, following the work of *Hjort* [1973] on the east Greenland shelf. Two linear equations make up the age model, reflecting the sedimentation rate change at the transition from the Holocene marine mud to the Last Glacial glaciomarine pebbly mud [*Jennings et al.*, 2002] (Figure 2). The sedimentation rate throughout the Holocene is constant at 20 cm kyr^{-1}. The last ~0.34 kyr are missing from the sedimentary record.

Chronology of core 327 is based on 4 AMS ^{14}C dates calibrated after a correction for a standard marine reservoir of 400 years as reported in previous works [*Andrews et al.*, 2001a; *Castañeda et al.*, 2004] (Figure 2). The age model developed here is given by a second-order polynomial equation: age (cal yrs BP) = $0.0412x^2 + 1.8997x + 385.71$ ($R^2 = 0.9996$), where x is the depth expressed in cm. Sedimentation rates range from ~550 $cm.kyr^{-1}$ at the very top of the core to ~37 $cm.kyr^{-1}$ at the base. The 3 m-long record of core 327 spans only the late Holocene (< 4.8 ka) and lacks the last 0.38 kyr.

Despite its proximity to core 327, core 2269 displays on average a higher sedimentation rate. The 11 calibrated AMS ^{14}C dates (400-year reservoir age correction), along with the Saksunarvatn tephra at 10.18 calibrated ka BP, indicate that sediment accumulated at a constant rate of ~200 cm kyr^{-1} during the entire Holocene [*Andrews et al.*, 2003; *Giraudeau et al.*, 2004] (Figure 2). The present study investigated the bottom 14 meters of core 2269, spanning 3.2 to 10.0 ka. A composite 2269/327 record was constructed using the stratigraphic frameworks obtained on both cores to analyze the Holocene time interval.

3.2. Dinocysts

On core 1207, 1 cm-thick sediment slices were subsampled every 2 cm for the interval corresponding to the last 10,000 calibrated years. Core 2269 was subsampled every 5 or 10 cm, and core 327, every ~5 cm on the entire record. Temporal resolution of analyses is thus relatively high, ranging from ~135 years in the lowest sedimentation rate interval in core 327 to ~100 years in core 1207 and ~25-50 years in core 2269. This allows the investigation of millennial- to submillennial scale sea surface circulation changes.

Samples from the entire 1207 and 327 records, as well as samples spanning 10.0 to 3.2 ka from core 2269, were treated following standard techniques described by *de Vernal et al.* [1999] in order to recover dinocysts. On average, 300 dinocysts were counted and identified for each sample, following the taxonomic nomenclature of *Rochon et al.* [1999] and *Head et al.* [2001]. Heterotrophic brown cysts such as *Brigantedinium* spp., *Quinquecuspis* spp. or *Lejeunecysta* spp. are often hard to distinguish one from another when not properly oriented on the slide. Thus, when unidentifiable, these cysts were grouped in the Protoperidinioid category. Concentrations were calculated using the marker grain method [*Matthews*, 1969].

3.3. Sea-surface condition reconstructions

Dinocysts, at least the autotrophic ones, thrive in the photic zone along with coccolithophores and diatoms in order to achieve photosynthesis. It has been shown that the distribution of the different dinocyst assemblages in the Nordic seas is closely related to water masses [*Matthiessen*, 1995], which make them good tracers of past sea surface conditions [*de Vernal et al.*, 1994, 2001].

The best analogue technique of the PPPbase software [cf. *Guiot and Goeury*, 1996] was used for quantitative reconstructions of sea surface conditions based on dinocyst assemblages. It allows the reconstruction of sea surface temperatures (SST) and sea surface salinities (SSS) in February and August, as well as sea ice cover extent, on the basis of the similarity between modern and fossil dinocyst spectra. Logarithm transformation of the relative abundances (per mil) of taxa is made to increase the weight of the secondary taxa,

which often have more specific ecological affinities than ubiquitous dominant taxa, and therefore to better discriminate assemblages in relation to environmental parameters [*de Vernal et al.*, 2001, 2005]. The dinocyst database used here comprises 940 reference sites from the North Atlantic, North Pacific and Arctic oceans and their adjacent seas [*de Vernal et al.*, 2005]. Hydrographical data at 0 m of water depth (SSTs and SSSs, in February and August) for each of these reference sites were compiled from the 2001 World Ocean Atlas [*National Oceanographic Data Center* (*NODC*), 2001], which gathers instrumental measurements from 1900 to 2001. The extent (in months yr^{-1}) of sea ice cover with concentration greater than 50% was determined after the 1953-2003 data set of the *National Snow and Ice Data Center* [2003]. These two databases have the advantage of spanning 100 and 50 years, respectively. Hydrographical parameters assigned to each reference site are therefore averaged over a longer time period, which is more suited for surface sediments that might integrate several decades. The same sources were used to assess modern values of sea surface parameters at the two sites. Sea surface condition reconstructions were then made for the three records.

Details on the approach used for quantitative reconstruction as well as the degree of accuracy of these reconstructions are thoroughly documented by *de Vernal et al.* [2005]. This method was proved particularly effective for reconstructing harsh environments such as those that characterized the northern Atlantic during the last glacial maximum. The accuracy of the method falls within the range of the modern hydrographical parameters variability and is better in more stable, open ocean environments [*de Vernal et al.*, 2005]. It shows a larger spread of estimated versus measured values in shallow and ice marginal areas such as those considered in the present study, which is explained by the high variability of sea surface conditions at annual, decadal or centennial timescales, and by the lack of accuracy of instrumental data in these specific settings [*Mudie and Rochon*, 2001]. In such cases, quantitative reconstructions are somewhat less reliable than in ice-free or open-ocean environments and should be interpreted with caution. A qualitative examination of the paleo-environmental information given by the species assemblages is essential to validate the temporal trends of the quantitative reconstructions.

4. Results

4.1. Dinocyst records

The very different environments in which the cores were collected are reflected in the total dinocyst concentrations. They are lower in the colder Greenland environment of core 1207 (generally a few thousand dinocysts g^{-1}, with rare peaks of the order of 10^4 dinocysts g^{-1}, Figure 3b) than in the composite 2269/327, where much higher concentrations, of the order of 10^5 to 10^6 dinocysts g^{-1}, are reached, peaking between 4.5 and 3.2 ka (Figure 3a). The general pattern of increasing concentrations from Greenland to north Iceland is in agreement with previous studies of dinocyst populations in surface sediment samples [*Matthiessen et al.*, 2001; *Marret et al.*, 2004]. In particular, the high total dinocyst concentrations recorded at site 2269/327 past 4.5 ka are of the order of those presently recorded off northern Iceland in the vicinity of the Arctic Front [*Marret et al.*, 2004], and might depict the setting up of this highly productive frontal boundary which separates the Arctic waters from the Atlantic waters carried by the NIIC around western Iceland.

Despite differences in hydrographical context and associated overall dinoflagellate production, both the east Greenland and the north Iceland shelves support an almost equally diverse (in terms of number of species) dinocyst population throughout the Holocene. However, the species assemblages are significantly different between the two sites, and changes in their composition are more pronounced at the east Greenland margin site.

In core 2269/327, variations in the assemblages are mostly driven by changes in the relative abundances of *Operculodinium centrocarpum*, cysts of *Pentapharsodinium dalei*, and *Nematosphaeropsis labyrinthus*, followed by *Spiniferites ramosus* and *Spiniferites elongatus*, which altogether often account for more than 80% of the total spectra (Figure 3a). The overwhelming dominance in the lower Holocene of cysts of the ubiquitous polar to subpolar taxa *P. dalei*, with sustained occurrences of heterotrophic taxa such as *Brigantedinium* spp. and Protoperidinioids, are indicative of harsher conditions characterized by large seasonal differences in the physicochemical status of the surface waters and extensive sea ice cover as encountered in sheltered coastal waters of polar and Arctic domains [*de Vernal et al.*, 2001]. Heterotrophic taxa can indeed be seen as an indication of

sea ice cover; while the growth of autotrophic taxa is inhibited because a poor penetration of light, heterotrophs, which depend on food availability such as sea ice diatoms, can develop [*Matthiessen*, 1995]. Two transitions are worth noticing. At ~6.2 ka, percentages of *S. elongatus* and *Bitectatodinium tepikiense* increase to the expense of *S. ramosus*. *B. tepikiense* shows affinities for stratified waters with large seasonal temperature amplitudes and reduced sea ice cover [*Rochon et al.*, 1999], and therefore suggests the setting up of a highly dynamical frontal system. At ~4.9 ka, *O. centrocarpum* increases dramatically from ~10% to 50%. This increase is mainly offset by a drop in cysts of *P. dalei* and to a lesser extent in *S. elongatus*. The distribution of the cyst of *P. dalei* is often associated with strong seasonal temperature gradients and the presence of the Polar Front [*Marret et al.*, 2004], whereas both the global [*Rochon et al.*, 1999] and regional [*Boessenkool et al.*, 2001; *Marret et al.*, 2004] biogeographical dinocyst datasets point to the affinities of *O. centrocarpum* for cold-temperate, nutrient-rich surface waters such as the North Atlantic Drift. The replacement of cysts of *P. dalei* with *O. centrocarpum* at ~4.9 ka therefore suggests a decrease in polar waters supplies and the flooding of the north Icelandic shelf with modified Atlantic-sourced waters. This assumption is further strengthened by the gradual increase, from 3 ka onward, of the abundance of *N. labyrinthus*, a taxa which presently outcompetes other dinocysts species in surface sediment off southwestern Iceland bathed by the IC [*Marret et al.*, 2004]. The above-described change in dominance between the cysts of *P. dalei* and *O. centrocarpum*/*N. labyrinthus* is also apparent in the dinocyst record of core 1207 (Figure 3b), hereby suggesting that a change from polar to more Arctic/Atlantic conditions developed off both northern Iceland and eastern Greenland settings throughout the Holocene. However, both the timing and the amplitude of this regime change show some discrepancies on each side of the Denmark Strait.

In core 1207, secondary taxa account for a greater part of the spectra variations. Since these subordinate taxa often thrive in environments with narrower variability in sea surface parameters, the fluctuations of their relative abundances carry more information on environmental changes than those of the dominant ubiquitous taxa. Hence we can infer from the assemblage changes in core 1207 that hydrographical parameters on the east Greenland shelf went through more pronounced fluctuations than on the northern Iceland shelf. The most obvious transition occurs at ~7.2 ka when heterotrophic taxa (*Islandinium minutum*,

Brigantedinium spp., Protoperidinioids and *Selenopemphix quanta*), which make up 10 to 30% of the total assemblages in the early Holocene, disappear in favour of autotrophic taxa *S. elongatus* and *O. centrocarpum*. *I. minutum* occupies a restricted ecological niche in the North Atlantic with maximum abundance in surface sediments off central and northeastern Greenland and in the Greenland Sea, which are characterized by permanent to quasi-permanent sea ice cover [e.g., *de Vernal et al.*, 2001; *Head et al.*, 2001]. This drastic change in trophic characteristics of the assemblages suggest that the surface water regime went through a major reorganization at about 7.2 ka, from polar conditions with extensive sea ice cover to more open ocean-like conditions. A second reorganization is seen around 4.9 ka, when oceanic taxa *N. labyrinthus*, with maximum abundance in Atlantic/Irminger-influenced areas off Iceland [*Marret et al.*, 2004], and *I. pallidum*, which is highly successful in cold, fully marine environments [*de Vernal*, 2001; *Matthiesen et al.*, 2005], appear. These transitions from neritic to more open-ocean assemblages bears to a certain extent some resemblance with the proximal and distal assemblages observed along the southeastern Greenland coast by *Boessenkool et al.* [2001]. The proximal assemblage is found on the inner shelf, where the influence of polar waters is the strongest, and comprises a significant proportion of heterotrophic taxa such as *I. minutum*. The distal assemblage, dominated by both *O. centrocarpum* and *N. labyrinthus*, characterizes the continental slope, where the influence of Atlantic waters is more pronounced. After ~4.9 ka, as recorded in core 2269/327, most of the variations in percentages of taxa concern the dominant species *O. centrocarpum*, cysts of *P. dalei* and *N. labyrinthus*, with a notable increase of the latter after 1.8 ka.

4.2. Sea surface reconstructions

In spite of discrepancies in timing and amplitude of inferred hydrological regime changes, both the northern Iceland and eastern Greenland dinocyst records suggest that a shift from polar/Arctic to more Arctic/Atlantic conditions developed in the area of the Denmark Strait from the early to the late Holocene. The reconstructed sea surface parameters (Figure 4) are coherent with this inferred long-term pattern. They also emphasize the major differences in environmental settings between the two sites. February SSTs are constantly

lower on the Greenland shelf than north of Iceland, with a difference of up to 3°C. In contrast, the gap between the 1207 and 2269/327 August SSTs records is much smaller; summer SSTs off Greenland can even be warmer than in the Iceland Sea, especially in the early Holocene. As a result, the temperature contrast (summer minus winter SSTs), hereafter referred to as seasonality, is generally higher, throughout the Holocene, off eastern Greenland, with the exception of a few short episodes. Apart from the very beginning of the Holocene, sea ice conditions are more severe on the Greenland shelf, lasting up to 6 months yr^{-1}, compared to the north Iceland shelf where there is no more than 1.5 months yr^{-1} of sea ice cover.

On the northern Iceland shelf, reconstructions for the top of the core yield values close to the present (Figure 4a); reconstructed summer SSTs are slightly higher than today's values, part of this discrepancy being attributable to the fact that core 2269/327 lacks the last 0.38 ka, but they nevertheless fall within the range of modern variability (summer SSTs: 6.5°C±2.2, *NODC* [2001]). A comparison of our dinocyst-based reconstructions with diatom-based estimates for the last 5 calibrated kyr B.P. from a nearby coring site [HM107-03, same water depth, ca. 100 nm eastward, *Jiang et al.*, 2002] is shown in Figure 5. These summer SST reconstructions are based on a regional surface sediment diatom database that is highly representative of the range of environmental variables around Iceland [*Jiang et al.*, 2001]. With the exception of the last 1000 years, and despite an offset of ~1°C, both the trends and the range of variation of summer SSTs are strongly coherent between the two methods, supporting our dinocyst-based estimates from the northern Iceland shelf.

In contrast, the gap between reconstructed hydrographical parameters and modern values seems to be much more important on the east Greenland shelf, with a difference of up to 5°C in summer SSTs, 4 in summer SSSs and 6 months in sea ice cover (Figure 4b). Both the quality of the instrumental dataset and the peculiar hydrological context off eastern Greenland may, at least in part, explain these discrepancies: instrumental measurements in the region are very rare as shown by the absence of measured values for modern February SSSs in the *NODC* records [2001]. In addition, the location of site 1207 in the vicinity of the Polar Front, a hydrological boundary characterized by highly variable sea surface conditions on annual to centennial time scales [e.g. *Isemer and Hasse*, 1985], makes modern values on the basis of sparse measurements less reliable in this specific setting. Another possible

source of divergence could be related to dinocyst production being lower during episodes of harsh conditions [*Matthiessen et al.*, 2001]; fossil assemblages would thus preferentially represent the most favorable years. Finally, a close examination of the dinocyst database reveals a lack of reference modern assemblages in the Denmark strait region. The closest analogues are therefore selected on the northern Iceland shelf and in the Norwegian Sea, which probably creates a bias towards warmer conditions. Still, we consider that the relative variations in the reconstructed parameters are valid, as they are supported by qualitative examination of the assemblages. Absolute values of reconstructions should therefore be taken with care and interpretations of the results should rather be based on these relative variations of sea surface conditions and on assemblage changes.

Despite Greenland shelf being a colder environment than the Iceland shelf, long-term tendencies at both sites share some common features. Winter SSTs depict an increase from the mid-Holocene onward and sea ice seems to have been more extensive during the early Holocene. SSS shifts from low to more oceanic values in the mid-Holocene are also observed on both shelves. The long-term trends in seasonality show some similarities at both sites as well, as they are characterized by overall decreasing values throughout the Holocene (Figure 4). On a shorter timescale, however, there are discrepancies with respect to the timing and amplitude of sea surface condition oscillations.

In both cores, very different environments from today characterize the early Holocene, as shown by the dinocyst assemblages and by the SSS and SST reconstructions. On the northern Iceland shelf, these reconstructions depict a distinct regime, with lower SSSs (~33.5), higher seasonality and a longer sea ice extent prior to 6.2 ka. Some marked high-amplitude oscillations are observed during this period, but no longer-term trend stands out (Figure 4a). Off east Greenland (Figure 3b), the early Holocene assemblage characterized by dominant heterotrophic and sea ice adapted taxa corresponds to very low SSSs (~30 and ~32 in summer and in winter, respectively), associated with generally higher summer SSTs (~9°C) than in the rest of the record. Throughout this interval ending at about 7.2 ka, summer SSTs strongly decrease, accordingly with an increase in the sea ice extent. Rapid, high-amplitude fluctuations attest overall instable sea surface conditions (Figure 4b).

In the mid-Holocene, major changes are recorded. After ~6.2 ka in core 2269/327, the regime change is expressed as a clear shift in most of the reconstructed parameters,

towards higher values for SSTs and SSSs, and lower values for sea ice extent and seasonality. SSSs reach modern values and are much more stable than in the early Holocene. The variations in assemblages (Figure 3a) suggest recurrent millennial-scale, high-amplitude changes of modern-like conditions, mostly visible in the summer SSTs and seasonality records (Figure 4a).

In core 1207, the sea surface conditions record a two-step change. By about 7.2 ka a first transition is recorded when lower summer SSTs are reached and SSSs shift to much higher values (~32 and ~33.5 in summer and winter, respectively). This regime ends at ~4.9 ka, corresponding with the second major change in assemblages. After ~4.9 ka, SSSs increase significantly and remain stable. Short-term variations are more weakly expressed in this record than in the one north of Iceland, and changes in the dinocyst assemblages mainly reflect the sea ice extent record (Figure 4b).

5. Discussion

5.1 Long-term trends of Holocene climate in the northwest Atlantic

Sea surface reconstructions on the eastern Greenland and northern Iceland shelves depict coherent long-term Holocene trends. From the early to the late Holocene, February SSTs increase slightly, while August SSTs are more stable, except for a warm interval lasting from 10 to 8 ka in core 1207. As a result, seasonality decreases throughout the Holocene (Figure 4). SSS reconstructions, in winter as well as in summer, yield generally lower values in the early to mid-Holocene, a period that is also characterized by a more extensive sea ice cover. This situation is consistent with more pronounced low-salinity water supplies from the Arctic, which favour a stronger stratification through the formation of a buoyant and relatively fresh surface water layer. This strong stratification, by preventing the diffusion of heat from the atmosphere through the water column, results in a reduced thermal inertia in a surface layer that may have been relatively shallow. The surface water response to air temperatures is thus faster; summer warming up and winter cooling are more pronounced and seasonal contrast increases. This mechanism was probably reinforced in the early Holocene by a higher summer insolation and a weaker winter insolation [*Berger and*

Loutre, 1991], as well as by additional freshwater supplies at the Greenland site due to the waning of the Greenland Ice Sheet, which lasted until ~8 ka [*Funder*, 1989]. Such a scenario is likely to explain the diatom-based summer SST reconstructions given by *Andersen et al.* [2004], which point to 2 to 4°C warmer early-Holocene SSTs off eastern Greenland and northern Iceland compared to the mid-late Holocene period. In the mid- to late Holocene, higher SSSs and shorter sea ice extent reflect an overall diminishing influence of polar waters and enhanced advection of Atlantic-source waters to the Denmark Strait region (Figure 4). The resulting weaker stratification leads to enhanced mixing and better diffusion of heat in the water column; seasonal changes of temperature are thus damped, which might explain the increasing winter SSTs and decreasing seasonality.

This long-term trend of sea surface conditions is only partly consistent with previous studies in the same region, some of which yield a cooling summer trend in the late Holocene [e.g. *Andersen et al.*, 2004]. However, as said earlier, comparison with *Jiang et al.*'s [2002] diatom-based reconstructions shows a good overall coherency with our data. In addition, some indications of a long term warming for the last 10 000 yrs, at least in winter or on an annual basis, can be inferred from the slightly diminishing relative abundance of cold planktonic foraminifera *Neogloboquadrina pachyderma* sinistral in a core from the Denmark Strait [VM28-14, *Bond et al.*, 1997], and to some extent from increased bulk carbonate accumulation in the mid-Holocene to late Holocene off northern Iceland [e.g. *Andrews and Giraudeau*, 2003], a measure of productivity induced by nutrient-rich Atlantic waters. Warmer winter SSTs in the late Holocene are suggested by Moros et al. [2004b] as well.

The inferred weakening of polar water supplies on the eastern Greenland shelf and off northern Iceland seems at odd with the ice-rafted detritus (IRD) records in core 1207 [*Jennings et al.*, 2002] and on the east Greenland margin in general [*Andrews et al.*, 1997], as well as the quartz percentages record in core 2269 [*Moros et al.*, submitted], which are commonly interpreted as evidences for a late Holocene cooling trend and strengthened EGC and EIC circulation in the Denmark Strait region. A possible explanation for such a discrepancy could be related to Greenland outlet glacier ablation mechanisms. *Reeh et al.* [1999] and *Reeh* [2004] showed that glacier ablation is controlled by two different mechanisms, depending on the presence or absence of fast ice, which is in turn related to winter cold and summer warmth. A temperature increase of only a few degrees would be

enough to switch from a floating glacier regime to an iceberg-calving glacier regime. While the former is associated with little IRD deposition on the shelf, the latter has a higher potential for transporting IRD out of the fjords [*Reeh et al.*, 1999; *Reeh*, 2004].

A second explanation, sustained by our sea ice and temperature reconstructions might lay in the influence of sea ice upon the drifting of lithic grains-bearing icebergs calved from the Greenland ice sheet. As proposed by *Funder et al.* [1998] from observations in the Arctic areas and along East Greenland, and discussed by *Moros et al.* [2004a], IRD production is maximum in periods when there is both seasonally open water (low sea ice extent) and glacier fronts in an advanced position. The middle to late steady increase in IRD recorded in cores 1207 [*Jennings et al.*, 2002] and 2269 [*Moros et al.*, 2006] might therefore be viewed as primarily related to (1) lower sea ice concentrations in the Denmark Strait region due to enhanced influence of Atlantic waters and increased winter SSTs as indicated by our reconstructions, (2) the Neoglacial readvance of the Greenland Ice Sheet [*Fulton*, 1989; *Cuffey and Clow*, 1997] and nearby mountain glaciers in North Iceland [*Stötter et al.*, 1999]. Comparison of IRD/quartz records with the relative abundance of the dinocyst species *N. labyrinthus* shows a close correspondence between the two proxies (Figure 6). Nowadays, highest occurrences of *N. labyrinthus* are found off western Iceland, in the path of the IC, as well as in the Labrador Sea under the Atlantic-influenced WGC, whereas it is absent from regions with quasi-permanent sea ice cover such as the northeastern Greenland shelf [*Rochon et al.*, 1999]. The coherency between the *N. labyrinthus* and IRD/quartz records illustrates the key influence of Atlantic water inflow upon the delivery of ice-rafted lithic material to the Denmark Strait region. Hence we propose that the increased IRD content in late Holocene sediments off eastern Greenland and northern Iceland is an indication of a fundamental shift in delivery of IRD to the Denmark Strait region. This shift was triggered by the coupled dynamics of continental ice sheet, and surface circulation changes linked to warmer winter SSTs and associated decreasing sea ice extent.

5.2. Spatial heterogeneity in surface water conditions across the NW Atlantic

The long-term coherent pattern of sea surface condition changes recorded off eastern Greenland and northern Iceland must be viewed as the response of the Iceland and

Greenland seas to the progressively reduced influence of polar waters relative to the Atlantic waters in the western Nordic seas. This regional coherency is further amplified by the EIC, which effectively connects both shelf settings. However, much damper long-term trends on the North Iceland shelf as well as several short-term discrepancies between the two records point out the role of distinct local surface circulation features that may respond differently or in a delayed manner to a combination of climate forcings.

Discrepancies are particularly pronounced on a shorter millennial to centennial timescale. Moreover, the discrepancies also concern the timing of the main changes: most records from the northern Iceland shelf present a clear shift around 6.2 ka, whereas a strong regime change associated with a drop in summer SSTs and a dramatic increase in SSSs occurs at ~7.4 ka off Greenland. A second major change in core 1207 takes place at ~4.9 ka, this time apparent only in the SSS (increase) and sea ice extent (decrease) records (Figure 4b). A possible explanation for these discrepancies between the two sites could be linked to the proximity of site 1207 to the Greenland ice sheet. We can hypothesize that site 1207, which lies close to the east Greenland coast on the inner shelf, was more directly affected by meltwater coming from the Greenland ice sheet in the early and mid-Holocene. In contrast, the northern Iceland site does not seem to have been as much influenced by meltwater supplies, as SSSs as low as those measured off eastern Greenland do not appear in our record.

The spatial and temporal heterogeneity in the northwestern Atlantic is further illustrated when comparing hydrological changes in our records with those from site P-013, located south of Greenland (Figure1; see also *de Vernal and Hillaire-Marcel* [2000] and *Solignac et al.* [2004] for further details). Site P-013, in the northeastern Labrador Sea, is under the influence of the West Greenland Current (WGC), which carries a mix of cold polar water from the ECG and warm salty water from the western branch of the IC (Figure 1).

Records from east and south Greenland depict anti-correlated long-term trends that are especially clear in the winter SSTs and sea ice extent signals of the mid-Holocene and late Holocene (Figure 7). These discrepancies between the records imply that waters from the Arctic that reached the eastern Greenland were not carried all the way to the southern Greenland site. The observed long-term corresponding trends from the eastern Greenland

and northern Iceland shelves additionally suggest that an important part of this meridional flow of polar waters was deflected towards the east via the EIC.

The IC component of the WGC probably played an important role as well in determining sea surface conditions south of Greenland. The thermal optimum from ~8.0 to 5.5 ka in core P-013 could be related to an enhanced western branch of the IC carrying more intensively warm waters to the south of Greenland. After 5.5 ka, the influence of the IC in the north-eastern Labrador Sea apparently decreased, resulting in colder SSTs and more extensive sea ice cover.

Despite the theoretical surface circulation connection between southern Greenland and northern Iceland via both branches of the IC (Figure 1), we see an overall anticorrelation of the reconstructed winter sea surface temperature and sea ice extent records between both core sites (P-013 and 2269/327) (Figures 4a and 7). Part of this inconsistency may lay in the fact that the 2269/327 record, being influenced by both the EIC and the NIIC, delivers a mixed signal, in which the variations of the two currents occult one another. Another explanation, sustained by the record of dinocyst assemblages from 2269/327, could be a balance between the two branches of this surface current throughout the Holocene, the western branch feeding the southern Greenland and Labrador Sea areas being strengthened (reduced) during period of reduced (strengthened) flow of Irminger water around Iceland.

Coherence is clearly shown between the record of core P-013 and a continental record from Lake N14 in southern Greenland (Figure 1; Figure 8). In the latter record, *Andresen et al.* [2004] interpreted the relative contribution of biogenic silica as a proxy for atmospheric conditions over South Greenland, low values corresponding to low primary production in a cold and arid environment, whereas high values are associated to higher annual production related to warm and humid conditions. The biogenic silica record follows reconstructed SSTs of site P-013, although only after ~8.2 ka for the summer SSTs due to the strong influence of meltwaters until then [*Funder*, 1989] that form a floating freshwater surface layer. The coherence between the south Greenland lake and core P-013 data after 8.2 ka points to the determinant influence of the western branch of the IC in the southern Greenland area and Labrador Sea. Some correlations can be proposed as well with the August SSTs from core 2269/327, with the maximum reconstructed values at ~4.7 ka in core 2269/327 being recorded in biogenic silica as well (Figure 8). This coherence between the

southern Greenland and north Iceland records suggests that this short interval was a time of equilibrium in the influence of the IC between its western and northern branches, at least in summer. The second 2269/327 SST maximum at ~2.7 ka could correlate with the warm event seen in both the February SSTs from core P-013 and the southern Greenland lake at ~2.4 ka, although not enough evidence is available at this stage to assert it. Uncertainties about the reservoir age on the northern Iceland shelf [*Eiriksson et al.*, 2000a; *Haflidason et al.*, 2000] as well as a somewhat poorly constrained age model for core 327, emphasize the need for a more refined chronostratigraphy to further assess the coherence between the northern Iceland shelf and southern Greenland.

5.3. Atmospheric forcing in the NW Atlantic

Temperatures and precipitations in southern Greenland are presently related to the location of the low-pressure system along its track, which crosses this area from south of Greenland to the northeast. When the position of the Icelandic Low is closer to southern Greenland, easterly winds bring warm temperatures and increased precipitation. Inversely, a northeastern position near Iceland implies northwesterly winds that bring cold and arid weather over southern Greenland [*Andresen et al.*, 2004].

The connection between the continental record from South Greenland and the P-013 record in the path of the western branch of the IC suggests a coupling between the atmospheric processes described above and the dynamics of the IC. We hypothesize that a southwesterly position of the Icelandic Low that seems to prevail in the early to mid-Holocene (~9 to 5.5 ka) and associated easterly/southeasterly winds are responsible for a strengthening of the influence of Atlantic waters to the south of Greenland through the IC, thus increasing SSTs and SSSs and decreasing sea ice extent in core P-013. After 5.5 ka, overall lower biogenic silica percentages in the South Greenland Lake N14 indicate generally colder and more arid climate in southern continental Greenland [*Andresen et al.*, 2004] (Figure 8). The position of the Icelandic Low must thus have shifted to the northeast throughout the Holocene. We surmise that such a shift favoured the rerouting of Atlantic waters toward western Iceland and eastern Greenland to the prejudice of the southern Greenland region. Accordingly, at 5.5 ka, SSTs in core P-013 south of Greenland decrease,

suggesting a weakening of the influence of the western branch of the IC. On the eastern Greenland and north Iceland shelves, SSSs increase and stabilize, and winter SSTs increase steadily, indicating reduced water advection from the Arctic and enhanced flow of Atlantic waters through the northern branch of the IC. This scenario is mostly sustained by winter SST reconstructions and sea ice extent.

The shift of the Iceland Low throughout the Holocene bears some resemblance with the dominant mode of present winter climate variability in the North Atlantic region, that is, the North Atlantic Oscillation (NAO) [*Hurrell*, 1995]. The antiphase relationship documented in the present work between winter conditions in the southern Greenland region and the Denmark Strait area might be viewed as related to long-term changes in the phase of the NAO, with a progressive shift from a negative phase in the Early Holocene to a positive phase from the mid-Holocene onward. Lower (higher) sea ice concentration and higher (lower) SSTs south of Greenland, combined with higher (lower) sea ice extent and fresher (saltier) and colder (warmer) sea surface conditions in the Greenland Sea region are indeed a signature of a negative (positive) NAO phase [*Chapman and Walsh*, 1993; *Visbeck et al.*, 2003]. Our observations are coherent with the work of *Tremblay et al.* [1997] on driftwood records in the Arctic Ocean, in which a strong EGC associated with a negative phase of the NAO and a southerly position of the Icelandic Low characterize the early Holocene, followed by a weak EGC linked to a positive phase of the NAO in the mid-Holocene to late Holocene. However, such a long-term change in the phase of the NAO does not win unanimous support among the different studies; other reconstructions, based for example on alkenone data [*Rimbu et al.*, 2003] or diatom assemblages [*Andersen et al.*, 2004] suggest an opposite evolution of this atmospheric circulation pattern. It must be kept in mind as well that local atmospheric forcings other than the NAO might play a determinant role in climate and sea surface variability in the western North Atlantic. Notably, instrumental records do not seem to show any connection between the NAO index and the Atlantic inflow off western and northern Iceland [*Ólafsson*, 1999]. We therefore surmise that any assumption of NAO-forced evolution of the sea surface conditions throughout the Holocene in the Nordic seas should take into account additional local processes.

6. Conclusion

Comparison of Holocene sea surface conditions at three different environments of the North Atlantic, each under the influence of a different combination of currents but nevertheless in interaction with each other, depicts a strong spatial heterogeneity.

Site 1207 on the east Greenland shelf, characterized by polar waters carried by the EGC, shows warming winter SSTs and diminishing sea ice extent trends throughout the Holocene. The same is observed at site 2269/327 on the north Iceland shelf, which lies in the path of the warm NIIC and the Arctic EIC, while site P-013 south of Greenland, influenced by the EGC and the IC, depicts opposite trends. This suggests that increased polar water supplies on the east Greenland shelf during the early to mid-Holocene were mostly deflected towards the northern Iceland shelf and did not efficiently reach the south of Greenland where conditions are indicative of a sustained Atlantic water influence. A decoupled dynamics of the western branch of the IC and of the NIIC could be the cause of such a discrepancy.

Our surface water reconstructions are at first glance at odd with the commonly assumed late Holocene cooling of the Denmark Strait region as previously suggested by IRD records. On the basis of the dinocyst-based reconstruction of sea ice extent off eastern Greenland and northern Iceland, as well as of the close relationship between the abundances of an Atlantic dinocyst species, *Nematosphaeropsis labyrinthus*, and IRD contents in the studied cores, we believe that IRD delivery in the Denmark Strait region during the Holocene is favoured by a combination of sustained iceberg calving from the Greenland ice sheet, as well as reduced sea ice cover to allow the transfer of lithic materials from its source to distant areas such as the north Iceland shelf. Consequently, the late Holocene increase in IRD sedimentation across this region might be viewed as triggered by an increased Atlantic water inflow (and associated lower sea ice extent), and the Neoglacial readvance of the Greenland ice sheet after its early Holocene decay.

The coherence between core P-013 on the southern Greenland rise and a continental record in southern Greenland puts forward a close coupling between the atmosphere and the ocean, with a general pattern of the Icelandic Low shifting northeastward throughout the Holocene. Combined with a weakening EGC throughout the Holocene, this atmospheric

evolution is reminiscent of a long-term evolution of the NAO (from a negative phase in the early Holocene to a positive phase onward). Any firm assumption of a NAO-forced Holocene history of the hydrography of the NW Atlantic, however, needs additional work, and must consider the evolution of additional local atmospheric forcing such as those presently acting in the Denmark Strait and nearby regions.

Acknowledgements

We are indebted to Anne Jennings and John T. Andrews, INSTAAR, Boulder, CO, for access to the samples, as well as to C. Andresen (GeoBiosphere Science Centre, Lund, Sweden), A. Jennings, H. Jiang (East China Normal University, Shanghai) and M. Moros (Bjerknes Centre for Climate Research, Bergen, Norway) for sharing their data. Fruitful discussions with M. Moros and J.-L. Turon (DGO-UMR EPOC, Bordeaux, France), as well as comments from an anonymous reviewer and J. Matthiessen (Alfred Wegener Institute, Bremerhaven, Germany) helped improve this paper. Core MD99-2269 was collected as part of IMAGES V, Leg 3 cruise of the RV *Marion Dufresne*, under the leadership of J.-L. Turon (chief scientist) and Y. Balut (IPEV, chief of operations), and support from IPEV and CNRS/INSU. This study is a contribution to project GR-240 of the Canadian Foundation for Climate and Atmospheric Sciences, and to the project TARDHOL of the French Programme National d'Études de la Dynamique du Climat of CNRS-INSU. Support was also provided by the Natural Sciences and Engineering Research Council of Canada. Special thanks are due to David Fortin for helpful comments on this manuscript.

References

Alley, R. B., A. M. Agustsdottir, and P. J. Fawcett, Ice-core evidence of late-Holocene reduction in North Atlantic Ocean heat transport, *Geophysical Monograph, 112*, 301-312, 1999.

Andersen, C., N. Koç, A. Jennings, and J.T. Andrews, Nonuniform response of the major surface currents in the Nordic Seas to insolation forcing: Implications for the Holocene climate variability, *Paleoceanography, 19*, PA2003, doi:10.1029/2002PA000873, 2004.

Andresen, C. S., S. Björck, O. Bennike, and G. Bond, Holocene climate changes in southern Greenland: evidence from lake sediments, *Journal of Quaternary Science, 19*, 783-795, 2004.

Andresen, C. S., G. Bond, A. Kuijpers, P. C. Knutz, and S. Björck, Holocene climate variability at multidecadal time scales detected by sedimentological indicators in a shelf core NW off Iceland, *Marine Geology, 214*, 323-338, 2005.

Andrews, J. T., and J. Giraudeau, Multi-proxy records showing significant Holocene environmental variability: the inner N. Iceland shelf (Hunafloi), *Quaternary Science Reviews, 22*, 175-193, 2003.

Andrews, J. T., J. Hardardóttir, G. B. Kristjansdóttir, K. Grönvold, and J. S. Stoner, A high-resolution Holocene sediment record from Hunuaflóaáll, N Iceland margin: century- to millennial-scale variability since the Vedde tephra, *The Holocene, 13*, 625-638, 2003.

Andrews, J. T., G. Helgadóttir, A. Geirsdóttir, and A. E. Jennings, Multicentury-scale records of carbonate (hydrographic?) variability on the N Iceland margin over the last 5000 yrs, *Quaternary Research, 56*, 199-206, 2001a.

Andrews, J. T., R. Kihl, G. B. Kristjánsdóttir, L. M. Smith, G. Helgadóttir, A. Geirsdóttir and A. E. Jennings, Holocene sediment properties of the East Greenland and Iceland continental shelves bordering Denmark Strait (64-68°N), North Atlantic, *Sedimentology*, 49, 5-24, 2002.

Andrews, J. T., G. B. Kristjánsdóttir, A. Geirsdóttir, J. Hardardóttir, G. Helgadóttir, A. E. Sveinbjörnsdóttir, A. E. Jennings and L. M. Smith, Late Holocene (~ 5 cal ka) trends and century-scale variability of N. Iceland marine records: measures of surface hydrography, productivity, and land/ocean interactions, in The Oceans and Rapide Climate Change: Past, Present, and Future, Geographical Monograph Series, vol. 126, pp. 69-81, AGU, Washington, D.C., 2001b.

Andrews, J. T., L. M. Smith, R. Preston, T. Cooper and A. Jennings, Spatial and temporal patterns of iceberg rafting (IRD) along the East Greenland margin, ca. 68°N, over the last 14 cal. ka, *Journal of Quaternary Science, 12*, 1-13, 1997.

Belkin, I. M., S. Levitus, J. Antonov and S.-A. Malmberg, "Great salinity anomalies" in the North Atlantic, *Progress in Oceanography, 41*, 1-68, 1998.

Berger, A. L. and M. F. Loutre, Insolation values for the climate of the last 10 million years, *Quaternary Science Reviews, 10*, 297-317, 1991.

Bianchi, G. G. and I. N. McCave, Holocene periodicity in North Atlantic climate and deep-ocean flow south of Iceland, *Nature, 397*, 515-517, 1999.

Blindheim, J., V. Borovkov, B. Hansen, S.-Aa. Malmberg, W. R. Turrell, and S. Østerhus, Upper layer cooling and freshening in the Norwegian Sea in relation to atmospheric forcing, *Deep-Sea Research I, 47*, 655-680, 2000.

Boessenkool, K. P., M.-J. van Gelder, H. Brinkhuis and S. R. Troelstra, Distribution of organic-walled dinoflagellate cysts in surface sediments from transects across the Polar Front offshore southeast Greenland, *Journal of Quaternary Science, 16*, 661-666, 2001.

Bond, G., W. Showers, M. Cheseby, R. Lotti, P. Almasi, P. de Menocal, P. Priore, H. Cullen, I. Hajdas and G. Bonani, A pervasive millemial-scale cycle in North Atlantic Holocene and glacial climates, *Science, 278*, 1257-1266, 1997.

Campbell, I. D., C. Campbell, M. J. Apps, N. W. Rutter and A. B. G. Bush, Late Holocene ~1500 yr climatic periodicities and their implications, *Geology, 26*, 471-473, 1998.

Castañeda, I., M. Smith, G. B. Kristjánsdóttir and J. T. Andrews, Temporal changes in Holocene $\delta^{18}O$ records from the northwest and central North Iceland Shelf, *Journal of Quaternary Science 19*, 321-334, 2004.

Chapman, W. L., and J. E. Walsh, Recent variations of sea ice and air temperature in high latitudes, *Bulletin of the American Meteorological Society, 74*, 33-47, 1993.

Cuffey, K.M., and G.D. Clow, Temperature, accumulation, and ice sheet elevation in central Greenland through the last glacial transition, *Journal of Geophysical Research, 102*, 26383-26369, 1997.

de Vernal, A., M. Henry, J. Matthiessen, P. J. Mudie, A. Rochon, K. Boessenkool, F. Eynaud, K. Grøsfjeld, J. Guiot, D. Hamel, R. Harland, M. J. Head, M. Kunz-Pirrung, E. Levac, V. Loucheur, O. Peyron, V. Pospelova, T. Radi, J.-L. Turon, and E. Voronina, Dinoflagellate cyst assemblages as tracers of sea-surface conditions in the northern North Atlantic, Arctic and sub-Arctic seas: the new "n = 677" database and application for quantitative paleoceanographical reconstruction, *Journal of Quaternary Science*, 16, 681-699, 2001.

de Vernal, A., F. Eynaud, M. Henry, C. Hillaire-Marcel, L. Londeix, S. Mangin, J. Matthiessen, F. Marret, T. Radi, A. Rochon, S. Solignac, and J.-L. Turon, Reconstruction of sea-surface conditions at middle to high latitudes of the Northern Hemisphere during the

Last Glacial Maximum (LGM) based on dinoflagellate cyst assemblages, *Quaternary Science Reviews*, *24*, 897-924, 2005.

de Vernal, A., M. Henry, and G. Bilodeau, Technique de préparation et d'analyse en micropaléontologie, *Les Cahiers du GEOTOP 3*, Université du Québec à Montréal, unpublished report, 1999.

de Vernal, A., and C. Hillaire-Marcel, Sea-ice cover, sea-surface salinity and halo-/thermocline structure of the northwest North Atlantic: modern versus full glacial conditions, *Quaternary Science Reviews*, *19*, 65-85, 2000.

de Vernal, A., J.-L. Turon, and J. Guiot, Dinoflagellate cyst distribution in high-latitude marine environments and quantitative reconstruction of sea-surface salinity, temperature and seasonality, *Canadian Journal of Earth Sciences*, *31*, 48-62, 1994.

Dickson, R., J. Lazier, J. Meicke, P. Rhines, and J. Swift, Long-term coordinated changes in the convective activity of the North Atlantic, *Progress in Oceanography*, *38*, 241-295, 1996.

Dickson, R. R., J. Meincke, S. Malmberg, and A. Lee, The 'Great Salinity Anomaly' in the northern North Atlantic 1968–1982, *Progress in Oceanography*, *20*, 103-151, 1988.

Eiriksson, J., K. L. Knudsen, H. Haflidason, and J. Heinemeier, Chronology of late Holocene climatic events in the northern North Atlantic based on AMS ^{14}C dates and tephra markers from the volcano Hekla, Iceland, *Journal of Quaternary Science*, *15*, 573-580, 2000a.

Eiriksson, J., K. L. Knudsen, H. Haflidason, and P. Henriksen, Late-glacial and Holocene paleoceanography of the North Icelandic shelf, *Journal of Quaternary Science*, *15*, 23-42, 2000b.

Fulton, R. J. (Ed.), *Quaternary Geology of Canada and Greenland*, Geology of Canada N° 1 ed., 1-11 pp, 1989.

Funder, S., Quaternary geology of ice-free areas and adjacent shelves of Greenland, in *Quaternary Geology of Canada and Greenland, Geology of Canada 1*, edited by R. J. Fulton, pp. 743-792, Geological Survey of Canada, Ottawa, 1989.

Funder, S., C. Hjort, J. Y. Landvik, S.-I. Nam, N. Reeh, and R. Stein, History of a stable ice margin – East Greenland during the middle and upper Pleistocene, *Quaternary Science Reviews, 17*, 77-123, 1998.

Giraudeau, J., A. E. Jennings, and J. T. Andrews, Timing and mechanisms of surface and intermediate water circulation changes in the Nordic Seas over the last 10,000 cal years: a view from the North Iceland shelf, *Quaternary Science Reviews*, *23*, 2127-2139, 2004.

Guiot, J., Methodology of the last climatic cycle reconstruction in France from pollen data, *Palaeogeography, Palaeoclimatology, Palaeoecology*, *80*, 49–69, 1990.

Guiot, J., and C. Goeury, PPPbase, a software for statistical analysis of paleoecological data. *Dendrochronologia, 14*, 295–300, 1996.

Haflidason, H., J. Eiriksson, and S. van Kreveld, The tephrochronology of Iceland and the North Atlantic region during the middle and late Quaternary: a review, *Journal of Quaternary Science, 15*, 3-22, 2000.

Head, M. J., R. Harland, and J. Matthiessen, Cold marine indicators of the late Quaternary: the new dinoflagellate cyst genus *Islandinium* and related morphotypes, *Journal of Quaternary Science, 16*, 621–636, 2001.

Helgadóttir, G., Paleoclimate (0 to >14 ka) of W and NW Iceland: an Iceland/USA contribution to P.A.L.E, *Cruise report B9-97*, Marine Research Institute of Iceland, Reykjavik, 1997.

Hjort, C., A sea correction for East Greenland, *Geologiska Föreningen Stockholm Förhandlingar, 95*, 132-134, 1973.

Hopkins, T. S., The GIN Sea- A synthesis of its physical oceanography and literature review 1972-1985, *Earth Science Reviews, 30*, 175-318, 1991.

Hurrell, J. W., Decadal trends in the North Atlantic Oscillation: Regional temperatures and precipitation, *Science, 269*, 376-379, 1995.

Isemer, H.-J., and L. Hasse (Eds.), *The Bunker Climate Atlas of the North Atlantic Ocean, vol. 1: Observations*, pp.57-60, Springer, Berlin, 1985.

Jennings, A. E., K. L. Knudsen, M. Hald, C. V. Hansen, and J. T. Andrews, A mid-Holocene shift in Arctic sea-ice variability on the East Greenland shelf, *The Holocene, 12*, 49-58, 2002.

Jiang, H., M. S. Seidenkrantz, K. L. Knudsen, J. Eiriksson, Diatom surface sediment assemblages around Iceland and their relationships to oceanic environmental variables, *Marine Micropaleontology, 41*, 73-96, 2001.

Jiang, H., M. S. Seidenkrantz, K. L. Knudsen, J. Eiriksson, Late-Holocene summer sea-surface temperatures based on a diatom record from the north Icelandic shelf, *The Holocene, 12*, 137-147, 2002.

Johannessen, O. M., Brief overview of the physical oceanography, in *The Nordic Seas*, edited by B. G. Hurdle, pp. 103-127, Springer, New York, 1986.

Knudsen, K. L, J. Eiriksson, E. Jansen, H. Jiang, F. Rytter, and E. R. Gudmundsdottir, Paleoceanographic changes off North Iceland through the last 1200 years: foraminifera,

stable isotopes, diatoms, and ice rafted debris, *Quaternary Science Reviews, 23*, 2231-2246, 2004.

Malmberg, S.-A., The water masses between Iceland and Greenland, *Journal of Marine Research Institute, 9,* 127-140, 1985.

Malmberg, S.-A., The ecological impact of the East Greenland Current on the North Icelandic water, *NATO ASI series*, vol. G7, 389-404, 1999.

Malmberg, S.-A., and S. Jónsson, Timing of deep convection in the Greenland and Iceland Seas, *ICES Journal of Marine Science*, *54*, 300-309, 1997.

Marchal, O., I. Cacho, T. F. Stocker, J. O. Grimalt, E. Calvo, B. Martrat, N. Shackelton, M. Vautravers, E. Cortijo, S. Van Kreveld, C. Andersson, N. Koç, M. Chapman, L. Sbaffi, J.-C. Duplessy, M. Sarnthein, J.-L. Turon, J. Duprat, and E. Jansen, Apparent cooling of the sea surface in the northeast Atlantic and Mediterranean during the Holocene, *Quaternary Science Reviews*, *21*, 455-483, 2002.

Marret, F., J. Eiríksson, K. L. Knudsen, J.-L. Turon, and J. D. Scourse, Distribution of dinoflagellate cyst assemblages in surface sediments from the northern and western shelf of Iceland, *Review of Paleobotany and Palynology*, *128*, 35-53, 2004.

Marret, F. and K. A. F. Zonneveld, Atlas of modern organic-walled dinoflagellate cyst distribution, *Review of Palaeobotany and Palynology, 125*, 1-200, 2003.

Matthews, J., The assessment of a method for the determination of absolute pollen frequencies, *New Phytologist*, *68*, 161–166, 1969.

Matthiessen, J., Distribution patterns of dinoflagellate cysts and other organic-walled microfossils in recent Norwegian-Greenland Sea sediments, *Marine Micropaleontology, 24*, 307-334, 1995.

Matthiessen, J., K.-H. Baumann, A. Schröder-Ritzrau, C. Hass, H. Andruleit, A. Baumann, S. Jensen, A. Kohly, U. Pflaumann, C. Samtleben, P. Schäfer, and J. Thiede, Distribution of calcareous, siliceous and organic-walled planktic microfossils in surface sediments of the Nordic Seas and their relation to surface-water masses, in *The Northern North Atlantic: a Changing Environment*, edited by P. Schäfer et al., pp. 105-127, Springer, Berlin, 2001.

Matthiessen, J., A. de Vernal, M. Head, Y. Okolodkov, K. Zonneveld and R. Harland, Modern organic-walled dinoflagellate cysts in Arctic marine environments and their (paleo-) environmental significance, *Paläontologische Zeitschrift, 79/1*, 3-51, 2005.

Moros, M., J. F. McManus, T. Rasmussen, A. Kuijpers, T. Dokken, I. Snowball, T. Nielsen, and E. Jansen, Quartz content and the quartz-to-plagioclase ratio determined by X-ray diffraction: a proxy for ice rafting in the northern North Atlantic? *Earth and Planetary Science Letters, 218*, 389-401, 2004a.

Moros, M., K. Emeis, B. Risebrobakken, I. Snowball, A. Kuijpers, J. McManus and E. Jansen, Sea surface temperatures and ice rafting in the Holocene North Atlantic: climate influences on northern Europe and Greenland, *Quaternary Science Reviews, 23*, 2113–2126, 2004b.

Moros, M., J. T. Andrews, D. E. Eberl, and E. Jansen, The Holocene history of drift ice in the northern North Atlantic: different spatial and temporal modes, submitted to *Paleoceanography*.

Mudie, P. J. and A. Rochon, Distribution of dinoflagellate cysts in the Canadian Arctic marine region, *Journal of Quaternary Science, 16*, 603-620, 2001.

Naval Oceanography Command Detachment, *Sea Ice Climatic Atlas: Vol. II Arctic East. Navair 50-1c-541*, 147 pp., Asheville, 1986.

National Oceanographic Data Centre (NODC), *World Ocean Atlas*, http://www.nodc.noaa.gov/OC5/WOD01/pr_wod01.html, 2001.

National Snow and Ice Data Center (NSIDC), *Arctic and Southern Ocean Sea Ice Concentrations*, http://nsidc.org/data/docs/noaa/g00799_arctic_southern_sea_ice/index.html, 2003.

O'Brien, S. R., P. A. Mayewski, L. D. Meeker, D. A. Meese, M. S. Twickler, and S. I. Whitlow, Complexity of Holocene climate as reconstructed from a Greenland ice core, *Science, 270*, 1962-1964, 1995.

Ólafsson, J., Connection between oceanic conditions off N-Iceland, Lake Mývatn temperature, regional wind direction variability and the North Atlantic Oscillation, *Rit Fiskideildar, 16*, 41-57, 1999.

Reeh, N., Holocene climate and fjord glaciations in Northeast Greenland: implications for IRD deposition in the North Atlantic, *Sedimentary Geology, 165*, 333-342, 2004.

Reeh, N., C. Mayer, H. Miller, H. H. Thomsen, and A. Weidick, Present and past climate control on fjord glaciations in Greenland: Implications for IRD-deposition in the sea, *Geophysical Research Letters, 26*, 1039-1042, 1999.

Rimbu, N., G. Lohmann, J.-H. Kim, H. W. Arz, and R. Schneider, Arctic/North Atlantic Oscillation signature in Holocene sea surface temperature trends as obtained from alkenone data, *Geophysical Research Letters, 30*, 1280, doi:10.1029/2002GL016570, 2003.

Rochon, A., A. de Vernal, J.-L. Turon, J. Matthiessen, and M. J. Head, Distribution of recent dinoflagellate cysts in surface sediments from the North Atlantic Ocean and adjacent seas in relation to sea-surface parameters. Contribution Series, vol. 35, pp. 7–54, American Association of Stratigraphic Palynologists, Houston, 1999.

Solignac, S., A. de Vernal, and C. Hillaire-Marcel, Holocene sea-surface conditions in the North Atlantic- contrasted trends and regimes in the western and eastern sectors (Labrador Sea vs. Iceland Basin), *Quaternary Science Reviews*, *23*, 319-334, 2004.

Steig, E., Mid-Holocene climate change, *Science*, *286*, 1485-1487, 1999.

Stötter, J., M. Wastl, C. Caseldine, and T. Haberle, Holocene paleoclimatic reconstructions in Northern Iceland: approaches and results, *Quaternary Science Reviews, 18*, 457-474, 1999.

Tremblay, L. B., L. A. Mysak and A. S. Dyke, Evidence from driftwood records for century-to-millennial scale variations of the high latitude atmospheric circulation during the Holocene, *Geophysical Research Letters, 24*, 2027-2030, 1997.

Visbeck, M., E. P. Chassignet, R. G. Curry, T. L. Delworth, R. R. Dickson, and Krahmann, G., The ocean's response to North Atlantic Oscillation variability, in *The North Atlantic Oscillation: Climate Significance and Environmental Impact*, *Geophysical Monograph Series* vol. 134, pp. 113-145, AGU, Washington, DC. 2003.

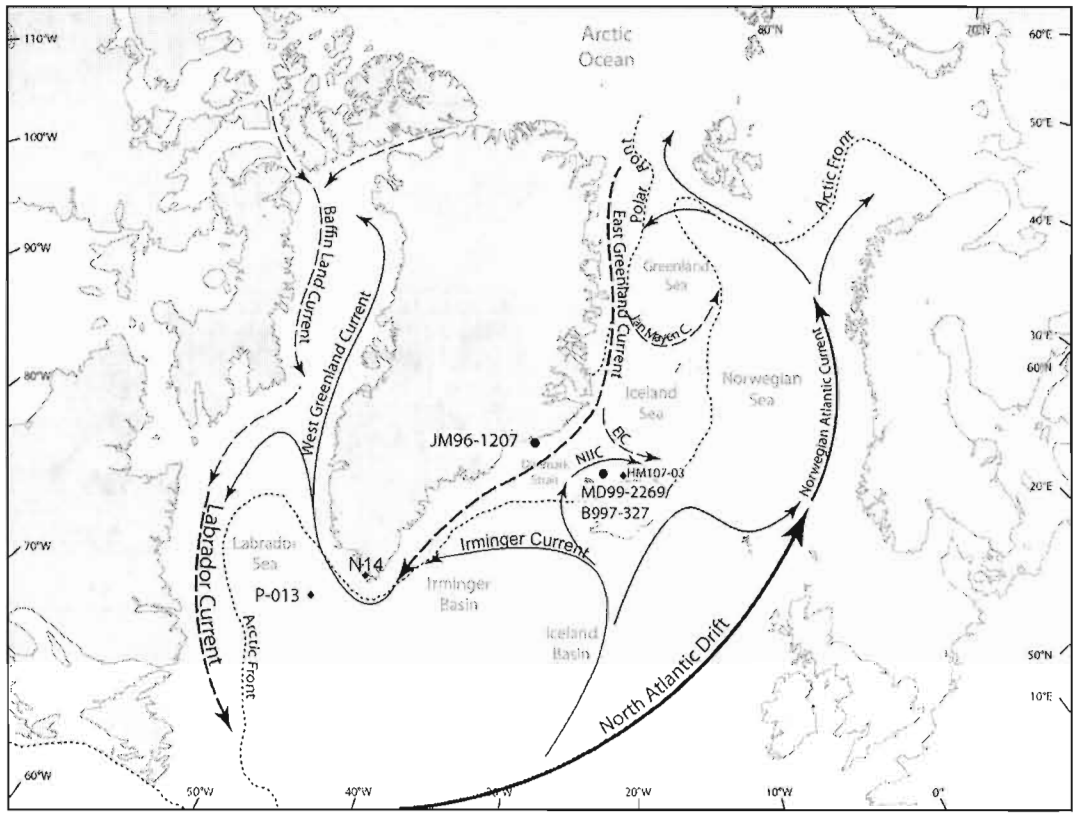

Figure 1. Location of the study cores MD99-2269, B997-327 and JM96-1207, and trajectories of the main ocean surface currents. Dashed arrows represent cold currents and solid arrows represent warm currents. The dotted lines illustrate the Arctic and Polar fronts, that is, the maximum sea ice extension in winter and summer, respectively, as defined from the 1953–2003 data set provided by the National Snow and Ice Data Center (NSIDC) [2003] and the sea ice atlas prepared by the Naval Oceanography Command Detachment [1986]. Locations of cores P-013 and HM107-03 and Lake N14 [Andresen et al., 2004], to which we refer in the text, are indicated. Isobaths indicate water depths of 2000, 1000 and 200 m.

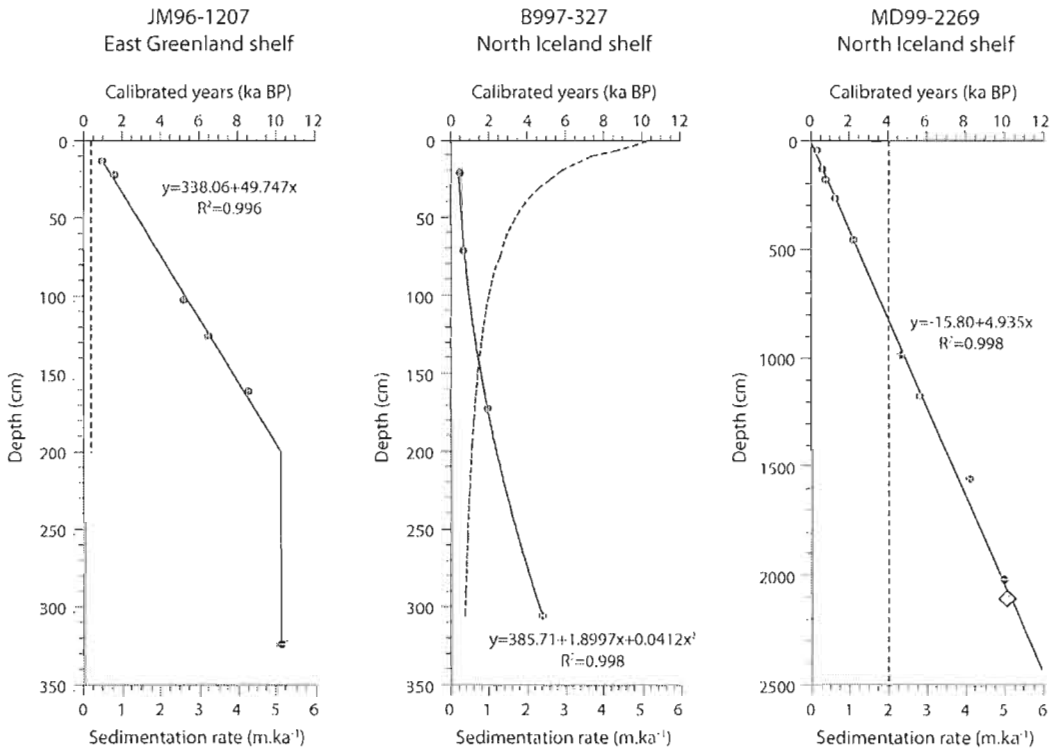

Figure 2. Age models of cores JM96-1207, B997-327 and MD99-2269. Dots represent ^{14}C dates. The diamond in core MD99-2269 corresponds to a tephra marker at 10.18 ka [Giraudeau et al., 2004]. One of the 14C dates of core MD99-2269 is absent from the graph as it is older than 12 calibrated ka. It was nevertheless taken into account in the regression calculations. Interpolated ages are indicated by black curves. Sedimentation rates are indicated by vertical dashed curves. Note that a different depth scale was used for core MD99-2269.

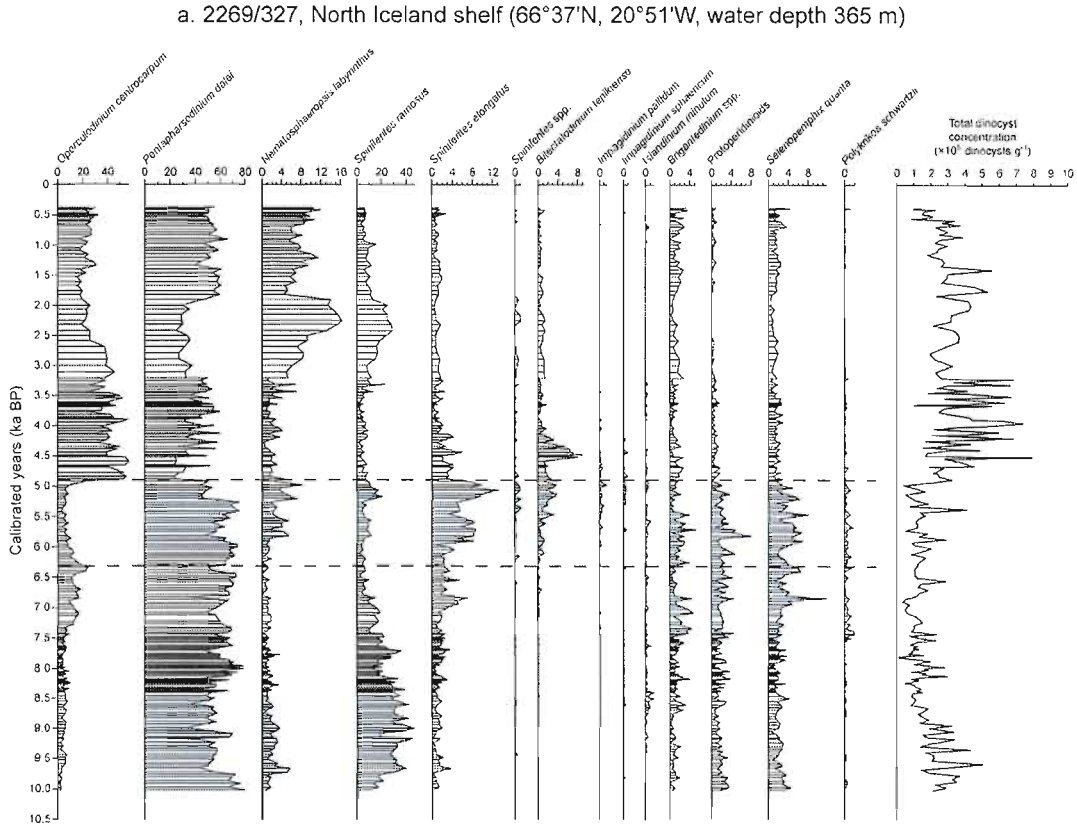

Figure 3. Diagram of dinocyst assemblages (expressed in percentages) and total dinocyst concentrations (black curves on the right) for the past 10,000 calibrated years in cores (a) 2269/327 and (b) 1207. Note the different scales used for dominant and accompanying taxa. Dashed lines indicate transitions discussed in the text.

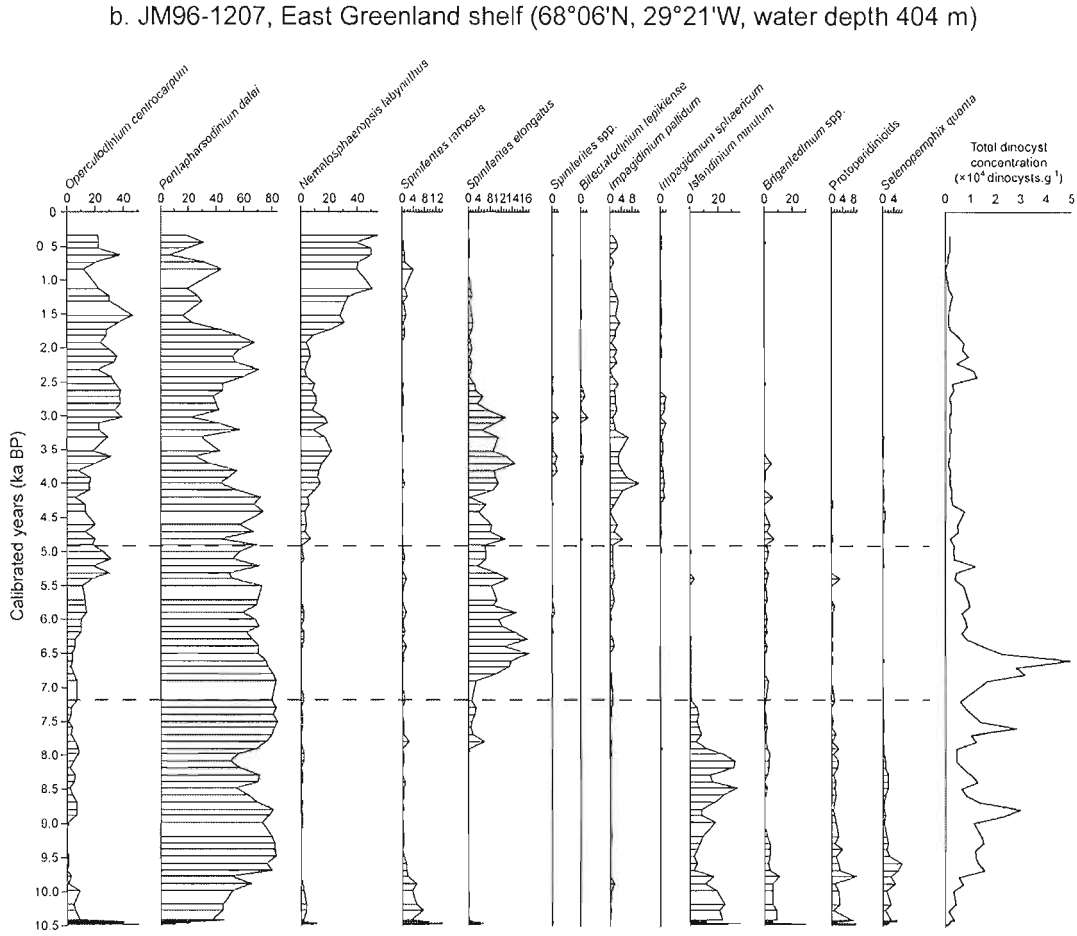

Figure 3. (continued)

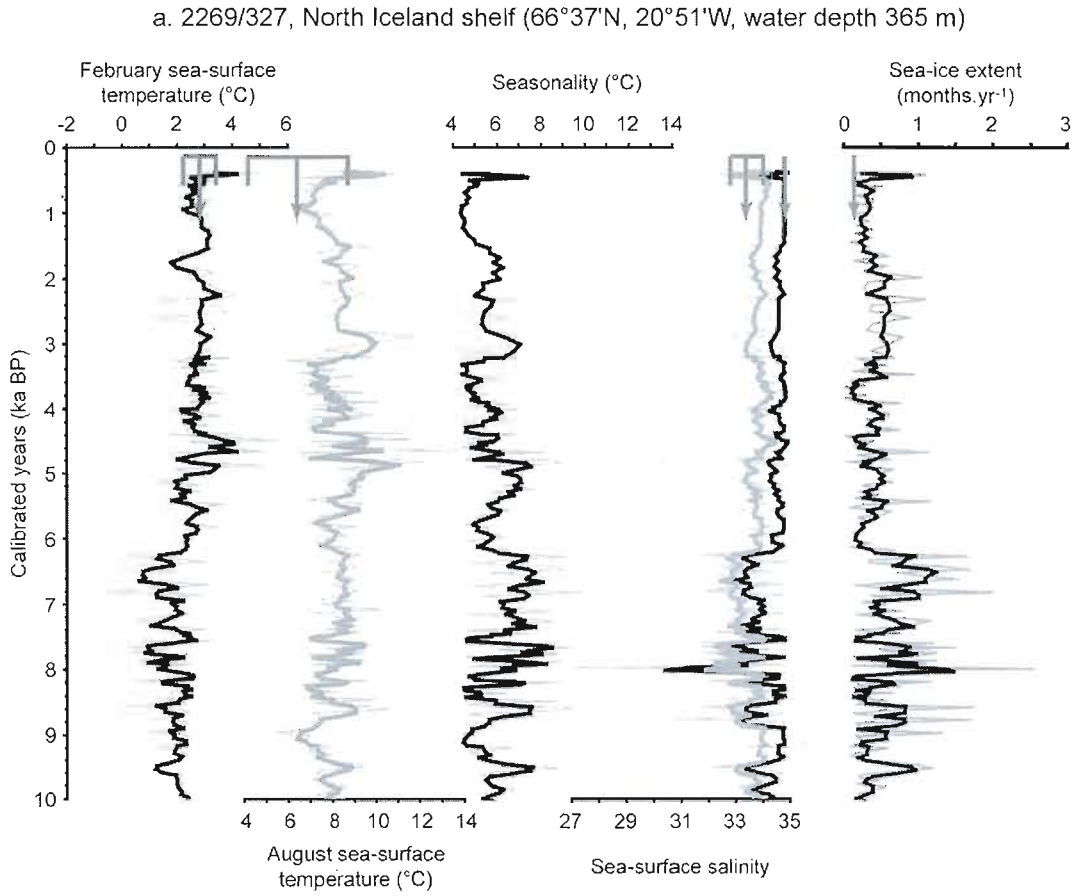

Figure 4. Reconstructions of sea surface conditions for the past 10,000 calibrated years for cores (a) 2269/327 and (b) 1207. Reconstructions are based on the five closest analogues following the procedure described by de Vernal et al. [2005]. Bold curves are smoothed records (three-point running mean). Black curves in temperature and salinity are February values, grey curves are August values. Dark grey arrows represent modern values, compiled from the 1900-2001 record of the National Oceanographic Data Center (NODC) [2001] and the 1953-2003 ice record from the NSIDC [2003]. The width of the base of the arrows shows the standard deviation of these modern instrumental measurements. No modern value was available for February SSSs in core 1207.

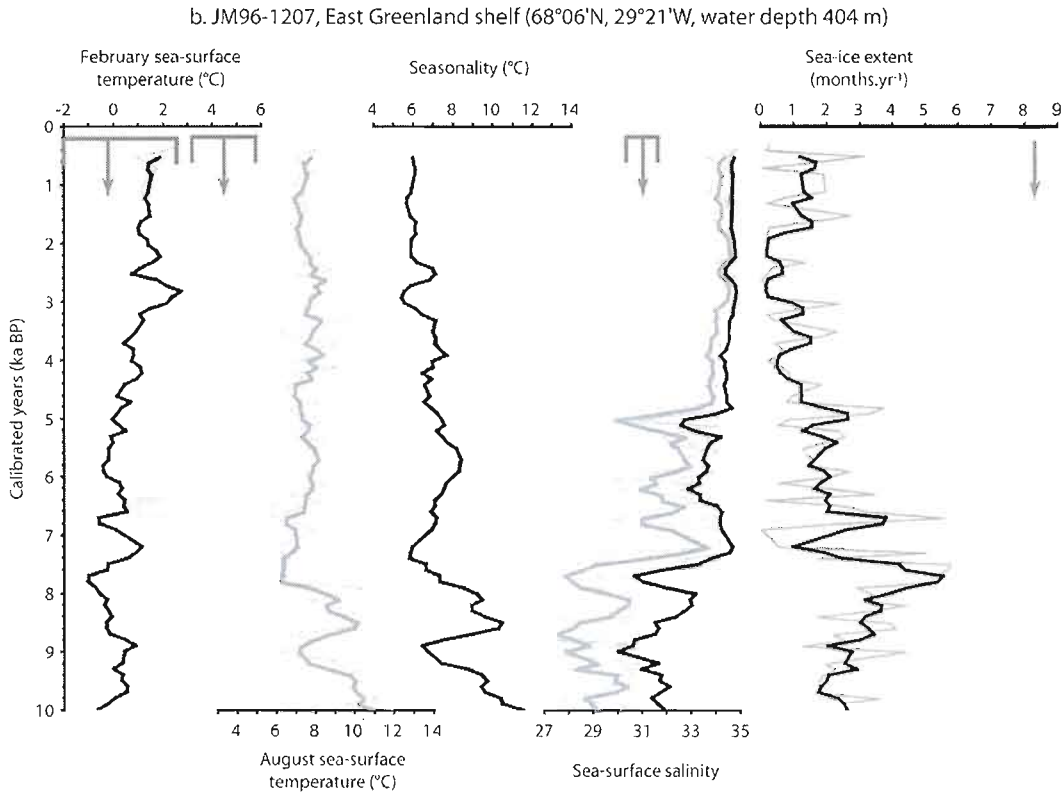

Figure 4. (continued)

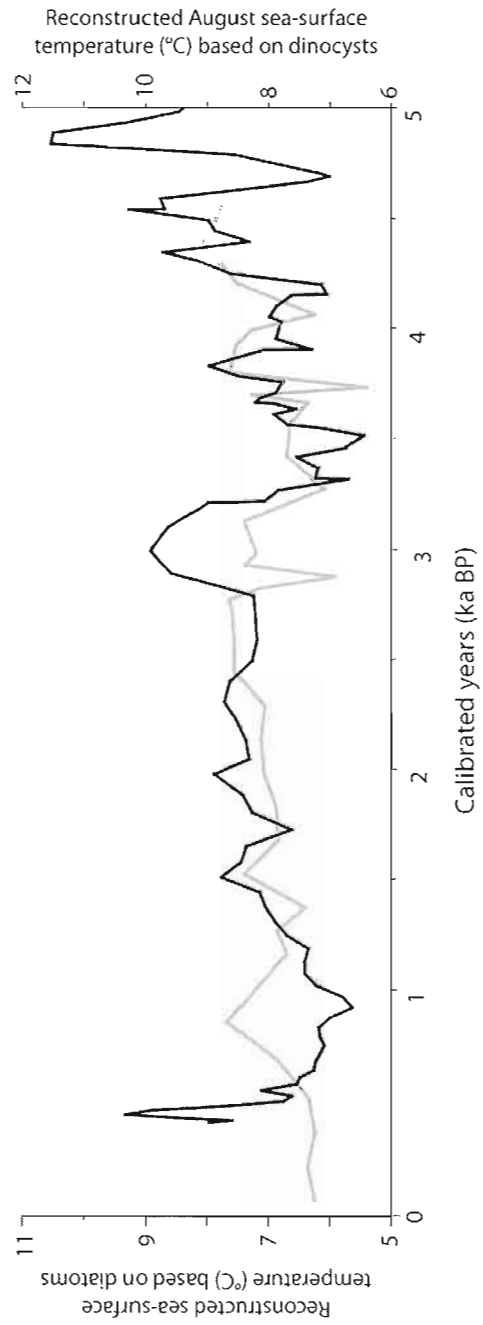

Figure 5. Comparison of diatom-based reconstructions of summer SSTs (core HM107-03, 66°30'N, 19°04'W [Jiang et al., 2002], grey curve) with dinocyst-based August SSTs from core 2269/327 (black curve). Note that the scales were shifted in order to better illustrate the common variations.

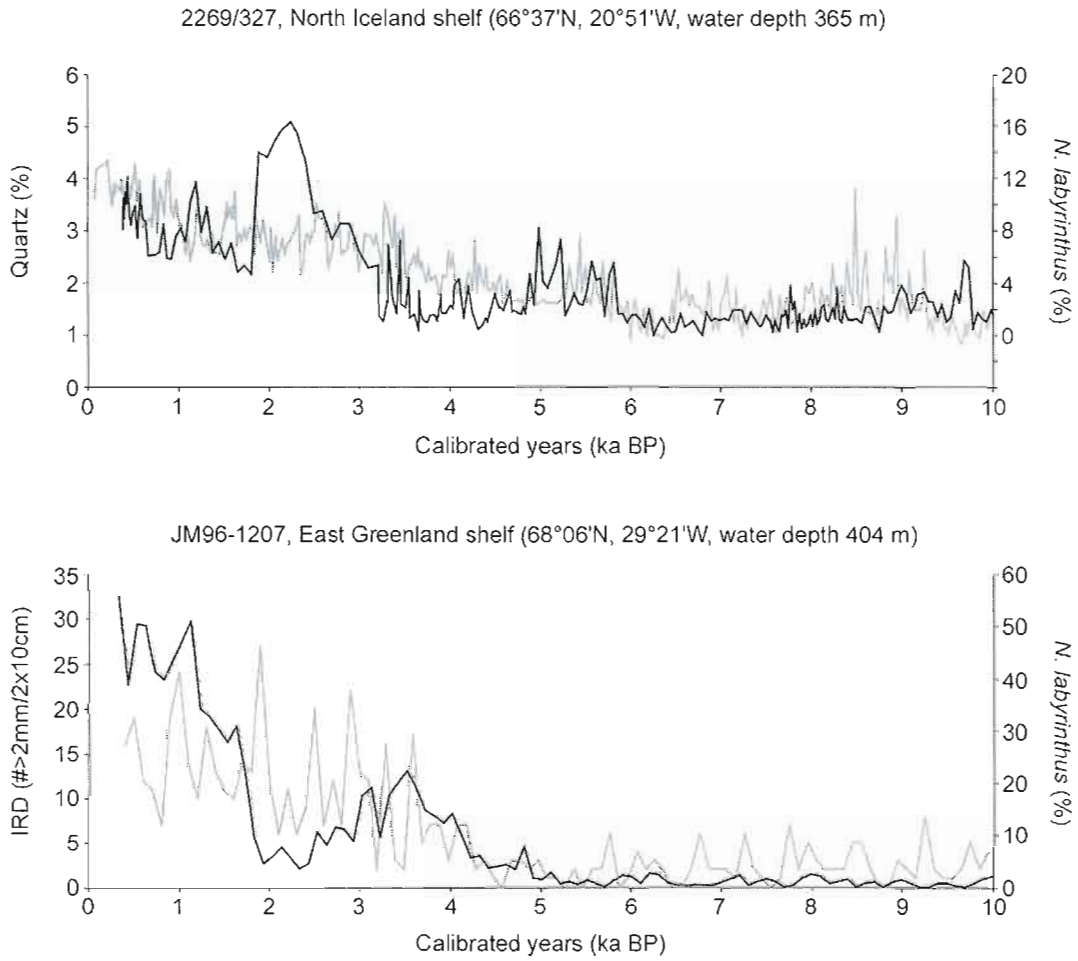

Figure 6. Comparison of the relative percentages of *N. labyrinthus* (black curves) with the IRD (core 1207 [Jennings et al., 2002]) and quartz (core 2269 [Moros et al., 2006]) records (grey curves).

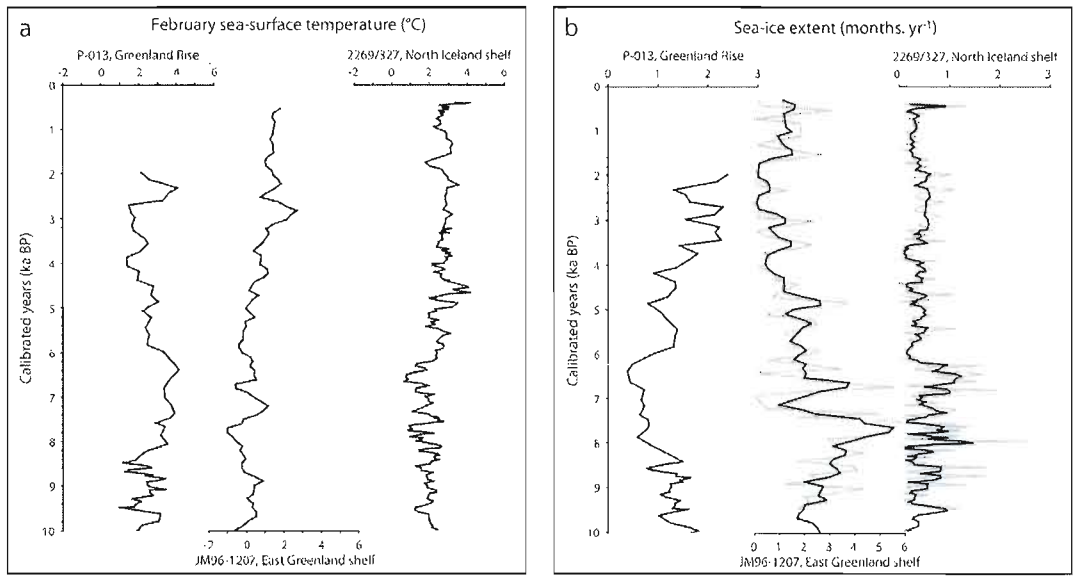

Figure 7. Comparison of some of the reconstructed parameters from cores 2269/327 and 1207 with those from core P-013, Greenland Rise [Solignac et al., 2004]. Note the different horizontal scales. Bold curves are smoothed records (three-point running mean). Reconstructions for record P-013 were updated with the latest "n=940" dinocyst database [de Vernal et al., 2005] and the updated World Ocean Atlas [NODC, 2001].

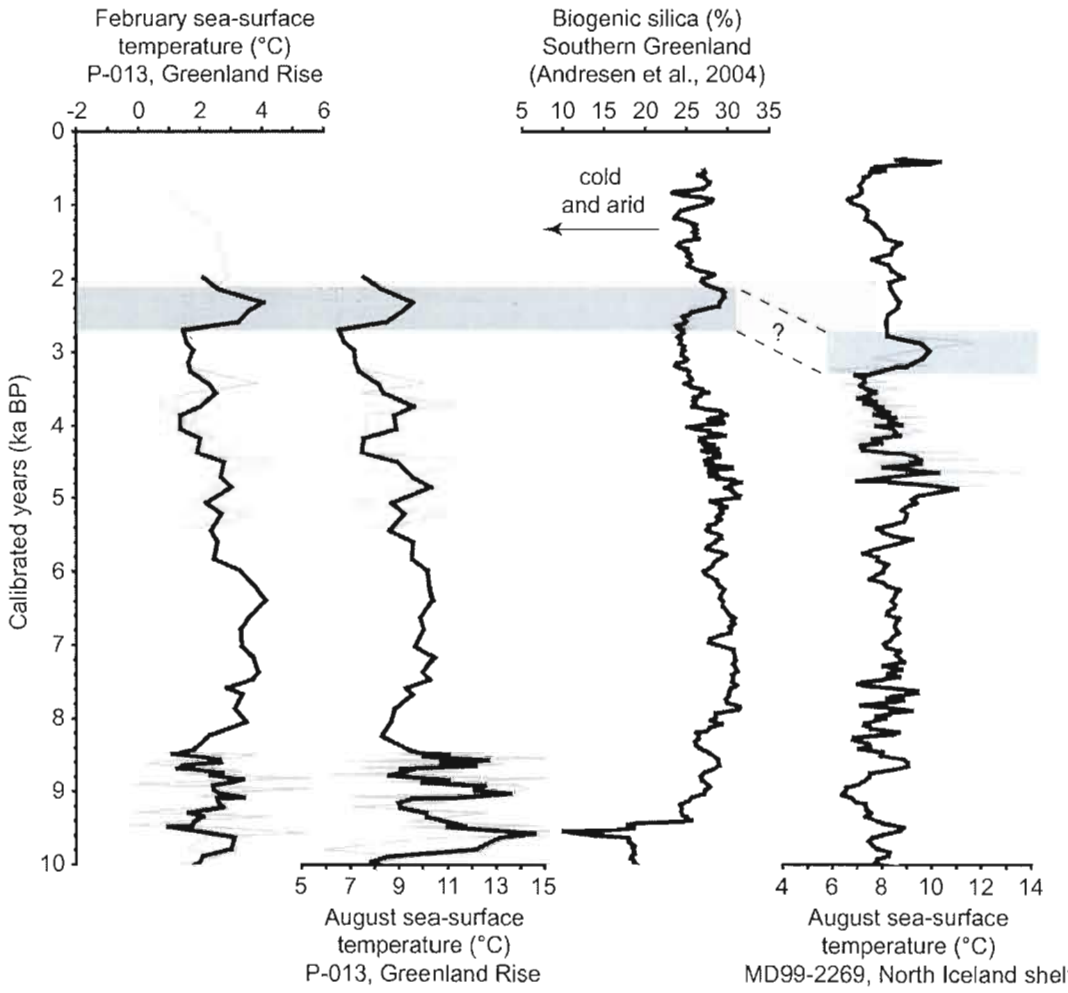

Figure 8. Comparison of dinocyst-based reconstructions of SSS and SST from cores P-013 and 2269/327 with a continental biogenic silica record from Lake N14, southern Greenland [Andresen et al., 2004].

CHAPITRE II

REORGANISATION OF THE UPPER OCEAN CIRCULATION IN THE MID-HOLOCENE IN THE NORTHEASTERN ATLANTIC

Sandrine Solignac[1], Michael Grelaud[2], Anne de Vernal[1], Jacques Giraudeau[3], Matthias Moros[4], Ian Nicholas McCave[5] and Babette Hoogakker[5]

[1]GEOTOP-UQAM, C.P. 8888, Succursale Centre-ville, Montréal, QC, H3C 3P8

[2]CEREGE, Europôle de l'Arbois, 13 545 Aix-en-Provence, France

[3]Environnements et Paléoenvironnements Océaniques, UMR CNRS 5805, Université Bordeaux 1, Avenue des Facultés, 33405 Talence cedex, France

[4]Bjerknes Centre for Climate Research, Allegaten 55, Bergen, 5007, Norvège et Baltic Sea Research Institute, Seestrasse 15, Rostock, 18119, Allemagne

[5]Department of Earth Sciences, University of Cambridge, Downing Street, Cambridge, CB2 3EQ, Royaume-Uni

Article soumis pour publication dans la *Revue canadienne des sciences de la Terre*

Résumé

Des études micropaléontologiques ont été menées sur deux carottes sédimentaires, l'une provenant de la ride de Reykjanes (LO09-14, 59°12.30'N, 31°05.94'O) et l'autre, du chenal des Féroé-Shetland (HM03-133-25, 60°06.55'N, 06°04.18'W), dans le but de retracer les changements hydrographiques du Courant Nord Atlantique (CNA) au cours de l'Holocène. Les assemblages de dinokystes et de coccolithes ont été analysés et interprétés d'après leur distribution biogéographique moderne. La méthode des meilleurs analogues a été appliquées aux assemblages de dinokystes afin de reconstituer quantitativement la température (TSO) et la salinité (SSO) de surface de l'océan. Les enregistrements des deux traceurs mettent en évidence des changements significatifs des conditions de surface de l'océan et suggèrent une réorganisation majeure de la configuration des courants de surface dans le nord-est de l'Atlantique Nord entre 7 et 5.4 ka BP.

Aux deux sites, la SSO moyenne avant 6.5-7 ka BP était plus basse que durant l'Holocène moyen à supérieur, suggérant des apports en eaux de fonte par le CNA. Les tendances à long terme des TSO, cependant, sont différentes aux deux sites, avec des TSO estivales plus chaudes que de nos jours sur la ride de Reykjanes de 9.3 à ~6 ka BP, et plus froides dans le chenal des Féroé-Shetland, jusqu'à ca. 5.4 ka BP. Ces tendances contrastées suggèrent que la diminution de l'insolation estivale n'était pas l'unique forçage direct à l'origine des changements des conditions de surface de l'océan dans les nord-est de l'Atlantique Nord. Un découplage des deux courants influençant le chenal des Féroé-Shetland, le CNA et le courant de Pente, est un mécanisme possible qui pourrait expliquer les différences observées aux deux sites. Il est proposé qu'un CNA plus fort durant l'Holocène inférieur à moyen se soit traduit par une hausse des TSO sur la ride de Reykjanes et une diminution dans le chenal des Féroé-Shetland. À l'inverse, un CNA plus faible après 5-6 ka BP, menant à des TSO plus basses sur la ride de Reykjanes, pourrait avoir entraîné une plus forte contribution relative du courant de Pente plus chaud et plus salé dans le chenal des Féroé-Shetland, résultant en une hausse régionales des TSO et SSO.

Abstract

A micropaleontological investigation was conducted on two sediment cores, one from the Reykjanes Ridge area (LO09-14, 59°12.30'N, 31°05.94'W) and the other from the Faroe-Shetland Channel (HM03-133-25, 60°06.55'N, 06°04.18'W) in order to document hydrographical changes of the North Atlantic Current (NAC) during the Holocene. Dinocyst and coccolith assemblages were analyzed and interpreted in view of their modern biogeographical distribution, and quantitative reconstructions of sea surface temperature (SST) and salinity (SSS) were conducted based on the best analogue technique applied to dinocyst assemblages. Both proxy records exhibit significant changes of sea-surface conditions and suggest a major reorganisation of surface circulation patterns in the northeastern North Atlantic between 7 and 5.4 ka BP.

At both sites, mean SSS before 6.5-7 ka BP was lower than during the mid- to late Holocene, suggesting dispersal of melwater supplies through the NAC. Long term trends of SST, however, show contrasted patterns with higher than present summer SST on the Reykjanes Ridge from 9.3 to ~6 ka BP, and lower than present SST in the Faroe-Shetland Channel until ca. 5.4 ka BP. The contrasted SST trends on the Reykjanes Ridge and in the Faroe-Shetland Channel suggest that decreasing summer insolation was not the only direct forcing behind changes in sea-surface conditions in the northeastern North Atlantic. Decoupling of the two currents influencing the Faroe-Shetland Channel, the NAC and the Slope Current (SC) is thus proposed as a possible mechanism explaining the different records at the two sites. We hypothesize that a strong NAC during the early-middle Holocene resulted in a SST increase on the Reykjanes Ridge and decrease in the Faroe-Shetland Channel. Inversely, a weaker NAC after 5-6 ka BP, leading to an SST decreased on the Reykjanes Ridge, would have fostered an enhanced relative contribution of the warmer, saltier SC in the Faroe-Shetland Channel, thus resulting in a regional SST and SSS increase.

1. Introduction

The flow of Atlantic waters to the high latitudes of the North Atlantic plays a major role in the heat transfers to the pole regulating the climate from western Europe, as well as in convection processes through which deep water formation occurs. It is thus essential to understand how warm, saline water supplies to the Nordic seas and the Arctic Ocean vary through time and what the consequences of these variations are. Studying these fluctuations throughout the Holocene allows the assessment of the interrelationships between Atlantic water fluxes and various scenarios of climate.

Many studies have shown decreasing sea surface temperatures during the Holocene, commonly attributed to insolation changes (e.g. Marchal et al., 2002; Kaplan and Wolfe, 2006). However, heterogeneities with respect to the amplitude and spatial extent of hydrographical changes (e.g., Solignac et al., 2004, 2006; de Vernal and Hillaire-Marcel, 2006) highlight the need for a better coverage of key regions of oceanic circulation in the mid- and high latitudes of the North Atlantic.

Here we present a Holocene record from the Faroe-Shetland Channel, which is one of the three pathways for poleward Atlantic water fluxes, along with the Iceland-Faroe Gap and the Denmark Strait (e.g., Hansen and Østerhus, 2000). Two micropaleontological tracers, coccoliths and dinoflagellate cysts (dinocysts), were analyzed in order to identify changes in the surface hydrography of the Faroe-Shetland Channel. Comparison with a record from the Reykjanes Ridge, southwest of Iceland, led to document the spatial patterns of the changes in sea-surface conditions and permit to propose possible mechanisms responsible for them.

Dinoflagellates and coccolithophores make up an important proportion of the plankton in the world ocean. The distribution of their various species is strongly influenced by hydrographical parameters such as sea-surface temperature and salinity and a good correspondence is observed between the characteristics of the overlying water masses and dinocyst/coccolith assemblages preserved in the sediment (e.g., Eide, 1990; Baumann et al., 2000; Lévesque, 1995; see also de Vernal and Marret, 2007 and references therein for a review on dinocyst fossil assemblages). Coccolith and dinocyst assemblages may suffer from specific drawbacks, such as calcite dissolution in coccoliths (Siesser, 1993; Samtleben and

Schröder, 1992) or the higher sensitivity to oxidation of some dinocyst species (Zonneveld et al., 2001). Analyzing both proxies therefore allows us to somewhat discriminate between ecological signals and taphonomic processes, and thus to obtain a more accurate picture of the paleoceanography of the Holocene in the northeastern Atlantic.

2. Oceanographic setting

The study area extends from the Faroe-Shetland Channel to the Reykjanes Ridge and thus lies under the influence of poleward-flowing Atlantic waters. These waters are usually described as warm and saline compared with the cold and fresher polar/arctic waters flowing south from the Arctic Ocean. However, here, it is essential to highlight the differences between the various water masses comprised under the general term "Atlantic waters".

The Gulf Stream splits into a northern and a southern branch at ~55°W (Reverdin et al., 2003), and its northern branch eventually splits up as well. A first limb turns north before crossing the Mid-Atlantic Ridge (MAR, e.g., Holliday et al., 2006) and flows along the western flank of the Reykjanes Ridge in the Irminger Sea, forming the Irminger Current (IC) and transporting ~8 Sv of water (Pollard et al., 2004). As it continues towards Greenland, the IC makes one of the northern limbs of the North Atlantic Subpolar Gyre (Fig.1). The upper water masses in the Subpolar Gyre are referred to as Subarctic Intermediate Water[1] (SAIW), which takes its source in the polar Labrador Current (Pollard et al., 2004). SAIW is typically characterized by a strong, shallow, seasonal salinity-driven stratification and is relatively cold and fresh (Read, 2001, Pollard et al., 2004, Holliday, 2006). It extends eastward to ~32°W at 55-56°N and further east (25-26°W) more in the south (53°N), forming the Subarctic Front with warmer, more saline waters from the North Atlantic Current (Read, 2001).

The remainder of the northern branch of the Gulf Stream flows eastward as the North Atlantic Current (NAC, ~16 Sv; Read, 2001) roughly along the 50°N parallel, crossing the North Atlantic Basin. Despite some discrepancies among authors in the interpretation of the oceanic currents in the North Atlantic, there is a general agreement on a "multi-branch" structure of the NAC. The northernmost NAC branch (Fig. 1) coincides with the Subarctic

[1] Water mass denominations vary among authors – here we use those provided by Read, 2001

Front (Pollard et al., 2004; Flatau et al., 2003; Brambilla, 2006). The southern NAC branch partly recirculates in the Iceland Basin (Brambilla, 2006) and carries a water mass referred to as Western North Atlantic Water (WNAW), which is highly seasonally stratified, warm and saline (Read, 2001). Part of the southern branch then flows south along the eastern flank of the Reykjanes Ridge, and eventually both northern and southern NAC branches cross again the MAR towards the west and join the northward path of the Irminger Current along the western flank of the Reykjanes Ridge (Fig. 1; Pollard et al., 2004).

Another 3.3 Sv of the southern branch of the NAC continues towards the Iceland-Faroe Gap (Fig. 1), and either gets modified along the way (Hansen and Østerhus, 2000) or mixes with upwelling water masses from the Rockall Plateau (Read, 2001), becoming the slightly fresher and colder Modified North Atlantic Water (MNAW) in the vicinity of the Iceland-Faroe Gap. Part of it then flows east/southeast as the Faroe Current and reaches the Faroe-Shetland Channel (Fig. 1).

A third branch of the NAC flows northeastward into the southern Rockall Trough and then on Rockall Plateau and Hatton Bank (Fig. 1). This branch is referred to as the Rockall-Hatton branch and carries WNAW (Pollard et al., 2004). In addition, a major distinction with the Iceland Basin characterizes the Rockall Trough and the Faroe-Shetland Channel: here another type of water mass influences the region (Pollard et al., 2004; Hansen and Østerhus, 2000). The Slope Current originates in the intergyre region in the Bay of Biscay (Read 2001) and carries 3 Sv of water into the Rockall Trough all the way to the Faroe-Shetland Channel (Hansen and Østerhus, 2000; Pollard et al., 2004; Fig. 1). It is characterized by a water mass referred to as Eastern North Atlantic Water (ENAW, Read, 2001, Pollard et al., 1996, 2004), which is significantly warmer, more saline and much less stratified than waters derived from the NAC (i.e., MNAW and WNAW). The upper water mass in the Faroe-Shetland Channel therefore results from the mixing of colder, fresher MNAW from the Faroese side, and warmer, more saline ENAW from the Scottish slope (occasionally mixed with some WNAW from the Rockall Hatton Branch of the NAC).

3. Material and methods

Two records from the northeastern Atlantic were used in this study. The westernmost one, LO09-14 (59°12.30'N, 31°05.94'W, 1493 m water depth), is located on the Reykjanes Ridge, southwest of Iceland (Fig. 1). This record is a composite made out of 4 cores, i.e. box core LO09-14 LBC, giant gravity core LO09-14 GGC, gravity core LO09-14 GC (all 3 retrieved at the same site), as well as neighbour core DS97-2P (58°56'33N, 30°24'59W, 1685 m water depth), which was used to fill the gap from 1.2 to 2.2 ka BP between the LBC and the GGC (Grelaud, 2004; Moros et al., 2004). The easternmost site, HM03-133-25 (60°06.55'N, 06°04.18'W, 1156 m water depth) is located in the Faroe-Shetland Channel, halfway between Scotland and the Faroe Islands (Fig. 1).

The LO09-14 site thus lies in the vicinity of the subarctic front, the position of which controls the relative contributions of SAIW and WNAW. The HM03-133-25 site, lying in the middle of the Faroe-Scotland Channel, is influenced by a combination of MNAW that circulates through the Iceland-Faroe Gap, and ENAW that flows, along with a varying amount of WNAW, through the Rockall Trough.

This major difference is reflected in today's environmental parameters (National Oceanographic Data Center (NODC), 2001), the sea surface temperature in the Reykjanes Ridge area averaging 10.9°C and 6.8°C in summer and winter, respectively, as compared to 11.6°C and 8.4°C in the Faroe-Shetland Channel. Sea surface salinity is higher in the Faroe-Shetland Channel (35.29 in summer and 35.28 in winter) than in the Reykjanes Ridge area (34.97 in summer and 35.14 in winter). No sea ice is observed at any of the sites, at least since 1950 (National Snow and Ice Data Center (NSIDC), 2003).

3.1. Chronologies

Ages on the three LO09-14 cores were calculated from 34 AMS ^{14}C dates measured on the foraminifera species *Globigerina bulloides*. Detailed age models can be found in Andersen et al. (2004) and Moros et al. (2004). DS97-2P was dated with 20 AMS ^{14}C ages measured on planktonic foraminifera. The age model is discussed in more depth in Prins et

al. (2001). Sedimentation rates on all cores allow a temporal resolution varying from less than 10 years to ~150 years.

The chronology for core HM03-133-25 is based on AMS-^{14}C dating. ^{14}C ages were converted into calendar years using the 5.0.1 version of the CALIB software of Stuiver and Reimer (1993), with a reservoir age of 400 years. A spline fit was used to convert depths into calendar ages. Sedimentation rates vary from 18 to 86 cm.kyr^{-1}, and temporal resolution of our analyses, from ~47 to 395 years. Full details on the establishment of the age model are given in McCave et al. (in prep.).

3.2. Micropaleontological tracers

The assemblages of two microfossil groups, coccoliths and dinoflagellate cysts (or dinocysts), were analyzed on both cores and on the same samples in order to allow direct comparison of the two proxies.

Sediment sample preparation for coccoliths were conducted using standardized techniques detailed in Andrews and Giraudeau (2003). Accordingly, census counts were expressed as both species relative abundances (%) and concentrations (specimens.g^{-1} of dry bulk sediment). Coccoliths were identified with an optical microscope at the species level, except for *Syracosphaera* spp., which might include more than one species. In core HM03-133-25, the distinction was made between two morphotypes of *Emiliania huxleyi* according to the degree of calcification of their central grid as identified by Beaufort and Heussner (2001, see also references therein). These morphotypes are hereafter referred to as open (slightly calcified) and closed (highly calcified) *E. huxleyi*.

Samples were treated for dinocyst population analyses following standard techniques described in de Vernal et al. (1999). Ideally, 300 dinocysts should be counted for each sample in order to get statistically significant results. However, very little sediment was left for palynological treatments in core LO09-14, and it was often not possible to reach 300 individuals. Here we used only the samples for which more than 50 dinocysts were counted for quantitative reconstructions. Dinocysts were identified according to the taxonomic nomenclature of Rochon et al. (1999) and Head et al. (2001). Brown cysts of heterotrophic taxa such as *Brigantedinium* spp., *Quinquecuspis* spp. or *Lejeunecysta* spp. had to be

grouped in the Protoperidinioid class when unidentifiable. When properly oriented on the slide and easy to recognize, they were identified at the species level. Total dinocyst concentrations were calculated using the marker grain method (Matthews, 1969).

About 15 different dinocyst species were observed in each core. In order to synthetize the information on species occurrence and to highlight the major shifts in the assemblages, a principal components analysis (PCA) was performed on each of the two dinocyst records, as well as on each of the two coccolith records for comparison purposes.

3.3. Quantitative hydrographical parameter reconstructions

The best analogue technique was applied (e.g., Guiot, 1990) on the dinocyst assemblages for quantitative reconstructions of sea-surface conditions based on the similarity between modern and fossil dinocyst spectra. Sea-surface temperatures (SST) and sea-surface salinities (SSS) in winter and summer, as well as sea-ice cover extent were reconstructed, as these parameters have been shown to be determining in the distribution of dinocyst assemblages (de Vernal et al., 2001, 2005).

The taxa relative abundances were logarithmically transformed in order to give more weight to secondary taxa that thrive in more specific ecological niches than the ubiquitous dominant taxa. The modern dinocyst assemblage database used here comprises the 1075 reference sites from the North Atlantic, North Pacific and Arctic oceans and their adjacent seas presented in de Vernal et al. (2005), as well as additional ones (unpublished data) that bring the total number of sites to 1189. Hydrographical data (SSTs and SSSs, in winter and summer) at 0 m of water depth, averaged over the period 1900 to 2001 (NODC, 2001), were assigned to each of these reference sites, as well as the extent (in months.year^{-1}) of sea-ice cover with concentrations greater than 50% (averaged over the period 1953 to 2003; NSIDC, 2003). Sea-surface condition reconstructions were then made for the two records based on the modern assemblages and their corresponding hydrographical data. More details on this statistical approach can be found in de Vernal et al. (2005).

4. Results

Dinocyst and coccolith assemblages in cores HM03-133-25 and LO09-14 depict strong fluctuations that reveal important changes in the surface hydrography of the northeastern Atlantic during the Holocene (Fig. 2). Here we focus on the main changes, as depicted by the first two (or three in some cases) principal components (PC) extracted from the dinocyst and coccolith records and by the quantitative dinocyst-based reconstructions.

4.1. HM03-133-25, Faroe-Shetland Channel

The first two PC of the coccolith record explain 38% and 33% of the variance, respectively (Fig. 3b). In other words, they are almost equally important in summarizing the variability of the assemblages, and together they capture the major variations. In contrast, the higher complexity of the dinocyst record is illustrated by the PC explaining lower proportions of the variance (18%, 12% and 6% for the three first components, respectively). This indicates that a higher number of PC is needed to see all the changes in dinocyst assemblages, which is directly linked to the higher number of species. Here we retained the first three components, as it is beyond the scope of this paper to look into all the higher frequency fluctuations. The interesting aspect to note is the excellent correspondence between dinocyst PC 1 and coccolith PC 2, and, to a lesser extent, between dinocyst PC 2-3 and coccolith PC 1 (Fig. 3a), showing that the two plankton groups varied in a parallel way.

In the dinocyst record, the strongest change, around 7 ka BP, is related to the drop of the relative abundance of *Nematosphaeropsis labyrinthus* (Fig. 2a and 3a), while the other fluctuations are mainly driven by *Spiniferites ramosus* (10.0 to 5.4 ka BP) and *Spiniferites mirabilis* (maximum from 9.8 to 9.4 ka BP). *S. mirabilis* is a subtropical to temperate taxon that is generally not encountered in regions with summer SST below 12°C. In the North Atlantic, it is observed in the Mediterranean Sea, on the shelf off Portugal and France, and on the southern Rockall Plateau (Rochon et al., 1999). Its presence in the Faroe-Shetland Channel at the very beginning of the Holocene thus allows the identification of a thermal optimum.

In the coccolith record, closed *Emiliania huxleyi* increases significantly at ~6.8 ka BP, while the other PC fluctuations correspond to the variations of *Gephyrocapsa muellerae*, *Calcidiscus leptoporus* and *Coccolithus pelagicus*, which all decrease between 8.7 and 8.5 ka BP (Fig. 2a). The high percentages of temperate *G. muellerae* (up to ~20%), which presently does not constitute more than 10% of modern assemblages from this region (Ziveri et al., 2004), is coherent with a thermal optimum depicted by *S. mirabilis*.

In the second half of the Holocene, the main change in dinocyst assemblages occurs around 3.5 ka BP with *N. labyrinthus*, *Selenopemphix quanta* and *Trinovantedinium applanatum* appearing (Fig. 3a). This is much subdued compared to variations of the coccolith assemblages (Fig. 3a), for which the first PC show very strong fluctuations, mainly due to *C. leptoporus* (Fig. 2a). The modern distribution of *C. leptoporus* is rather complex and patchy in the North Atlantic, making it difficult to interpret these fluctuations. Higher relative abundances are observed offshore Portugal and France compared with higher latitudes (Ziveri et al., 2004). The reappearance of *C. leptoporus* in the middle to late Holocene could then be partly due to generally warmer conditions.

Reconstructed sea surface conditions based on dinoflagellate cysts fluctuate accordingly to the main transitions identified by the PC. The highest SSTs of the entire Holocene are observed before 9.4 ka BP, along with the lowest SSSs and the strongest seasonality (Fig. 4a). At 9.4 ka BP, SSTs drop while SSSs increase. Until 5.4 ka BP, although almost always below today's values, SSTs depict significant millennial oscillations. These are also apparent in the SSS records, with a two-step increase at 9 and 7 ka BP, after which they reach values closer to the modern ones (Fig. 4a).

At 5.4 ka BP, SSTs and SSSs increase drastically and remain rather stable for the rest of the Holocene. This stability is somewhat at odds with the variability observed in the dinocyst assemblages and even more with that of the coccolith assemblages (Fig. 2a and 3a). Also, there is a slight offset between the reconstructed SST and SSS values at 0.3 ka BP (Fig. 4a) and modern values (NODC, 2001). This may be partly due to a certain lack of modern assemblages in the Faroe-Shetland Channel (de Vernal et al., 2005). As a result, the pool of reference sites to select the best analogues from is reduced and does not fully reflect the subtle variations in dinocyst assemblages. Sea surface condition reconstructions after 5.4 ka BP should thus be taken with a little care. However, warmer SSTs in the mid- to late

Holocene are supported by the greater proportions of closed *E. huxleyi* in the coccolith record. Dandonneau et al. (2006) observed a shift from *G. muellerae*-dominated to closed *E. huxleyi*-dominated assemblages along a transect crossing the NAC, as the water mass characteristics change from temperate to subtropical, suggesting a preference for warmer waters for closed *E. huxleyi*. Hence, although our dinocyst-based reconstructions might lack detail after 5.4 ka BP, SSTs were still on average higher than during the first half of the Holocene.

4.2. LO09-14, Reykjanes Ridge

On the Reykjanes Ridge, the strongest change occurs around 6.5 ka BP, as illustrated by the first PC of both dinocyst and coccolith records (17% and 34% of the variance, respectively). It corresponds with an increase of cold *C. pelagicus* and a decrease of warm *G. oceanica* in the coccolith record, and with a drop of *N. labyrinthus* in the dinocyst record, as seen in the Faroe-Shetland Channel. *N. labyrinthus* is presently found in various environments in the world ocean and appears to be adapted to a wide range of hydrological parameters. In the North Atlantic, however, it reaches its highest relative abundance in the Subpolar Gyre in the Labrador and Irminger seas (Rochon et al., 1999), i.e., in slightly colder and fresher water with a seasonal, salinity-driven stratification (Read, 2001). Boessenkool et al. (2001), in a study on dinocyst assemblages from the Greenland coast, hypothesized that *N. labyrinthus* might be better adapted to stratified conditions compared with turbulence-tolerant *Operculodinium centrocarpum*. Generally higher percentages of *N. labyrinthus* in the first half of the Holocene might thus be related to lower SSS associated with more stratified upper waters, rather than a lower SST signal, especially as the concomitant presence of warm *S. mirabilis*, higher percentages of subtropical to temperate *G. oceanica* (Ziveri et al., 2004) and the absence of cold water thriving coccolith *C. pelagicus* in core LO09-14 argue against harsher conditions during this interval.

Secondary changes are less marked than in core HM03-133-25 (Fig. 3b). In the dinocyst record, the second PC indicates a transition at 9-9.4 ka BP, with an increase of dinocyst *S. ramosus* followed by *S. mirabilis*, and a decrease of coccolith *G. muellerae*. Another transition occurs around 8 ka BP, when percentages of *S. mirabilis* drop and

coccoliths *C. lepoptorus* and *G. oceanica* decrease, indicating the start of climate deterioration.

After ~6.5 ka BP, the second axis of the PCA performed on the coccolith assemblages depict a strong fluctuation from 3 to 1.4 ka BP due to an increase of *G.muellerae*. At 1.4 ka BP, *G. muellerae* and *C. leptoporus* are partly replaced by *C. pelagicus*. These shifts do not stand out clearly in the PCA performed on the dinocyst assemblages, although the reappearance of *N. labyrinthus* at ~3 ka BP and a sudden increase of *Echinidinium* spp. at 1.4 ka BP are observed (Fig. 2b and 3b).

Quantitative reconstructions in core LO09-14 show a cooling from 10.3 to 9.4 ka BP, followed by SST peaking until 8 ka BP and gradually decreasing until ~6.5 ka BP. In contrast, SSSs are relatively low until 5.9 ka BP. Reconstructions of sea-surface conditions for the interval from 6 to 3 ka BP obviously suffer from the lack of data as mentioned earlier. After 3 ka BP, SSTs increase slightly and eventually reach values that agree remarkably well with modern values at this site (Fig. 4b).

5. Discussion

5.1. Reorganisation of eastern North Atlantic surface hydrography in the mid-Holocene

The most prominent changes depicted by the principal components analyses performed on coccolith and dinocyst assemblages from both cores occurred between 7 and 5.4 ka BP, and in this respect are coherent with previous studies suggesting major mid-Holocene climate changes (e.g., Steig, 1999; deMenocal et al., 2000). This shows that a large scale reorganization of the North Atlantic oceanic system took place during this period, at least in the surface layers, where phytoplankton communities develop. The time interval from 7 to 5.4 ka BP corresponds with two important changes in terms of climate forcing (e.g., Kaplan and Wolfe, 2006): the last remnants of the Laurentide ice sheet disappeared around 6 ka BP (Dyke et al., 2003), supplying the ocean with fresh meltwaters until then (Fairbanks, 1989), and summer insolation, which peaked at 10 ka BP, reached its steepest decline rates after 6 ka BP (Berger and Loutre, 1991).

5.1.1. Meltwater influence on the North Atlantic hydrography

In both records, percentages of *N. labyrinthus* were relatively high until around 6.5-6.0 ka BP (Fig. 2). As mentioned earlier, this could be an indication of more stratified waters, at least seasonally, due to generally lower SSS (Fig. 3). The mid-Holocene decrease in *N. labyrinthus* is coherent with other records from the Iceland Basin, namely cores MD95-2015 (Eynaud et al., 2004), MD99-2254 (Solignac et al., 2004), HU91-045-072 and HU91-045-080 (de Vernal, unpublished data; see Fig. 1 for localisations).

The low SSS until ~6 ka BP might correspond to the influence of meltwaters from the Laurentide ice sheet. Whereas sites in the vicinity of the ice sheet, such as in the Labrador Sea (e.g., core P094, Fig. 1, de Vernal and Hillaire-Marcel, 2006) experienced direct meltwater effects resulting in a much more dramatic SSS decrease in the early Holocene, distant sites in the path of the NAC could have been influenced in a more subtle way. Meltwaters from the Laurentide ice sheet eventually joined the Labrador Current, which mixes with the Gulf Stream at the southern boundary of the Subpolar Gyre (Fig. 1) and contributes to the Subarctic Intermediate Water eventually subducting under the NAC and influencing its properties through mixing processes (Pollard et al., 2004). Reduced salinity in the Labrador Current would thus have an effect on the salinity of the NAC. In core HM03-133-25, where the NAC has a somewhat lesser influence, SSS in the early Holocene were higher than on the Reykjanes Ridge, and the shift to even higher values in the late Holocene was more gradual (Fig. 4a).

5.1.2. Summer insolation decrease during the Holocene

Whereas meltwater supplies have a regional effect on the ocean surface hydrography, insolation changes affect the entire globe. The decrease of summer insolation throughout the Holocene (Berger and Loutre, 1991) is thought to be responsible for the onset of the Neoglaciation around 5.7 ka BP in numerous records (Marchal et al., 2002 and references therein).

The influence of the high summer insolation during the early Holocene is visible in the SST record of core LO09-14 on the Reykjanes Ridge, which depicts a thermal optimum

from 9.4 to around 8 ka BP. Although the drop in SST from 8 to 6.5 ka BP is much sharper than the gradual decrease of summer insolation (Berger and Loutre, 1991), it is coherent with increasing percentages of the cold coccolith species *C. pelagicus* (Fig. 2b), alkenone data obtained on the same core (Moros et al., 2004; Fig. 5), as well as other records indicating a thermal maximum ending around 6.5 ka BP in this region (e.g., Giraudeau et al., 2000; de Vernal and Hillaire-Marcel, 2006; see also Kaufman et al., 2004 and references therein).

In the Faroe-Shetland Channel, however, SSTs do not depict the same trend. The SST optimum occurred earlier than on the Reykjanes Ridge, which is in agreement with the study of Kaufman et al. (2004) on the timing of the Holocene thermal maximum in the western Arctic, and with sedimentological and dinocyst studies showing that modern-like oceanic circulation started as early as the end of the Younger Dryas in the region, with Atlantic waters flowing through the northern Rockall Trough and the Faroe-Shetland Channel (Stoker et al., 1989; Howe et al., 1998). The thermal optimum then stopped abruptly at 9.4 ka BP and SSTs remained generally low until 5.4 ka BP, after which they rose. The relatively warm conditions observed during the mid-late Holocene in the Faroe-Shetland Channel suggest that the effects of diminishing insolation were not straightforward and did not generate a homogeneous cooling and reflect a change in the strength and/or spatial configuration of oceanic currents.

5.2. Possible mechanisms of hydrographical variations during the Holocene

Changes in sea surface parameters can result from differences in the relative contribution of the various currents influencing a given region. Notably, Holliday (2003) showed that SST and SSS variations in the Rockall Trough are primarily explained by the degree of mixing between the WNAW-carrying NAC and the ENAW-carrying Slope Current. Similarly, the Faroe-Shetland Channel is influenced by waters from the Rockall Trough, mixed with MNAW coming from the NAC-derived Faroe Current (Hansen and Østerhus, 2000). Hence, a stronger influence of either WNAW or MNAW relative to ENAW would result in colder, fresher waters in the Faroe-Shetland Channel.

The lower SSTs and SSSs recorded from 9.4 to 5.4 ka BP in core HM03-133-25 might then reflect a stronger flow of NAC reaching the site, through the Rockall Channel

and/or through the Iceland-Faroe Gap and the Faroe Current. Hence, despite the high insolation at the beginning of the Holocene, a weakened relative contribution of the Slope Current, once the NAC reached its full strength at ~9.4 ka BP (as indicated by the start of the thermal optimum in core LO09-14), led to colder and fresher sea surface conditions.

After 6-5 ka BP, the influence of the NAC on the Faroe-Shetland Channel diminished and was compensated by a stronger relative contribution of the warmer, more saline Slope Current. Interestingly, a record further south in the Rockall Trough (core VM29-191, Bond et al., 2001; Fig. 1) depicts generally lower percentages of ice-rafted debris after 5.2 ka BP, suggesting warmer conditions (Bond et al., 2001; Moros et al., 2006). This record agrees quite well with ours (Fig. 6). In addition, foraminifera-based SST (Risebrobakken et al., 2003) from core MD95-2011, located in the eastern Norwegian Sea under the most ENAW-influenced branch of the Norwegian Current (Poulain et al., 1996; Hansen and Østerhus, 2000), depict generally warmer conditions in the mid- to late Holocene. Here too, our SST record parallels that of core MD95-2011 (Fig. 7). Hence, it seems that several sites in the path of ENAW-influenced currents were characterized by increasing SST from the mid-Holocene onwards.

Comparison with today's climate brings to the light possible mechanisms that might cause such changes. Notably, atmospheric circulation variability can have significant effects on the oceanic circulation. Today, the leading mode of atmospheric variability in the North Atlantic region is the North Atlantic Oscillation (NAO; Hurrell, 1995). Many studies have focused on the present-day air-sea interactions caused by the NAO, which seems to be linked with significant changes in the oceanic circulation. This led several authors to suggest that the changes in the hydrography of the North Atlantic during the Holocene might be the result of a long term modulation of the NAO (e.g., Rimbu et al., 2003). However, much disagreement on whether the Holocene witnessed a shift from a dominance of positive to negative NAO-like atmospheric patterns or vice versa is apparent in the literature (e.g., Tremblay et al., 1997; Risebrobakken et al., 2003).

Nilsen et al. (2003, 2004), based on model experiments, inferred a negative correlation between the poleward flows of Atlantic waters in the Iceland-Faroe Gap and the Faroe-Shetland Channel. They suggested that an increase of the NAO index creates stronger winds that result in a decreased inflow in the Iceland-Faroe Gap and increased inflow in the

Faroe-Shetland Channel. It is not clear however if the enhanced flow in the Faroe-Shetland Channel implies a higher contribution of ENAW and thus higher SST and SSS. Care should also be taken as local climatic features can override the NAO signature. In the Faroe-Shetland Channel, Holliday (2003) studied the effect of the NAO on the amount of WNAW entering the Rockall Trough and thus freshening the water masses, and stated that no constant, direct relationship between the Rockall Trough water masses and the NAO is observed.

Other studies focused on the recent variations of the subpolar gyre strength, as observed by Häkkinen and Rhines (2004) from altimetry data. These variations do not seem to be linked to wind stress changes associated with the NAO. Hatun et al. (2005) related them to variations of SSS in the mid-latitude North Atlantic and showed that when the subpolar gyre is strong, its influence on the NAC is high, whereas the influence of the subtropical gyre is low. This would be coherent with decreasing SST on the Reykjanes Ridge after 6.5 ka BP, due to the NAC carrying a greater proportion of SAIW relative to WNAW. The second effect of the strength of the supolar gyre is to control the influence of the relatively fresh NAC in the Rockall Trough. When the gyre is strong, the influence of the NAC decreases, making the relative contribution of the Slope Current stronger. This, again, would be coherent with our data. A similar pattern of subpolar gyre strength, associated with decoupled Atlantic water-carrying currents could have characterized the eastern north Atlantic during the Holocene, although on a longer time scale.

6. Conclusion

Comparison of the dinocyst and coccolith records from the Reykjanes Ridge and the Faroe-Shetland Channel shows a remarkable agreement between the two proxies, supporting further the interpretation of assemblage variations in terms of ecological changes affecting the upper water column. Our records unequivocally indicate a major reorganisation of the northeastern North Atlantic system in the mid-Holocene, between 7 and 5.4 ka BP. This time interval corresponds with the end of meltwater supplies from decaying ice sheets (Dyke et al., 2003) and with the summer insolation decrease getting steeper (Berger and Loutre, 1991). Quantitative reconstructions of SSS yield relatively low values until 6.5-7 ka BP at

both sites, suggesting that meltwater supplies might have had a significant influence, probably through the NAC. In contrast, SST trends are very different at the two sites.

The Reykjanes Ridge record depicts an early to mid-Holocene thermal optimum coherent with previous studies and interpreted as the result of a high summer insolation. The gradual decrease in SST from 8 ka BP onwards was much sharper than the gradual insolation decrease, suggesting a non-linear response of the ocean. This is even clearer in the Faroe-Shetland Channel, where, after a short and very early thermal optimum (10.0 to 9.4 ka BP), SSTs remained relatively cold until 5.4 ka BP when a slight increase is recorded. A possible mechanism to explain this trend involves a variable influence of the poleward Atlantic-water carrying currents in the area. Our study site today lies under the influence of the NAC and the warmer, saltier Slope Current. A stronger NAC during the first half of the Holocene could have resulted in a weaker relative contribution of the Slope Current and thus lower SST and SSS. Some studies have shown modern mechanisms that might be compatible with this hypothesis, such as an anticorrelation between the flows of Atlantic waters through the Iceland-Faroe Gap and through the Faroe-Shetland Channel (Nilsen et al., 2003), and a changing balance between the influence of the subpolar gyre and that of the subtropical gyre on the waters flowing towards the Nordic seas (Hatun et al., 2005).

Acknowledgements

This study is a contribution of the Polar Climate Stability Network (PCNS) supported by the Canadian Foundation of Climate and Atmospheric Science (CFCAS). We also acknowledge financial support from the Natural Sciences and Engineering Research Council (NSERC) of Canada and the Fonds québécois de la recherche sur la nature et les technologies (FQRNT).

References

Andersen, C., N. Koç and M. Moros, 2004: A highly unstable Holocene climate in the subpolar North Atlantic: evidence from diatoms. *Quat. Sci. Rev.*, **23**, 2155-2166.

Baumann, K. H., H. A. Andruleit and C. Samtleben, 2000: Coccolithophores in the Nordic Seas: comparison of living communities with surface sediment assemblages. *Deep Sea Res. II*, **47**, 1743-1772.

Beaufort, L. and S. Heussner, 2001: Seasonal dynamics of calcareous nannoplankton on a West European continental margin: The Bay of Biscay. *Mar. Micropal.*, **43**, 27-55.

Berger, A. L. and M. F. Loutre, 1991: Insolation values for the climate of the last 10 million years. *Quat. Sci. Rev.*, **10**, 297-317.

Boessenkool, K. P., M.-J. van Gelder, H. Brinkhuis, and S. R. Troelstra, 2001: Distribution of organic-walled dinoflagellate cysts in surface sediments from transects across the polar front offshore southeast Greenland. *J. Quat. Sci.*, **16**, 661-666.

Bond, G., W. Showers, M. Cheseby, R. Lotti, P. Almasi, P. de Menocal, P. Priore, H. Cullen, I. Hajdas and G. Bonani, 1997: A pervasive millennial-scale cycle in North Atlantic Holocene and glacial climates. *Science*, **278**, 1257-1266.

Bond, G., B. Kromer, J. Beer, R. Muscheler, M. N. Evans, W. Showers, S. Hoffmann, R. Lotti-Bond, I. Hajdas and G. Bonani, 2001: Persistent Solar Influence on North Atlantic Climate During the Holocene. *Science*, **294**, 2130-2136.

Brambilla, E., 2006: The upper limb of the North Atlantic overturning circulation : investigation of the subtropical-subpolar gyre exchange and Subpolar Mode Water. Scripps Institution of Oceanography Technical Report, http://repositories.cdlib.org/sio/techreport/52

Dandonneau, Y., Y. Montel, J. Blanchot, J. Giraudeau and J. Neveux, 2006: Temporal variability in phytoplankton pigments, picoplankton and coccolithophores along a transect through the North Atlantic and tropical southwestern Pacific. *Deep-Sea Res. I*, **53**, 689-712.

de Vernal, A., M. Henry and G. Bilodeau, 1999: Technique de préparation et d'analyse en micropaléontologie. Les Cahiers du GEOTOP 3, Université du Québec à Montréal, unpublished report.

de Vernal, A., M. Henry, J. Matthiessen, P. J. Mudie, A. Rochon, K. P. Boessenkool, F. Eynaud, K. Grosfjeld, J. Guiot, D. Hamel, R. Harland, M. J. Head, M. Kunz-Pirrung, E. Levac, V. Loucheur, O. Peyron, V. Pospelova, T. Radi, J.-L. Turon and E. Voronina, 2001: Dinoflagellate cyst assemblages as tracers of sea-surface conditions in the northern North Atlantic, Arctic and sub-Arctic seas: the new $n = 677$ database and its application for quantitative palaeoceanographic reconstruction. *J. Quat. Sci.*, **16**, 681-698.

de Vernal, A., F. Eynaud, M. Henry, C. Hillaire-Marcel, L. Londeix, S. Mangin, J. Matthiessen, F. Marret, T. Radi, A. Rochon, S. Solignac and J.-L. Turon, 2005: Reconstruction of sea-surface conditions at middle to high latitudes of the Northern Hemisphere during the Last Glacial Maximum (LGM) based on dinoflagellate cyst assemblages. *Quat. Sci. Rev.*, **24**, 897–924.

de Vernal, A. and C. Hillaire-Marcel, 2006: Provincialism in trends and high frequency changes in the northwest North Atlantic during the Holocene. *Global and Planetary Change*, **54**, 263–290.

de Vernal, A. and F. Marret, 2007: Organic-walled dinoflagellate cysts: tracers of sea-surface conditions. *Proxies in Late Cenozoic Paleoceanography, Developments in Marine Geology*, No. 1, C. Hillaire-Marcel and A. de Vernal, Eds., Elsevier, 371-408.

deMenocal, P., J. Ortiz, T. Guilderson, J. Adkins, M. Sarnthein, L. Baker and M. Yarusinsky, 2000: Abrupt onset and termination of the African Humid Period: rapid climate responses to gradual insolation forcing. *Quat. Sci. Rev.*, **19**, 347-361.

Dyke, A. S., A. Moore and L. Roberson, 2003: Deglaciation of North America. Geological Survey of Canada Open File Report 1574 (CD ROM).

Eide, L. K., 1990: Distribution of coccoliths in surface sediments in the Norwegian-Greenland Sea. *Mar. Micropal.*, **16**, 65-75.

Eynaud, F., J. L. Turon and J. Duprat, 2004: Comparison of the Holocene and Eemian palaeoenvironments in the South Icelandic Basin : dinoflagellate cysts as proxies for the North Atlantic surface circulation. *Rev. of Palaeobotany and Palynology*,**128**, 55-79.

Fairbanks, R. G., 1989: A 17,000-year glacio-eustatic sea level record: influence of glacial melting rates on the Younger Fryas event and deep-ocea circulation. *Nature*, **342**, 637-642.

Flatau, M. K., L. Talley, and P. P. Niiler, 2003: The North Atlantic Oscillation, surface current velocities, and SST changes in the subpolar North Atlantic. *J. Clim.*, **16**, 2355-2369.

Giraudeau, J., M. Cremer, S. Manthé, L. Labeyrie and G. Bond, 2000: Coccolith evidence for instabilities in surface circulation south of Iceland during Holocene times. *Earth Plan. Sci. Lett.*, **179**, 257-268.

Grelaud, M., 2004: Rôle du couplage océan/atmopshère dans la variabilité climatique Holocène rapide : le cas de la Dérive Nord Atlantique. Unpublished MSc thesis, Université Bordeaux I, 31 pp.

Guiot, J., 1990: Methodology of the last climatic cycle reconstruction in France from pollen data. *Palaeogeography, Palaeoclimatology, Palaeoecology*, **80**, 49–69.

Häkkinen, S. and P. B. Rhines, 2004: Decline of subpolar North Atlantic circulation during the 1990s. *Science*, **304**, 555-559.

Hansen, B. and S. Østerhus, 2000: North Atlantic-Nordic Seas exchanges. *Prog. Oceanog.*, **45**, 109-208.

Hatun, H. A. B. Sandø, H. Drange, B. Hansen and H. Valdimarsson, 2005: Influence of the Atlantic subpolar gyre on the thermohaline circulation. *Science*, **309**, 1841-1844.

Head, M. J., R. Harland and J. Matthiessen, 2001: Cold marine indicators of the late Quaternary: The new dinoflagellate cyst genus *Islandinium* and related morphotypes. *J. Quat. Sci.*, **16**, 621-636.

Holliday, N. P., 2003: Air-sea interaction and circulation changes in the northeast Atlantic. *J. Geophys. Res.*, **108**, 3259, doi:10.1029/2002JC001344.

Holliday, N. P., J. J. Waniek, R. Davidson, D. Wilson, L. Brown, R. Sanders, R. T. Pollard and J. T. Allen, 2006: Large-scale physical controls on phytoplankton growth in the Irminger Sea Part I: Hydrographic zones, mixing and stratification. *J. Mar. Syst.*, **59**, 201-218.

Howe, J. A., R. Harland, N. M. Hine and W. E. N. Austin, 1998: Late Quaternary stratigraphy and paleoceanographic change in the northern Rockall Trough, North Atlantic Ocean. *Geological Processes on Continental Margins: Sedimentation, Mass-Wasting and Stability*, *Special Publications*, No. 129, M.S. Stoker, D. Evans and A. Cramp, Eds., Geological Society, 269-286.

Hurrell, J. W., 1995: Decadal trends in the North Atlantic Oscillation: Regional temperatures and precipitation. *Science*, **269**, 676-679.

Kaplan, M. R. and A. P. Wolfe, 2006: Spatial and temporal variability of Holocene temperature in the North Atlantic region. *Quat. Res.*, **65**, 223-231.

Kaufman, D. S., T. A. Ager, N. J. Anderson, P. M. Anderson, J. T. Andrews, P. J. Bartlein, L. B. Brubaker, L. L. Coats, L. C. Cwynar, M. L. Duvall, A. S. Dyke, M. E. Edwards, W. R. Eisner, K. Gajewski, A. Geirsdottir, F. S. Hu, A. E. Jennings, M. R. Kaplan, M. W. Kerwin, A. V. Lozhkin, G. M. MacDonald, G. H. Miller, C. J. Mock, W. W. Oswald, B. L. Otto-Bliesner, D. F. Porinchu, K. Rühland, J. P. Smol, E.J. Steig and B.B. Wolfe, 2004: Holocene thermal maximum in the western Arctic (0-180°W). *Quat. Sci. Rev.*, **23**, 529-560.

Lévesque, L., 1995: Distribution des assemblages de coccolithes dans les sediments récents des moyennes latitudes de l'Atlantique Nord: développement de fonctions de transfert paléocéanographiques. MSc Thesis, Université du Québec à Montréal, 93 pp.

Marchal, O., I. Cacho, T. F. Stocker, J. O. Grimalt, E. Calvo, B. Martrat, N. Shackelton, M. Vautravers, E. Cortijo, S. van Kreveld, C. Andersson, N. Koç, M. Chapman, L. Sbaffi, J.-C. Duplessy, M. Sarnthein, J.-L. Turon, J. Duprat and E. Jansen, 2002: Apparent cooling of the

sea surface in the northeast Atlantic and Mediterranean during the Holocene. *Quat. Sci. Rev.*, **21**, 455-483.

Matthews, J., 1969: The assessment of a method for the determination of absolute pollen frequencies. *New Phytologist*, **68**, 161-166.

Moros, M., K. Emeis, B. Risebrobakken, I. Snowball, A. Kuijpers, J. McManus, and E. Jansen, 2004: Sea surface temperatures and ice rafting in the Holocene North Atlantic: climate influences on northern Europe and Greenland. *Quat. Sci. Rev.*, **23**, 2113-2126.

Moros, M., J. T. Andrews, D. D. Eberl and E. Jansen, 2006: Holocene history of drift ice in the northern North Atlantic: Evidence for different spatial and temporal modes. *Paleoceanography*, **21**, PA2017, doi:10.1029/2005PA001214.

National Oceanographic Data Center (NODC), 2001: World ocean atlas, http://www.nodc.noaa.gov/OC5/WOD01/pr_wod01.html, Silver Springs, Md.

National Snow and Ice Data Center (NSIDC), 2003: Arctic and Southern Ocean sea ice concentrations. http://nsidc.org/data/docs/noaa/g00799_arctic_southern_sea_ice/index.html, Boulder, CO.

Nilsen, J. E. O., Y. Gao, H. Drange, T. Furevik and M. Bentsen, 2003: Simulated North Atlantic-Nordic Seas water mass exchanges in an isopycnic coordinate OGCM. Geophys. *Res. Lett.*, **30**, 1536, doi:10.1029/2002GL016597.

Nilsen, J. E. O., H. Hatun, A. B. Sando, I. Bethke, O. Laurantin, Y. Gao, H. Drange and T. Furevik, 2004: On the recent time history and forcing of the inflow of Atlantic Water to the Arctic Mediterranean. Extended abstract, *International Scientific Symposium on Climate Change in the Arctic*, Reykjavik, Iceland, Arctic Climate Impact Assessment.

Pollard, R. T., M. J. Griffiths, S. A. Cunningham, J. F. Read, F. F. Pérez and A. F. Rios, 1996: Vivaldi 1991 - A study of the formation, circulation and ventilation of Eastern North Atlantic Central Water. *Prog. Oceanog.*, **37**, 167-192.

Pollard, R. T., J. F. Read and N. P. Holliday, 2004: Water masses and circulation pathways through the Iceland Basin during Vivaldi 1996. *J. Geophys. Res.*, **109**, C04004, doi:10.1029/2003JC002067.

Poulain, P.-M., A. Warm-Varnas and P. P. Niiler, 1996. Near-surface circulation of the Nordic seas as measured by Lagrangian drifters. *J. Geophys. Res.*, **101**, 18,237-18,258.

Prins, M. A., S. R. Troelstra, R. W. Kruk, K. van der Borg, A. F. M. de Jong, and G. J. Weltje, 2001: The Late Quaternary sedimentary record of Reykjanes Ridge, North Atlantic. *Radiocarbon*, **43**, 939–947.

Read, J. F., 2001: CONVEX-91: water masses and circulation of the Northeast Atlantic subpolar gyre. *Prog. Oceanog.*, **48**, 461-510.

Reverdin, G., P. P. Niiler and H. Valdimarsson, 2003: North Atlantic Ocean surface currents. *J. Geophys. Res.*, **108**, 3002, doi:10.1029/2001JC001020.

Rimbu, N., G. Lohmann, J.-H. Kim, W. Arz and R. Schneider, 2003: Arctic/North Atlantic Oscillation signature in Holocene sea surface temperature trends as obtained from alkenone data. *Geophys. Res. Lett.*, **30**, 1280, doi:10.1029/2002GL016570.

Risebrobakken, B., E. Jansen, C. Andersson, E. Mjelde and K. Hevroy, 2003: A high-resolution study of Holocene paleoclimatic and paleoceanographic changes in the Nordic Seas. *Paleoceanography*, **18**, 1017, doi:10.1029/2002PA000764.

Rochon, A., A. de Vernal, J.-L. Turon, J. Matthiessen and M. J. Head, 1999: Distribution of dinoflagellate cyst assemblages in surface sediments from the North Atlantic Ocean and adjacent basins and quantitative reconstruction of sea-surface parameters. *Special Contribution Series of the American Association of Stratigraphic Palynologists*, No. 35, Houston, TX, 7-54.

Samtleben, C.and A. Schröder, 1992: Living coccolithophore communities in the Norwegian-Greenland Sea and their record in sediments. *Mar. Micropal.*, **19**, 333-354.

Siesser, W.G., 1993: Calcareous nannoplankton. *Fossil prokaryotes and protists*, J. H. Lipps, Ed., Blackwell Scientific Publications, 169-201.

Solignac, S., A. de Vernal and C. Hillaire-Marcel, 2004: Holocene sea-surface conditions in the North Atlantic – contrasted trends and regimes in the western and eastern sectors (Labrador Sea vs. Iceland Basin). *Quat. Sci. Rev.*, **23**, 319-334.

Solignac, S., J. Giraudeau and A. de Vernal, 2006: Holocene sea surface conditions in the western North Atlantic : Spatial and temporal heterogeneities. *Paleoceanography*, **21**, doi:10.1029/2005PA001175.

Steig, E.J., 1999: Mid-Holocene climate change. *Science*, **286**, 1485-1487.

Stoker, M. S., R. Harland, A. C. Morton and D. K. Graham, 1989: Late Quaternary stratigraphy of the northern Rockall Trough and Faroe-Shetland Channel, northeast Atlantic Ocean. *J. Quat. Sci.*, **4**, 211-222.

Stuiver, M., and P. J. Reimer, 1993: Extended ^{14}C database and revised CALIB radiocarbon calibration program. *Radiocarbon*, **35**, 215-230.

Tremblay, L. B., L. A. Mysak and A. S. Dyke, 1997: Evidence from driftwood records for century-to-millenial scale variations of the high latitude atmospheric circulation during the Holocene. *Geophys. Res. Lett.*, **24**, 2027-2030.

Ziveri, P., K.-H. Baumann, B. Böckel, J. Bollmann and J. R. Young, 2004. Biogeography of selected Holocene coccoliths in the Atlantic Ocean. *Coccolithophores: From Molecular Processes to Global Impacts*, H. R. Thiersten and J. R. Young, Eds., Springer Verlag, 403-428.

Zonneveld, K. A. F., G. J. M. Versteegh and G. J. de Lange, 2001a. Palaeoproductivity and post-depositional aerobic organic matter decay reflected by dinoflagellate cyst assemblages of the Eastern Mediterranean S1 sapropel. *Mar. Geol.*, **172**, 181-195.

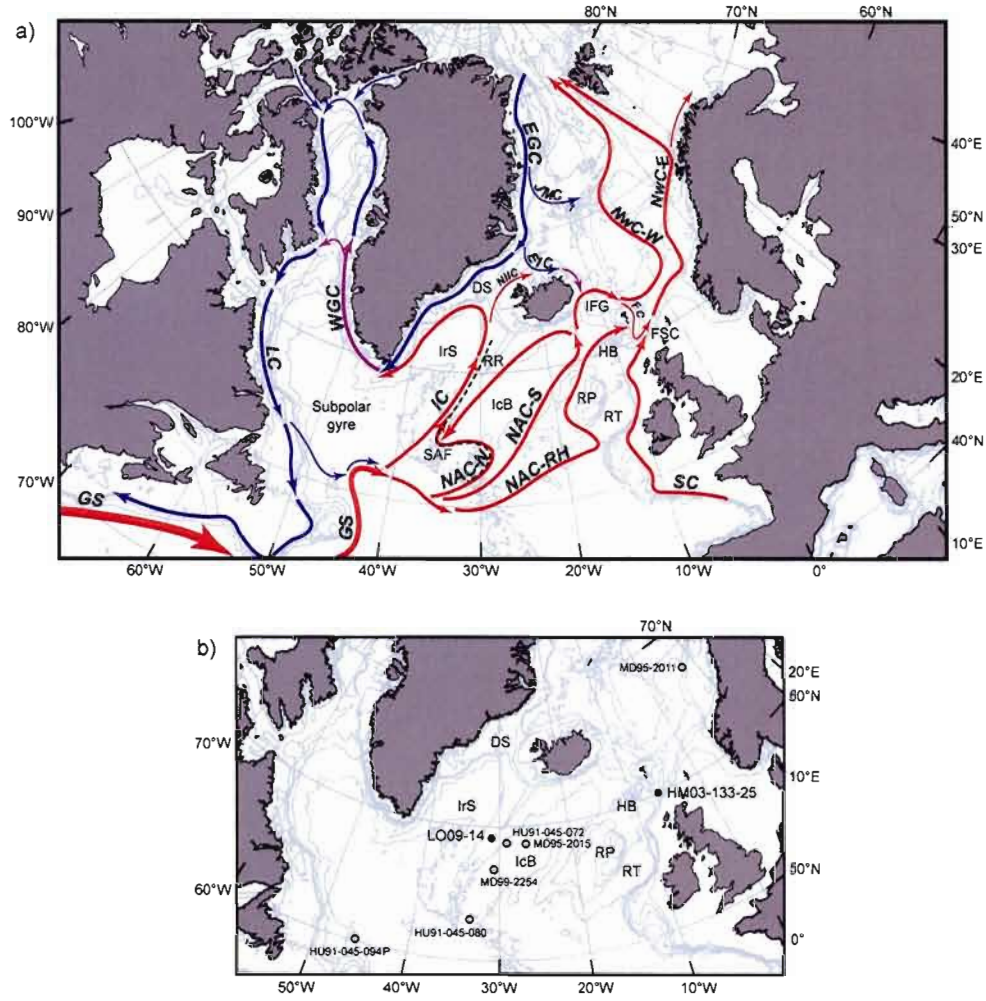

Figure 1. a) Trajectories of the main ocean surface currents (GS: Gulf Stream, LC: Labrador Current, WGC: West Greenland Current, EGC: East Greenland Current, JMC: Jan Mayen Current, EIC: East Iceland Current, NIIC: North Icelandic Irminger Current, IC: Irminger Current, NAC-N: northern branch of the North Atlantic Current, NAC-S: southern branch, NAC-RH: Rockall-Hatton branch, SC: Slope Current, FC: Faroe Current, NwC-W: western branch of the Norwegian Current, new: eastern branch), and location of the regions discussed in the text (DS: Denmark Strait, IrS: Irminger Sea, RR: Reykjanes Ridge, IcB: Iceland Basin, RP: Rockall Plateau, RT: Rockall Trough, HB: Hatton Banks, IFG: Iceland-Faroe Gap, FSC: Faroe-Shetland Channel). Blue arrows represent cold currents and red arrows represent warm currents. The dashed line corresponds with the Subarctic Front (SAF).
b) Location of cores HM03-133-25 and LO09-14 and other cores discussed in the text. Isobaths correspond to 2000, 1000 and 200 m water depths.Trajectories of the main ocean surface currents.

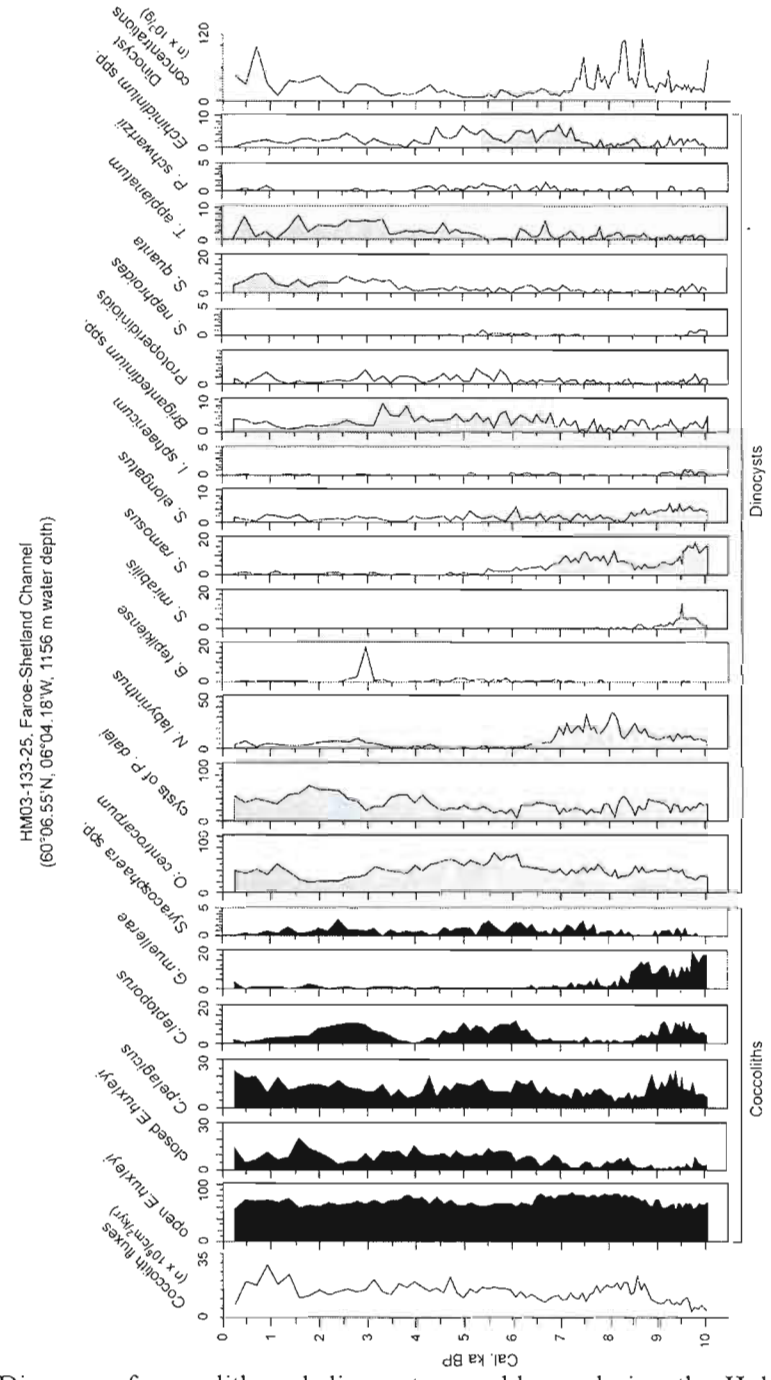

Figure 2a. Diagram of coccolith and dinocyst assemblages during the Holocene in core HM03-133-25. Percentages of each species are relative to either the sum of coccoliths (in black) or dinocysts (in grey). Note the different scales used for dominant and accompanying taxa.

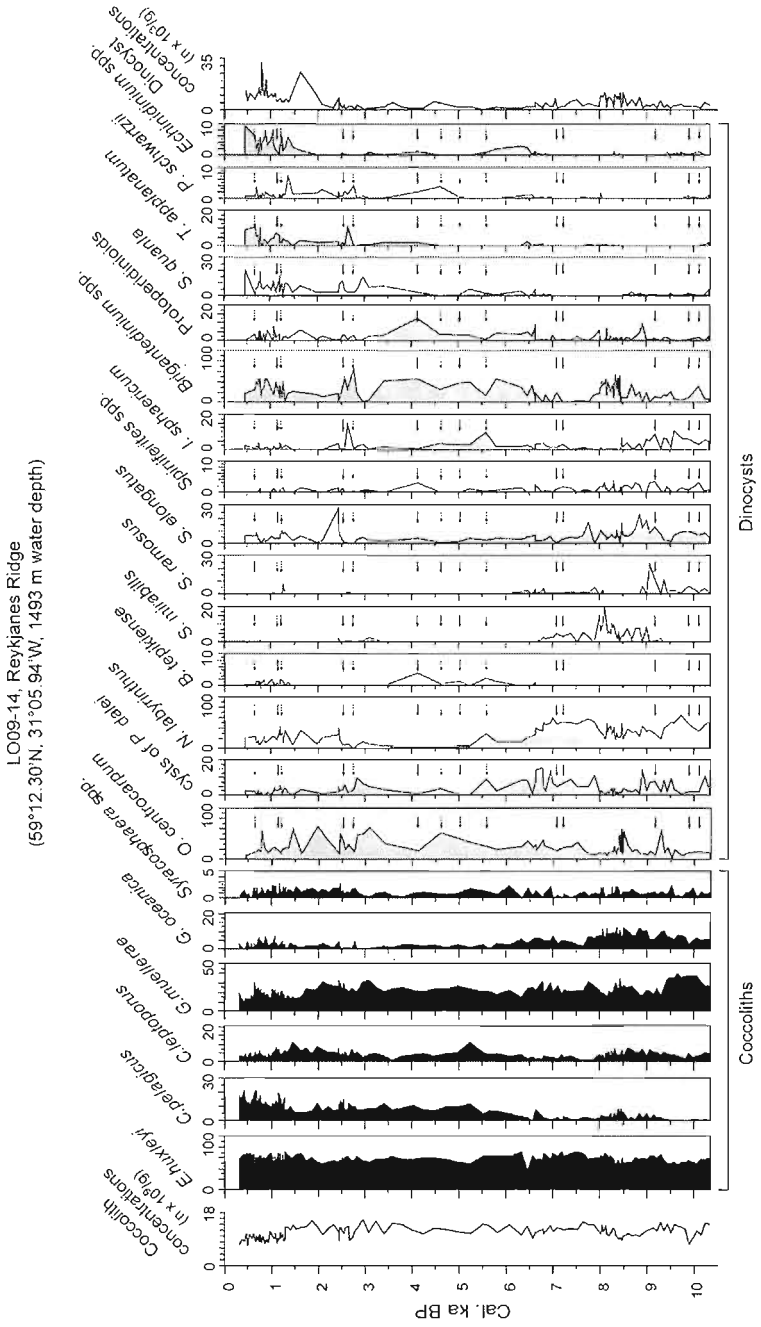

Figure 2b. Diagram of coccolith and dinocyst assemblages during the Holocene in core LO09-14. Percentages of each species are relative to either the sum of coccoliths (in black) or dinocysts (in grey). Note that different scales were used for dominant and accompanying taxa, and that open and closed morphotypes of E. huxleyi were not distinguished in this core. Arrows indicate levels for which too few dinocysts were counted for quantitative reconstructions.

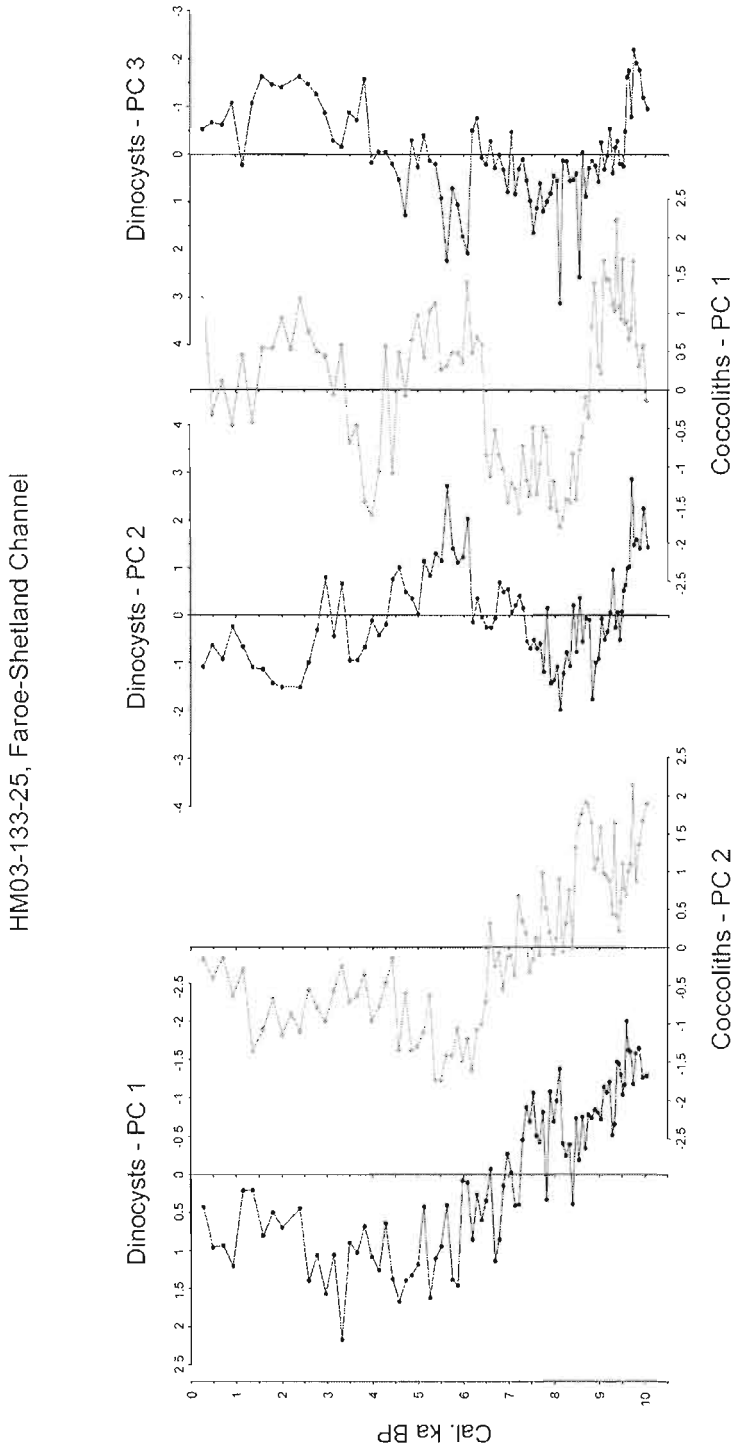

Figure 3a. Eigenvalues of the first principal components extracted from the dinocyst (black) and coccolith records (grey) of core HM03-133-25.

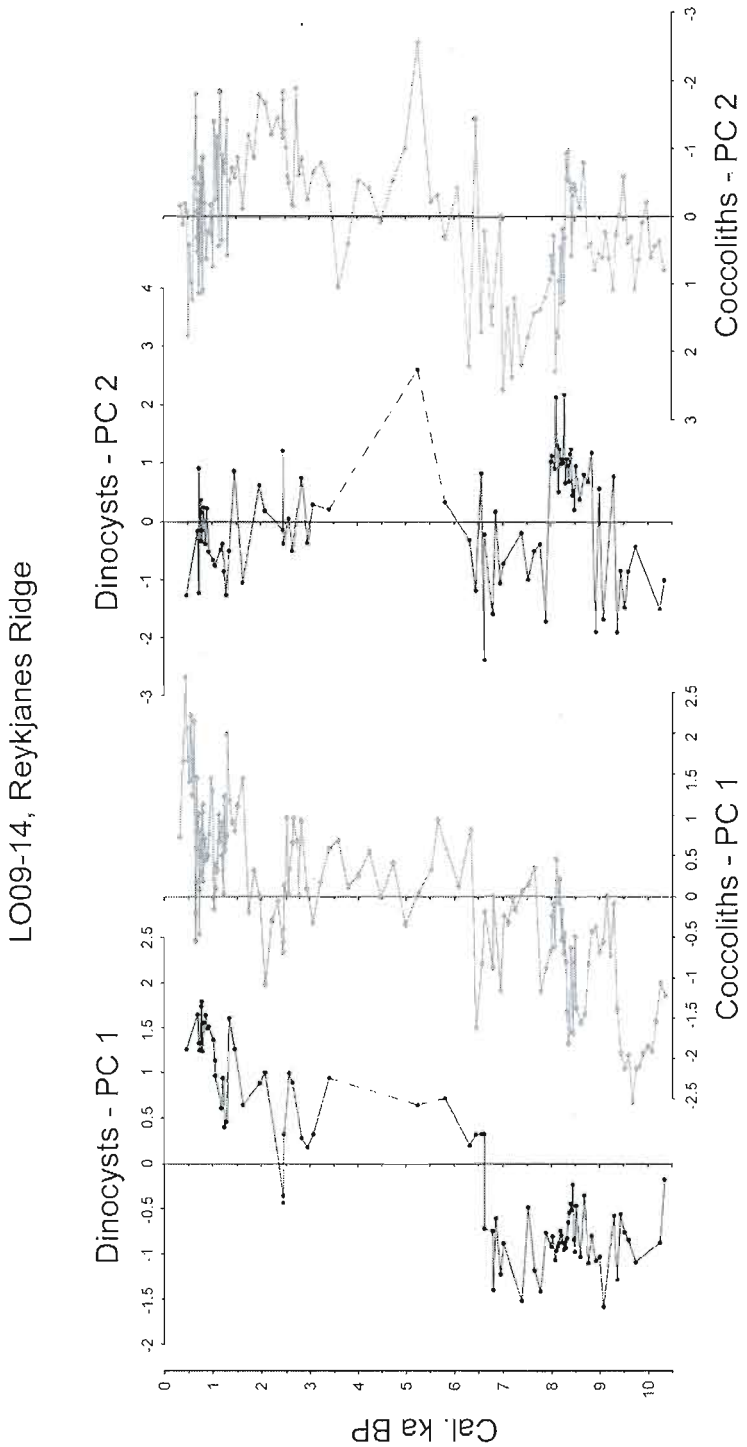

Figure 3b. Eigenvalues of the first principal components extracted from the dinocyst (black) and coccolith records (grey) of core LO09-14. Dashed lines link data points in the interval of sparse quantitative results.

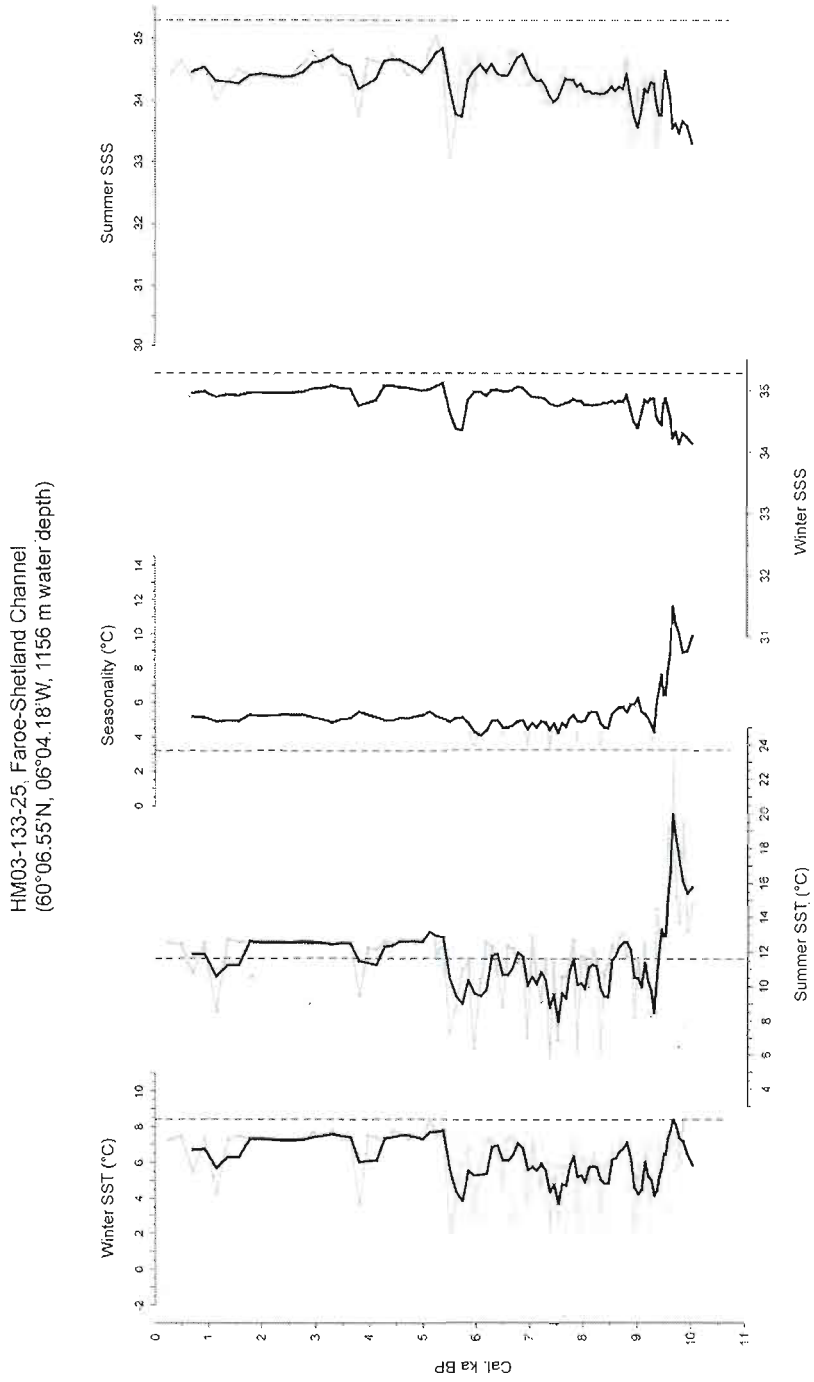

Figure 4a. Reconstruction of sea surface conditions during the Holocene in core HM03-133-25 based on dinocyst assemblages and using the best analogue method described in de Vernal et al. (2005). Bold curves are smoothed records (3-point running mean). Vertical dashed lines are modern values at this site, along with standard deviations of the measurements (grey areas) (NODC, 2001).

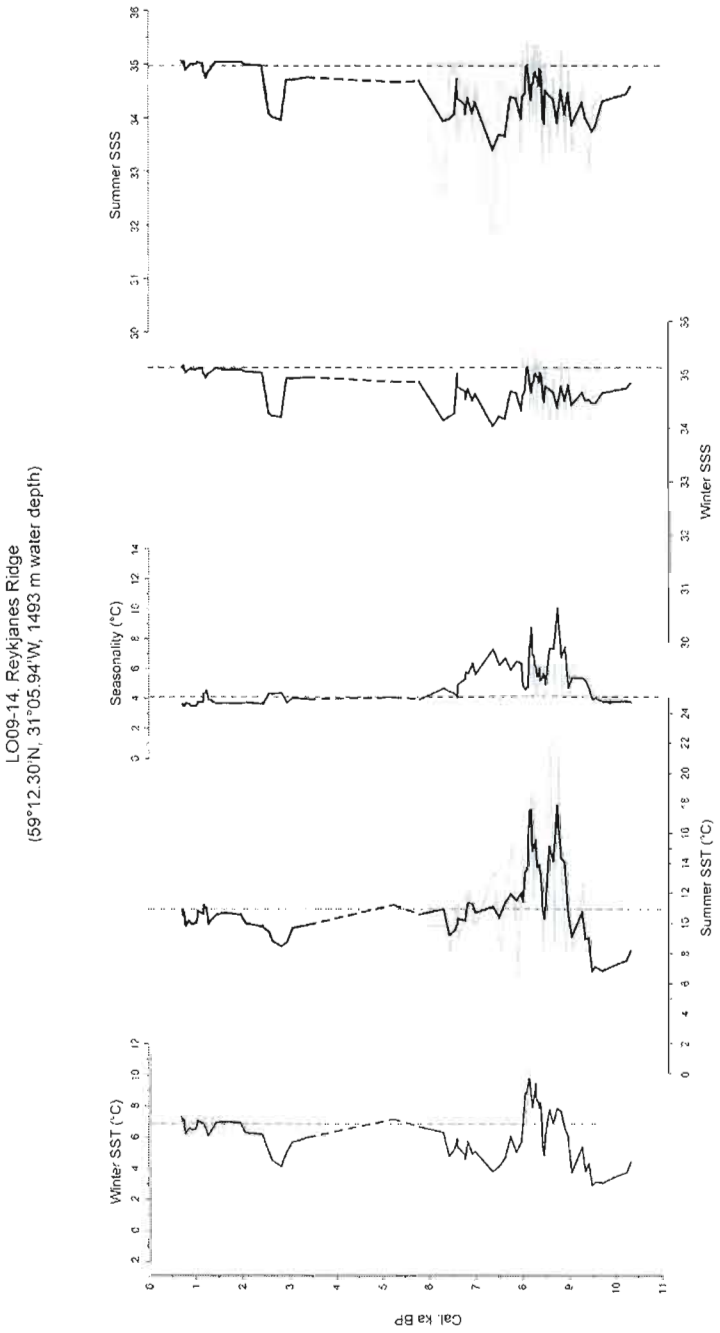

Figure 4b. Reconstruction of sea surface conditions during the Holocene in core LO09-14 based on dinocyst assemblages and using the best analogue method described in de Vernal et al. (2005). Bold curves are smoothed records (3-point running mean). Vertical dashed lines are modern values at this site, along with standard deviations of the measurements (grey areas) (NODC, 2001). Dashed lines link data points in the interval of sparse quantitative results.

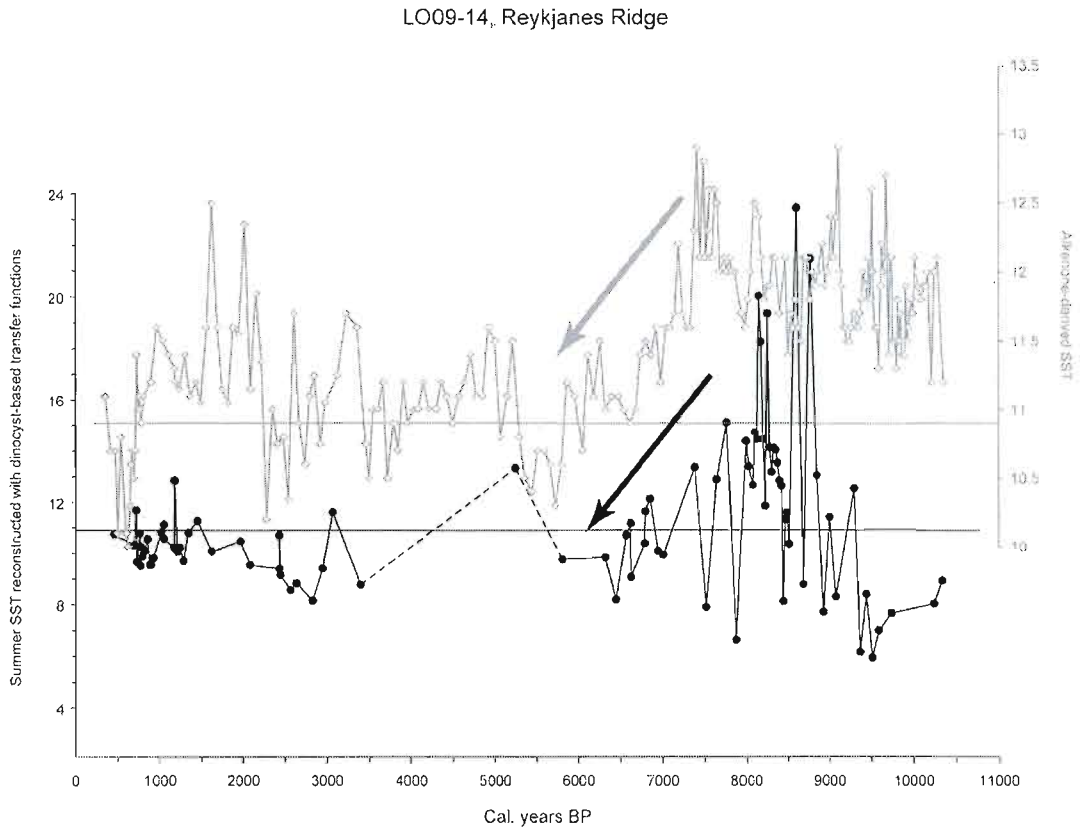

Figure 5. Comparison of dinocyst-based (black curve, 3-point running mean) and alkenone-derived (grey curve, Moros et al., 2004) SST records of core LO09-14. Note that different scales were used for the two records, as the amplitude of dinocyst-based SST changes is much larger than that of the alkenone record. Horizontal lines are the modern SST value at this site (NODC, 2001). Dashed lines link data points in the interval of sparse quantitative results.

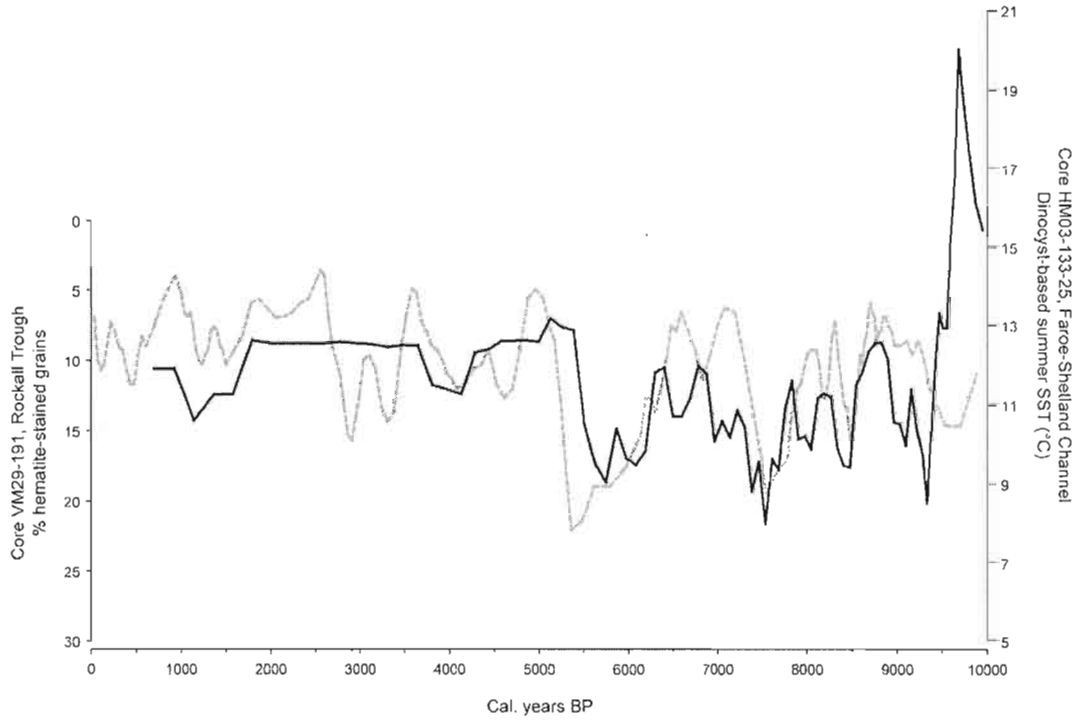

Figure 6. Comparison of dinocyst-based SST (black curve, 3-point running mean) of core HM03-133-25 with percentages of hematite-stained grains of core VM29-191, Rockall Trough (grey curve, Bond et al., 2001). Note the inverse scale for the hematite-stained grains.

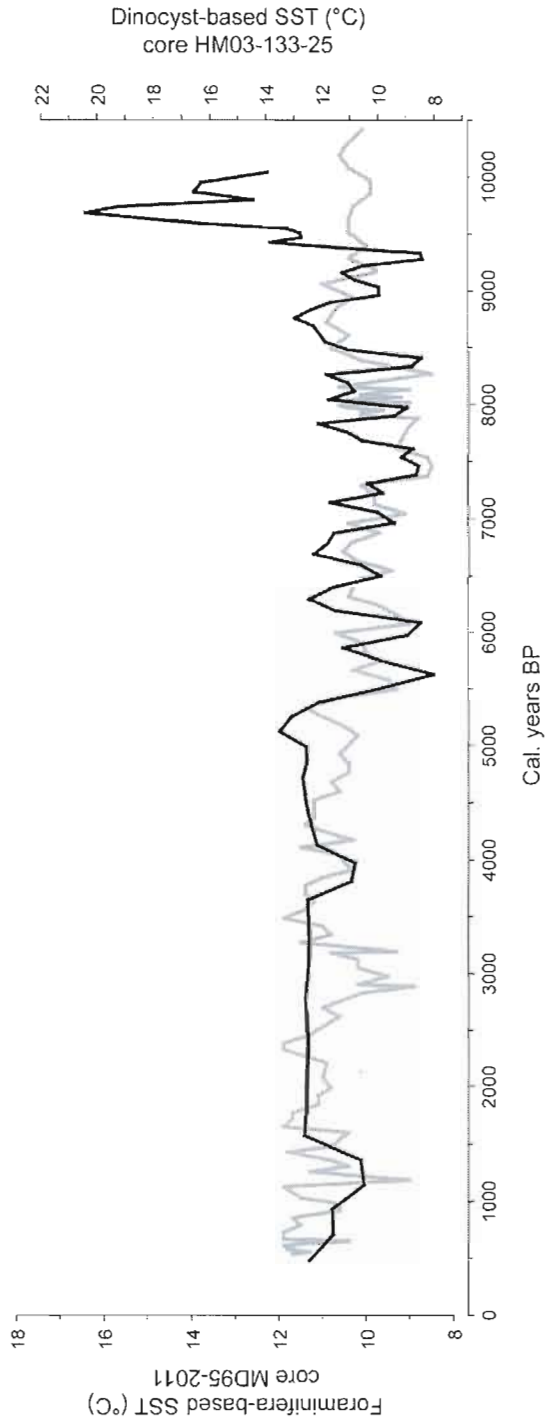

Figure 7. Comparison of dinocyst-based SST (black curve, 3-point running mean) of core HM03-133-25 with foraminifera-based SST of core MD95-2011, Voring Plateau (grey curve, Risebrobakken et al., 2003). Note the different scales used for the two records.

CHAPITRE III

COMPARISON OF COCCOLITH AND DINOCYST ASSEMBLAGES IN THE NORTHERN NORTH ATLANTIC: HOW WELL DO THEY RELATE WITH SURFACE HYDROGRAPHY?

Sandrine Solignac[1], Anne de Vernal[1] and Jacques Giraudeau[2]

[1]GEOTOP-UQAM, C.P. 8888, Succursale Centre-ville, Montréal, QC, H3C 3P8

[2]Environnements et Paléoenvironnements Océaniques, UMR CNRS 5805, Université Bordeaux 1, Avenue des Facultés, 33405 Talence cedex, France

Article sous presse dans la revue *Marine Micropaleontology*

Résumé

Des dénombrements de coccolithes et de kystes de dinoflagellés (ou dinokystes) dans des échantillons de sédiments de surface ont été compilés à partir de base de données existantes ainsi que de nouveaux comptages afin de mettre sur pieds une base de données de 87 sites pour lesquels les deux groupes de microfossiles ont été analysés. Cette base de données permet une comparaison directe de la distribution des assemblages de coccolithes et de dinokystes dans l'Atlantique Nord subtropical à subpolaire. De plus, la relation entre ces assemblages et les paramètres environnementaux de surface de l'océan est étudiée, afin d'identifier d'éventuelles différences dans l'écologie des deux groupes de plancton.

La comparaison met en évidence une excellente correspondance entre les assemblages de dinokystes, les assemblages de coccolithes et la distribution des masses d'eau de surface couvertes par notre base de données, notamment dans les domaines subtropical et tempéré. Dans le domaine subpolaire, les assemblages de coccolithes sont nettement moins diversifiés en termes d'espèces que ceux de dinokystes. Ainsi, la distinction entres les différentes masses d'eau subpolaires à partir des assemblages de coccolithes n'est pas aussi claire que dans les régions subtropicales et tempérées, alors que la distribution des assemblages de dinokystes est clairement reliée à l'hydrographie de surface même dans le domaine subpolaire.

Des analyses de correspondance canonique menées sur les assemblages de coccolithes et de dinokystes montrent que la température de surface de l'océan est le paramètre environnemental ayant la plus grande influence sur la distribution des deux groupes. Les assemblages de dinokystes semblent également être influencés par la distance à la côte, et pourraient ainsi fournir des informations supplémentaires comparé aux assemblages de coccolithes. Les autres facteurs environnements significatifs incluent la salinité de surface et la productivité, mais leur influence relative change selon que des échantillons provenant de conditions environnementales « extrêmes » sont inclus ou non dans la base de données. Les résultats suggèrent qu'il est difficile de faire ressortir tous les différents environnements par des analyses multivariées en raison de la complexité des interrelations entre les divers paramètres environnementaux. Malgré cela, chaque masse d'eau de surface couverte par notre base de données est caractérisée par une combinaison unique de paramètres environnementaux, ainsi que par des associations distinctes d'assemblages de dinokystes et de coccolithes. Cela montre que ces groupes de microfossiles sont étroitement liés aux conditions de surface de l'océan, particulièrement la température, la salinité et la productivité.

Abstract

Coccolith and dinoflagellate cyst (or dinocyst) population counts were compiled from existing surface sediment databases as well as new counts in order to establish an 87-sample database for which assemblages of both microfossil groups are known. This database allowed a direct comparison of the distribution of coccolith and dinocyst assemblages in the subtropical to subpolar North Atlantic. In addition, the relationship between these assemblages and sea surface environmental parameters was addressed, in order to identify possible differences in the ecology of the two plankton groups.

The comparison highlights an excellent correspondence between dinocyst assemblages, coccolith assemblages and the distribution of the surface water masses represented in our database, notably in the subtropical and temperate domains. In the subpolar domain, coccolith assemblages are much less diversified than dinocyst assemblages in terms of species. As a result, the discrimination between the subpolar water masses based on coccolith assemblages is not as clear as in the subtropical/temperate regions, whereas dinocyst assemblages show a distribution pattern closely related with surface hydrography.

Canonical correspondence analyses performed on coccolith and dinocyst assemblages show that sea surface temperature is the primary environmental parameter influencing the distribution of both groups. Dinocyst assemblages also seem to respond to the distance to the coast, and may therefore bring additional information compared with coccolith assemblages. Other significant environmental factors include sea surface salinity and productivity, but their relative importance changes depending on the inclusion of samples from extreme environmental settings in the database. Results suggest that the complexity of the interrelationships between the various environmental parameters makes it difficult to adequately bring to light all the different environments and their associated coccolith/dinocyst assemblages in multivariate analyses. However, each surface water mass represented in our database is characterized by a unique combination of environmental parameters as well as by distinct associations of coccolith and dinocyst assemblages, thus showing that these microfossil groups closely relate to sea surface conditions, including temperature, salinity and productivity.

Keywords: dinoflagellate cyst, coccolith, North Atlantic, distribution, hydrography, multivariate analysis

1. Introduction

Numerous mineralogical, isotopic, molecular or micropaleontological proxies have been developed in order to reconstruct sea-surface hydrographical parameters. Few studies however use a combination of these indicators for paleoceanographic reconstructions, even though comparison of different proxy records obtained on the same samples are known to yield significant discrepancies (e.g., Calvo et al., 2002; Dolven et al., 2002 and Risebrobakken et al., 2003), highlighting the need for a better understanding of the various proxy signals.

Here we examine two widely used micropaleontological proxies, coccoliths and dinoflagellate cysts (or dinocysts), which are the fossil remains of coccolithophores and dinoflagellates, respectively. These microorganisms thrive in the upper water column, mainly in the photic zone, making them good tracers of sea-surface conditions such as temperature and/or salinity. Many studies have indeed shown a significant relationship between the coccolith or dinocyst assemblages and the overlying water masses and used these microfossils for qualitative and quantitative paleohydrological reconstructions (e.g., Geitzenauer et al., 1976, Eide, 1990, Samtleben and Schröder, 1992, de Vernal et al., 1994, 1997, Baumann et al., 2000).

Although a few projects aimed at comparing the two proxies, either in their modern distribution or in long-term records (e.g., Baumann and Matthiessen, 1992, Hass et al., 2001, Matthiessen et al., 2001, Vink et al., 2003), none of these were conducted on a large spatial scale in the North Atlantic. The mid-latitude North Atlantic, the Labrador Sea and the Nordic Seas are characterized by strong physico-chemical gradients at the sea surface. They are also the scene of major oceanographic processes, such as deep-water convection, thus having a primary role in both the thermohaline circulation and the climate system. In view of the complexity of the area, it appears essential to use several complementary tracers to accurately assess past hydrographical changes. Hence, the goal of this study was to compare the modern distribution of coccolith and dinocyst assemblages and to identify potentially distinct environmental requirements for the two groups that might help refining paleoceanographic reconstructions.

2. Oceanographic setting

The northern North Atlantic area is characterized by poleward-flowing warm and saline waters carried by the Gulf Stream and its northern branches (the North Atlantic Drift, the Irminger Current and the Norwegian Current; Poulain et al., 1996, Hansen and Osterhus, 2000, Read, 2001, Pollard et al., 2004), as well as by the cold, fresh, southward East Greenland and Labrador currents (Fig. 1, Lazier and Wright, 1993, Woodgate et al., 1999). These contrasting water masses mix in the Nordic Seas through secondary branches of the main currents such as the warm North Iceland Irminger Current and the cold Iceland and Jan Mayen currents. Mixing between Atlantic and Arctic waters also occurs in the Labrador Sea where the Irminger Current meets the East Greenland Current, forming the relatively warm West Greenland Current. In the south, another branch of the Gulf Stream, known as the Azores Current, originates near the Grand Banks (40°N, 45°W), flows southeastward and then eastward between 33.5 and 35°N until it reaches the African coast and the Gulf of Cadiz (Reverdin et al., 2003; Fig. 1). North of the Azores Current, the coast of Portugal is influenced by the southward Portugal Current, as well as by the southward Portugal Coastal Countercurrent along the coast during downwelling season and the poleward Portugal Coastal Current during upwelling season. These two coastal currents extend from the shore to about 10-11°W (Martins et al., 2002).

A decreasing gradient of sea-surface temperature and salinity is thus observed from the south to the north/northwest of the study area. In addition, the Scotian/Newfoundland shelves are a region worth highlighting. The temperature and salinity gradients are steepest here, as this frontal area is characterized by an extremely variable circulation due to the mixing of polar and subtropical water masses, carried by the Labrador Current, the St. Lawrence River and the Gulf Stream (Longhurst, 1998). This could explain that the highest interannual temperature variability and the strongest seasonality (up to 14°C) are observed in this region (NODC, 2001). It is also worth noting that the sites nearer Newfoundland are generally colder (in winter) than the ones from Nova Scotia, due to a periodical influence of eddies from the Gulf Stream/North Atlantic Drift on the latter (Smith and Schwing, 1991). Localized coastal upwelling can also occur on the Scotian Shelf, especially in summer, when

favourable winds blow from the southwest to the northeast, bringing nutrients to the surface (Petrie et al., 1987).

3. Materials and methods

3.1. Coccolith and dinocyst modern databases

The sites used in this study are located in the North Atlantic between 34° and 73°N, from offshore Nova Scotia and Newfoundland to the coast of Portugal and up to the Nordic Seas (Fig. 2), thus covering a wide range of hydrological parameters, from subtropical to arctic conditions. Though uneven, their distribution is optimized in areas with steep environmental gradients.

Coccolith population counts were compiled from different sources and added to some new counts (see Table 1 for more details) in order to establish a North Atlantic modern database comprising 163 surface sediment samples (Fig. 2). Identification of the different coccolith species was not always consistent among the different sources; it was therefore necessary to standardize the counts according to updated taxonomical concepts (Giraudeau and Beaufort, 2007, and references therein). The resulting database comprises 12 coccolith taxa (see Appendix A for details on the taxonomy). The deep-dwelling species *Florisphaera profunda* was excluded, as it was not taken into account in some of the samples. However, many of our sites lie north of the 10°C isotherm at 100 m depth (NODC, 2001), decreasing the probability that *F. profunda* made up an important part of the coccolithophore communities, as temperature seems to be a limiting factor (Okada and Honjo, 1973). Also, a few *Algirosphaera robusta* were identified in some of the samples but this species was not included in the database as it was not clear if its absence in the other samples was a real ecological signal or if it was not taken into account either. Unfortunate as it is, we believe that excluding *A. robusta* from our counts did not create a significant bias, since its relative abundance never reached more than 2% in the samples in which it was identified. Morever, both *F. profunda* and *A. robusta* are species that dwell between 100 and 200 m (Okada and Honjo, 1973, Knappertsbusch, 1993, Samtleben et al., 1995), i.e., at significantly lower depths than other coccolithophores,. In this respect, they can be seen as part of another

planktonic community that is not influenced by the hydrography of the very surface of the ocean, making their exclusion from the database less of a problem.

In order to eliminate any bias related to small-scale hydrographical features, depositional processes or sampling artefacts, which might result in a strong spatial variability, we chose to present the counts from only 87 of these sites, on which dinocyst population counts were also conducted, rather than comparing neighbouring samples from the two groups. However, the 87 samples are not evenly distributed in the study area, and in some instances references will be made to the more extensive database they are taken from in order to avoid any misinterpretation of the species distribution. In these 87 sites, 9 coccolith taxa were observed (Appendix A).

An extensive modern dinocyst database with 1075 sites was established in the course of the last decade (de Vernal et al., 2005 and references therein), covering the northeastern Pacific, the Arctic, the North Atlantic and their adjacent seas. Here, for comparison purposes, we selected only the samples common to the coccolith database, providing us with an 87-site database in which counts of both microfossils were carried out (Fig. 2, Table 1). In total, 45 dinocyst taxa were used for statistical treatments (Appendix B).

3.2. Environmental data

Winter (January to March), spring (April to June), summer (July to September), fall (October to December) sea-surface temperatures (SST) and salinities (SSS) were evaluated at each site from the NODC Ocean Atlas (2001). In addition, the interannual temperature variability was assessed through the annual SST standard deviation calculated on the 100 years of measurements (NODC, 2001). It will be referred to as sdSST. The sea surface temperature seasonal contrast ($\Delta SST_{sum\text{-}win}$) was calculated as the difference between the summer and winter sea surface temperatures. These two variables were estimated in order to identify taxa that are more sensitive to strong environmental variability.

Productivity values for each season (Antoine et al., 1996) were compiled for each site as well, as it has been shown that microfossil assemblages are related to primary productivity (e.g., Devillers and de Vernal, 2000; Ziveri et al., 2004; Radi and de Vernal, submitted), and because this parameter is directly related to important physical and chemical

properties of the water column, such as the depth and seasonal cycle of the mixed layer and its nutrient content. Finally, the distance to the nearest coastline was measured and included in the environmental database as an indicator of the neritic/open ocean setting of the various sites.

3.3. Statistical analyses

Multivariate analyses were used in order to highlight a possible structure in the distribution of the coccolith and dinocyst assemblages in relation with the surface water masses of the study region. We chose the canonical correspondence analysis (CCA) among the various multivariate analyses available, because, as a direct gradient analysis, it allows the identification of the environmental parameters potentially responsible for the distribution of the species assemblages (Ter Braak, 1986). In the graphic representation of the CCA results, the position of the eigenvectors representing the parameters provides information about their contribution to the variability within the assemblages: the closer to being parallel to either CCA axis a vector is, the higher its correlation with this particular axis, and the longer a vector is, the stronger the apparent influence of this parameter on the distribution of the species (Ter Braak, 1986). Similarly, the positions of the vectors relative to each other can bring useful information: the closer to being parallel two vectors are, the more (anti)correlated the variables (depending on their respective directions), whereas the closer to being orthogonal, the more independent. The CANOCO software of Ter Braak and Smilauer (1998) also allows the computation of the statistical significance of a parameter's contribution to the assemblage variability (here p values lower than 0.05 indicate a statistically significant relationship). Two CCA were thus performed using CANOCO, one on the 87-site coccolith database and the other on the corresponding dinocyst database.

Logarithmic transformations were conducted on both coccolith and dinocyst relative abundances in order to increase the weight of the rare species relative to the overwhelmingly dominant ones in the multivariate analyses. These dominant species, such as the coccolith *E. huxleyi* or the dinocyst *O. centrocarpum*, can tolerate large environmental variations in their habitats. Inversely, rarer species tend to have narrower ecological requirements, and

therefore might provide more precise information on the environment to be reconstructed than the ubiquitous dominant species.

4. Results

A qualitative examination of the assemblages from the various domains included in the 87-site database reveals clearly distinct coccolith assemblages for each of the subtropical and temperate regions (offshore Portugal, Celtic Sea, south of Rockall Channel, Iceland Basin, Newfoundland and Scotian shelves, fig. 3). The distinction is less obvious in the subpolar domain due to much poorer assemblages in terms of taxon diversity. The different regions are well represented in the dinocyst assemblages as well. As a consequence, a good correspondence is observed between coccolith and dinocyst assemblages in the subtropical and temperate regions (Fig. 3). In the subpolar domain, dinocyst assemblages are much more diversified in terms of species than coccolith assemblages and allow a better representation of the overlying water masses (Fig. 3).

4.1. Coccolith assemblages in the North Atlantic

The CCA performed on the 87-site database shows a transition from warm assemblages along the Portugal coast, in the Rockall region and on the Scotian Shelf, to colder assemblages from the Iceland Sea along the first axis, which explains 51% of the variance (Fig. 4). Note that the term "warm" is used here in opposition to the coldest Icelandic sites, and that assemblages similar to our warm ones in other studies covering lower latitudes might be referred to as cool (e.g., Ziveri et al., 2004). The warm assemblages are characterized by subtropical to temperate taxa *Gephyrocapsa muellerae*, *Gephyrocapsa oceanica*, *Syracosphaera* spp., *Umbilicosphaera sibogae*, and *Helicosphaera* spp. (Ziveri et al., 2004), while the subarctic assemblages are overwhelmingly dominated by *Coccolithus pelagicus* and/or *Emiliania huxleyi* (Fig. 3 and 4a), as observed in numerous previous studies (e.g., Geitzenauer et al., 1977; Eide, 1990; Samtleben and Schröder, 1992; Baumann et al., 2000). Accordingly, a correlation between the first axis and SST of all seasons (R=-0.72 to -0.84, Table 2) is observed, with a higher coefficient for fall SST. The fact that sites from a given geographical area are close to each other on the plot confirms the good correspondence

between coccolith assemblages and water masses observed in other studies (e.g., Roth, 1994, Lévesque, 1995). Sites from the different subarctic seas (Labrador, Iceland, Norwegian and Irminger seas), however, are somewhat more difficult to discriminate (Fig. 4b), due to the fact that only two species make up more than 90% of the assemblages. A subtle distinction can be made between the subpolar gyre sites (Irminger and Labrador seas) and the Nordic Seas sites (Norwegian and Iceland seas), with generally higher occurrences of *C. leptoporus* and to a lesser extent *Helicosphaera* spp. in the former (Fig. 3). This is consistent with the work of Okada and McIntyre (1979), who observed these two species in the northwestern North Atantic (although with rare occurrences). However, this distinction with the Nordic Seas is hard to interpret due to a patchy and complex distribution of *C. leptoporus* in the North Atlantic (Ziveri et al., 2004) that is not clearly related to a particular environmental factor.

The second axis, which represents 26% of the variance, puts forward an opposition between *G. oceanica* on the one hand, and *G. muellerae*, *Syracosphaera* spp. and *Rhabdosphaera* spp. on the other (Fig. 4a). It shows an inverse correlation with SSS (-0.71 to -0.74, Table 2), especially in summer and fall. *G. muellerae*, *Syracosphaera* spp. and *Rhabdosphaera* spp. seem to favour more saline environments, as opposed to *G. oceanica*, which is found in both fresher (Scotian shelf) and saline environments (Portugal coast). Interestingly, it seems from the position of summer SST and summer SSS on the plot that these two variables are quite independent since their vectors are at ~90° from each other. Such a result is surprising, as a strong correlation is generally observed between SST and SSS in the North Atlantic, where warm, saline Atlantic waters flow next to cold, fresh polar/Arctic waters. This apparent contradiction may find its explanation in the peculiar hydrographical setting of the Scotian and Newfoundland shelves, where relatively warm summer SST are associated with very low SSS due to the influence of freshwater from the St. Lawrence River (Loder et al., 1997). These sites alone are enough to weaken the otherwise strong correlation between SST from SSS in the database. Accordingly, the assemblages from Nova Scotia (and to a lesser extent Newfoundland) are distinct from the rest of the database (Fig. 3), with the highest relative abundances of *C. leptoporus* and *G. oceanica*.

4.2. Dinocyst assemblages

The CCA performed on the 87 dinocyst assemblages reveals a major difference with the coccolith assemblages (Fig. 5). While in the latter, the various environments are reflected by variations in the relative abundances of no more than 9 species, in the dinocyst assemblages, the differentiation between the environments is much more pronounced, with some species unique to certain settings. This is clearly seen in Fig. 3, where sites from offshore Portugal and from the Celtic Sea stand out due to species that are not found in any of the other samples presented here, such as *Lingulodinium machaerophorum*, dominant at the Portuguese sites, and *Dubridinium* spp. and *Quinquecuspis concreta* in the Celtic Sea (Marret and Scourse, 2002). As a result, the other sites are clustered together on the plot. Nevertheless, a closer examination of this cluster reveals again a distribution of the sites coherent with their geographic region (Fig. 5c).

The first axis of the CCA (44% of the variance) performed on the dinocyst assemblages puts forward an opposition between warm and cold taxa, again coherent with a predominant influence of SST on the composition of the assemblages (Fig. 5). The dinocyst assemblages are strongly correlated with SST of all seasons (R=0.76 to 0.85), with a stronger coefficient for spring (Table 3). The warmest assemblages are from offshore Portugal and are dominated by *L. machaeoroporum*, a taxa known for its preference for temperate to tropical environments (Marret and Zonneveld, 2003), followed by North Atlantic Drift-influenced assemblages dominated by *Operculodinium centrocarpum* along with *Spiniferites elongatus* and/or *Spiniferites mirabilis* and by *Spiniferites ramosus*-dominated assemblages from the Celtic Sea. These secondary species are gradually replaced with subpolar species *Nematosphaeropsis labyrinthus* and/or cysts of *Pentapharsodinium dalei* towards the Norwegian Sea. With dinocyst assemblages, the distinction between the different subarctic seas is more obvious than with the coccolithes (Fig. 4b and 5c), with *N. labyrinthus* having much higher relative abundances in the subpolar gyre compared with the Nordic Seas and the coldest sites in the north of the Iceland Sea comprising high proportions of cold species

Impagidinium pallidum and *Islandinium minutum* (Fig. 3, Matthiessen, 1995; Head et al., 2001). The first axis is also correlated with winter and fall productivity (R= 0.78 and 0.70).

The second axis (33% of the variance) correlates positively with the distance from the coast (R=0.57) and negatively with spring productivity (R=-0.59). Here the distinction between neritic species, such as *L. machaerophorum*, and open ocean taxa, such as *Impagidinium* species or *N. labyrinthus* (Rochon et al., 1999; Marret et al., 2004), along the second axis is not very clear. However, a strong neritic/open ocean component has been shown in the distribution of dinocyst assemblages in previous studies (e.g., Rochon et al., 1999; Marret and Zonneveld, 2003; Radi et al., 2007), and a clear increase in the relative abundance of cysts of *P. dalei* is observed in the Iceland Sea as we get nearer to the shore (Fig. 3), supporting the hypothesis that the distance from the coast is an important variable controlling the dinocyst assemblages.

At the scale of our database, SSS seem to have a weaker influence on the assemblages, as they are not correlated with the two first axes of the CCA. However, a significant (p<0.05) negative correlation is observed between the fourth axis (8% of the variance) and summer and winter salinities (R= -0.57 and -0.67, Table 3). Also, as with the coccolith assemblages, distinctive assemblages on the Scotian and Newfoundland shelves stand out with some of the highest relative abundances of *Brigantedinium* spp., which shares dominance with *O. centrocarpum* and to a lesser extent, cysts of *P. dalei*. This group can be further divided into two sub-assemblages, one with high percentages of *Bitectatodinium tepikiense*, and the other with higher contributions of *Brigantedinium* spp., *S. mirabilis* and *S. ramosus*, corresponding to the sites nearer Newfoundland and nearer Nova Scotia, respectively. These distinctive assemblages cannot be explained by SST alone and might indicate the influence of SSS.

5. Discussion

5.1. Comparing coccolith and dinocyst assemblages in recent sediments from the North Atlantic

Coccolith and dinocyst assemblages in surface sediments of the North Atlantic reveal clear relationships with the overlying water masses. Both databases succeed in reflecting the main oceanographic domains in the study area. More importantly, in the warmest regions (offshore Portugal, Celtic Sea, Rockall channel region, Iceland Basin, Norwegian Sea, and Scotian Shelf), the coccolith assemblage zones closely correspond with those of the dinocysts (Fig. 3, Table 4). This coherency is of major importance in paleoceanography. One of the downsides of interpreting relative abundances is the closed sum effect, i.e. the fact that the variations of the different species in a given assemblage are not independent from each other as the sum of the abundances must always be 100%. However, coccolith and dinocyst counts are independent. Having some species from each group varying in a roughly parallel way (e.g., coccolith *G. muellerae* and dinocyst *S. mirabilis* in zones I to III, or coccolith *E. huxleyi* and dinocyst *O. centrocarpum* in zones VII and VIII, fig. 3) gives further support to the significance of these variations, thus reducing the risk of interpreting possible non ecological artefacts as environmental changes (e.g., post-sedimentation processes such as transport, dissolution, etc.). In warm environments, the two proxies can also possibly act as approximate replacements for each other in case one of them cannot be analyzed, due to poor carbonate preservation for example. In the subarctic seas, however, much richer dinocyst assemblages allow a better representation of the various surface water masses than the coccolith assemblages, which are overwhelmingly dominated by only two species, *E.huxleyi* and *C. pelagicus*.

The other major difference between the two groups is the fact that some dinocyst taxa exhibit a preference for neritic environments. Some coccolithophores are adapted to shallow water domains, but all coccoliths in our database relate to species that thrive essentially in the open ocean. In our samples, the almost exclusive presence of the coccolith species *G. oceanica* in sites near the coasts of Portugal and Nova Scotia (Fig. 3) result from an insufficient sampling in the mid-latitudes rather than neritic affinities. Indeed, this species is an important contributor to the mid-latitude open ocean assemblages when considering the extensive 163-site coccolith database (see section 3.1) and reference studies (e.g., Bollmann, 1997; Ziveri et al., 2004). Some dinocyst taxa such as *L. machaeorophorum* and cysts of *P. dalei* are also present in higher proportions in sites nearest to a coast. Comparison with the entire dinocyst database presented in de Vernal et al. (2005) confirms that these species do

have a preference for neritic environments (although cysts of *P. dalei* are not restricted to coastal settings). Dinocyst assemblages might thus bring additional information compared to the coccoliths, for example in environments influenced by both oceanic and coastal processes.

5.2. Relating microfossil assemblages to environmental parameters

The coherence between coccolith and dinocyst assemblages and the overlying water masses naturally leads to the question of controlling environmental factors. The first observation that can be made based on the CCA performed on coccolith and dinocyst assemblages concerns the importance of the database used for the multivariate analyses. Including a few samples from peculiar environments can either hide meaningful relationships, or, conversely, create anomalously strong correlations, while at the same time it allows the discrimination of the effects of covarying environmental parameters on the distribution of the assemblages. Each of these cases is encountered in our data.

The fact that SSS are not correlated to SST only in the Nova Scotia/Newfoundland sites (section 4.1) makes them stand out from the other sites and is enough to yield a strong correlation between the second axis of the CCA performed on the coccolith assemblages and SSS (Fig. 4, Table 2). However, when these sites are removed from the database, SSS are correlated with the first axis (R=-0.61 to -0.70) and with SST (Fig. 6a). The relationship between assemblages and SSS thus seems to hold for a great part due to the covariance of SSS and SST. This does not mean that SSS has no influence on coccolith assemblages; the fact remains that, for a given temperature range (here, 13-16°C in summer), contrasting SSS as observed between sites from the Celtic Sea/Rockall region (34.9-35.5) and Nova Scotia/Newfoundland (30.7-32.0) result in contrasting assemblages (Fig. 3). The addition of the Nova Scotia/Newfoundland sites in the database thus allows us to isolate the effect of SSS on assemblages; but one must keep in mind that the relationship between assemblages and SSS might not be as strong for sites from a more hydrographically homogenous region.

Conversely, in the dinocyst database, the distribution of the sites on the plot is clustered in 3 groups (Fig. 5) due to the very peculiar assemblages from offshore Portugal and the Celtic Sea. This clustered distribution conceals meaningful relationships. For

example, when the Portugal and Celtic Sea sites are removed from the database, the relationship with SST is much clearer, with a gradual transition from warmer to colder sites along the first axis of the CCA (Fig. 6b). In addition, the Nova Scotia/Newfoundland sites stand out and create a strong relationship between the second axis and SSS (Fig. 6b), as in the CCA performed on the 87 coccolith assemblages (Fig. 4).

Several other CCA tests, in which various "outlier" sites (Portugal, Celtic, Newfoundland and/or Nova Scotia sites) were removed from both coccolith and dinocyst databases in order to reduce their influence, yielded yet other ordinations of the controlling environmental parameters (data not shown). The results obtained with the CCA performed on different "sub-databases" thus highlight the difficulties of determining precisely how well a given environmental variable explains the distribution of the assemblages, as the importance of the variable changes with the database used for the analyses. However, in all cases, SST emerges as the main controlling factor. Depending on the database, SST from different seasons might yield significant relationships with either coccolith or dinocyst assemblages, making it hard to determine whether SST from a particular season have a stronger influence than the others. Also, dinocysts and coccoliths seem to respond to SST from different seasons (Tables 2 and 3). It is not clear whether it is a random artefact or a true ecological signal related to distinct seasonal development cycles of the two groups.

Following SST, productivity, SSS and the distance to the coast (for the dinocysts only) are other important variables controlling the distribution of the assemblages. Again, depending on the database used in the analyses, they can correlate to either the first axis of the CCA, along with SST, or to the second axis (or even the fourth axis, as with the 87 dinocyst samples). This results from different relationships between the parameters in the various water masses; for example, high winter productivity is associated with high winter SST offshore Portugal, but also with low winter SST in some parts of the Labrador Sea or on the Scotian Shelf (Fig. 7). Similarly, high winter productivity is associated with high fall productivity offshore Portugal, in the Celtic and on the Scotian Shelf, but not in the Labrador Sea (Fig. 7). Including or excluding sites from only one or all of these regions thus yields different correlation coefficients between the ordination axes and the environmental parameters.

Hence, care should be taken when trying to identify key environmental parameters controlling the distribution of phytoplankton from a geographically extended database that includes numerous distinct environments. However, the clear zonation of the hydrological parameters that appears on Figure 7, along with a similar zonation of the assemblages (Fig. 3), confirms again the good correspondence of the overlying water mass properties with both the dinocyst and coccolith assemblages.

It also suggests that it might be more adequate to consider the effects of a combination of environmental parameters on coccolith and dinocyst assemblages rather than to try to assess the influence of each individual parameter. Indeed, some regions are better discriminated from the others with respect to SST (e.g., offshore Portugal, where SST are the highest), while others are differentiated by the annual productivity cycle (e.g., summer productivity is much higher in the central Irminger Sea (zone VIIa) than in the Norwegian Sea near the Vöring Plateau (zone Va), whereas the other parameters are very similar, fig. 7). Complex interrelationships between environmental variables make it difficult to reduce the data to a few axes of variance in a multivariate analysis, but the fact remains that coccolith and dinocyst assemblages do exhibit variations corresponding to those of the environmental variables taken together. Table 4 synthetizes the correspondence between coccolith assemblages, dinocyst assemblages, and the main characteristics of the water masses in which they develop.

5.3. Further work

Although it is difficult to establish the relative influence of the various environmental parameters on the distribution of coccolith and dinocyst assemblages, interesting observations, which might be worth investigating further, can still be made from a qualitative examination of Figure 7.

Notably, the zonation in the environmental parameters mentioned earlier is particularly clear in the productivity records. Although primary productivity does not influence the assemblages *per se* (except for dinocyst assemblages that contain heterotrophic taxa), it is directly related to the nutrient content of the upper water layers, as well as to physical factors. Indeed, productivity annual cycles are for a great part linked to the

mixing/stratification cycle specific to each region, which is in turn related to the interaction between seasonal physical forcings such as irradiance, wind stress, freshwater supplies, sea ice, upwelling, etc. (e.g., Sverdrup, 1953; Longhurst, 1995, 1998; Gudmundsson, 1998; Waniek et al., 2005; Holliday et al., 2006). A strong stratification allows the phytoplankton to remain in the photic zone, while deep mixing brings up nutrients from the deeper water masses; the interplay between these two processes as well as their seasonal occurrences determines the timing, the duration and the species composition of phytoplankton blooms (e.g., Waniek and Holliday, 2006). In particular, such links between dinocysts/coccoliths and stratification have been shown by Vink et al. (2003) and Marret and Scourse (2002), although the emphasis was put on the intensity of the stratification rather than its timing.

Hence, some of the assemblages might reflect the influence of the stratification cycle and the availability of nutrients. For example, polar/Arctic water-influenced regions might benefit from fresh/melt water supplies from glaciers and sea ice. These create a shallow halocline that stabilizes the water column earlier in the year, triggering an early bloom (Longhurst, 1995; Waniek et al., 2005; Holliday et al., 2006) as seen in the Iceland Sea where the winter and spring productivity is higher than in the Irminger and Norwegian seas. The highest summer productivity in the Irminger Sea compared to the Norwegian Sea seems to be linked to highest nutrients in summer in the former (NODC, 2001), and may be related to a stabilization of the water column later in the year (Holliday et al., 2006), which prevents phytoplankton from utilizing the nutrients in spring. This is coherent with results from Waniek and Holliday (2006) that indicate late blooms in the Irminger Sea. These distinct productivity/stratification annual cycles could possibly explain some of the differences in the species composition of coccolith and dinocyst assemblages. For example, *N. labyrinthus* is much more common in dinocyst assemblages from the Irminger Sea than from the Norwegian Sea, which share very similar hydrographical parameters except for the afore-mentioned summer productivity. Further studies are needed to assess this possible relationship.

6. Conclusion

Comparison of dinoflagellate and coccolith assemblages in the North Atlantic illustrates a number of important points:

- Each of the subtropical regions (offshore Portugal, Celtic Sea, south of Rockall Channel, Iceland Basin, Newfoundland and Scotian shelves) represented in our database is characterized by distinct dinocyst and coccolith assemblages, as well as by unique combinations of environmental parameters. This confirms that the assemblages from surface sediments reflect the overlying sea surface conditions and it shows an excellent correspondence between coccolith and dinocyst assemblages, illustrating the robustness of both proxies for paleoceanography purposes.
- In the subpolar domain, however, poor species diversity in the coccolith assemblages makes them less adequate for discriminating the different water masses than dinocyst assemblages. In contrast, distinct dinocyst assemblages are observed in the different subpolar seas (Labrador, Irminger, Iceland and Norwegian seas), highlighting again their potential as paleoceanographic tracers for high latitude environments.
- Multivariate analyses put forward the strong influence of SST on the distribution of both coccolith and dinocyst assemblages. For the dinocyst assemblages only, the distance from the shore also appears to be an important parameter influencing their distribution. Thus, unlike coccolith assemblages, dinocyst assemblages could bring supplementary information on oceanic vs coastal processes.
- Other controlling factors include seasonal SSS and productivity, but their relative importance highly depends on the sites included in the database. The interrelationships of the various parameters can differ from one region to another, which makes it difficult to summarize the data with a few CCA axes. This suggests that reasoning in terms of water masses characterized by a combination of parameters rather than trying to isolate the effects of the various parameters might be more appropriate and should help understand better the ecological requirements of phytoplankton assemblages.
- The annual productivity cycle associated with each region integrates various biogeochemical and physical ocean processes and suggests that timing and duration of upper water column stratification might be important factors influencing dinocyst and coccolith assemblages, but more studies are needed to assess this further.

- Further work should include more surface sediment samples on which both coccolith and dinocyst are analyzed, notably in the Iceland Basin and in the south Norwegian Sea, as well as in the 40-50°N band, so as to cover more extensively temperate regions, and to increase the potential of coccolith assemblages which show a higher diversity in tropical and temperate water masses. Identification of the various morphotypes of coccolith taxa might also improve the discrimination of regional/local surface water environments, as it has been shown that some coccolith taxa such as *Gephyrocapsa* spp. and *C. leptoporus* are composed of distinct morphotypes with significant differences in their ecological preferences and hence their biogeographic distributions (Bollmann, 1997, Ziveri et al., 2004 and references therein).

Acknowledgements

The authors want to thank Fabienne Marret, Department of Geography, University of Liverpool, and Karen Luise Knudsen, Geologisk Institut, Aarhus Universitet, for access to surface samples from the Celtic Sea and Icelandic shelf, as well as Harald Andruleit, Bundesanstalt für Geowissenschaften und Rohstoffe, Federal Institute for Geosciences and Natural Resources, Hannover, for sharing coccolith data from the Nordic Seas with Linda Lévesque (formerly at GEOTOP, Université du Québec à Montréal). Special thanks to Bianca Fréchette, GEOTOP, Université du Québec à Montréal, for her help in the interpretation of the statistical analyses, and to Fabienne Marret and an anonymous reviewer for their helpful comments. This study is a contribution to the Polar Climate Stability Network, supported by the Canadian Foundation for Climate and Atmospheric Sciences (CFCAS). Support from the Natural Sciences and Engineering Research Council (NSERC) of Canada and the Fonds québécois de la recherche sur la nature et les technologies (FQRNT) is acknowledged.

References

Antoine, D., André, J.M., Morel, A., 1996. Oceanic primary production. 2. Estimation at global scale from satellite (costal zone colour scanner) chlorophyll. Global Biogeochemical Cycles 10, 57–69.

Baumann, K.-H., Matthiessen, J., 1992. Variations in surface water mass conditions in the Norwegian Sea: evidence from Holocene coccolith and dinoflagellate cyst assemblages. Marine Micropaleontology 20, 129-146.

Baumann, K.-H., Andruleit, H. A., Samtleben, C., 2000. Coccolithophores in the Nordic Seas: comparison of living communities with surface sediment assemblages. Deep Sea Research II 47, 1743-1772.

Bollmann, J., 1997. Morphology and biogeography of *Geophyrocapsa* coccoliths in Holocene sediments. Marine Micropaleontology 29, 319-250.

Calvo, E., J. Grimalt, Jansen, E., 2002. High resolution U37K sea surface temperature reconstruction in the Norwegian Sea during the Holocene. Quaternary Science Reviews 21, 1385-1394.

de Vernal, A., Turon, J.-L., Guiot, J., 1994. Dinoflagellate cyst distribution in high latitude environments and quantitative reconstruction of sea-surface temperature, salinity and seasonality. Canadian Journal of Earth Sciences 31, 48–62.

de Vernal, A., Rochon, A., Turon, J.-L., Matthiessen, J., 1997. Organic-walled dinoflagellate cysts: palynological tracers of sea surface conditions in middle to high latitude marine environments. Geobios 30, 905–920.

de Vernal, A., Eynaud, F., Henry, M., Hillaire-Marcel, C., Londeix, L., Mangin, S., Matthiessen, J., Marret, F., Radi, T., Rochon, A., Solignac, S., Turon, J.-L., 2005. Reconstruction of sea-surface conditions at middle to high latitudes of the Northern Hemisphere during the Last Glacial Maximum (LGM) based on dinoflagellate cyst assemblages. Quaternary Science Reviews 24, 897-924.

Devillers, R., de Vernal, A., 2000. Distribution of dinoflagellate cysts in surface sediments of the northern North Atlantic in relation to nutrient content and productivity in surface waters. Marine Geology 166, 103-124.

Dolven, J.K., Cortese, G., Bjørklund, K.R., 2002. A high-resolution radiolarian-derived paleotemperature record for the Late Pleistocene-Holocene in the Norwegian Sea. Paleoceanography 17 (4), 1072, doi:10.1029/2002PA000780.

Eide, L. K., 1990. Distribution of coccoliths in surface sediments in the Norwegian-Greenland Sea. Marine Micropaleontology 16, 65-75.

Geitzenauer, K.R., Roche, M.B., McIntyre, A., 1976. Modern Pacific coccolith assemblages: derivation and application to late Pleistocene paleotemperature analysis. In: Cline, R.M., Hays, J.D. (Eds.), Investigation of late Quaternary paleoceanography and paleoclimatology. Geological Society of America, Washington DC, pp. 423-448.

Geitzenauer, K.R., Roche, M.B., McIntyre, A., 1977. Coccolith biogeography from North Atlantic and Pacific surface sediments. In: Ramsey, A.T.S. (Ed.), Oceanic Micropaleontology. Academic Press, New York, pp. 973-1008.

Giraudeau, J., Beaufort, L., 2007. Coccolithophores: From extant populations to fossil assemblages. In: Hillaire-Marcel, C., de Vernal, A. (Eds.), Proxies in Late Cenozoic Paleoceanography. Elsevier, Amsterdam, pp. 409-439.

Gudmundsson, K., 1998. Long-term variation in phytoplankton productivity during spring in Icelandic waters. ICES Journal of Marine Science 55, 635-643.

Hansen, B., Osterhus, S., 2000. North Atlantic-Nordic Seas exchanges. Progress in Oceanography 45, 109-208.

Hass, H. C., Andruleit, H., Baumann, A., Baumann, K.-H., Kohly, A., Jensen, S., Matthiessen, J., Samtleben, C., Schäfer, P., Schröder-Ritzrau, A., Thiede, J., 2001. The potential of synoptic plankton analyses for paleoclimatic investigations: five plankton groups from the Holocene Nordic Seas. In: Schäfer, P., Ritzrau, W., Schlüter, M., Thiede, J. (Eds.), The northern North Atlantic: a changing environment. Springer, Berlin, pp. 291-318.

Head, M.J., Harland, R., Matthiessen, J., 2001. Cold marine indicators of the late Quaternary: the new dinoflagellate cyst genus *Islandinium* and related morphotypes. Journal of Quaternary Science 16, 621-636.

Holliday, N. P., Waniek, J. J., Davidson, R., Wilson, D., Brown, L., Sanders, R., Pollard, R. T., Allen, J. T., 2006. Large-scale physical controls on phytoplankton growth in the Irminger Sea Part I: Hydrographic zones, mixing and stratification. Journal of Marine Systems 59, 201-218.

Knappertsbusch, M., 1993. Geographic distribution of living and Holocene coccolithophores in the Mediterranean Sea. Marine Micropaleontology 21, 219-247.

Lazier, J.R.N., and D.G. Wright, 1993: Annual velocity variations in the Labrador Current. Journal of Physical Oceanography, 23, 659-678.

Lévesque, L., 1995. Distribution des assemblages de coccolithes dans les sédiments récents des moyennes latitudes de l'Atlantique Nord: développement de fonctions de transfert paléocéanographiques. M.Sc. thesis, Université du Québec à Montréal, Canada.

Loder, J.W., Han, G., Hannah, C.G., Greenberg, D.A., Smith, P.C., 1997. Hydrography and baroclinic circulation in the Scotian Shelf region: winter versus summer. Canadian Journal of Fisheries and Auqatic Sciences 54, 40-56.

Longhurst, A., 1995. Seasonal cycles of pelagic production and consumption. Progress in Oceanography 36, 77-167.

Longhurst, A., 1998. Ecological geography of the sea. Academic Press, San Diego.

Marret, F., Scourse, J., 2002. Control of modern dinoflagellate cyst distribution in the Irish and Celtic seas by seasonal stratification dynamics. Marine Micropaleontology 47, 101-116.

Marret, F., Zonneveld K.A.F., 2003. Atlas of modern organic-walled dinoflagellate cyst distribution. Review of Palaeobotany and Palynology 125, 1-200.

Marret, F., Eiriksson, J., Knudsen, K.L., Turon, J.-L., Scourse, J.D., 2004. Distribution of dinoflagellate cyst assemblages in surface sediments from the northern and western shelf of Iceland. Review of Palaeobotany and Palynology 128, 35-53.

Martins, C. S., Hamann, M., Fuiza, A.F.G., 2002. Surface circulation in the eastern North Atlantic from drifters and altimetry. Journal of Geophysical Research 107 (C12), 3217, doi:10.1029/2000JC000345.

Matthiessen, J., 1995. Distribution patterns of dinoflagellate cysts and other organic-walled microfossils in recent Norwegian-Greenland Sea sediments. Marine Micropaleontology 24, 307-334.

Matthiessen, J., Baumann, K.-H., Schröder-Ritzrau, A., Hass, C., Andruleit, H., Baumann, A., Jensen, S., Kohly, A., Pflaumann, U., Samtleben, C., Schäfer, P., Thiede, J., 2001. Distribution of calcaerous, siliceous and organic-walled planktic microfossils in surface sediments in the Nordic Seas and their relation to surface-water masses. In: Schäfer, P., Ritzrau, W., Schlüter, M., Thiede, J. (Eds.), The northern North Atlantic: a changing environment. Springer, Berlin, pp. 105-127.

National Oceanographic Data Centre (NODC), *World Ocean Atlas*, http://www.nodc.noaa.gov/OC5/WOD01/pr_wod01.html, 2001.

Okada, H., Honjo, S., 1973. The distribution of oceanic coccolithophorids in the Pacific. Deep-Sea Research 20, 355-374.

Okada, H., McIntyre, A., 1979. Seasonal distribution of modern coccolithophores in the western North Atlantic Ocean. Marine Biology 54, 319-328.

Petrie, B., Topliss, B.J., Wright, D.J., 1987. Coastal upwelling and eddy development off Nova Scotia. Journal of Geophysical Research 21, 939-955.

Pollard, R.T., Read, J.F., Holliday, N.P., 2004. Water masses and circulation pathways through the Iceland Basin during Vivaldi 1996. Journal of Geophysical Research 109, C04004, doi:10.1029/2003JC002067.

Poulain, P.-M., Warm-Varnas, A., Niiler, P.P., 1996. Near-surface circulation of the Nordic seas as measured by Lagrangian drifters. Journal of Geophysical Research 101 (C8), 18,237-18,258.

Pujos, A., 1988. Stratigraphical and paleoecological distribution of calcareous nannofossils throughout the Quaternary in the Caribbean Sea. 11th Caribbean Geological Conference, Barbados, 20-26 July 1986, pp. 8:1-8:13.

Radi, T., Pospelova, V., de Vernal, A., Vaughn Barrie, J., 2007. Dinoflagellate cysts as indicators of water quality and productivity in British Columbia estuarine environments. Marine Micropaleontology 62, 269-297.

Radi, T., de Vernal, A., submitted. Dinocysts as proxy of primary productivity in mid-high latitudes of the northern hemisphere. Submitted to Marine Micropaleontology.

Read, J.F., 2001. CONVEX-91: water masses and circulation of the Northeast Atlantic subpolar gyre. Progress in Oceanography 48, 461-510.

Reverdin, G., Niiler, P.P., Valdimarsson, H., 2003. North Atlantic Ocean surface currents. Journal of Geophysical Research 108 (C1), 3002, doi:10.1029/2001JC001020.

Risebrobakken, B., Jansen, E., Andersson, C., Mjelde, E., Hevrøy, K., 2003. A high-resolution study of Holocene paleoclimatic and paleoceanographic changes in the Nordic Seas. Paleoceanography 18, 1017, doi:10.1029/2002PA000764.

Rochon, A., de Vernal, A., Turon, J.-L., Matthiessen, J., Head, M.J., 1999. Distribution of recent dinoflagellate cysts in surface sediments from the North Atlantic ocean and adjacent seas in relation to sea-surface parameters. American Association of Stratigraphic Palynologists Contribution Series 35, Houston, TX.

Roth, P.H., 1994. Distribution of coccoliths in oceanic sediments. In: Winter, A., Siesser W.G. (Eds.), Coccolithophores. Cambridge University Press, Cambridge, pp. 199-218.

Samtleben, C., Schröder, A., 1992. Living coccolithophore communities in the Norwegian-Greenland Sea and their record in sediments. Marine Micropaleontology 19, 333-354.

Samtleben, C., Schäfer, P., Andruleit, H., Baumann, A., Baumann, K.-H., Kohly, A., Matthiessen, J., Schröder-Ritzrau, A., 1995. Plankton in the Norwegian-Greenland Sea: from living communities to sediment assemblages – an actualistic approach. Geologische Rundschau 84, 108-136.

Smith, P.C., Schwing, F.B., 1991. Mean circulation and variability on the eastern Canadian continental shelf. Continental Shelf Research 11, 977-1012.

Sverdrup, H.U., 1953. On conditions for the vernal blooming of phytoplankton. Journal du Conseil International pour l'Exploration de la Mer 18, 287-295.

Ter Braak C.J.F., 1986. Canonical Correspondence Analysis: A New Eigenvector Technique for Multivariate Direct Gradient Analysis. Ecology 67, 1167-1179.

Ter Braak, C.J.F., Smilauer, P., 1998. CANOCO reference manual and user's guide to CANOCO for Windows: Software for canonical community ordination (version 4). Centre for Biometry, Wageningen.

Vink, A., Baumann, K. H., Böckel, B., Esper, O., Kinkel, H., Volbers, A., Willems, H., Zonneveld, K.A.F., 2003. Coccolithophorid and dinoflagellate synecology in the south and equatorial Atlantic: improving the paleoecological significance of phytoplanktonic microfossils. In: Wefer, G., Mulitza, S., Ratmeyer, V. (Eds.), The South Atlantic in the late Quaternary: Reconstruction of material budgets and current systems. Springer, Berlin, pp. 101-120.

Waniek, J.J., Holliday, N.P., Davidson, R., Brown, L., Henson, S.A., 2005. Freshwater control of onset and species composition of Greenland shelf spring bloom. Marine Ecology Progress Series 288, 45-57.

Waniek, J. and Holliday, N.P., 2006. Large-scale physical controls on phytoplankton growth in the Irminger Sea. Part II: model study of the physical and meteorological preconditioning. Journal of Marine Systems 59, 219-237.

Woodgate, R.A., Fahrbach, E., and Rohardt, G., 1999: Structure and transport of the East Greenland Current at 75°N from moored current meters. Journal of Geophysical Research 104, 18,059-18,072.

Ziveri, P., Baumann, K.-H., Böckel, B., Bollmann, J., Young, J.R., 2004. Biogeography of selected Holocene coccoliths in the Atlantic Ocean. In: Thierstein, H.R., Young, J.R. (Eds.), Coccolithophores – from molecular processes to global impact. Springer, Berlin, pp. 403-428.

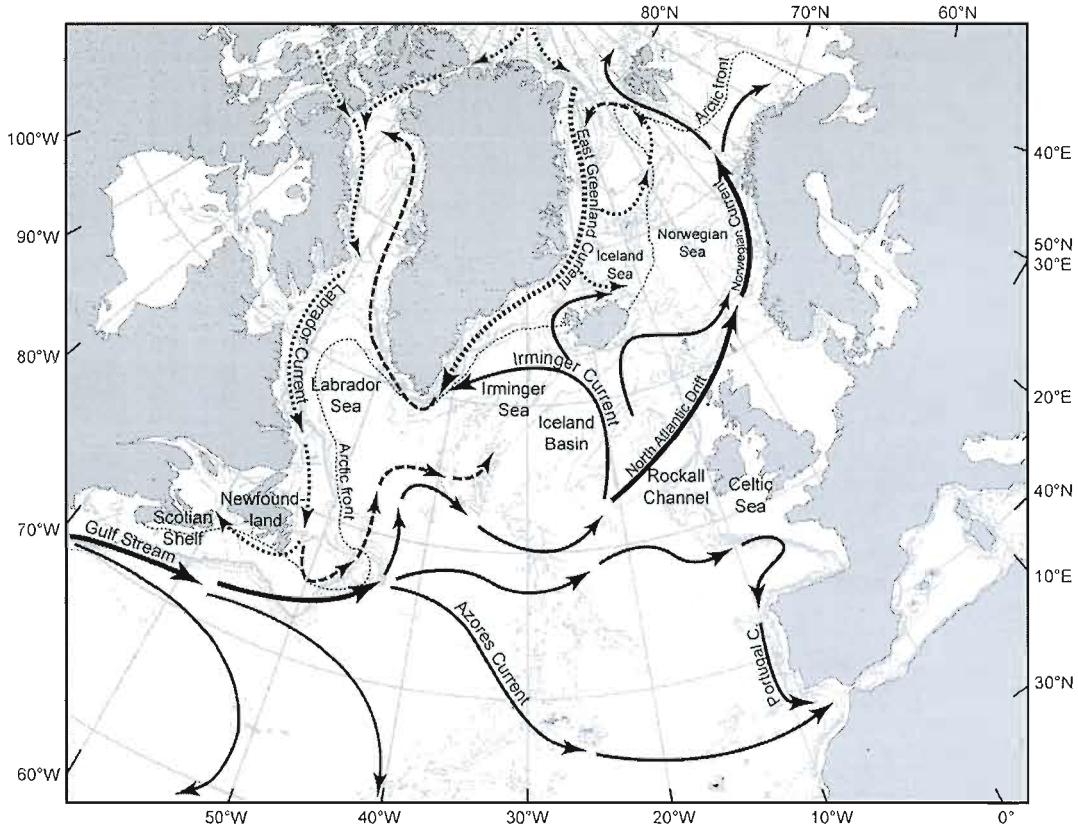

Figure 1. Surface oceanic currents of the study area. Solid, dotted and dashed arrows represent warm, cold and mixed currents, respectively.

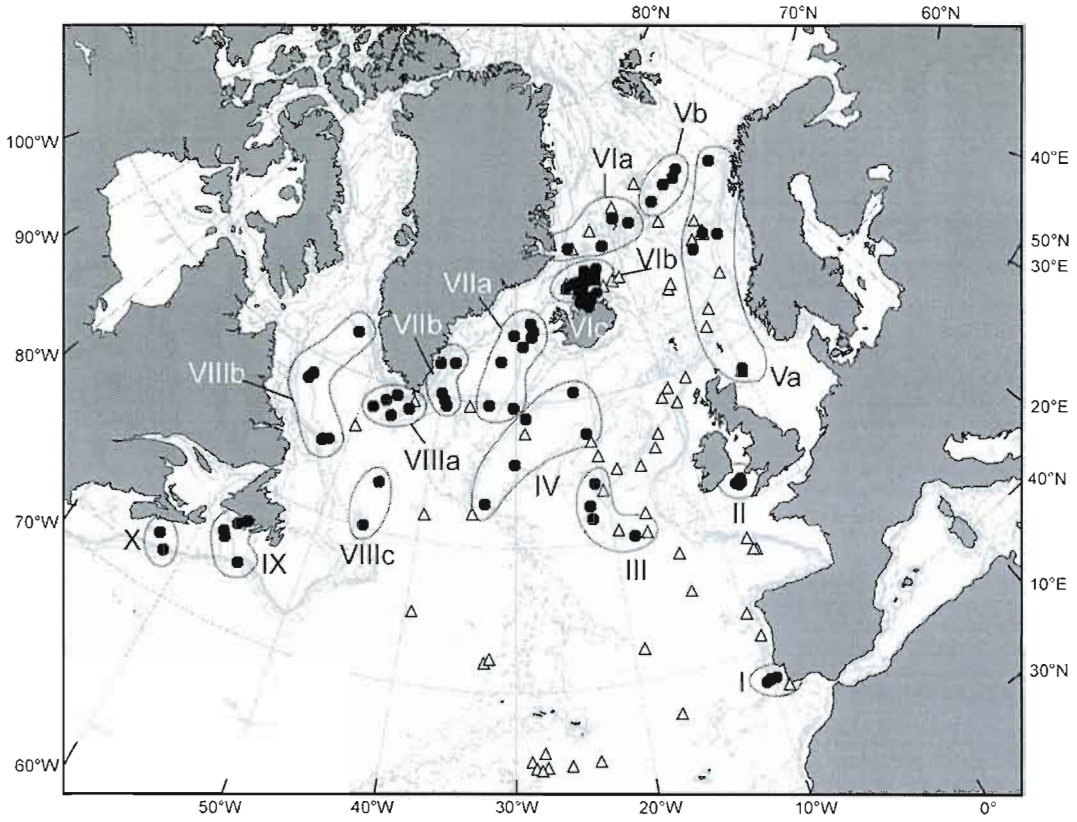

Figure 2. Location of surface sediment samples. White triangles are samples on which only coccoliths were analyzed, black dots are samples on which both coccoliths and dinocysts were analyzed. See table 1 for more information on the sources of the different samples. Shaded areas with associated roman numbers are the geographical zones used in figures 3 to 7.

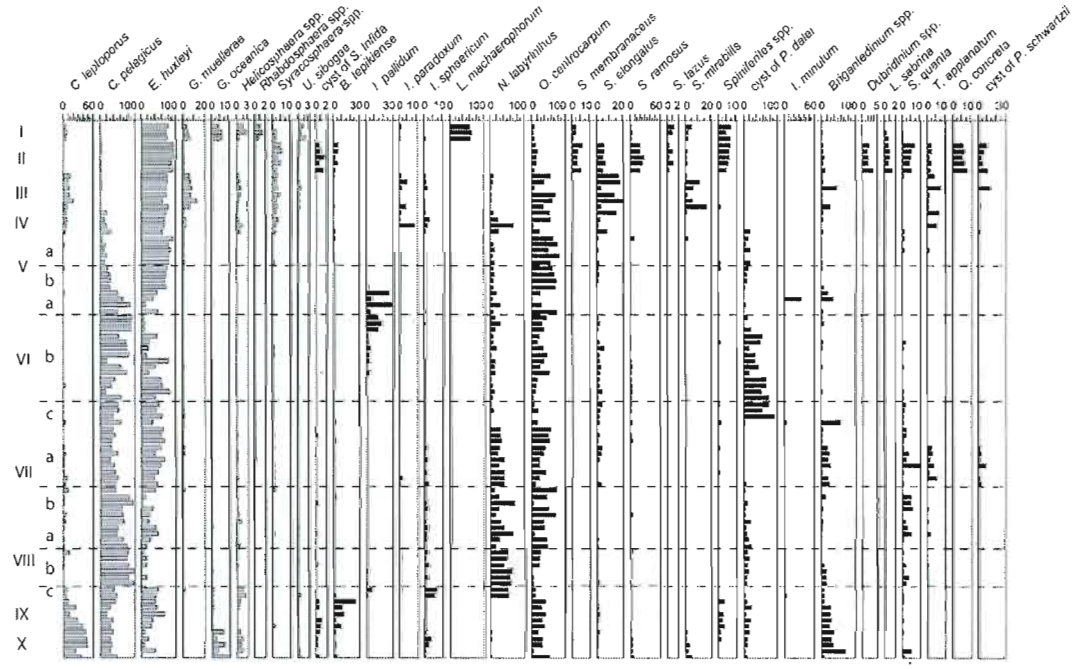

Figure 3. Coccolith (in grey) and dinocyst (in black) assemblages from the 87 sites. Zones are strictly based on the geographic location of the sites. I: offshore Portugal. II: Celtic Sea. III: south of Rockall Channel. IV: Iceland Basin. V: Norwegian Sea (Va: North Sea and Norwegian Sea samples, Vb: samples closer to the Greenland Sea). VI: Iceland Sea (VIa: northern Iceland Sea, VIb: southern Iceland Sea, VIc: North Iceland shelf). VII: Irminger Sea (VIIa: south of Denmark Strait and central Irminger Sea, VIIb: samples closer to the eastern Greenland coast). VIII: Labrador Sea (VIIIa: south of Greenland, VIIIb: northern and western Labrador Sea, VIIIc: southern subpolar gyre). IX: Newfoundland shelf. X: Scotian shelf. Note that some of the dinocyst species occurring in very low numbers are not reported on the diagram for more clarity. Exhaustive data can be found in original publications of regional datasets (de Vernal et al., 2005 and references therein).

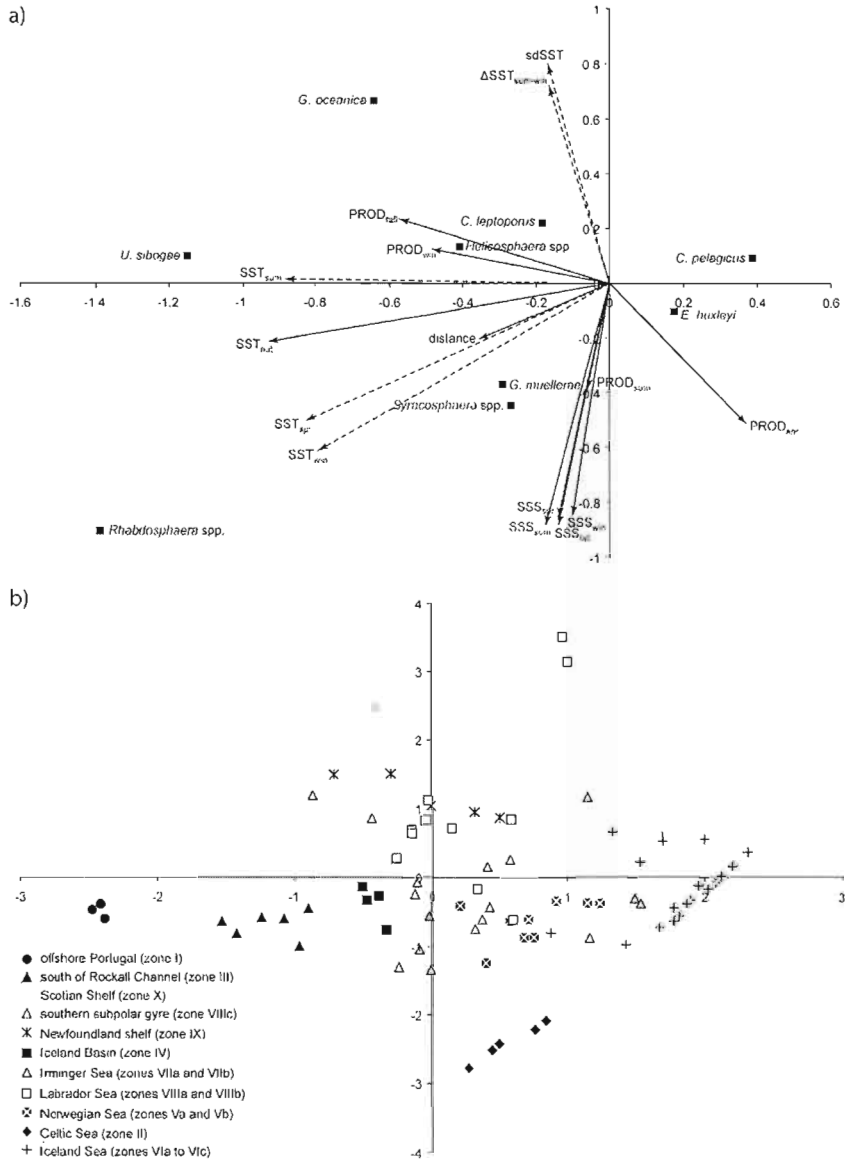

Figure 4. Ordination diagram of the CCA performed on the 87 coccolith assemblages. a) Species and environmental parameter scores. Dotted arrows indicate a non significant relationship between the parameter and the distribution of the assemblages. b) Site scores. SSTwin, SST spr, SSTsum, SSTaut are winter, spring, summer and fall sea surface temperatures, respectively. sdSST is the standard deviation of the annual sea surface temperature. ΔSSTsum-win is the seasonality, i.e., the difference between summer and winter sea surface temperatures. SSSwin, SSS spr, SSSsum, SSSaut are winter, spring, summer and fall sea surface salinities, respectively. PRODwin, PROD spr, PRODsum, PRODaut are winter, spring, summer and fall productivity, respectively. distance is the distance between the site and the shore.

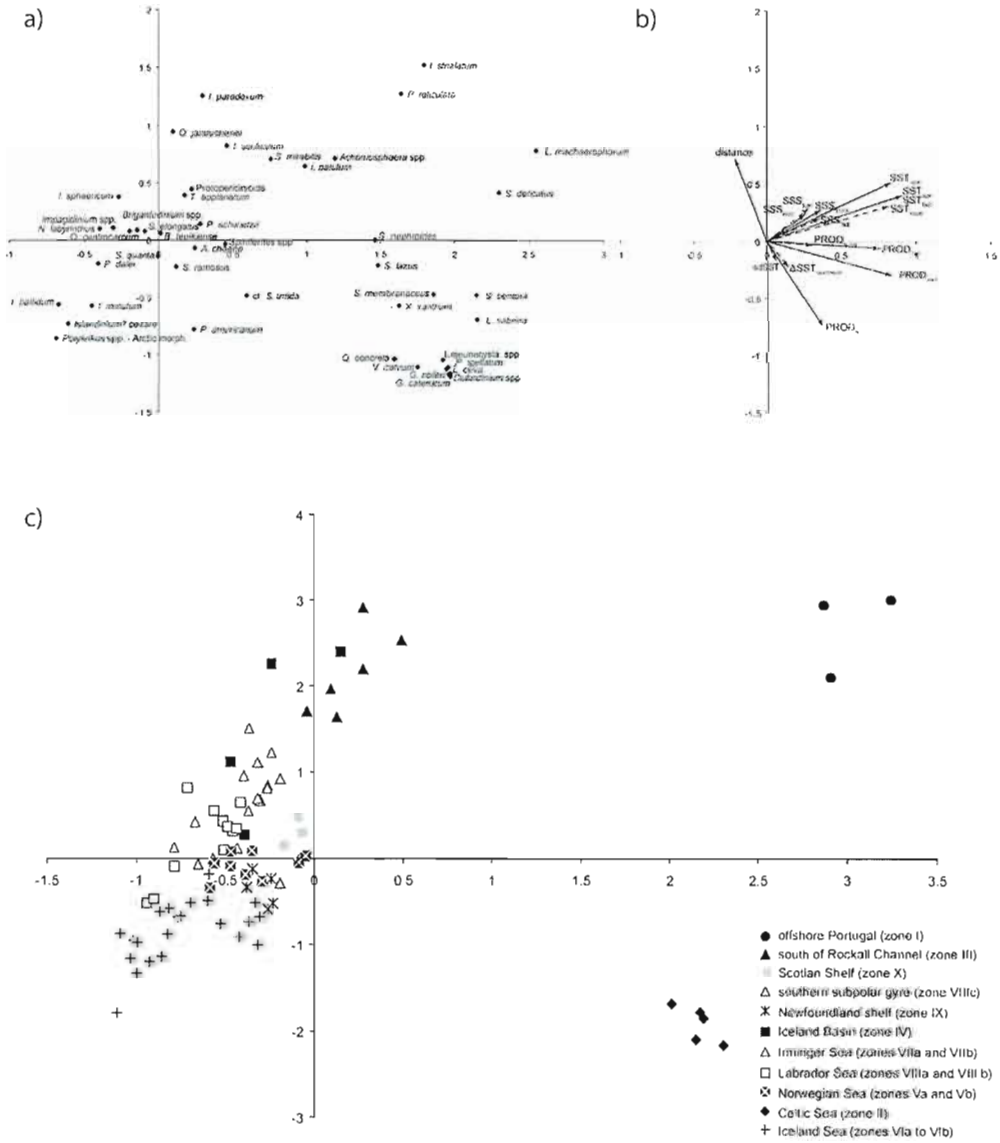

Figure 5. Ordination diagram of the CCA performed on the 87 dinocyst assemblages. a) Species scores. b) Environmental parameter scores. Dotted arrows indicate a non significant relationship between the parameter and the distribution of the assemblages. c) Site scores. Environmental parameter abbreviations are the same as in fig. 4.

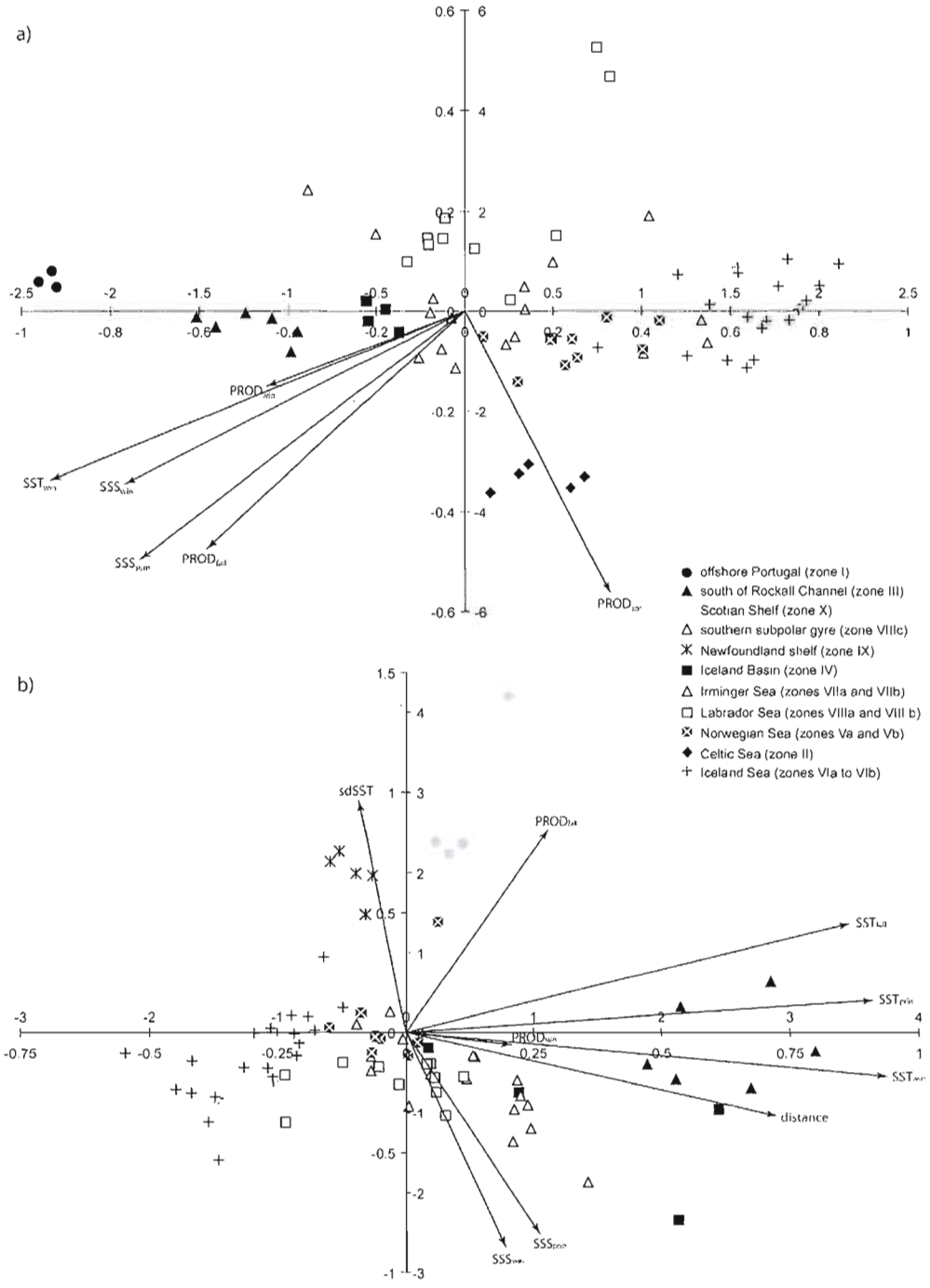

Figure 6. a) Ordination diagram of the CCA performed on the coccolith assemblages after removing sites from the Scotian and Newfoundland shelves. b) Ordination diagram on the CCA performed on the dinocyst assemblages after removing sites from offshore Portugal and from the Celtic Sea.

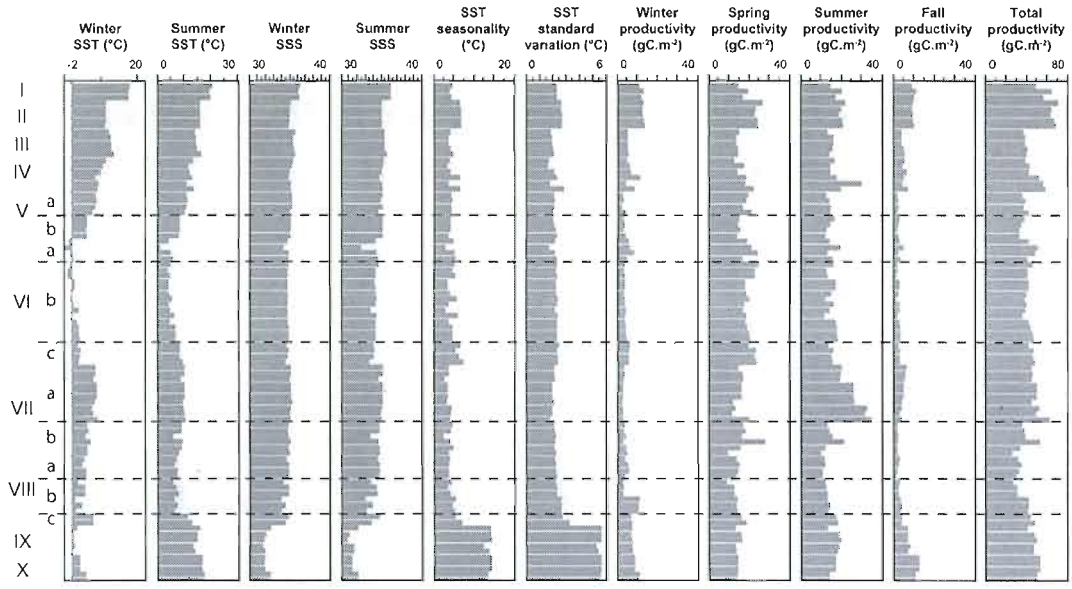

Figure 7. Major environmental parameters. Zones are based on the geographic location of the sites (see fig. 2), which are in the same order as in figure 4.

Site	Longitude	Latitude	Water depth (m)	Corresponding site in the dinocyst database	Source	Site	Longitude	Latitude	Water depth (m)	Corresponding site in the dinocyst database	Source
7465	-9 98	42.70	2462	-	a	A102	-39.45	59.53	2930	-	c
7467	-17 17	37.32	3098	-	a	A103	-39.67	59.86	2700	A103	c
72108	-7 03	46.67	4285	-	a	A104	-40.22	60.29	2231	A104	c
72306	-19.13	42.22	3756	-	a	A105	-41.02	62.32	660	A105	c
01-10	4.52	64.75	860	-	a	A106	-38.83	62.54	2180	A106	c
F1.10	-7 07	59 50	1366	-	a	A107	-32.18	62.91	2820	A107	c
F1.28	-10.92	58.78	1841	-	a	A109	-28.94	63.87	1625	A109	c
F1.34	-12.75	56.52	2300	-	a	A110	-28.94	63.87	1625	A110	c
F1 39B	-15.65	54 63	2209	-	a	A111	-28.93	63.87	1600	A111	c
F1.47	-14.08	48.18	4207		a	A112	-30.18	64.67	2200	A112	c
F1 KR2	-9 28	58.08	2005	-	a	A113	-22.08	60.57	2400	A113	c
F1.KR4	-1 50	61.97	1621	-	a	A114	-21.17	57.55	2370	A114	c
F1.KR5	-0.03	63.00	1947	-	a	A115	-20.83	57 00	1875		c
F1 KR7	-9.78	59.25	482		a	A116	-20 32	55.95	1544		c
F1.KR10	-13.53	55.60	2216	-	a	A118	-21.08	54.08	2900	A118	c
F1.KR11	-16.32	51 48	4654	-	a	A119	-21.93	52.57	3955	A119	c
F1.KR12	-16.63	50.13	4787	-	a	A120	-21.93	52.57	3965	A120	c
F2.KR1	-34.77	52.28	3800	-	a	A121	-21.88	51.72	2838	A121	c
F2.KR3	-28.88	57 93	2270	-	a	A123	-17.92	50.10	4279	A123	c
GO KR1	-7.52	47.63	1925	-	a	L162	-52.87	54.82	1364	L162	c
GO.KR3	-7.32	46.77	3746		a	L163	-52.13	55.03	2648	L163	c
HS.1	-9.53	40.95	4200		a	L164	-52.75	54.90	1984	L164	c
HS.2	-9 47	40.97	3700	-	a	L165	-49.75	56.62	3992	-	c
HS.3	-9.42	40.92	4200	-	a	A168	-39.31	59.49	2949	A168	c
HS.4	-8.67	37.10	1150		a	A169	-36.13	59 63	3025	-	c
M1 16	-13 92	45.42	4780		a	A170	-33.58	59.85	2255	A170	c
65	-28 02	34 62	3452	-	a	A171	-30.36	59.68	1319	A171	c
68	-27.65	34 80	2520	-	a	A173	-28.74	58.94	2237	A173	c
69	-25 80	34.82	4675	-	a	A174	-30.23	55.75	2926	A174	c
70	-23.70	34.95	5118	-	a	A175	-33.53	53.06	3024	A175	c
74226	-28.45	34.72	3592		a	L177	-45.26	53.33	3378	L151	c
74227	-28.77	35.25	3210		a	L178	-45.69	50.20	3448	L178	c
74229	-27 80	35.80	3419	-	a	N239	-0 28	58 14	128	-	c
2066	**-17.59**	**66.15**	**199**	**A935**	b	N240	-0 22	58 14	130	-	c
2639	**-15.45**	**67.93**	**1101**	**A936**	b	**N241**	**0.02**	**58.22**	**139**	**N241**	c
2646	**-15.38**	**68.08**	**1303**	**A937**	b	**A258**	**-62.79**	**43.83**	**230**	**A258**	c
2667	**-15.75**	**67.00**	**187**	**A938**	b	**A259**	**-62.81**	**43.82**	**235**	**A259**	c
2674	**-16.84**	**66.74**	**148**	**A939**	b	**A260**	**-62.80**	**43.83**	**231**	**A260**	c
2730	**-18.86**	**66.50**	**464**	**A940**	b	**A261**	**-61.76**	**42.88**	**833**	**A261**	c
2739	-20.33	67.04	500	-	b	**A262**	**- -61.75**	**42.89**	**804**	**A262**	c
2742	-20 50	67.75	726	-	b	**A284**	**-10.30**	**37.75**	**3350**	**A264**	c
2746	**-20.85**	**67.77**	**800**	**A945**	b	**A265**	**-9.49**	**37.88**	**1150**	**A265**	c
2748	-20.69	68.04	973	-	b	**A266**	**-9.95**	**37.87**	**2465**	**A266**	c
2752	**-19.35**	**67.92**	**1021**	**A947**	b	**N267**	**2.91**	**67.08**	**1306**	**J301**	d
2757	**-18.83**	**67.92**	**622**	**A948**	b	**N268**	**9.27**	**72.35**	**2518**	**J306**	d
2760	**-17.75**	**67.92**	**1127**	**A949**	b	**N269**	**15.84**	**71.20**	**1676**	**J310**	d
2764	**-17.50**	**68.08**	**1198**	**A950**	b	**N270**	**7.49**	**71.99**	**2768**	**J311**	d
2770	**-16.95**	**68.60**	**492**	**A951**	b	**N271**	**4.99**	**72.01**	**2974**	**J312**	d
2775	**-14.67**	**68.60**	**1552**	**A952**	b	**N272**	**0.67**	**71.44**	**2872**	**J313**	d
2778	**-15.76**	**68.33**	**1418**	**A953**	b	N273	-0 81	73.17	2755	-	d
2780	**-17.85**	**67.60**	**1019**	**A954**	b	**N274**	**7.78**	**67.02**	981	**J324**	d
2784	**-18.19**	**67.48**	**810**	**A955**	b	N275	5.78	67 65	1434	-	d
2788	**-18.37**	**67.32**	**545**	**A956**	b	N276	6 01	67.78	1305	-	d
2793	**-18.85**	**67.28**	**488**	**A957**	b	N277	6.02	67 80	1302	-	d
2794	-19.05	67.23	458	-	b	**N278**	5 88	67 69	1312	-	d
2798	-17.69	66.58	425	-	b	N279	3.71	67.70	1256	-	d
2875	**-27.60**	**64.57**	**777**	**A965**	b	N280	5 94	68 68	3003	-	d
2879	**-27.23**	**64.93**	**355**	**A966**	b	**N281**	**5.84**	**67.67**	**1312**	**J326**	d
2894	**-27.53**	**65.48**	**664**	**A967**	b	N282	5 93	67.74	1247	-	d
Celt4	**-6.50**	**51.35**	**86**	**A987**	b	N283	0.05	70 05	3299	-	d
Celt5	**-6.15**	**51.20**	**104**	**A988**	b	N284	-5 54	70 96	1713	-	d
Celt6	**-5.90**	**51.23**	**93**	**A989**	b	**N285**	**-8.42**	**71.63**	**1958**	**J328**	d
Celt7	**-6.06**	**51.28**	**98**	**A990**	b	N287	-14.07	71 29	1209	-	d
Celt8	**-5.83**	**51.50**	**89**	**A991**	b	**N288**	**-19.35**	**70.40**	**397**	**J335**	d
A074	**-55.62**	**44.66**	1381	A074	c	N289	-18.35	70.36	1679	-	d
G075	**-57.59**	**45.85**	**473**	**G075**	c	**N290**	**-12.43**	**70.01**	**1822**	**J337**	d
G076	**-57.94**	**46.19**	**468**	**G076**	c	N291	-4 15	65 53	2821	-	d
G077	**-56.37**	**47.51**	**355**	**G077**	c	N202	-7.81	72 35	2628	-	d
G078	**-57.05**	**47.07**	**333**	**G078**	c	N293	-3.51	65 80	2926	-	d
L087	**-53.88**	**62.65**	**2424**	**L087**	c	N294	-18 38	54 84	1054	-	d
L090	**-45.87**	**59.49**	**1105**	**L090**	c	N205	-20.29	53.54	2201	-	d
L091	**-47.09**	**58.92**	**2805**	**L091**	c	N296	-19.44	50 88	3843	-	d
L092	**-48.36**	**58.21**	**3379**	**L092**	c	N297	-0.07	70.04	3247	-	d
L093	**-57.46**	**58.36**	**2865**	**L093**	c	**N298**	**-5.56**	**70.96**	**1737**	**J327**	d
L094	**-57.12**	**58.76**	**3032**	**L094**	c	N299	-8.45	71 65	1949	-	d
A095	-32 73	42 03	1970	-	c	N300	-17.92	67.89	1135		d
A096	-32.26	42 33	3250	-	c	N301	-18 77	67.89	895	-	d
A097	-39.44	45.09	1966	-	c	N302	-18.62	67.86	820		d
A098	-39 78	51.88	2970	-	c	N303	-14.20	67.34	1036	-	d
A099	**-45.90**	**57.98**	**2405**	**A099**	c	N304	-11.07	67.66	1841	-	d
A100	**-43.97**	**58.79**	**1615**	**A100**	c	N305	-12.50	67 51	1774	-	d
A101	-43.44	59.37	1015	-	c						

In bold, sites analyzed for dinocyst counts as well
a: A. Pujos, 1988
b: S. Solignac, GEOTOP, this study
c: L. Lévesque (1995), GEOTOP-UQÀM-McGill
d: Baumann et al., 2000

Table 1. List of the 163 samples used for modern coccolith population counts.

Environmental parameter	Correlation coefficients with the axes		Marginal effects	Conditional effects	
	Axis 1 (51%)	Axis 2 (26%)	%	%	*p*
SSTwin	-0.72	-0.51	26.11	1.52	0.079
SSTspr	-0.75	-0.42	26.11	1.52	0.072
SSTsum	-0.80	0.01	25.37	1.14	0.270
SSTfall	***-0.84***	***-0.18***	***28.57***	***44.11***	***0.001***
SSSwin	***-0.09***	***-0.71***	***12.56***	***1.90***	***0.028***
SSSspr	***-0.13***	***-0.71***	***12.81***	***3.42***	***0.001***
SSSsum	***-0.16***	***-0.74***	***13.79***	***3.80***	***0.003***
SSSfall	***-0.13***	***-0.74***	***13.55***	***19.39***	***0.001***
PRODwin	***-0.43***	***0.10***	***10.84***	***5.32***	***0.001***
PRODspr	***0.33***	***-0.42***	***9.36***	***9.89***	***0.001***
PRODsum	-0.05	-0.31	2.96	0.00	0.238
PRODfall	***-0.51***	***0.20***	***13.30***	***1.90***	***0.025***
distance	***-0.31***	***-0.17***	***7.14***	***4.56***	***0.002***
ΔSSTsum-win	-0.15	0.60	10.10	0.00	-
sdSST	-0.15	0.67	11.58	1.52	0.065

Tableau 2. Summary of the CCA performed on the 87 coccolith assemblages. Percentages in brackets beneath each axis are the proportion of the variance explained by the axis. Significant relationships ($p>0.05$) between the environmental parameters and the distribution of the assemblages are in bold italic characters. Shaded areas indicate the strongest correlation coefficients between the parameters and the axes. The percentages in the marginal effect column show the proportion of the variance explained by a given environmental parameter when taken individually, without correction for a possible covariance with some of the environmental parameters. The percentages in the conditional effect column show the proportion of the variance explained by a given environmental parameter after correction for the covariance between the parameters. Environmental parameter abbreviations are the same as in fig. 4.

Environmental parameter	Correlation coefficients with the axes			Marginal effects	Conditional effects	
	Axis 1 (44%)	Axis 2 (33%)	Axis 4 (8%)	%	%	*p*
SST_{win}	***0.77***	***0.42***	***-0.11***	***17.81***	***3.11***	***0.005***
SSTspr	***0.85***	***0.32***	***0.03***	***19.59***	***37.21***	***0.001***
SSTsum	0.76	0.25	0.40	16.45	0.68	0.933
SSTfall	***0.83***	***0.32***	***0.21***	***19.02***	***2.44***	***0.021***
SSSwin	***0.23***	***0.18***	***-0.67***	***5.48***	***7.85***	***0.001***
SSSspr	0.25	0.22	-0.63	5.70	1.89	0.094
SSSsum	***0.33***	***0.21***	***-0.58***	***6.70***	***4.60***	***0.001***
SSSfall	0.31	0.15	-0.62	6.27	1.76	0.156
PRODwin	***0.78***	***-0.24***	***0.19***	***16.67***	***6.09***	***0.001***
PRODspr	***0.35***	***-0.59***	***-0.12***	***8.40***	***9.20***	***0.001***
PRODsum	0.27	-0.02	0.12	3.06	1.76	0.117
PRODfall	***0.70***	***-0.05***	***0.42***	***14.03***	***2.17***	***0.038***
distance	***-0.19***	***0.57***	***0.00***	***7.12***	***16.91***	***0.001***
ΔSSTsum-win	0.12	-0.16	0.68	4.70	0.00	-
sdSST	***0.05***	***-0.11***	***0.67***	***4.56***	***4.47***	***0.001***

Tableau 3. Summary of the CCA performed on the 87 dinocyst assemblages. Percentages in brackets beneath each axis are the proportion of the variance explained by the axis. Significant relationships ($p<0.05$) between the environmental parameters and the distribution of the assemblages are in bold italic characters. Shaded areas indicate the strongest correlation coefficients between the parameters and the axes. The percentages in the marginal effect column show the proportion of the variance explained by a given environmental parameter when taken individually, without correction for a possible covariance with some of the environmental parameters. The percentages in the conditional effect column show the proportion of the variance explained by a given environmental parameter after correction for the covariance between the parameters. Environmental parameter abbreviations are the same as in fig. 4.

Tableau 4. Synthesis of the coccolith and dinocyst assemblages associated with each region, along with the major hydrographical characteristics in which they develop. Taxa in bold characters are dominant in the assemblages; when more then one is in bold, the first one has on average higher relative abundances.

Region	Coccolith assemblage	Dinocyst assemblage	Water mass characteristics
Offshore Portugal (zone I)	***E. huxleyi*** *G.muellerae* *C. leptoporus* *G. oceanica*	*L. machaerophorum* *Spiniferites* spp. *S. mirabilis*	Warmest winter (15.4 ± 0.1°C) and summer (19.5 ± 0.6°C), highest SSS (36.07 ± 0.04 in summer). Highly productive zone (56.1 ± 7.7 $gC.m^{-2}$) with some of the highest elevated winter and fall productivity (~9.9-11.6 $gC.m^{-2}$).
Celtic Sea (zone II)	***E. huxleyi*** *Syracosphaera* spp.	***S. ramosus*** *Spiniferites* spp. *S. quanta* *Q. concreta* cysts of *P. schwartzii* *S. elongatus*	Mild winter (9.0 ± 0.1°C) and summer (15.6 ± 0.1°C), lower SSS (34.95 ± 0.01 in summer) than in the surrounding open ocean settings, most productive zone (66.3 ± 3.0 $gC.m^{-2}$ annually) with some of the highest elevated winter and fall productivity (~9.3 – 12.5 $gC.m^{-2}$).
South of Rockall Channel (zone III)	***E. huxleyi*** *G. muellerae* *C. leptoporus*	***O. centrocarpum*** *S. elongatus* *S. mirabilis*	Mild winter (10.5 ± 0.5°C) and summer (14.4 ± 1.0°C), high SSS (35.38 ± 0.10 in summer), low productivity (38.5 ± 1.3 $gC.m^{-2}$), mostly in spring (14.2 ± 0.8 $gC.m^{-2}$) and summer (15.1 ± 1.4 $gC.m^{-2}$).
Iceland basin (zone IV)	***E. huxleyi*** *C. pelagicus* *C. leptoporus* *G. muellerae*	***O. centrocaprum*** ***N. labyrinthus*** *S. elongatus*	Mild to cold winter (7.6 ± 1.1°C) and summer (11.8 ± 0.9°C), medium SSS (34.97 ±0.18 in summer), medium productivity (46.1 ± 7.4 $gC.m^{-2}$), mostly in spring (16.4 ± 2.7 $gC.m^{-2}$) and summer (18.6 ± 6.3 $gC.m^{-2}$).
Norwegian Sea (zone V)	***E. huxleyi*** *C. pelagicus*	***O. centrocarpum*** cysts of *P. dalei* *N. labyrinthus*	Cold winter (5.3 ± 1.2°C) and summer (9.6 ± 1.9°C), medium SSS (34.96 ± 0.15 in summer), low productivity (38.4 ± 7.8 $gC.m^{-2}$), mostly in spring (17.6 ± 3.0 $gC.m^{-2}$) and summer (14.6 ± 2.4 $gC.m^{-2}$), generally lower towards the Greenland Sea.
Iceland Sea (zone VI)	*C. pelagicus* ***E. huxleyi***	***O. centrocarpum*** *I. pallidum* cysts of ***P. dalei*** *N. labyrinthus*	Very cold winter (0.7 ± 1.1°C) and summer (5.3 ± 1.8°C), warmer towards the North Iceland shelf. Low SSS, significantly lower in summer (34.04 ± 0.46) than in winter (34.68 ± 0.13). Low to medium productivity (42.6 ± 3.9 $gC.m^{-2}$), most pronounced in spring (20.4 ± 2.4 $gC.m^{-2}$ some of the highest values in the database after the Celtic Sea), and summer.
Irminger Sea (zone VII)	*E. huxleyi* ***C. pelagicus***	***O. centrocarpum*** ***N. labyrinthus*** *Brigantedinium* spp. *S. quanta* *T. applanatum* cysts of *P. schwartzii*	Denmark Strait and central Irminger Sea: cold winter (6.2 ± 0.5°C) and summer (9.6 ± 0.6 °C), medium SSS (34.95 ± 0.15 in summer), medium productivity (48.9 ± 5.3 $gC.m^{-2}$) due to the highest summer productivity values of all the databse (26.3 ± 5.5 $gC.m^{-2}$). East Greenland coast: colder winter and summer (4.2 ± 0.5 and 8.1 ± 1.4°C), lower SSS (34.4 ± 0.5), low productivity (39.4 ± 7.9 $gC.m^{-2}$), mostly in spring and summer.
Labrador Sea (zone VIII)	***C. pelagicus*** *E. huxleyi*	***N. labyrinthus*** *O. centrocarpum* cysts of *P. dalei* *Brigantedinium* spp.	Very cold winter and summer (3.2 ± 1.6 and 7.5 ± 2.0°C), colder towards the north/west compared to the south of Greenland. Low SSS (34.09 ± 0.65 in summer), significantly lower in summer than in winter in the western part of the Labrador Sea. Generally low productivity (34.9 ± 7.2 $gC.m^{-2}$), except in the southernmost western sites where high winter productivity values are observed.
Newfoundland shelf (zone IX)	***E. huxleyi*** ***C. pelagicus*** ***C. leptoporus***	***O. centrocarpum*** *Brigantedinium* spp. *B. tepikiense* cysts of *P. dalei*	Very cold winter (0.6 ± 0.5°C) and mild summer (14.2 ± 0.9°C), very low SSS, significantly lower in summer (31.31 ± 0.53) than in winter (31.97 ± 0.42). Medium productivity (46.3 ± 3.6 $gC.m^{-2}$), most pronounced in summer and spring, significant in winter and fall.
Scotian shelf (zone X)	***C. leptoporus*** *C. pelagicus* *E. huxleyi* *G. oceanica*	***Brigantedinium*** spp. ***O. centrocarpum*** cysts of *P. dalei* *S. ramosus* *S. mirabilis*	Very cold winter (2.7 ± 0.9°C) and mild summer (16.6 ± 0.3°C), very low SSS (31.50 ± 0.41 in summer). Medium to high productivity (51.3 ± 1.5 $gC.m^{-2}$), mostly in summer and spring, significant in winter. Highest fall productivity of all the database (11.6 ± 0.9 $gC.m^{-2}$).

Appendix A. Coccolith taxonomy. The complete list refers to species identified within the original coccolith database (163 samples). Species in bold are the coccolith taxa whose counts were subjected to the CCA analyses.

Calcidiscus leptoporus (Murray et Blackman 1898) Loeblich Jr and Tappan 1978.
Includes forms assigned by A. Pujos to *Coccolithus pataecus* Gartner 1967.

Ceratolithus cristatus Kamptner 1950

Coccolithus pelagicus (Wallich 1877) Schiller 1930

Emiliania huxleyi (Lohmann 1902) Hay and Mohler in Hay et al., 1967

Gephyrocapsa muellerae Bréheret 1978

Gephyrocapsa oceanica Kamptner 1943

Helicosphaera Kamptner 1954
Mainly refers in the present database to *Helicosphaera carteri* (Wallich 1877) Kamptner 1954.

Pontosphaera Lohmann 1902

Rhabdosphaera Haeckel 1894
Mainly refers in the present database to *Rhabdosphaera clavigera* Murray and Blackman 1898

Scapholiths: rhombolith-type coccoliths inadequately assigned to the artificial species *Scapholithus fossilis*, now ranked in the family Calciosoleniaceae Kamptner 1937, and its two species *Calciosolenia brasiliensis* (Lohmann 1919) Young in Young et al. 2003 and *Calciosolenia murrayi* Gran 1912

Syracosphaera Lohmann 1902
Mainly refers in the present database to *Syracosphaera pulchra* Lohmann 1902

Umbilicosphaera sibogae (Weber-Ban Bosse 1901) Gaarder 1970
Includes forms assigned by A. Pujos to *Umbellosphaera mirabilis* Gartner 1967

Appendix B. Dinocyst taxonomy. Note that some of the 45 taxa used in the statistical analyses do not appear as they group taxa already on this list (e.g., *Impagidinium* spp., Protoperidinoids, etc.).

Achomosphaera spp. Evitt 1963
Ataxiodinium choane Reid 1974
Bitectatodinium tepikiense Wilson 1973
Brigantedinium spp. Reid 1977
    Includes *Brigantedinium cariacoense* (Wall 1967) Lentin et Williams 1993 and *Brigantedinium simplex* Wall 1965 ex Lentin et Williams 1993
cf. *Scripsiella trifida* Lewis 1991
Cyst of *Gymnodinium catenatum* Graham 1943
Cyst of *Gymnodinium nolleri* Ellegaard & Moestrup 1999
Cyst of *Pentapharsodinium dalei* Indelicato et Loeblich III 1986
Cyst of *Polykrikos schwartzii* Bütschli 1873
Impagidinium aculeatum (Wall 1967) Lentin et Williams 1981
Impagidinium pallidum Bujak 1984
Impagidinium paradoxum (Wall 1967) Stover et Evitt 1978
Impagidinium patulum (Wall 1967) Stover et Evitt 1978
Impagidinium sphaericum (Wall 1967) Lentin et Williams 1981
Impagidinium strialatum (Wall 1967) Stover et Evitt 1978
Islandinium minutum (Harland et Reid in Harland et al. 1980) Head et al. 2001
Islandinium? cezare (de Vernal et al. 1989 ex de Vernal in Rochon et al. 1999) Head et al. 2001
Lejeunecysta oliva (Reid 1977) Turon & Londeix 1988
Lejeunecysta sabrina (Reid 1977) Bujak 1984
Lingulodinium machaerophorum (Deflandre et Cookson 1955) Wall 1967
Nematosphaeropsis labyrinthus (Ostenfeld 1903) Reid 1974
Operculodinium centrocarpum sensu Wall et Dale 1966
Operculodinium janduchenei Head et al. 1989
Protoperidinium stellatum (Wall in Wall et Dale 1968) Rochon et al. 1999
Pixidinopsis reticulata (McMinn et Sun 1994) Marret et de Vernal 1997
Protoperidinium americanum (Gran et Braarud 1935) Balech 1974
Quinquecuspis concreta (Reid 1977) Harland 1977
Selenopemphix nephroides (Benedek 1972) Benedek et Sarjeant 1981
Selenopemphix quanta s.l.
    Includes *Selenopemphix quanta* (Bradford 1975) Matsuoka 1985 and cysts of *Protoperidinium nudum* (Meunier 1919) Balech 1974
Spiniferites bentorii (Rossignol 1964) Wall et Dale 1970
Spiniferites delicatus Reid 1974
Spiniferites elongatus s.l.
    Includes *Spiniferites elongatus* Reid 1974 and *Spiniferites frigidus* Harland et Reid in Harland et al. 1980
Spiniferites lazus Reid 1974
Spiniferites membranaceus s.l.

Includes *Spiniferites membranaceus* (Rossignol 1964) Sarjeant 1970 and *Spiniferites belerius* Reid 1974

Spiniferites mirabilis s.l.

Includes *Spiniferites mirabilis* (Rossignol 1967) Sarjeant 1970 and *Spiniferites hyperacanthus* (Deflandre et Cookson 1955) Cookson et Eisenack 1974

Spiniferites ramosus s.l.

Includes *Spiniferites ramosus* (Ehrenberg 1838) Mantell 1854 and *Spiniferites bulloideus* (Deflandre et Cookson 1955) Sarjeant 1970

Trinovantedinium applanatum (Bradford 1977) Bujak et Davies 1983

Votadinium calvum Reid 1977

Xandarodinium xanthum Reid 1977

Appendix C. Coccolith taxa relative abundances of previously unavailable data from the 87-site database.

Site	*Calcidiscus leptoporus*	*Coccolithus pelagicus*	*Emiliania huxleyi*	*Gephyrocapsa muellerae*	*Gephyrocapsa oceanica*	*Helicosphaera* spp.	*Rhabdosphaera* spp.	*Syracosphaera* spp.	*Umbilicosphaera sibogae*
2666	**5.56**	**61.11**	**33.33**	**0.00**	**0.00**	**0.00**	**0.00**	**0.00**	**0.00**
2639	**0.00**	**78.46**	**21.54**	**0.00**	**0.00**	**0.00**	**0.00**	**0.00**	**0.00**
2646	**0.00**	**84.35**	**14.78**	**0.00**	**0.00**	**0.00**	**0.00**	**0.87**	**0.00**
2667	**0.00**	**50.00**	**50.00**	**0.00**	**0.00**	**0.00**	**0.00**	**0.00**	**0.00**
2674	**1.33**	**36.00**	**60.33**	**2.00**	**0.00**	**0.00**	**0.00**	**0.33**	**0.00**
2730	**0.00**	**55.50**	**43.12**	**0.92**	**0.00**	**0.00**	**0.00**	**0.46**	**0.00**
2746	**0.00**	**59.26**	**39.81**	**0.93**	**0.00**	**0.00**	**0.00**	**0.00**	**0.00**
2752	**0.00**	**54.55**	**45.45**	**0.00**	**0.00**	**0.00**	**0.00**	**0.00**	**0.00**
2757	**0.00**	**76.19**	**23.81**	**0.00**	**0.00**	**0.00**	**0.00**	**0.00**	**0.00**
2760	**0.00**	**20.00**	**80.00**	**0.00**	**0.00**	**0.00**	**0.00**	**0.00**	**0.00**
2764	**0.00**	**77.54**	**21.74**	**0.00**	**0.00**	**0.00**	**0.00**	**0.72**	**0.00**
2770	**0.57**	**89.71**	**9.71**	**0.00**	**0.00**	**0.00**	**0.00**	**0.00**	**0.00**
2775	**0.00**	**92.56**	**7.44**	**0.00**	**0.00**	**0.00**	**0.00**	**0.00**	**0.00**
2778	0.00	90.60	9.02	0.38	0.00	0.00	0.00	0.00	0.00
2780	**0.00**	**41.18**	**58.82**	**0.00**	**0.00**	**0.00**	**0.00**	**0.00**	**0.00**
2784	**5.56**	**33.33**	**61.11**	**0.00**	**0.00**	**0.00**	**0.00**	**0.00**	**0.00**
2788	**0.00**	**15.38**	**84.62**	**0.00**	**0.00**	**0.00**	**0.00**	**0.00**	**0.00**
2793	**0.00**	**61.68**	**38.32**	**0.00**	**0.00**	**0.00**	**0.00**	**0.00**	**0.00**
2875	**0.71**	**35.46**	**63.12**	**0.71**	**0.00**	**0.00**	**0.00**	**0.00**	**0.00**
2879	**0.00**	**42.37**	**56.11**	**0.38**	**0.00**	**0.38**	**0.00**	**0.75**	**0.00**
2894	**0.50**	**33.83**	**65.17**	**0.00**	**0.00**	**0.00**	**0.00**	**0.50**	**0.00**
A074	10.00	46.60	40.60	0.00	1.10	0.90	0.00	0.30	0.50
A099	5.99	68.26	23.45	0.40	0.40	1.30	0.00	0.20	0.00
A100	3.80	52.15	41.74	0.90	0.90	0.50	0.00	0.00	0.00
A103	10.20	46.20	39.50	2.20	0.20	0.40	0.00	1.30	0.00
A104	3.60	82.80	12.40	0.80	0.00	0.40	0.00	0.00	0.00
A105	2.00	95.40	2.40	0.00	0.00	0.20	0.00	0.00	0.00
A106	1.60	64.00	32.40	1.30	0.00	0.50	0.00	0.20	0.00
A107	3.60	44.10	49.90	1.40	0.00	0.20	0.00	0.80	0.00
A109	3.00	35.20	58.30	2.60	0.00	0.10	0.10	0.70	0.00
A110	5.51	52.51	38.68	2.40	0.00	0.30	0.00	0.50	0.10
A111	3.50	27.90	66.00	1.60	0.00	0.30	0.20	0.50	0.00
A112	3.90	40.96	53.35	1.00	0.00	0.20	0.00	0.60	0.00
A113	6.99	18.68	71.13	1.00	0.20	0.50	0.00	1.30	0.20
A114	8.81	1.80	79.08	6.91	0.10	0.30	0.00	2.70	0.30
A118	14.51	1.00	73.57	6.91	0.70	0.60	0.00	2.70	0.00
A119	10.69	3.30	74.93	7.29	0.20	1.00	0.00	2.20	0.40
A120	12.49	3.20	70.83	8.69	0.20	1.30	0.00	2.60	0.70

Site	*Calcidiscus leptoporus*	*Coccolithus pelagicus*	*Emiliania huxleyi*	*Gephyrocapsa muellerae*	*Gephyrocapsa oceanica*	*Helicosphaera* spp.	*Rhabdosphaera* spp.	*Syracosphaera* spp.	*Umbilicosphaera sibogae*
A121	12.41	2.40	72.17	7.71	0.40	1.00	0.10	3.40	0.40
A123	21.74	1.10	60.32	13.03	0.70	0.70	0.10	2.00	0.30
A168	6.79	65.93	26.07	0.20	0.00	0.70	0.00	0.30	0.00
A170	8.00	51.40	37.20	1.60	0.20	0.70	0.00	0.90	0.00
A171	4.50	46.75	45.95	1.40	0.00	0.40	0.10	0.90	0.00
A173	3.71	31.56	61.22	1.20	0.10	0.90	0.10	1.20	0.00
A174	8.79	13.59	70.13	3.20	0.50	0.70	0.00	3.10	0.00
A175	7.20	19.10	67.30	3.20	0.30	1.40	0.00	1.50	0.00
A258	45.00	37.30	10.00	0.00	6.80	0.90	0.00	0.00	0.00
A259	45.60	28.30	21.70	0.00	2.60	1.80	0.00	0.00	0.00
A260	48.30	32.93	9.48	0.40	7.39	1.10	0.00	0.40	0.00
A261	24.70	29.30	39.10	1.00	3.70	1.90	0.00	0.00	0.30
A262	35.90	49.00	4.50	0.00	9.80	0.00	0.00	0.00	0.80
A264	7.21	1.70	77.66	4.11	4.21	1.70	1.00	0.80	1.60
A265	7.91	2.00	72.37	5.31	5.71	2.60	1.50	1.80	0.80
A266	6.93	1.10	74.10	6.63	5.92	0.80	0.80	1.71	2.01
Celt4	**0.00**	**4.11**	**91.78**	**0.00**	**0.00**	**0.00**	**0.00**	**4.11**	**0.00**
Celt5	**0.00**	**3.10**	**91.80**	**0.00**	**0.00**	**0.00**	**0.00**	**5.10**	**0.00**
Celt6	**0.00**	**1.20**	**95.10**	**1.20**	**0.00**	**0.00**	**0.00**	**2.50**	**0.00**
Celt7	**0.00**	**5.24**	**89.63**	**1.01**	**0.00**	**0.00**	**0.00**	**4.13**	**0.00**
Celt8	0.00	4.40	92.30	1.10	0.00	0.00	0.00	2.20	0.00
G075	23.62	29.23	44.24	0.70	1.50	0.70	0.00	0.00	0.00
G076	11.91	17.92	69.77	0.00	0.20	0.00	0.00	0.20	0.00
G077	29.27	35.36	34.57	0.00	0.30	0.00	0.00	0.50	0.00
G078	38.40	27.60	32.00	0.00	0.80	0.00	0.00	1.20	0.00
L087	12.50	79.80	7.10	0.20	0.00	0.40	0.00	0.00	0.00
L090	0.60	49.85	48.15	0.20	0.00	0.40	0.00	0.80	0.00
L091	2.69	66.87	29.14	0.20	0.20	0.50	0.00	0.20	0.20
L092	2.90	78.62	16.68	0.40	0.00	0.90	0.00	0.50	0.00
L093	2.59	78.54	17.47	0.40	0.40	0.40	0.00	0.20	0.00
L094	2.30	80.64	15.77	0.20	0.20	0.50	0.00	0.20	0.20
L162	0.00	99.10	0.00	0.00	0.90	0.00	0.00	0.00	0.00
L163	1.90	80.80	15.20	1.10	0.30	0.20	0.00	0.30	0.20
L164	0.20	99.30	0.00	0.00	0.50	0.00	0.00	0.00	0.00
L177	8.00	39.00	47.70	1.90	1.50	1.70	0.00	0.20	0.00
L178	6.40	47.50	41.20	1.10	0.90	2.30	0.00	0.00	0.60
N241	1.30	6.00	91.20	1.00	0.20	0.00	0.00	0.30	0.00

Site	2636	2639	2645	2667	2674	2730	2746	2752	2757	2760	2764	2770	2775	2778	2780	2784	2788	2793	2875	2879	2894	4071
Achomosphaera spp.	0.0	0.0	0.0	0.0	0.0	0.0	0.0	0.0	0.0	0.0	0.0	0.0	0.0	0.0	0.0	0.0	0.0	0.0	0.0	0.0	0.0	0.0
Ataxiodinium choane	1.0	0.0	0.0	0.0	0.0	0.0	0.0	0.0	0.0	0.0	0.0	0.0	0.0	0.0	0.0	0.0	0.0	0.0	0.0	0.0	0.0	0.3
Bitectatodinium tepikiense	1.4	0.2	0.0	0.0	0.0	0.2	1.1	0.0	0.0	0.2	0.0	0.5	0.0	0.0	0.0	0.1	0.4	0.2	0.2	0.2	1.2	25.9
Brigantedinium spp.	58.1	1.2	0.0	0.3	0.7	0.7	4.7	1.7	8.4	0.0	4.5	10.3	5.6	0.5	0.0	0.7	4.2	2.6	6.4	4.4	3.0	11.0
cf. *Scrippsiella trifida*	0.0	0.0	0.0	0.0	0.0	0.0	0.0	0.0	0.0	0.0	0.0	0.0	0.0	0.0	0.0	0.0	0.0	0.0	0.0	0.4	0.0	0.6
cysts of *Gymnodinium catenatum*	0.0	0.0	0.0	0.0	0.0	0.0	0.0	0.0	0.0	0.0	0.0	0.0	0.0	0.0	0.0	0.0	0.0	0.0	0.0	0.0	0.0	0.0
cysts of *Gymnodinium nolleri*	0.0	0.0	0.0	0.0	0.0	0.0	0.0	0.0	0.0	0.0	0.0	0.0	0.0	0.0	0.0	0.0	0.0	0.0	0.0	0.0	0.0	0.0
cysts of *Pentapharsodinium dalei*	4.1	20.0	37.6	74.3	93.2	57.9	44.3	56.0	50.0	36.0	20.0	1.5	12.8	24.1	68.4	68.0	55.8	74.5	0.2	2.4	0.8	9.2
cysts of *Polykrikos schwartzii*	0.3	0.0	0.0	0.0	0.0	0.5	0.0	0.0	0.0	0.0	0.0	0.0	0.0	0.0	0.0	0.0	0.0	0.4	0.9	0.8	0.5	0.0
cysts of *Polykrikos* sp. - Arctic morphotype	0.0	0.0	0.0	0.0	0.0	0.0	0.0	0.2	0.0	0.0	0.0	0.0	0.0	0.0	0.0	0.0	0.0	0.0	0.0	0.0	0.0	0.0
Dubridinium spp.	0.0	0.0	0.0	0.0	0.0	0.0	0.0	0.0	0.0	0.0	0.0	0.0	0.0	0.0	0.0	0.0	0.0	0.0	0.0	0.0	0.0	0.0
Impagidinium aculeatum	0.0	0.0	0.0	0.0	0.0	0.0	0.0	0.0	0.0	0.0	0.0	0.0	0.0	0.0	0.0	0.0	0.0	0.0	0.0	0.0	0.0	0.0
Impagidinium pallidum	0.0	4.2	3.8	0.3	0.0	0.0	0.0	3.1	2.1	4.2	5.7	17.5	14.2	14.2	0.6	0.2	0.6	0.2	0.0	0.0	0.0	0.0
Impagidinium paradoxum	0.0	0.0	0.0	0.0	0.0	0.0	0.0	0.0	0.0	0.0	0.0	0.0	0.0	0.0	0.0	0.0	0.0	0.0	0.0	0.0	0.0	0.0
Impagidinium patulum	0.0	0.0	0.0	0.0	0.0	0.0	0.0	0.0	0.0	0.2	0.0	0.0	0.0	0.0	0.0	0.0	0.0	0.0	0.0	0.0	0.0	0.0
Impagidinium sphaericum	0.0	0.0	0.0	0.0	0.0	0.2	0.2	0.0	0.2	0.0	0.0	0.9	0.3	0.0	0.0	0.2	0.0	0.1	0.4	0.4	0.0	0.3
Impagidinium spp.	0.0	0.0	0.0	0.0	0.0	0.0	0.0	0.0	0.0	0.0	0.0	0.0	0.0	0.0	0.0	0.0	0.0	0.0	0.0	0.0	0.0	0.0
Impagidinium striatum	0.0	0.0	0.0	0.0	0.0	0.0	0.0	0.0	0.0	0.0	0.0	0.0	0.0	0.0	0.0	0.0	0.0	0.0	0.0	0.0	0.0	0.0
Islandinium minutum	5.1	0.0	1.0	0.0	0.3	1.1	0.2	1.9	0.0	0.2	2.0	2.6	0.8	3.1	0.0	0.3	0.3	0.5	0.0	0.0	0.0	0.6
Islandinium? cezare	0.3	0.0	0.2	0.0	0.0	0.0	0.0	0.0	0.0	0.0	0.0	0.0	0.3	0.2	0.0	0.0	0.0	0.0	0.0	0.0	0.0	0.0
Lejeunecysta oliva	0.0	0.0	0.0	0.0	0.0	0.0	0.0	0.0	0.0	0.0	0.0	0.0	0.0	0.0	0.0	0.0	0.0	0.0	0.0	0.0	0.0	0.0
Lejeunecysta sabrina	0.0	0.0	0.0	0.0	0.0	0.0	0.0	0.0	0.0	0.0	0.0	0.0	0.0	0.0	0.0	0.0	0.0	0.0	0.0	0.0	0.0	0.0
Lejeunecysta spp.	0.0	0.0	0.0	0.0	0.0	0.0	0.0	0.0	0.0	0.0	0.0	0.0	0.0	0.0	0.0	0.0	0.0	0.0	0.0	0.0	0.0	0.0
Lingulodinium machaerophorum	0.0	0.0	0.0	0.0	0.0	0.0	0.0	0.0	0.0	0.0	0.0	0.0	0.0	0.0	0.0	0.0	0.0	0.0	0.0	0.0	0.0	0.0
Nematosphaeropsis labyrinthus	1.4	14.8	5.7	3.7	0.8	9.4	13.5	9.2	10.5	15.8	20.2	30.3	16.8	14.9	5.1	7.0	14.7	7.8	31.4	31.2	34.1	2.4
Operculodinium centrocarpum	17.0	53.5	49.3	9.7	2.1	22.2	27.6	24.3	19.7	39.3	37.6	32.4	45.2	39.7	20.2	16.8	13.1	8.6	56.9	52.8	54.3	43.8
Operculodinium janduchenei	0.0	0.0	0.0	0.0	0.0	0.0	0.0	0.0	0.0	0.0	0.0	0.0	0.0	0.0	0.0	0.0	0.0	0.0	0.0	0.0	0.0	0.0
Pyxidinopsis reticulata	0.0	0.0	0.0	0.0	0.0	0.0	0.0	0.0	0.0	0.0	0.0	0.0	0.0	0.0	0.0	0.0	0.0	0.0	0.0	0.0	0.0	0.0
Protoperidinioids	0.3	0.0	0.0	0.0	0.0	0.0	0.0	0.0	0.0	0.0	0.0	0.0	0.0	0.0	0.0	0.0	0.0	0.0	0.0	0.0	0.0	0.0
Protoperidinium americanum	0.0	0.0	0.0	0.2	0.0	0.3	0.0	0.0	0.0	0.0	0.0	0.0	0.5	0.0	0.0	0.0	0.4	0.4	0.0	0.0	0.0	0.0
Protoperidinium stellatum	0.0	0.0	0.0	0.0	0.0	0.0	0.0	0.0	0.0	0.0	0.0	0.0	0.0	0.0	0.0	0.0	0.0	0.0	0.0	0.0	0.0	0.0
Quinquecuspis concreta	0.0	0.0	0.0	0.0	0.0	0.1	0.0	0.0	0.0	0.0	0.0	0.0	0.0	0.0	0.0	0.0	0.4	0.0	0.1	0.0	0.0	0.0
Selenopemphix nephroides	0.0	0.0	0.0	0.0	0.1	0.0	0.0	0.0	0.0	0.0	0.0	0.0	0.0	0.0	0.0	0.0	0.0	0.0	0.0	0.0	0.0	0.0
Selenopemphix quanta	0.7	0.0	0.0	2.0	0.7	1.4	0.6	0.2	1.9	0.2	0.7	0.2	0.8	0.2	0.4	0.5	0.9	0.6	2.3	2.4	0.7	0.6
Spiniferites bentorii	0.0	0.0	0.0	0.0	0.0	0.0	0.0	0.0	0.0	0.0	0.0	0.0	0.0	0.0	0.0	0.0	0.0	0.0	0.0	0.0	0.0	0.0
Spiniferites delicatus	0.0	0.0	0.0	0.0	0.0	0.0	0.0	0.0	0.0	0.0	0.0	0.0	0.0	0.0	0.0	0.0	0.0	0.0	0.0	0.0	0.0	0.0
Spiniferites elongatus	2.0	3.1	2.0	4.3	1.6	2.6	3.6	0.5	2.2	1.8	5.4	3.0	0.8	1.2	2.1	2.1	4.3	0.9	0.2	1.6	1.2	0.6
Spiniferites lazus	0.0	0.0	0.0	0.0	0.0	0.0	0.0	0.0	0.0	0.0	0.0	0.0	0.0	0.0	0.0	0.0	0.0	0.0	0.0	0.0	0.0	0.0
Spiniferites membranaceus	0.0	0.0	0.0	0.2	0.0	0.0	0.0	0.0	0.0	0.0	0.0	0.0	0.0	0.0	0.0	0.0	0.0	0.0	0.0	0.0	0.0	0.0
Spiniferites mirabilis	0.0	0.0	0.0	0.0	0.0	0.0	0.0	0.0	0.0	0.0	0.0	0.0	0.0	0.0	0.0	0.0	0.0	0.0	0.0	0.0	0.0	0.0
Spiniferites ramosus	5.7	3.1	0.4	3.8	0.4	3.4	4.2	2.8	3.9	2.2	3.9	0.2	1.9	1.9	3.2	4.2	4.7	2.7	1.2	3.2	4.3	0.9
Spiniferites spp.	1.7	0.0	0.0	1.0	0.0	0.2	0.0	0.0	1.1	0.0	0.0	0.2	0.0	0.0	0.0	0.0	0.5	0.0	0.0	0.0	0.0	3.9
Trinovantedinium applanatum	0.0	0.0	0.0	0.2	0.0	0.0	0.0	0.0	0.0	0.0	0.0	0.0	0.0	0.0	0.0	0.0	0.0	0.1	0.0	0.0	0.0	0.0
Votadinium calvum	0.0	0.0	0.0	0.0	0.0	0.0	0.0	0.0	0.0	0.0	0.0	0.0	0.0	0.0	0.0	0.0	0.1	0.0	0.0	0.0	0.0	0.0
Xandarodinium xanthum	0.0	0.0	0.0	0.0	0.0	0.0	0.0	0.0	0.0	0.0	0.0	0.0	0.0	0.0	0.0	0.0	0.0	0.0	0.0	0.0	0.0	0.0

Appendix D. Dinocyst taxa relative abundances in the 87-site database.

Site	A099	A100	A103	A104	A105	A106	A107	A109	A110	A111	A112	A113	A114	A118	A119	A120	A121	A123	A168	A170	A171	A173
Achomosphaera spp.	0.0	0.0	0.0	0.0	0.0	0.0	0.0	0.0	0.0	0.0	0.0	0.0	0.0	0.0	0.0	0.0	0.0	0.0	0.0	0.0	0.0	0.0
Alexandrium choane	0.0	0.0	0.0	0.0	0.0	0.0	0.0	0.0	0.0	0.0	0.0	0.0	0.0	0.1	0.0	0.0	0.0	0.0	0.0	0.0	0.0	0.0
Bilecitatodinium tepikiense	0.2	0.3	0.5	1.3	0.0	0.3	0.0	0.3	0.7	0.0	0.0	1.2	1.2	1.2	0.0	1.2	0.2	0.3	0.6	0.0	1.0	2.8
Brigantedinium spp	6.1	5.6	1.4	12.1	1.2	8.1	4.1	17.7	25.0	20.6	27.6	7.1	26.6	5.3	6.8	45.7	4.1	5.7	0.3	22.4	23.9	8.2
cf. *Scrippsiella trifida*	0.0	0.0	0.0	0.0	0.4	0.0	0.0	0.0	0.0	0.0	0.0	0.0	0.0	0.0	0.0	0.0	0.0	0.0	0.0	0.0	0.0	0.0
cysts of *Gymnodinium catenatum*	0.0	0.0	0.0	0.0	0.0	0.0	0.0	0.0	0.0	0.0	0.0	0.0	0.0	0.0	0.0	0.0	0.0	0.0	0.0	0.0	0.0	0.0
cysts of *Gymnodinium nolleri*	0.0	0.0	0.0	0.0	0.0	0.0	0.0	0.0	0.0	0.0	0.0	0.0	0.0	0.0	0.0	0.0	0.0	0.0	0.0	0.0	0.0	0.0
cysts of *Pentapharsodinium dalei*	21.2	6.6	3.7	1.7	13.3	3.0	2.0	0.0	0.0	0.3	0.0	0.3	0.2	0.2	0.0	0.0	0.0	0.3	3.0	0.0	8.0	20.7
cysts of *Polykrikos schwartzii*	0.7	0.0	0.3	0.0	0.2	1.0	0.0	2.5	3.8	1.4	8.6	0.0	2.0	0.0	0.0	13.2	0.1	0.3	0.0	3.4	4.0	2.8
cysts of *Polykrikos* sp. - Arctic morphotype	0.0	0.0	0.0	0.0	0.0	0.0	0.0	0.0	0.0	0.0	0.0	0.0	0.0	0.0	0.0	0.0	0.0	0.0	0.0	0.0	0.0	0.0
Dubridinium spp.	0.0	0.0	0.0	0.0	0.0	0.0	0.0	0.0	0.0	0.0	0.0	0.0	0.0	0.0	0.0	0.0	0.0	0.0	0.0	0.0	0.0	0.0
Impagidinium aculeatum	0.2	0.0	0.1	0.0	0.0	0.0	0.0	0.0	0.0	0.3	0.0	0.6	1.5	0.4	5.7	0.0	0.0	0.0	0.0	0.0	0.0	0.6
Impagidinium pallidum	0.0	0.0	0.0	0.0	0.4	0.0	0.0	0.0	0.0	0.0	0.0	0.0	0.0	0.0	0.0	0.0	0.0	0.0	0.0	0.0	0.0	0.6
Impagidinium paradoxum	0.0	0.0	0.0	0.0	0.0	0.0	0.3	0.0	0.0	0.0	0.0	1.2	2.9	1.6	4.5	1.8	0.3	0.0	0.0	1.7	0.7	0.0
Impagidinium patulum	0.0	0.0	0.0	0.0	0.0	0.0	0.0	0.0	0.0	0.0	0.0	0.0	0.0	0.0	1.1	0.0	0.0	0.0	0.0	0.0	0.0	0.0
Impagidinium sphaericum	0.9	1.9	0.5	0.0	1.2	1.8	1.2	1.1	0.7	2.0	0.0	0.6	0.2	0.8	1.1	2.1	0.0	0.3	0.2	0.0	2.7	0.9
Impagidinium spp.	0.0	0.0	0.0	0.4	0.0	0.0	0.0	0.0	0.0	0.0	0.0	0.0	0.0	0.0	0.0	0.0	0.0	0.0	0.0	0.0	0.0	0.0
Impagidinium striatum	0.0	0.0	0.0	0.0	0.0	0.0	0.0	0.0	0.0	0.0	0.0	0.0	0.2	0.0	0.0	0.3	0.0	0.0	0.0	0.0	0.0	0.0
Islandinium minutum	0.0	0.0	0.0	0.0	0.0	0.0	0.0	0.0	0.0	0.0	0.0	0.0	0.0	0.0	0.0	0.0	0.0	0.0	0.0	0.0	0.0	0.0
Islandinium? cezare	0.0	0.0	0.0	0.0	0.0	0.0	0.0	0.0	0.0	0.0	0.0	0.0	0.0	0.0	0.0	0.0	0.0	0.0	0.0	0.0	0.0	0.0
Lejeunecysta oliva	0.0	0.0	0.0	0.0	0.0	0.0	0.0	0.0	0.0	0.0	0.0	0.0	0.0	0.0	0.0	0.0	0.0	0.0	0.0	0.0	0.0	0.0
Lejeunecysta sabrina	0.0	0.0	0.0	0.0	0.0	0.0	0.0	0.0	0.0	0.0	0.0	0.0	0.0	0.0	0.0	0.0	0.0	0.0	0.0	0.0	0.0	0.0
Lejeunecysta spp.	0.0	0.0	0.0	0.0	0.0	0.0	0.0	0.0	0.0	0.0	0.0	0.0	0.0	0.0	0.0	0.0	0.0	0.0	0.0	0.0	0.0	0.0
Lingulodinium machaerophorum	0.0	0.0	0.0	0.0	0.0	0.0	0.0	0.0	0.0	0.0	0.0	0.0	0.0	0.0	0.0	0.0	0.0	0.0	0.0	0.0	0.0	0.0
Nematosphaeropsis labyrinthus	29.9	39.5	12.8	25.0	71.5	24.6	43.9	25.7	21.7	42.4	24.1	8.9	2.7	0.3	8.0	5.3	5.2	4.6	1.5	41.4	40.9	26.3
Operculodinium centrocarpum	36.0	40.8	74.3	47.0	6.8	50.5	41.6	43.5	36.2	25.1	25.9	55.8	37.9	57.5	40.9	11.1	73.3	62.1	72.1	25.9	14.0	25.7
Operculodinium janduchenei	0.4	0.3	0.5	3.4	0.0	0.3	0.6	0.0	0.0	0.3	0.0	0.9	0.5	0.2	1.1	0.3	0.1	0.3	0.0	0.0	0.0	0.0
Pixidinopsis reticulata	0.0	0.0	0.0	0.0	0.0	0.0	0.3	0.0	0.0	0.0	0.0	0.3	0.0	0.0	0.0	0.0	0.0	0.0	0.0	0.0	0.0	0.0
Protoperidinioids	0.0	0.0	0.0	1.3	0.0	0.0	0.0	0.0	0.0	0.3	0.0	0.0	0.0	0.1	0.0	0.0	0.0	0.0	0.0	0.0	0.0	0.0
Protopendinium americanum	0.0	0.0	0.0	0.0	0.0	0.0	0.0	0.0	0.0	0.0	0.0	0.0	0.0	0.0	0.0	0.0	0.0	0.0	0.0	0.0	0.0	0.0
Protoperidinium stellatum	0.0	0.0	0.0	0.0	0.0	0.0	0.0	0.0	0.0	0.0	0.0	0.0	0.0	0.0	0.0	0.0	0.0	0.0	0.0	0.0	0.0	0.0
Quinquecuspis concreta	0.0	0.0	0.0	0.0	0.0	0.0	0.0	0.0	0.0	0.0	0.0	0.0	0.0	0.0	0.0	0.0	0.0	0.0	0.0	0.0	0.0	0.0
Selenopemphix nephroides	0.0	0.0	0.0	0.0	0.0	0.0	0.0	0.0	0.0	0.0	0.0	0.3	0.0	0.2	0.0	0.0	0.0	0.0	0.0	0.0	0.0	0.0
Selenopemphix quanta	1.7	2.9	0.5	5.2	4.7	5.6	0.6	0.6	3.8	2.5	10.3	0.0	0.5	0.8	0.0	0.3	0.3	0.0	0.2	0.0	0.7	1.3
Spiniferites bentorii	0.0	0.0	0.0	0.0	0.0	0.0	0.0	0.0	0.0	0.0	0.0	0.0	0.0	0.0	0.0	0.0	0.0	0.0	0.0	0.0	0.0	0.0
Spiniferites delicatus	0.0	0.0	0.0	0.0	0.0	0.0	0.0	0.0	0.0	0.0	0.0	0.0	0.0	0.0	0.0	0.0	0.0	0.3	0.0	0.0	0.0	0.0
Spiniferites elongatus	0.4	1.3	1.5	0.9	0.2	1.5	1.5	4.2	3.8	2.3	0.0	15.1	3.4	16.3	18.2	3.2	13.6	19.4	0.5	0.0	3.7	7.8
Spiniferites lazus	0.0	0.0	0.0	0.0	0.0	0.0	0.0	0.0	0.0	0.0	0.0	0.0	0.0	0.0	0.0	0.0	0.0	0.0	0.0	0.0	0.0	0.0
Spiniferites membranaceus	0.0	0.0	0.0	0.4	0.0	0.0	0.0	0.0	0.0	0.0	0.0	0.0	0.0	0.0	0.0	0.0	0.0	0.0	0.0	0.0	0.0	0.0
Spiniferites mirabilis	0.0	0.0	0.0	0.0	0.0	0.0	0.0	0.0	0.0	0.0	0.0	1.5	16.7	1.3	11.4	6.7	1.6	6.0	0.0	0.0	0.3	0.0
Spiniferites ramosus	1.3	0.3	3.7	0.4	0.0	2.0	1.7	0.3	0.0	0.0	0.0	0.0	0.0	0.2	1.1	0.9	0.1	0.0	5.6	0.0	0.3	1.3
Spiniferites spp.	0.2	0.3	0.2	0.4	0.0	0.3	0.9	0.8	0.3	0.0	0.0	0.0	1.2	0.0	0.0	0.3	0.0	0.0	0.0	0.0	0.0	0.9
Trinovantedinium applanatum	0.7	0.3	0.2	0.4	0.2	1.0	1.5	2.2	3.1	2.0	3.4	6.2	0.7	4.3	0.0	7.6	1.2	0.6	0.0	5.2	0.0	0.0
Votadinium calvum	0.0	0.0	0.0	0.0	0.0	0.0	0.0	0.0	0.0	0.0	0.0	0.0	0.0	0.0	0.0	0.0	0.0	0.0	0.0	0.0	0.0	0.0
Xandarodinium xanthum	0.0	0.0	0.0	0.0	0.0	0.0	0.0	0.0	0.0	0.0	0.0	0.0	0.2	0.0	0.0	0.0	0.0	0.0	0.0	0.0	0.0	0.0

Appendix D. (continued)

Site	A174	A175	A258	A259	A260	A261	A262	A264	A265	A266	Cet4	Cet5	Cet6	Cet7	Cet8	G075	G076	G077	G078	L087	L090	L091
Achomosphaera spp	0.0	0.0	0.0	0.0	0.0	0.0	0.6	0.0	0.0	0.4	0.0	0.0	0.0	0.0	0.0	0.0	0.0	0.0	0.0	0.0	0.0	0.0
Ataxodinium choane	0.3	0.0	0.0	0.0	0.0	0.0	0.0	0.0	0.0	0.0	0.2	0.7	0.5	0.2	0.2	0.6	0.7	0.0	0.3	0.2	0.0	0.0
Bitectatodinium tepikiense	0.3	0.7	2.5	1.0	1.2	0.0	4.5	0.0	0.0	0.0	6.1	6.3	3.0	5.6	3.4	10.2	12.0	3.2	9.0	0.2	0.3	0.6
Brigantedinium spp	7.3	0.0	40.3	31.6	35.8	71.3	9.5	0.7	4.8	2.2	6.9	6.3	9.8	6.9	12.4	29.4	29.1	31.5	24.1	1.2	2.9	3.1
cf. Schpsielia lintida	0.0	0.0	0.8	0.5	0.5	0.0	0.6	0.0	0.0	0.0	0.7	0.9	1.7	0.8	1.5	0.6	0.0	1.2	1.0	0.0	0.2	0.0
cysts of Gymnodinium colenatum	0.0	0.0	0.0	0.0	0.0	0.0	0.0	0.0	0.0	0.0	0.2	0.2	0.2	0.2	0.5	0.0	0.0	0.0	0.0	0.0	0.0	0.0
cysts of Gymnodinium nolten	0.0	0.0	0.0	0.0	0.0	0.0	0.0	3.0	0.0	0.0	0.2	0.2	0.7	0.2	0.7	0.0	0.0	0.0	0.0	0.0	0.0	0.0
cysts of Pentapharsodinium dalei	4.0	0.0	19.5	12.7	13.9	3.5	10.0	0.0	0.0	0.4	1.1	0.7	1.0	0.8	0.7	25.2	7.3	22.7	16.1	12.9	11.4	15.9
cysts of Polykrikos schwartzii	1.0	0.7	0.0	0.0	0.0	0.0	0.0	0.0	0.0	0.0	9.3	6.7	4.0	5.6	10.5	0.0	0.0	0.0	0.0	0.0	0.9	0.3
cysts of Polykrikos sp. - Arctic morphotype	0.0	0.0	0.0	0.0	0.0	0.0	0.0	0.0	0.0	0.0	0.0	0.0	0.0	0.0	0.0	0.0	0.0	0.0	0.0	0.0	0.0	0.0
Dubridinium spp.	0.0	0.0	0.0	0.0	0.0	0.0	0.0	0.0	0.0	0.0	2.6	1.9	2.2	2.1	3.9	0.0	0.0	0.0	0.0	0.0	0.0	0.0
Impagidinium aculeatum	0.0	0.7	0.2	0.7	0.0	0.0	0.2	1.4	0.5	0.9	0.2	0.0	0.0	0.2	0.0	0.0	0.0	0.0	0.0	0.2	0.0	0.3
Impagidinium pallidum	0.3	0.7	0.0	0.0	0.0	0.0	0.0	0.0	0.0	0.0	0.2	0.0	0.0	0.2	0.0	0.0	0.0	0.0	0.0	0.6	0.4	0.2
Impagidinium paradoxum	1.0	8.8	0.0	0.0	0.0	0.0	0.0	1.4	0.7	0.9	0.2	0.0	0.0	0.0	0.0	0.0	0.0	0.0	0.0	0.2	0.0	0.0
Impagidinium patulum	0.0	0.0	0.2	0.5	0.5	1.2	3.0	2.8	0.5	0.9	0.0	0.0	0.0	0.0	0.0	0.0	0.0	0.0	0.0	0.0	0.0	0.0
Impagidinium sphaericum	3.0	2.2	1.0	3.5	2.4	0.6	0.9	0.0	0.0	0.9	0.0	0.0	0.0	0.0	0.0	0.0	0.0	0.0	0.0	2.0	1.2	1.3
Impagidinium spp.	0.0	0.0	0.0	0.2	0.0	0.0	0.0	0.7	0.0	0.0	0.0	0.0	0.0	0.0	0.0	0.0	0.0	0.4	0.0	0.0	0.0	0.0
Impagidinium striatum	0.0	0.0	0.0	0.0	0.0	0.0	0.0	0.0	0.5	0.0	0.0	0.0	0.0	0.0	0.0	0.0	0.0	0.0	0.0	0.0	0.0	0.0
Islandinium minutum	0.0	0.0	0.5	1.0	0.5	1.8	0.4	0.0	0.0	0.0	0.2	0.4	0.2	0.2	0.2	0.6	1.1	1.4	1.0	0.2	0.0	0.0
Islandinium? cezare	0.0	0.0	0.0	0.2	0.0	0.6	0.0	0.0	0.0	0.0	0.0	0.0	0.0	0.0	0.0	0.0	0.0	0.0	0.0	0.0	0.0	0.0
Lejeunecysta oliva	0.0	0.0	0.0	0.0	0.0	0.0	0.0	0.0	0.0	0.0	0.2	0.4	0.2	0.2	0.2	0.0	0.0	0.0	0.0	0.0	0.0	0.0
Lejeunecysta sabrina	0.0	0.0	0.0	0.0	0.0	0.0	0.0	0.0	0.5	0.9	0.7	0.9	1.0	0.8	1.5	0.0	0.0	0.0	0.0	0.0	0.0	0.0
Lejeunecysta spp	0.0	0.0	0.0	0.0	0.0	0.0	0.0	0.0	0.0	0.0	0.2	0.4	0.2	0.4	0.0	0.0	0.0	0.0	0.0	0.0	0.0	0.0
Lingulodinium machaerophorum	0.0	0.0	0.0	0.0	0.0	0.0	0.0	59.3	66.6	63.3	0.2	0.4	0.2	0.4	0.5	0.0	0.0	0.0	0.0	0.0	0.0	0.0
Nematosphaeropsis labyrinthus	20.9	69.1	4.2	3.7	2.4	1.8	3.6	0.0	1.0	0.9	0.0	0.0	0.0	0.0	0.0	0.6	0.7	0.8	0.6	51.4	65.2	20.3
Operculodinium centrocarpum	58.8	8.8	21.2	34.5	33.7	6.4	53.0	9.0	7.5	10.9	14.1	18.6	15.6	16.4	9.7	31.6	43.6	33.1	41.2	27.4	10.1	45.0
Operculodinium jenduchenei	0.0	0.0	0.0	0.0	0.0	0.0	0.0	0.0	0.0	0.4	0.0	0.0	0.0	0.0	0.0	0.0	0.0	0.0	0.0	0.0	0.0	0.0
Poulnopsis reticulata	0.0	0.0	0.0	0.0	0.0	0.0	0.0	2.1	0.2	0.9	0.0	0.0	0.0	0.0	0.0	0.0	0.0	0.0	0.0	0.2	0.0	0.0
Protoperidinioids	0.0	0.0	0.0	0.0	0.0	0.0	0.0	1.4	0.0	0.4	0.0	0.0	0.0	0.0	0.0	0.0	0.0	0.0	0.0	0.0	0.2	0.0
Protoperidinium americanum	0.0	0.0	0.0	0.0	0.0	0.0	0.0	0.0	0.0	0.0	0.2	0.2	0.2	0.2	0.2	0.0	0.0	0.0	0.0	0.0	0.0	0.0
Protoperidinium stellatum	0.0	0.0	0.0	0.0	0.0	0.0	0.0	0.0	0.0	0.0	0.2	0.4	1.0	0.4	0.5	0.0	0.0	0.0	0.0	0.0	0.0	0.0
Quinquecuspis concreta	0.0	0.0	0.0	0.0	0.0	0.0	0.0	0.0	0.0	0.0	5.8	6.5	5.2	6.2	8.0	0.0	0.0	0.0	0.0	0.0	0.0	0.0
Selenopemphix nephroides	0.0	0.0	0.0	0.0	0.0	0.0	0.0	0.7	0.5	0.0	0.2	0.2	0.0	0.2	0.2	0.0	0.0	0.0	0.0	0.0	0.0	0.0
Selenopemphix quanta	0.0	0.0	0.8	0.2	0.5	5.3	1.1	0.0	0.5	0.0	6.9	5.4	4.7	4.4	5.1	0.0	0.0	0.5	0.3	0.5	5.0	1.0
Spiniferites bentorii	0.0	0.0	0.0	0.0	0.0	0.0	0.0	0.0	0.0	0.4	0.2	0.2	0.0	0.2	0.0	0.0	0.0	0.0	0.0	0.0	0.0	0.0
Spiniferites delicatus	0.0	0.0	0.0	0.0	0.0	0.0	0.0	2.1	0.7	1.3	0.2	0.2	0.2	0.2	0.2	0.0	0.0	0.0	0.0	0.0	0.0	0.0
Spiniferites elongatus	2.7	1.5	1.7	1.2	1.0	0.6	0.9	0.0	0.2	0.0	5.5	5.8	5.2	6.2	4.6	0.8	1.8	1.4	0.6	0.4	0.2	1.1
Spiniferites fazus	0.0	0.0	0.0	0.0	0.0	0.0	0.0	1.4	1.0	0.0	0.4	0.9	0.5	1.2	0.5	0.0	0.0	0.0	0.0	0.0	0.0	0.0
Spiniferites membranaceus	0.0	0.0	0.0	0.7	0.0	0.0	0.0	2.8	2.6	0.9	5.8	3.7	3.2	3.3	5.1	0.0	0.0	0.0	0.0	0.0	0.0	0.0
Spiniferites mirabilis	0.3	0.0	2.1	1.0	3.4	2.3	5.3	4.8	2.6	3.1	0.7	2.0	1.5	1.9	0.5	0.0	0.0	0.0	0.0	0.0	0.0	0.0
Spiniferites ramosus	0.0	1.5	3.5	4.7	4.1	4.7	6.3	2.1	4.3	2.2	20.3	20.4	28.7	24.7	21.4	0.3	0.4	1.4	1.0	2.2	0.0	2.6
Spiniferites spp.	0.0	0.0	1.2	1.7	0.2	0.0	0.0	7.6	4.8	7.0	6.7	6.1	6.2	6.0	4.6	0.3	2.9	2.8	3.9	0.0	0.0	0.0
Trinovantedinium applanatum	0.0	5.1	0.0	0.0	0.0	0.0	0.0	0.0	0.0	0.0	2.6	2.2	1.5	2.3	1.7	0.0	0.0	0.0	0.0	0.0	1.9	0.3
Votadinium calvum	0.0	0.0	0.0	0.0	0.0	0.0	0.0	0.0	0.0	0.0	0.9	0.7	0.7	0.8	0.7	0.0	0.0	0.0	0.0	0.0	0.0	0.0
Xandarodinium xanthum	0.0	0.0	0.0	0.0	0.0	0.0	0.0	0.0	0.0	0.0	0.0	0.2	0.2	0.2	0.5	0.0	0.0	0.0	0.0	0.0	0.0	0.0

Appendix D. (continued)

Site	L092	L093	L094	L162	L163	L164	L177	L178	N241	N267	N268	N269	N270	N271	N272	N274	N281	N285	N288	N290	N298
Achomosphaera spp.	0.0	0.0	0.0	0.0	0.0	0.0	0.0	0.0	0.0	0.0	0.0	0.0	0.0	0.0	0.0	0.0	0.0	0.0	0.0	0.0	0.0
Alexandrium choanum	0.2	0.0	0.0	0.0	0.0	0.0	0.0	0.0	0.3	0.1	0.1	0.1	0.0	0.0	0.4	0.1	0.1	0.0	0.0	0.0	0.0
Bitectatodinium tepikiense	0.0	0.6	0.2	0.0	0.0	0.0	0.7	2.9	2.4	0.3	0.9	0.5	0.5	0.6	0.4	0.7	0.6	0.3	0.3	0.0	0.0
Brigantedinium spp.	0.9	2.2	9.6	17.2	15.9	17.3	11.7	11.0	0.4	1.0	4.1	3.5	2.5	1.8	8.9	3.8	3.4	22.4	36.9	1.0	7.5
cf. *Senegalia trifida*	0.0	0.0	0.2	0.0	0.0	0.0	0.0	0.0	0.1	0.0	0.0	0.0	0.0	0.0	0.0	0.0	0.0	0.0	0.0	0.0	0.0
cysts of *Gymnodinium catenatum*	0.0	0.0	0.0	0.0	0.0	0.0	0.0	0.0	0.0	0.0	0.0	0.0	0.0	0.0	0.0	0.0	0.0	0.0	0.0	0.0	0.0
cysts of *Gymnodinium nolleri*	0.0	0.0	0.0	0.0	0.0	0.0	0.0	0.0	0.0	0.0	0.0	0.0	0.0	0.0	0.0	0.0	0.0	0.0	0.0	0.0	0.0
cysts of *Pentapharsodinium dalei*	25.7	18.2	14.4	14.9	11.3	9.6	2.1	3.3	15.6	6.4	15.3	21.0	10.9	9.9	4.4	22.4	1.7	1.1	0.5	6.3	0.9
cysts of *Polykrikos schwartzii*	0.7	0.0	0.4	0.7	0.5	0.0	0.3	0.0	0.2	0.1	0.3	0.3	0.2	0.0	0.1	0.6	0.0	0.0	0.0	0.0	0.0
cysts of *Polykrikos* sp. - Arctic morphotype	0.0	0.0	0.0	0.0	0.0	0.0	0.0	0.0	0.0	0.0	0.0	0.0	0.0	0.0	0.0	0.0	0.0	0.0	0.0	0.0	0.0
Dubridinium spp.	0.0	0.0	0.0	0.0	0.0	0.0	0.0	0.0	0.0	0.0	0.0	0.0	0.0	0.0	0.0	0.0	0.0	0.0	0.0	0.0	0.0
Impagidinium aculeatum	0.0	0.2	0.0	0.0	0.0	0.0	2.1	0.0	0.0	0.0	0.0	0.0	0.0	0.0	0.0	0.0	0.0	0.0	0.0	0.0	0.0
Impagidinium pallidum	0.2	0.8	0.4	2.2	0.0	1.4	6.6	1.9	0.3	0.5	0.6	0.5	0.7	0.9	1.3	0.4	0.4	26.4	6.1	28.6	5.0
Impagidinium paradoxum	0.4	0.6	0.0	0.0	0.0	0.0	0.7	0.5	0.0	0.0	0.0	0.0	0.0	0.0	0.0	0.0	0.0	0.0	0.0	0.0	0.0
Impagidinium patulum	0.0	0.0	0.0	0.0	0.0	0.0	0.0	0.0	0.0	0.0	0.0	0.0	0.0	0.0	0.0	0.0	0.0	0.0	0.0	0.0	0.0
Impagidinium sphaericum	0.0	1.0	2.6	0.0	2.1	0.5	6.2	5.2	0.0	0.0	0.1	0.1	0.0	0.0	0.0	0.1	0.1	0.3	0.0	0.0	0.0
Impagidinium spp.	0.0	0.0	0.0	0.0	0.0	0.0	0.0	0.0	0.0	0.1	0.0	0.1	0.2	0.2	0.0	0.0	0.2	0.0	0.3	0.4	0.0
Impagidinium striatum	0.0	0.0	0.0	0.0	0.0	0.0	0.0	0.0	0.0	0.0	0.0	0.0	0.0	0.0	0.0	0.0	0.0	0.0	0.0	0.0	0.0
Islandinium minutum	0.0	0.0	0.7	0.0	2.6	2.4	1.4	4.8	0.0	0.1	0.1	0.1	0.0	0.0	0.4	0.0	0.2	1.1	35.5	0.2	0.2
Islandinium? *cezare*	0.0	0.0	0.0	0.7	0.0	0.0	0.3	0.0	0.0	0.0	0.0	0.0	0.0	0.0	0.0	0.8	0.1	0.5	8.7	0.2	1.1
Lejeunecysta oliva	0.0	0.0	0.0	0.0	0.0	0.0	0.0	0.0	0.0	0.0	0.0	0.0	0.0	0.0	0.0	0.0	0.0	0.0	0.0	0.0	0.0
Lejeunecysta sabrina	0.0	0.0	0.0	0.0	0.0	0.0	0.0	0.0	0.0	0.0	0.0	0.0	0.0	0.0	0.0	0.0	0.0	0.0	0.0	0.0	0.0
Lejeunecysta spp.	0.0	0.0	0.0	0.0	0.0	0.0	0.0	0.0	0.0	0.0	0.0	0.0	0.0	0.0	0.0	0.0	0.0	0.0	0.0	0.0	0.0
Lingulodinium machaerophorum	0.0	0.0	0.0	0.0	0.0	0.0	0.0	0.0	0.0	0.0	0.0	0.0	0.0	0.0	0.0	0.1	0.0	0.0	0.0	0.0	0.0
Nematosphaeropsis labyrinthus	17.0	49.9	40.0	61.9	57.9	59.1	52.4	55.2	1.2	10.3	10.9	13.5	11.8	9.9	10.8	14.5	8.6	19.7	6.4	32.2	10.1
Operculodinium centrocarpum	48.5	26.0	25.6	0.7	8.2	6.3	14.5	13.8	65.4	78.2	64.5	56.2	70.2	74.6	72.2	51.8	83.8	27.7	4.7	30.5	74.9
Operculodinium janduchenoi	0.0	0.0	0.0	0.0	0.0	0.0	0.0	0.0	0.0	0.0	0.0	0.0	0.0	0.0	0.0	0.0	0.0	0.0	0.0	0.0	0.0
Pyxidinopsis reticulata	0.0	0.0	0.0	0.0	0.0	0.0	0.0	0.0	0.0	0.0	0.0	0.0	0.0	0.0	0.0	0.0	0.0	0.0	0.0	0.0	0.0
Protoperidinioids	0.0	0.0	0.9	0.0	0.0	0.0	0.0	0.0	0.0	0.0	0.0	0.0	0.0	0.0	0.0	0.0	0.0	0.0	0.0	0.0	0.1
Protoperidinium americanum	0.0	0.0	0.0	0.0	0.0	0.0	0.0	0.0	0.0	0.2	0.0	0.1	0.0	0.0	0.0	0.0	0.0	0.0	0.0	0.0	0.0
Protoperidinium stellatum	0.0	0.0	0.0	0.0	0.0	0.0	0.0	0.0	0.0	0.0	0.0	0.0	0.0	0.0	0.0	0.0	0.0	0.0	0.0	0.0	0.0
Quinquecuspis concreta	0.0	0.0	0.0	0.0	0.0	0.0	0.0	0.0	0.0	0.0	0.0	0.0	0.0	0.0	0.0	0.0	0.0	0.0	0.0	0.0	0.0
Selenopemphix nephroides	0.0	0.0	0.0	0.0	0.0	0.0	0.0	0.0	0.0	0.0	0.0	0.0	0.0	0.0	0.0	0.0	0.0	0.0	0.0	0.0	0.0
Selenopemphix quanta	0.0	0.0	1.8	0.7	3.6	2.4	0.0	1.0	1.6	0.3	0.2	0.4	0.3	0.0	0.0	1.2	0.1	0.3	0.3	0.2	0.1
Spiniferites bentorii	0.0	0.0	0.0	0.0	0.0	0.0	0.0	0.0	0.0	0.0	0.0	0.0	0.0	0.0	0.0	0.0	0.0	0.0	0.0	0.0	0.0
Spiniferites delicatus	0.0	0.0	0.0	0.0	0.0	0.0	0.0	0.0	0.0	0.0	0.0	0.0	0.0	0.0	0.0	0.0	0.0	0.0	0.0	0.0	0.0
Spiniferites elongatus	1.2	0.4	0.0	0.7	0.0	1.0	0.0	0.0	1.3	0.4	1.2	1.6	1.6	1.2	0.2	1.1	0.4	0.0	0.3	0.0	0.1
Spiniferites lazus	0.0	0.0	0.0	0.0	0.0	0.0	0.0	0.0	0.0	0.0	0.0	0.2	0.1	0.0	0.0	0.1	0.0	0.0	0.0	0.0	0.0
Spiniferites membranaceus	0.0	0.0	0.0	0.0	0.0	0.0	0.0	0.0	0.0	0.0	0.0	0.0	0.0	0.0	0.0	0.1	0.0	0.0	0.0	0.0	0.0
Spiniferites mirabilis	0.0	0.0	0.0	0.0	0.0	0.0	0.0	0.0	2.4	0.1	0.0	0.0	0.1	0.1	0.0	0.2	0.1	0.0	0.0	0.0	0.0
Spiniferites ramosus	3.9	0.0	2.0	0.0	0.0	0.0	1.0	0.0	8.2	0.0	0.2	0.1	0.2	0.0	0.0	0.1	0.0	0.0	0.0	0.0	0.0
Spiniferites spp.	0.0	0.0	0.0	0.0	0.0	0.0	0.0	0.0	0.8	0.7	1.2	1.4	0.4	0.6	0.9	0.6	0.3	0.3	0.0	0.0	0.0
Trinovantedinium applanatum	0.5	0.2	1.1	0.0	0.0	0.0	0.0	0.5	0.0	0.1	0.2	0.2	0.3	0.1	0.1	1.2	0.1	0.0	0.0	0.4	0.0
Votadinium calvum	0.0	0.0	0.0	0.0	0.0	0.0	0.0	0.0	0.0	0.0	0.0	0.0	0.0	0.0	0.0	0.0	0.0	0.0	0.0	0.0	0.0
Xandarodinium xanthum	0.0	0.0	0.0	0.0	0.0	0.0	0.0	0.0	0.0	0.0	0.0	0.0	0.0	0.0	0.0	0.0	0.0	0.0	0.0	0.0	0.0

Appendix D. (continued)

Appendix E. Environmental parameters for each of the 87 sites of the database

Site	SSTwin (°C)	SSTspr (°C)	SSTsum (°C)	SSTfall (°C)	ΔSSTsum-win (°C)	sdSST (°C)	SSSwin	SSSspr	SSSsum	SSSfall	PRODwin ($gC.m^{-2}$)	PRODspr ($gC.m^{-2}$)	PRODsum ($gC.m^{-2}$)	PRODfall ($gC.m^{-2}$)	Distance to the coast (km)
2066	1.88	4.77	8.96	4.16	7.08	2.33	34.43	33.67	33.43	34.09	5.58	23.78	15.41	2.83	11.2
2639	0.02	1.91	5.80	2.17	5.78	2.33	34.66	34.55	34.32	34.44	3.42	18.57	11.53	1.61	155.7
2646	-0.22	1.56	5.24	1.86	5.46	2.32	34.67	34.59	34.29	34.42	3.31	20.06	12.09	1.51	174.8
2667	1.62	3.73	7.85	4.67	6.23	2.39	34.59	34.31	33.95	34.53	5.67	19.91	13.35	2.40	52.2
2674	1.99	4.02	7.97	4.39	5.98	2.36	34.67	34.19	33.92	34.57	5.17	22.62	15.32	2.98	29.9
2730	2.45	4.35	7.71	4.53	5.26	2.30	34.76	34.43	34.03	34.55	5.15	23.16	15.95	2.58	33.7
2746	1.78	2.75	4.43	2.39	2.65	2.13	34.70	34.62	33.54	34.37	3.97	17.28	14.33	2.69	164.4
2752	0.65	1.98	3.93	1.85	3.28	2.16	34.69	34.55	34.07	34.39	3.34	18.02	17.02	2.85	192.0
2757	0.58	1.93	3.87	1.91	3.29	2.19	34.70	34.56	34.12	34.38	3.21	18.36	17.33	2.86	186.3
2760	0.44	2.02	3.89	1.95	3.45	2.24	34.68	34.55	34.13	34.40	3.14	17.89	16.03	2.59	164.7
2764	0.18	1.73	3.91	1.64	3.73	2.22	34.67	34.53	34.12	34.40	2.94	18.77	15.30	2.33	179.6
2770	-0.76	0.80	3.82	1.14	4.58	2.17	34.63	34.64	34.15	34.32	2.97	22.86	12.40	1.85	228.8
2775	-0.26	0.74	4.67	1.90	4.93	2.28	34.84	34.74	34.58	34.55	3.34	24.63	15.92	1.58	237.8
2778	-0.64	1.12	4.52	1.38	5.16	2.27	34.66	34.63	34.21	34.38	3.34	22.70	13.15	1.50	200.1
2780	1.15	2.69	4.50	2.50	3.35	2.27	34.73	34.56	34.15	34.42	3.41	17.95	17.05	2.92	136.1
2784	1.68	3.56	6.28	3.36	4.60	2.27	34.75	34.61	34.16	34.50	3.59	19.04	17.69	3.11	129.4
2788	1.92	3.74	6.52	3.48	4.60	2.28	34.78	34.62	34.18	34.53	3.90	20.14	17.94	3.18	120.8
2793	1.95	3.83	6.48	3.76	4.53	2.26	34.78	34.61	34.16	34.51	4.22	20.55	18.33	3.19	117.9
2875	6.42	7.19	9.80	7.54	3.38	2.00	35.10	35.09	35.06	35.03	2.63	14.75	20.22	6.55	175.2
2879	6.25	7.02	9.65	7.46	3.40	2.05	35.09	35.09	35.07	35.02	3.13	16.51	19.55	6.01	139.1
2894	5.68	6.33	8.16	5.81	2.48	2.12	34.97	34.98	34.58	34.64	2.86	16.94	19.38	5.41	137.1
A074	1.36	5.48	15.43	8.66	14.07	5.55	32.69	32.52	32.01	31.94	6.92	13.12	13.26	7.16	244.1
A099	4.09	4.05	7.48	6.70	3.39	2.18	34.95	34.74	34.64	34.31	4.35	9.28	10.08	1.54	226.0
A100	3.29	3.98	6.89	4.88	3.60	2.09	34.55	34.71	34.37	34.47	3.46	13.70	11.33	2.86	106.7
A103	4.06	5.15	8.63	5.99	4.57	2.04	34.82	34.91	34.62	34.84	3.34	16.99	13.06	1.88	191.6
A104	4.41	4.94	8.51	6.47	4.10	2.08	34.73	34.87	34.68	34.83	3.00	18.13	14.07	2.05	147.6
A105	3.44	3.10	5.58	3.75	2.14	2.19	34.78	33.95	33.49	34.11	3.68	16.18	15.75	2.50	64.4
A106	4.92	5.74	8.93	6.05	4.01	2.15	35.00	35.00	34.50	34.95	2.33	28.00	21.21	1.72	141.6
A107	5.21	6.43	9.40	7.12	4.19	1.92	35.04	35.00	34.88	34.84	2.31	13.01	32.44	4.00	381.5
A109	6.51	7.19	9.80	7.64	3.29	1.92	35.09	35.09	35.03	35.00	2.55	16.29	26.04	4.92	260.8
A110	6.51	7.17	9.80	7.64	3.29	1.92	35.09	35.09	35.03	35.00	2.55	16.29	26.04	4.92	260.3
A111	6.51	7.17	9.80	7.64	3.29	1.92	35.09	35.09	35.03	35.00	2.55	16.29	26.04	4.92	260.3
A112	6.17	6.70	9.21	7.41	3.04	2.04	35.14	35.09	35.05	34.96	1.97	12.16	26.52	3.63	278.7
A113	8.19	9.01	11.38	9.84	3.19	1.58	35.16	35.20	35.12	35.15	5.86	17.73	14.81	4.41	346.0
A114	9.22	10.12	12.83	10.76	3.61	1.66	35.27	35.17	35.16	35.22	4.11	12.63	16.58	5.17	659.4
A118	9.87	11.52	13.74	13.10	3.87	1.79	35.54	35.33	35.37	35.23	4.80	14.89	13.24	3.59	723.6
A119	10.47	11.24	13.94	11.94	3.47	1.89	35.35	35.28	35.34	35.27	4.66	13.35	16.38	3.91	794.3
A120	10.47	11.24	13.94	11.94	3.47	1.89	35.35	35.28	35.34	35.27	4.66	13.35	16.38	3.91	794.3
A121	10.43	11.58	14.44	12.25	4.01	1.95	35.39	35.33	35.30	35.31	4.83	14.68	15.70	4.88	797.5
A123	11.35	12.97	16.13	14.06	4.78	2.04	35.54	35.60	35.55	35.51	5.32	14.83	13.91	5.25	573.9
A168	4.12	5.44	8.74	5.75	4.62	2.01	34.83	34.86	34.70	34.78	3.70	15.73	12.09	1.85	221.3
A170	5.73	7.29	9.63	7.34	3.90	1.87	34.93	34.94	34.81	34.82	2.53	11.49	31.53	2.90	509.9
A171	6.77	7.33	10.36	8.64	3.59	1.77	35.10	35.03	34.98	35.01	2.52	20.27	34.82	4.03	611.4
A173	7.15	7.86	10.71	9.26	3.56	1.74	35.06	35.07	34.97	35.12	3.71	18.17	29.77	4.26	630.4
A174	7.60	8.08	11.67	9.08	4.07	2.00	34.98	34.90	34.92	34.97	6.18	14.28	14.56	6.42	896.7
A175	6.25	8.36	12.57	8.94	6.32	2.30	34.75	34.81	34.69	34.70	10.94	18.97	17.48	4.64	973.1

Appendix E. (continued)

Site	SSTwin (°C)	SSTspr (°C)	SSTsum (°C)	SSTfall (°C)	ΔSSTsum-win (°C)	sdSST (°C)	SSSwin	SSSspr	SSSsum	SSSfall	PRODwin ($gC.m^{-2}$)	PRODspr ($gC.m^{-2}$)	PRODsum ($gC.m^{-2}$)	PRODfall ($gC.m^{-2}$)	Distance to the coast (km)
A258	2.17	5.61	16.47	11.29	14.30	5.60	31.80	31.71	31.20	31.38	8.26	14.49	17.35	12.31	94.1
A259	2.12	5.59	16.46	11.28	14.34	5.59	31.79	31 70	31.20	31.38	8.26	14.49	17.35	12.31	93.2
A260	2.15	5.62	16.47	11.29	14.32	5.59	31.80	31.71	31.20	31.38	8.26	14.49	17.35	12.31	93.6
A261	3.74	6.94	16.98	11.86	13.24	5.51	32.46	32.58	31.95	32.22	10.39	14.31	14.26	10.63	226.6
A262	3.74	6.89	16.97	11.88	13.23	5.52	32.46	32.57	31.94	32.22	10.39	14.31	14.26	10.63	225.9
A264	15.49	17.60	20.02	18.88	4.53	2.24	36.16	36.13	36.11	36.29	10.64	14.46	14.51	8.87	143.1
A265	15.27	16.92	18.86	17.98	3.59	2.25	36.01	35.97	36.04	36.14	12.61	19.82	20.46	11.05	75.3
A266	15.37	17.27	19.60	18.57	4.23	2.25	36.15	36 05	36.08	36.26	11.69	16.98	17.29	9.86	109.6
Celt4	9.09	11.25	15.44	12.85	6.35	2.58	35.03	34.88	34.94	35.07	12.39	26.67	21.70	9.28	88.3
Celt5	9.14	11.47	15.62	13.08	6.48	2.61	34.98	34.87	34.95	35.10	11.89	23.44	19.56	8.84	94.5
Celt6	9.06	11.52	15.68	13.11	6.62	2.63	34.95	34.84	34.95	35.06	12.22	22.86	18.54	9.33	78.0
Celt7	9.09	11.42	15.65	13.13	6.56	2.62	34.92	34.84	34.94	35.09	12.57	24.25	20.31	9.52	84.6
Celt8	8.84	11.30	15.50	13.19	6 66	2.64	34.83	34.74	34.96	35.02	13.25	24.60	20.71	9.77	58.9
G075	0 49	4.46	14.59	7.70	14.10	5.59	31.94	31 72	30.90	31.35	6.37	16.24	18.76	6.68	146.4
G076	0.37	4.55	14.51	7.56	14.14	5.57	31.74	31.64	30.67	31.40	7.00	16.76	19.51	6.73	141.4
G077	0.81	4.85	13.03	8.13	12.22	5.17	31.64	31.25	31.47	31.58	7.17	12.89	18.91	7.74	14.3
G078	0.18	3.68	13.74	7.11	13.56	5.35	31.84	31.76	31.52	31.78	7.48	13 49	18.18	7.14	54.2
L087	1.42	2.01	5.56	3.04	4.14	2.16	34.21	33.90	33.58	32.75	2.40	8.84	11.90	2.61	158.6
L090	2.66	3.15	6.09	2.55	3.43	2.17	34.79	34.28	34.65	34.36	4.70	15.30	11.91	2.48	84.2
L091	3.88	4.15	7.25	5.55	3.37	2.20	34.86	34.88	34.71	34.63	5.62	14.59	10.54	1.69	176.5
L092	3.86	4.09	7.24	4.39	3.38	2.27	34.87	34.84	34.66	34.59	3.21	13.69	10.60	1.37	284.2
L093	3.47	0.51	6.76	5.75	3.29	2.27	34.77	34.71	34.31	34.45	2.76	12.66	12.60	2.29	270.3
L094	3.45	0.36	7.38	6.66	3.93	2.25	34.77	34 90	34.36	34.42	2.48	12.72	13.04	2.36	302.2
L162	0.60	2.31	5.96	2.37	5.36	2.58	33.97	33.07	32.90	33.54	10.43	14.05	13.22	3.54	239.1
L163	2 61	3.07	7.14	4.28	4.53	2.55	34.39	33.33	33.75	34.13	10.15	13.84	14.23	3.74	291.4
L164	1.04	2.47	6.13	2.61	5.09	2.57	33.96	33.20	32.97	33.64	10.06	13.85	13.55	3.54	250.4
L177	5.68	6.81	10.85	7.49	5.17	2.62	34.79	34.27	34.64	34.93	6.31	16.23	17.31	3.65	692.2
L178	5.71	6.37	12.45	8.91	6.74	3.17	34.36	34 16	33.65	34.14	6.77	18.74	17.95	3.80	562.4
N241	6.76	9.05	13.17	9.94	6.41	2.83	35.11	35.07	35.03	35.16	8.58	22.36	19.79	7.03	125.8
N267	6.38	7.91	10.52	7.89	4 14	2.06	35.17	35.18	35.09	35.14	2.26	19.69	12.33	1.58	443.9
N268	4.05	5.30	8.07	4.86	4.02	1.99	35.08	35 10	35.04	35.08	2.91	15.17	16.51	2.88	390.1
N269	5.51	6.24	9.69	6.62	4.18	1.93	34.95	34.86	34.61	34.80	3.96	21.15	14.84	1.65	164.3
N270	4.07	5.00	7.93	5.27	3.86	2.05	35.09	35.12	35.05	35.05	3.19	14.50	14.44	2.45	430.3
N271	3.85	4.75	7.78	5.01	3.93	2.16	35.09	35.08	35.01	35.08	2.68	15.79	12.44	1.74	463.7
N272	4.08	5.05	7.55	5.62	3.47	2.25	35.06	35.07	35.02	35.08	3.98	13.97	11.93	2.09	308.7
N274	6.73	7.47	11.14	9.07	4.41	2.15	35.13	35.07	34.80	35.04	2.70	18.73	14.14	2.38	240.2
N281	6.39	7.26	10.64	8.55	4.25	2.05	35.14	35 12	35.01	35.09	1.73	17.06	14.86	2.27	338.8
N285	-0.44	0.05	4.19	0.86	4.63	2.14	34.69	34.49	34.20	34.20	5.13	19.45	14.01	2.59	53.1
N288	-1.82	0.99	0.98	-0.26	2.80	1.67	34.21	33.16	32.34	33.67	5.89	21.11	19.11	4.77	87.2
N290	-0.07	1.24	4.96	1.88	5.03	2.14	34.80	34.68	34.32	34.77	8.02	24.46	12.92	2.42	153.6
N298	0.47	1.30	5.60	3.44	5.13	2.28	34.79	34.72	34.54	34.73	4.37	16.89	15.84	3.35	89.9

CONCLUSION

Les résultats présentés dans cette thèse peuvent être regroupés en deux catégories, l'une portant sur les changements des conditions de surface de l'Atlantique Nord durant l'Holocène, et l'autre, plus méthodologique, sur la comparaison des dinokystes et des coccolithes dans les sédiments modernes et dans des enregistrements Holocène. Si dans les deux cas les résultats apportent de nouveaux éléments dans la compréhension du système océanique et dans le potentiel paléocéanographique des dinokystes et coccolithes, ils soulignent également certains aspects sur lesquels la priorité devrait être mise dans les recherches futures.

Jusqu'à récemment, l'Holocène était considéré comme une période exceptionnellement stable, durant laquelle aucun changement climatique marqué n'avait eu lieu (Dansgaard et al., 1993). On sait maintenant que, bien que beaucoup plus faibles que pendant la glaciation, des fluctuations climatiques significatives ont eu lieu au cours de l'Holocène, allant même jusqu'à avoir des conséquences sur les populations humaines (deMenocal, 2001). De nombreuses études montrent une baisse graduelle des températures atmosphériques et océaniques au cours de l'Holocène, en particulier aux moyennes et hautes latitudes de l'hémisphère Nord (e.g., Dahl-Jensen et al., 1998; Rimbu et al., 2003), généralement attribuée à la diminution de l'insolation estivale (Marchal et al., 2002). Les quelques derniers milliers d'années de l'Holocène seraient ainsi caractérisés par un mode climatique néoglaciaire (Mangerud et al., 1974). Cependant, des différences au niveau de la chronologie et de l'amplitude de l'optimum thermique de l'Holocène ont également été mises en évidence (e.g., Kaufmann et al., 2004; Kaplan et Wolfe, 2006). Les résultats présentés ici vont plus avant dans cette voie, et montrent clairement que de fortes hétérogénéités spatiales ont caractérisé l'évolution de l'hydrographie de surface de l'océan au cours de l'Holocène, illustrant l'importance de prendre en compte les mécanismes climatiques et hydrographiques locaux en plus de phénomènes globaux tels que les changements d'insolation.

Les deux premiers chapitres montrent que d'importants changements à la surface de l'Atlantique Nord ont eu lieu entre 7.4 et 4.9 ka BP (Fig. 1). L'Holocène moyen a donc été

une période de réorganisation majeure du système océanique, qui peut être reconstituée à partir des carottes étudiées, chacune provenant d'une région-clé de la circulation océanique. À ~6.5 ka BP, l'optimum thermique se termine sur la ride de Reykjanes (carotte LO09-14; voir aussi Giraudeau et al., 2000 et Moros et al., 2004), suggérant une diminution des flux d'eaux atlantiques transportées par la Dérive Nord Atlantique et le Courant d'Irminger, qui aurait aussi engendré le refroidissement observé au sud du Groenland (carotte P-013). L'évolution des températures aux autres sites est cependant en contradiction avec l'idée d'un refroidissement général. Sur la côte est du Groenland (carotte JM96-1207) et au nord-ouest de l'Islande (2269/327), les températures de surface en hiver augmentent au cours de l'Holocène, de façon graduelle au site groenlandais et plus subitement, à 6.2 ka BP, au site islandais. Dans le Chenal des Féroé-Shetland (carotte HM03-133-25), les températures d'été et d'hiver augmentent après 5.4 ka BP.

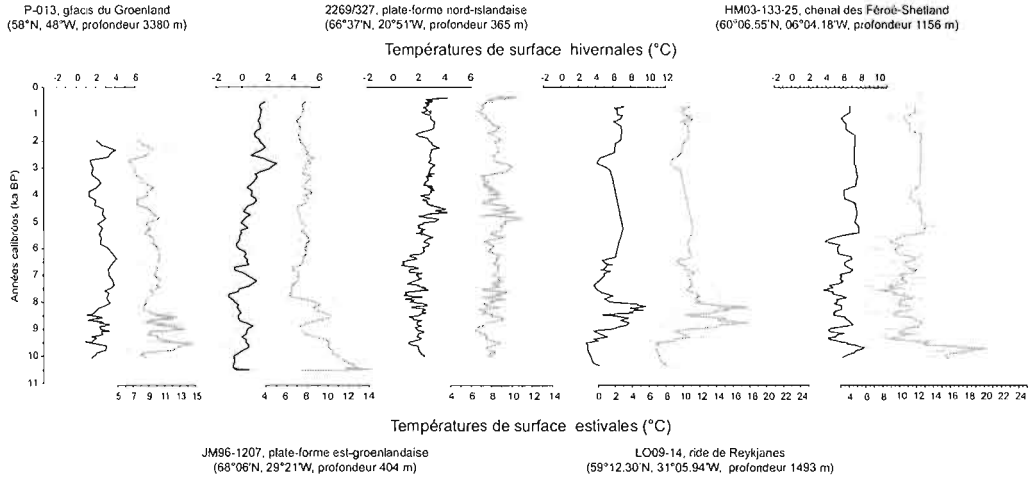

Figure 1. Synthèse des reconstitutions de températures de surface.

Ces hétérogénéités peuvent être expliquées par des changements dans la configuration des courants océaniques. Les différents sites sont sous l'influence de plusieurs courants ayant des températures et salinités distinctes. Plusieurs études ont montré qu'un changement dans la force relative des différents courants à un site donné résulte en un changement dans les conditions de surface (Gudmundsson, 1998; Holliday, 2003). Ainsi, le réchauffement observé dans la région du détroit du Danemark dans la deuxième moitié de l'Holocène peut être interprété comme le résultat d'une diminution de l'intensité des

courants de l'Est du Groenland (tel que proposé par Tremblay et al., 1997) et de l'Est de l'Islande, favorisant une contribution en eaux atlantiques accrue, comme en témoigne l'augmentation des pourcentages du dinokyste *N. labyrinthus* dans la carotte JM96-1207. Ces flux en eaux atlantiques, qui proviennent du courant d'Irminger du Nord de l'Islande, suggèrent un mécanisme de découplage des deux branches du courant d'Irminger: lorsque la branche sud-ouest s'affaiblit (carotte P-013, refroidissement), la branche nord-est est renforcée (carotte 2269/327, réchauffement).

Un changement dans le poids relatif des différents courants peut également expliquer la hausse des températures de surface dans le Chenal des Féroé-Shetland (carotte HM03-133-25). Actuellement, cette région est baignée par les eaux chaudes et salées du courant de Pente, qui prend sa source dans le Golfe de Gascogne, et par les eaux relativement plus froides et moins salées de la Dérive Nord Atlantique. Le réchauffement dans la deuxième moitié de l'Holocène, qui concorde avec des enregistrements plus au sud, dans le chenal de Rockall (Bond et al., 2001), et plus au nord, dans la mer de Norvège (Risebrobakken et al., 2003), pourrait être le résultat d'une diminution de l'influence de la Dérive Nord Atlantique et donc d'une empreinte plus claire des caractéristiques du courant de Pente. Il semblerait donc que l'Holocène moyen à supérieur ait été caractérisé par un affaiblissement général des apports en eaux atlantiques transportées par la Dérive Nord Atlantique et le courant d'Irminger, affaiblissement qui a eu des conséquences variables selon la région et les autres courants entrant en jeu.

De nombreux auteurs ont proposé qu'une telle réorganisation des courants dans l'Atlantique Nord au cours de l'Holocène pourrait être le résultat d'une modulation sur le long terme de l'Oscillation Nord Atlantique (*North Atlantic Oscillation* – NAO; Rimbu et al., 2003). La NAO se traduit par une corrélation inverse entre les températures atmosphériques de l'Europe et du Groenland liée au déplacement des cellules de haute et de basse pression et donc des vents dominants (Hurrell, 1995), qui à leur tour ont une influence sur la circulation océanique (e.g., Visbeck et al., 2003). Les résultats présentés dans le chapitre un suggèrent un affaiblissement du courant de l'Est du Groenland cohérent avec l'étude Tremblay et al. (1997), qui met en évidence un renforcement de l'index de la NAO au cours de l'Holocène. Cependant, toutes les études ne concordent pas sur ce point, et certaines semblent au contraire montrer le passage d'une phase positive à négative au cours

de l'Holocène (Rimbu et al., 2003; Lorenz et al., 2006). Il faut donc prendre l'hypothèse d'une modulation sur le long terme de la NAO avec prudence. Même actuellement, le lien avec la circulation océanique n'est pas toujours clair et, dans certaines régions, telles que le nord-est de l'Islande, des mécanismes locaux de variation hydrographique semblent prendre le dessus sur les effets de la NAO (Ólafsson, 1999). De la même façon, des études portant sur l'intensité de la gyre subpolaire et sur son influence sur les eaux atlantiques se dirigeant vers les mers Nordiques ne montrent pas de lien clair avec la NAO (Hakkinen et Rhines, 2004; Hatun et al., 2005). Enfin, d'autres études (Holliday, 2003) encore mettent en évidence une réponse du système océanique à la NAO significativement différente à court (moins d'un an) et à long terme (~3-8 ans), rendant difficile l'extrapolation de ce phénomène à l'échelle de l'Holocène.

De plus amples études sont donc indispensables pour éclaircir ce point, ou même simplement pour approfondir la question des fluctuations d'intensité des courants, sans nécessairement faire référence à la NAO. S'il est vraisemblable de penser que la contribution *relative* des différents courants influençant une région donnée a varié au cours de l'Holocène, il est difficile de déterminer si l'intensité *absolue* de chacun des courants ou de seulement certains d'entre eux a changé. Par exemple, le réchauffement dans la deuxième moitié de l'Holocène observé au site 2269/327 suggère une plus forte influence du courant d'Irminger du Nord de l'Islande, qui pourrait être le résultat du seul affaiblissement du courant de l'Est de l'Islande, du seul renforcement du courant d'Irminger du Nord de l'Islande, ou d'un changement simultané des deux courants. Il serait donc intéressant d'obtenir des enregistrements Holocène provenant de régions affectées par un seul des différents courants de l'Atlantique Nord afin de pouvoir isoler les fluctuations de chacun d'entre eux. Par exemple, un enregistrement provenant du nord de la côte est du Groenland permettrait d'étudier les variations du courant de l'Est du Groenland sans avoir à prendre en compte l'influence d'eaux atlantiques. Aussi, un site provenant du chenal entre l'Islande et les îles Féroé fournirait des informations sur les fluctuations de la Dérive Nord Atlantique, sans qu'elles soient en partie cachées par les variations du courant de Pente comme dans le Chenal des Féroé-Shetland. Lorsqu'il sera possible de déterminer la façon dont chaque courant a évolué au cours de l'Holocène, ainsi que la façon dont ils ont interagi dans les

régions où ils se rencontrent, il sera possible de proposer des mécanismes océaniques et climatiques plus précis.

D'un point de vue plus méthodologique, la comparaison des dinokystes et des coccolithes dans les enregistrements de l'est de l'Atlantique Nord (carottes LO09-14 et HM03-133-25) met en évidence des variations communes des deux groupes au cours de l'Holocène, suggérant que l'ensemble des communautés phytoplanctoniques ont été affectées par des changements des conditions de surface. Cependant, des contradictions sont également apparentes. Un exemple illustrant ce problème est le début de l'Holocène dans la carotte LO09-14 de la ride de Reykjanes, présentée dans le chapitre deux. Les assemblages de dinokystes sont caractérisés par de forts pourcentages de *Nematosphaeropsis labyrinthus*, qui, associés avec les autres espèces, indiquent d'après les reconstitutions quantitatives un épisode froid et désalé, qui est d'ailleurs cohérent avec les reconstitutions basées sur les assemblages de diatomées d'Andersen et al. (2004). Les assemblages de coccolithes suggèrent au contraire une période chaude en raison de pourcentages de *Gephyrocapsa muellerae* élevés. Il est primordial de comprendre la signification de telles contradictions pour affiner les reconstitutions paléocéanographiques. Dans cette optique, les distributions des assemblages actuels de dinokystes et de coccolithes ont été comparées afin de faire la lumière sur d'éventuelles différences écologiques. Le chapitre trois, qui présente les résultats de cette comparaison, met en avant une excellente correspondance entre les deux groupes, du moins dans les milieux tempérés. Cependant, si une relation évidente apparaît entre les assemblages de coccolithes et de dinokystes et les masses d'eau sus-jacentes, il est difficile de déterminer avec précision les facteurs environnementaux ayant la plus grande influence sur la distribution des espèces en raison d'une forte covariance entre ces facteurs.

Une des voies à explorer plus en profondeur dans le futur serait donc d'isoler les effets des paramètres environnementaux. Dans cette optique, analyser plus d'assemblages provenant de milieux uniques en termes de combinaisons de facteurs environnements devrait être privilégié. Par exemple, les résultats présentés dans le chapitre trois montrent qu'au large de la Nouvelle-Écosse et de Terre-Neuve, où la salinité de surface n'est pas corrélée à la température, les assemblages aussi bien de dinokystes que de coccolithes ressortent de par leur composition unique dans la base de données. Cela indique, beaucoup plus clairement

qu'en milieu océanique ouvert où salinité et température varient en général de pair, que la température de surface n'est pas l'unique facteur déterminant la distribution des espèces. Cependant, il reste à savoir si ces assemblages si particuliers sont le résultat d'un effet direct de la salinité sur le développement de certaines espèces, ou plutôt à un effet indirect, par exemple à travers son influence sur la stratification de la colonne d'eau. Pour cela, il serait utile non seulement d'agrandir la base de données de comparaison afin de couvrir des milieux plus variés, mais aussi de tester de plus nombreux paramètres environnementaux dans les analyses multivariées.

En effet, il ressort du chapitre trois que des assemblages différents sont retrouvés dans des environnements similaires en termes de température et de salinité. Cependant, lorsque la productivité saisonnière est introduite dans les données environnementales, la distinction entre les environnements apparaît beaucoup plus clairement et pourrait expliquer la différence entre les assemblages. Ainsi, bien que la base de données actuelle soit trop restreinte pour pouvoir déterminer avec certitude la relation entre assemblages et cycle annuel de productivité, il semble que prendre en compte un plus grand nombre de paramètres environnementaux permette une meilleure compréhension des variations des assemblages. Cela semble particulièrement vrai dans le cas de bases de données couvrant une région restreinte, où l'éventail des valeurs de température et de salinité est relativement réduit en comparaison par exemple à une base de données globale s'étendant de l'équateur aux pôles. Or, les variations hydrographiques de la surface océanique au cours de l'Holocène étaient d'amplitude relativement faible, et correspondraient donc plutôt aux variations d'assemblages d'une région restreinte, d'où l'importance de mieux comprendre les facteurs environnementaux déterminants. Outre la productivité saisonnière, il pourrait être intéressant de tester des facteurs tels que la stratification de la colonne d'eau ou la turbidité des eaux de surface. Malheureusement, ces données sont pour le moment difficiles à obtenir à grande échelle, ou, dans le cas de la stratification, les différentes bases de données existantes se contredisent fortement (Monteret et Levitus, 1997; Lorbacher et al. 2006).

Enfin, une troisième raison d'agrandir la base de données commune de dinokystes et coccolithes est d'obtenir un plus grand éventail de combinaisons d'assemblages des deux groupes afin de mieux comprendre nos enregistrements Holocène. En effet, dans l'état actuel des choses, la forte correspondance entre les assemblages actuels de coccolithes et de

dinokystes ne nous permet pas de comprendre les divergences entre les enregistrements passés des deux traceurs. Cela est particulièrement clair dans l'exemple de la carotte LO09-14 exposé plus tôt. Dans notre base de données actuelle, aucun de nos échantillons ne contient à la fois de forts pourcentages de *N. labyrinthus* et de *G. muellerae* comme c'est le cas au début de l'Holocène. Pour le moment, il est impossible de dire avec certitude si cette incohérence est due à une base de données trop restreinte, ou si cela indique que les conditions de surface de l'océan durant cet intervalle étaient entièrement différentes de tout ce qu'on peut retrouver aujourd'hui. Il est donc indispensable d'étendre notre base de données pour éclaircir la question. Alternativement, il a été suggéré que les divergences entre les traceurs micropaléontologiques pourraient être liées à des saisons de blooms différentes ou à des habitats plus ou moins profonds dans la colonne d'eau (Chapman et al., 1996; Sikes et Keigwin, 1996, Marchal et al., 2002), ce qui nous ramène encore une fois à l'importance de mieux comprendre l'écologie des traceurs.

En conclusion, cette thèse apporte de nouveaux éclairages sur l'évolution des conditions de surface de l'Atlantique Nord au cours de l'Holocène, en particulier sur le plan de la distribution spatiale des changements hydrographiques et de l'interaction entre les différents courants océaniques. De nombreux points restent cependant à éclaircir; pour cela, les études futures devraient se concentrer sur des régions-clés de la circulation de l'Atlantique Nord et, impérativement, sur la comparaison des différents traceurs paléocéanographiques.

RÉFÉRENCES

Alley, R.B., Mayewski P.A., Saltzman E.S., 1999b. Increasing North Atlantic climate variability recorded in a central Greenland ice core. *Polar Geography* 23, 119-131.

Andersen, C., Koç, N., Moros, M., 2004. A highly unstable Holocene climate in the subpolar North Atlantic: evidence from diatoms. *Quaternary Science Reviews* 23, 2155-2166.

Andruleit, H., 1997. Coccolithophore fluxes in the Norwegian-Greenland Sea: seasonality and assemblage alterations. *Marine Micropaleontology* 31, 45-64.

Baumann, K.-H., Matthiessen, J., 1992. Variations in surface water mass conditions in the Norwegian Sea: evidence from Holocene coccolith and dinoflagellate cyst assemblages. *Marine Micropaleontology* 20, 129-146.

Baumann, K.-H., Andruleit, H. A., Samtleben, C., 2000. Coccolithophores in the Nordic Seas: comparison of living communities with surface sediment assemblages. *Deep Sea Research II* 47, 1743-1772.

Berger, A. L. and M. F. Loutre, 1991. Insolation values for the climate of the last 10 million years. *Quaternary Science Reviews* 10, 297-317.

Blindheim, J., Borovkov, V., Hansen, B., Malmberg, S.-Aa., Turrell, W.R., Osterhus, S., 2000. Upper layer cooling and freshening in the Norwegian Sea in relation to atmospheric forcing. *Deep-Sea Research I* 47, 655-680.

Boessenkool, K.P., van Gelder, M.-J., Brinkhuis, H., Troelstra, S.R., 2001. Distribution of organic-walled dinoflagellate cysts in surface sediments from transects across the Polar Front offshore southeast Greenland. *Journal of Quaternary Science* 16, 661–666.

Bollmann, J., Henderiks, J., Brabec, B., 2002. Global calibration of *Gephyrocapsa* coccolith abundance in Holocene sediments for paleotemperature assessment. *Paleoceanography* 17, doi:10.1029/2001PA000742.

Bond, G., W. Showers, M. Cheseby, R. Lotti, P. Almasi, P. de Menocal, P. Priore, H. Cullen, I. Hajdas and G. Bonani, 1997. A pervasive millemial-scale cycle in North Atlantic Holocene and glacial climates. *Science* 278, 1257-1266.

Bond, G., Kromer, B., Beer, J., Muscheler, R., Evans, M.N., Showers, W., Hoffmann, S., Lotti-Bond, R., Hajdas, I., Bonani, G., 2001. Persistent Solar Influence on North Atlantic Climate During the Holocene. *Science* 294, 2130-2136.

Brand, L. E., 1994. Physiological ecology of marine coccolithophores. In *Coccolithophores*, sous la dir. de A. Winter et W.G. Siesser, p. 39-49. Cambridge: Cambridge University Press.

Calvo, E., J. Grimalt, Jansen, E., 2002. High resolution U37K sea surface temperature reconstruction in the Norwegian Sea during the Holocene. *Quaternary Science Reviews* 21, 1385-1394.

Chapman, M. R., Shackleton, N. J., 2000. Evidence of 550-year and 1000-year cyclicities in North Atlantic circulation patterns during the Holocene. *The Holocene* 10, 287-291.

Chapman, M. R., Shackleton, N.J., Zhao, M., Eglinton, G., 1996. Faunal and alkenone reconstructions of subtropical North Atlantic surface hydrography and paleotemperature over the last 28 kyr. *Paleoceanography* 11, 343-357.

Cortese, G., Dolven, J,K,, Bjørklund, K.R., Malmgren, B.A., 2005. Late Pleistocene–Holocene radiolarian paleotemperatures in the Norwegian Sea based on artificial neural networks. *Palaeogeography, Palaeoclimatology, Palaeoecology* 224, 311– 332.

Dahl-Jensen, D., Mosegaard, K., Gundestrup, N., Clow, G.D., Johnsen, S.J., Hansen, A.W., Balling, N., 1998. Past temperatures directly fromthe Greenland ice sheet. *Science* 282, 268–271.

Dansgaard, W., Johnsen, S.J., Clausen, H.B., Dahl-Jensen, D., Gundestrup, N.S., Hammer, C.U., Hvidberg, C.S., Steffensen, J.P., Sveinbjörnsdottir, A.E., Jouzel, J., Bond, G., 1993. Evidence for general instability of past climate from a 250-kyr ice-core record. *Nature* 364, 218-220.

de Vernal, A., Turon, J.-L., Guiot, J., 1994. Dinoflagellate cyst distribution in high latitude environments and quantitative reconstruction of sea-surface temperature, salinity and seasonality. *Canadian Journal of Earth Sciences* 31, 48–62.

de Vernal, A., Eynaud, F., Henry, M., Hillaire-Marcel, C., Londeix, L., Mangin, S., Matthiessen, J., Marret, F., Radi, T., Rochon, A., Solignac, S., Turon, J.-L., 2005. Reconstruction of sea-surface conditions at middle to high latitudes of the Northern Hemisphere during the Last Glacial Maximum (LGM) based on dinoflagellate cyst assemblages. *Quaternary Science Reviews* 24, 897-924.

de Vernal, A., Hillaire-Marcel, C., 2006. Provincialism in trends and high frequency changes in the northwest North Atlantic during the Holocene. *Global and Planetary Change* 54, 263–290.

de Vernal, A., et F. Marret. 2007. Organic-walled dinoflagellate cysts: tracers of sea-surface conditions. In *Proxies in Late Cenozoic Paleoceanography*, *Developments in Marine Geology*, vol. 1, sous la dir. de C. Hillaire-Marcel et A. de Vernal, p. 371-408. Amsterdam, Oxford: Elsevier.

deMenocal, P.B., 2001. Cultural Responses to Climate Change During the Late Holocene. *Science* 292, 667 – 673.

Denton, G.H., Karlén, W., 1973. Holocene climatic variations – Their pattern and possible cause. *Quaternary Research* 3. 155-205.

Dolven, J.K., Cortese, G., Bjorklund, K.R., 2002. A high-resolution radiolarian-derived paleotemperature record for the Late Pleistocene-Holocene in the Norwegian Sea. *Paleoceanography* 17, 1072, doi:10.1029/2002PA000780.

Duplessy, J.-C., Ivanova, E., Murdmaa, I., Paterne, M., Labeyrie, L., 2001. Holocene paleoceanography of the northern Barents Sea and variations of the northward heat transport by the Atlantic Ocean. *Boreas* 30, 2-16.

Eide, L. K., 1990. Distribution of coccoliths in surface sediments in the Norwegian-Greenland Sea. *Marine Micropaleontology* 16, 65-75.

Eiriksson, J., Knudsen, K.L., Haflidason, H., Heinemeier, J., 2000a. Chronology of late Holocene climatic events in the northern North Atlantic based on AMS ^{14}C dates and tephra markers from the volcano Hekla, Iceland. *Journal of Quaternary Science* 15, 573-580.

Eiriksson, J., Knudsen, K.L., Haflidason, H., Henriksen, P., 2000b. Late-glacial and Holocene paleoceanography of the North Icelandic shelf. *Journal of Quaternary Science* 15, 23-42.

Fensome, R.A., Taylor, F.J.R., Norris, G., Sargeant, W.A.S., Wharton, D.I., Williams, G.L., 1993. *A classification of living and fossil dinoflagellates*. Micropaleontology, Special publication number 7, p. 1-351. American Museum of Natural History.

Geitzenauer, K.R., Roche, M.B., McIntyre, A., 1976. Modern Pacific coccolith assemblages: derivation and application to late Pleistocene paleotemperature analysis. In *Investigation of late Quaternary paleoceanography and paleoclimatology*, sous la dir. De R.M. Cline et J.D. Hays, P. 423-448. Washington DC: Geological Society of America.

Giraudeau, J., Cremer, M., Manthé, S., Labeyrie, L., Bond, G., 2000. Coccolith evidence for instabilities in surface circulation south of Iceland during Holocene times. *Earth and Planetary Science Letters* 179, 257-268.

Giraudeau, J., Beaufort, L., 2007. Coccolithophores: From extant populations to fossil assemblages. In *Proxies in Late Cenozoic Paleoceanography, Developments in Marine Geology*, vol. 1, sous la dir. de C. Hillaire-Marcel et A. de Vernal, p. 409-439. Amsterdam, Oxford: Elsevier.

Gudmundsson, K, 1998. Long-term variation in phytoplankton productivity during srping in Icelandic waters. *ICES Journal of Marine Science* 55, 635-643.

Guiot, J., 1990. Methodology of the last climatic cycle reconstruction in France from pollen data. *Palaeogeography Palaeoclimatology Palaeoecology* 80, 49–69.

Häkkinen, S., Rhines, P.B. 2004. Decline of subpolar North Atlantic circulation during the 1990s. *Science* 304, 555-559.

Haq, B. U., 1998. Calcareous nannoplankton. In *Introduction to marine micropaleontology*, sous la dir. de B.U. Haq et A. Boersma, p. 79-107. Elsevier.

Hass, H. C., Andruleit, H., Baumann, A., Baumann, K.-H., Kohly, A., Jensen, S., Matthiessen, J., Samtleben, C., Schäfer, P., Schröder-Ritzrau, A., Thiede, J., 2001. The potential of synoptic plankton analyses for paleoclimatic investigations: five plankton groups from the Holocene Nordic Seas. In *The northern North Atlantic: a changing environment*, sous la dir. de P. Schäfer, W. Ritzrau, M. Schlüter et J. Thiede, p. 291-318. Berlin: Springer.

Hatun, H., Sandø, A.B., Drange, H., Hansen, B., Valdimarsson, H., 2005. Influence of the Atlantic Subpolar Gyre on the Thermohaline Circulation. *Science* 309, 1841-1844.

Holliday, N. P., 2003. Air-sea interaction and circulation changes in the northeast Atlantic. *Journal of Geophysical Research* 108, 3259, doi:10.1029/2002JC001344.

Hurrell, J. W., 1995. Decadal trends in the North Atlantic Oscillation: Regional temperatures and precipitation. *Science* 269, 676-679.

Kaplan, M.R., Wolfe, A.P., 2006. Spatial and temporal variability of Holocene temperature in the North Atlantic region. *Quaternary Research* 65, 223-231.

Kaufman, D.S., Ager, T.A., Anderson, N.J., Anderson, P.M., Andrews, J.T., Bartlein, P.J., Brubaker, L.B., Coats, L.L., Cwynar, L.C., Duvall, M.L., Dyke, A.S., Edwards, M.E., Eisner, W.R., Gajewski, K., Geirsdottir, A., Hu, F.S., Jennings, A.E., Kaplan, M.R., Kerwin, M.W., Lozhkin, A.V., MacDonald, G.M., Miller, G.H., Mock, C.J., Oswald, W.W., Otto-Bliesner, B.L., Porinchu, D.F., Rühland, K., Smol, J.P., Steig, E.J., Wolfe, B.B., 2004. Holocene thermal maximum in the western Arctic (0-180°W). *Quaternary Science Reviews* 23, 529-560.

Keeling, C.D., Whorf, T.P., 2000. The 1,800-year oceanic tidal cycle: A possible cause of rapid climate change. *Proceedings of the National Academy of Science* 97, 3814-3819.

Klitgaard-Kristensen, D., Sejrup, H. P., Haflidason, H., 2001. The last 18 kyr fluctuations in Norwegian surface conditions and implications for the magnitude of climatic change: evidence from the North Sea. *Paleoceanography* 16, 455-467.

Kucera, M., 2007. Planktonic foraminifera as tracers of past oceanic environments. In *Proxies in Late Cenozoic Paleoceanography, Developments in Marine Geology*, vol.

1, sous la dir. de C. Hillaire-Marcel et A. de Vernal, p. 213-262. Amsterdam, Oxford: Elsevier.

Lorbacher, K., Dommenget, D., Niiler, P.P., Köhl, A., 2006. Ocean mixed layer depth: A subsurface proxy of ocean-atmosphere variability. *Journal of Geophysical Research* 111, C07010, doi:10.1029/2003JC002157.

Lorenz, S. J., Kim, J. H., Rimbu, N., Schneider, R. R., Lohmann, G., 2006. Orbitally driven insolation forcing on Holocene climate trends: Evidence from alkenone data and climate modeling. *Paleoceanography* 21, PA1002, doi:10.1029/2005PA001152.

Mangerud, J., Andersen, S.T., Berglund, B.E., Donner, J.J., 1974. Quaternary stratigraphy of Norden, a proposal for terminology and classification. *Boreas* 3, 179–181.

Marchal, O., Cacho, I., Stocker, T.F., Grimalt, J.O., Calvo, E., Martrat, B., Shackelton, N., Vautravers, M., Cortijo, E., van kreveld, S., Andersson, C., Koç, N., Chapman, M., Sbaffi, L., Duplessy, J.-C., Sarnthein, M., Turon, J.-L., Duprat, J., Jansen, E., 2002. Apparent cooling of the sea surface in the northeast Atlantic and Mediterranean during the Holocene. *Quaternary Science Reviews* 21, 455-483.

Marret, F., Eiriksson, J., Knudsen, K.L., Turon, J.-L., Scourse, J.D., 2004. Distribution of dinoflagellate cyst assemblages in surface sediments from the northern and western shelf of Iceland. *Review of Palaeobotany and Palynology* 128, 35-53.

Marshall, J. et F. Schott. 1999. Open-ocean convection; observations, theory, and models. *Reviews of Geophysics* 37, 1-64.

Maslin, M., Pike, J., Stickley, C., Ettwein, V., 2003. Evidence of Holocene climate variability in marine sediments. In *Global Change in the Holocene*, sous la dir. de A. Mackay, R. Battarbee, J. Birks et F. Oldfield, p. 185-209. Londres: Arnold.

Matthiessen, K.-H., Schröder-Ritzrau, A., Hass, C., Andruleit, H., Baumann, A., Jensen, S., Kohly, A., Pflaumann, U., Samtleben, C., Schäfer, P., Thiede, J., 2001. Distribution of calcareous, siliceous and organic-walled planktic microfossils in surface sediments of the Nordic Seas and their relation to surface-water masses. In *The northern North Atlantic: a changing environment*, sous la dir. de P. Schäfer, W. Ritzrau, M. Schlüter et J. Thiede, p. 291-318. Berlin: Springer.

Monterey, G., Levitus, S., 1997. Seasonal variability of mixed layer depth for the world ocean. *NOAA Atlas NESDIS 14*, U.S. Gov. Printing Office, Wash., D.C., 96 pp.

Moros, M., Emeis, K., Risebrobakken, B., Snowball, I., Kuijpers, A., McManus, J., Jansen, E., 2004. Sea surface temperatures and ice rafting in the Holocene North Atlantic: climate influences on northern Europe and Greenland. *Quaternary Science Reviews* 23, 2113-2126.

National Snow and Ice Data Center (NSIDC), 2003. Arctic and Southern Ocean Sea Ice Concentrations, http://nsidc.org/data/docs/noaa/g00799_arctic_southern_sea_ice/index.html,

Nesje, A., Johannessen, T., 1992. What were the primary forcing mechanisms of high-frequency Holocene climate and glacier variations? *The Holocene* 2, 79-84.

Noren, A.J., Bierman, P.R., Steig, E.J., Lini, A., Southon, J., 2002. Millenial-scale storminess variability in the northeastern United States during the Holocene epoch. *Nature* 419, 821-824.

O'Brien, S. R., Mayewski, P.A., Meeker, L.D., Meese, D.A., Twickler, M.S., Whitlow, S.I., 1995. Complexity of Holocene climate as reconstructed from a Greenland ice core. *Science* 270, 1962-1964.

Ólafsson, J., 1999. Connection between oceanic conditions off N-Iceland, Lake Mývatn temperature, regional wind direction variability and the North Atlantic Oscillation. *Rit Fiskideildar* 16, 41-57.

Oppo, D.W., McManus, J.F., Cullen, J.L., 2003. Deepwater variability in the Holocene epoch. *Nature* 422, 277-278.

Paul, A., Schultz, M., 2002. Holocene climate varibility on centennial-to-millenial time scales: 2. Internal and forced oscillations as possible causes. In *Climate Development and History of the North Atlantic Realm*, sous la dir. de G. Wefer, W. Berger, K.-E. Behre et E. Jansen, p. 41-54. Berlin, Heidelberg: Springer Verlag.

Rahman, A., de Vernal, A., 1994. Surface oceanographic changes in the eastern Labrador Sea; nannofossil record of the last 31,000 years. *Marine Geology* 121, 247-263.

Rahmstorf, S., 2006. Thermohaline Ocean Circulation. In *Encyclopedia of Quaternary Sciences*, sous la direction de S.A. Elias. Amsterdam: Elsevier.

Rasmussen, T.L., Bäckström, D., Heinemeier, J., Klitgaard-Kristensen, D., Knutz, P.C., Kuijpers, A., Lassen, S., Thomsen, E., Troelstra, S.R., van Weering, T.C.E., 2002a. The Faroe-Shetland gateway: late Quartenary water mass exchange between the Nordic seas and the northeastern Atlantic. *Marine Geology* 188, 165-192.

Rasmussen, T.L., Thomsen, E., Troelstra, S.R., Kuijpers, A., Prins, M.A., 2002b. Millennial-scale glacial variability versus Holocene stability changes in planktic and bentic foraminifera faunas and ocean circulation in the North Atlantic during the last 60 000 years. *Marine Micropaleontology* 47, 143-176.

Rimbu, N., Lohmann, G., Kim, J.-H., Arz, H.W., Schneider, R., 2003. Arctic/North Atlantic Oscillation signature in Holocene sea surface temperature trends as obtained from alkenone data. *Geophysical Research Letters* 30, 1280, doi:10.1029/2002GL016570.

Risebrobakken, B., Jansen, E., Andersson, C., Mjelde, E., Hevroy, K., 2003. A high-resolution study of Holocene paleoclimatic and paleoceanographic changes in the Nordic Seas. *Paleoceanography* 18, 1017, doi:10.1029/2002PA000764.

Rochon, A., de Vernal, A., Turon, J.-L., Matthiessen, J., Head, M.J., 1999. *Distribution of recent dinoflagellate cysts in surface sediments from the North Atlantic ocean and adjacent seas in relation to sea-surface parameters*. American Association of Stratigraphic Palynologists Contribution Series 35, Houston, TX.

Samtleben, C., Schröder, A., 1992. Living coccolithophore communities in the Norwegian-Greenland Sea and their record in sediments. *Marine Micropaleontology* 19, 333-354.

Sarnthein, M., van Kreveld, S., Erlenkeuser, H., Grootes, P.M., Kucera, M., Pflaumann, U., Schulz, M., 2003. Centennial-to-millenial-scale periodicities of Holocene climate and sediment injections off the western Barents shelf, 75°N. *Boreas* 32, 447-461.

Sarnthein, M., Jansen, E., Weinelt, M., Arnold, M., Duplessy, J.-C., Erlenkeuser, H., Flatoy, A., Johannessen, G., Johannessen, T., Jung, S., Koç, N., Labeyrie, L., Maslin, M., Pflaumann, U., Schulz, H. 1995. Variations in Atlantic surface ocean paleoceanography, 50°-80°N: A time-slice record of the last 30,000 years. *Paleoceanography* 10, 1063-1094.

Schulz, M., Paul, A., 2002. Holocene climate variability on centennial-to-millenial time scales: 1. Climate records from the Noth-Atlantic realm. In *Climate Development and History of the North Atlantic Realm*, sous la dir. de G. Wefer, W. Berger, K.-E. Behre et E. Jansen, p. 41-54. Berlin, Heidelberg: Springer Verlag.

Siesser, W.G., 1993. Calcareous nannoplankton. In *Fossil prokaryotes and protests*, sous le dir. de J.H. Lipps, p.169-201, Blackwell Scientific Publications.

Sikes, E.L., Keigwin, L.D., 1996. A re-examination of northeast Atlantic sea surface temperature and salinity over the last 16 kyr. *Paleoceanography* 11, 327-342.

Solignac, S., de Vernal, A., Hillaire-Marcel, C., 2004. Holocene sea-surface conditions in the North Atlantic – contrasted trends and regimes in the western and eastern sectors (Labrador Sea vs. Iceland Basin). *Quaternary Science Reviews* 23, 319-334.

Solignac, S. 2005. Manifestations et forçages des oscillations millénaires et submillénaires de l'Holocène dans l'Atlantique Nord et les régions continentales amphi-atlantiques. Rapport de synthèse 16 (9), Montréal, Université du Québec à Montréal.

Swift, J. H., 1986. The Arctic waters. In *The Nordic seas*, sous la dir. de B.G. Hurdle, p. 129-153. New York: Springer.

Tremblay, L.B., Mysak, L.A., Dyke, A.S., 1997. Evidence from driftwood records for century-to-millenial scale variations of the high latitude atmospheric circulation during the Holocene. *Geophysical Research Letters* 24, 2027-2030.

Turrell, W.R., Hansen, B., Osterhus, S., Hughes, S., Ewart, K., Hamilton, J., 1999. Direct observations of inflow to the Nordic seas through the Faroe-shetland Channel 1994-1997. *ICES CM 1999/L:01*. Copenhague: International Council for the Exploration of the Sea.

Vink, A., Baumann, K. H., Böckel, B., Esper, O., Kinkel, H., Volbers, A., Willems, H., Zonneveld, K.A.F., 2003. Coccolithophorid and dinoflagellate synecology in the south and equatorial Atlantic: improving the paleoecological significance of phytoplanktonic microfossils. In *The South Atlantic in the Late Quaternary: Reconstruction of Material Budgets and Current Systems*, sous la dir. de G. Wefer, S. Mulitza et V. Ratmeyer, p. 101-120. Berlin, Heidelberg, New York, Tokyo: Springer Verlag.

Visbeck, M., Chassignet, E.P., Curry, R.G., Delworth, T.L., Dickson, R.R., Krahmann, G., 2003. The ocean's response to North Atlantic Oscillation variability. In *The North Atlantic Oscillation: Climate Significance and Environmental Impact, Geophysical Monograph Series*, vol. 134, p. 113-145. Washington DC: American Geophysical Union.

Wall, D., Dale, B., 1968. Modern dinoflagellate cysts and the evolution of the Peridiniales. *Micropaleontology* 14, 265-304.

Zielinski, G.A., Mayewski, P.A., Meeker, L.D., Whitlow, S., Twickler, M.S., Morrison, M., Meese, D.A., Gow, A.J., Alley, R.B. 1994. Record of volcanism since 7000 B.C. from the GISP2 Greenland ice core and implications for the volcano-climate system. *Science* 264, 948-952.

Zonneveld, K.A.F., Versteegh, G.J.M., de Lange, G.J., 2001. Palaeoproductivity and post-depositional aerobic organic matter decay reflected by dinoflagellate cyst assemblages of the Eastern Mediterranean S1 sapropel. *Marine Geology* 172, 181-195.